Lithofacies and Alteration of the Hurricane Zone, of the Boomerang volcanogenic massive sulphide deposit, Tulks Belt, Central Newfoundland, Canada

By Michelle English

A thesis submitted to the School of Graduate Studies in partial fulfillment of the requirements for the degree of

Master of Science

Department of Earth Sciences

Memorial University of Newfoundland

October 28th, 2019

St. John's, Newfoundland and Labrador

Abstract

The Hurricane zone of the Boomerang volcanogenic massive sulphide (VMS) deposit is part of the VMS-hosting Cambro-Ordovician Tulks volcanic belt. The Hurricane zone is one of three lenses in the deposit and consists of a sub-horizontal (semi-)massive sulphide lens with combined resources of 55,100 tonnes @ 13.4% Zn, 7.0% Pb, 1.20% Cu, 159.0 g/t Ag, and 2.00 g/t Au. Mineralization is hosted in intermediate to felsic volcaniclastic rocks of the ca. 488 Ma Pats Pond Group (Victoria Lake supergroup) and consists of banded sphalerite, galena, chalcopyrite, and pyrite, which are interpreted to have formed below the seafloor within subseafloor sediments. Four alteration assemblages are identified: intense sericite-quartz-pyrite, sericite-quartz-chlorite-pyrite, intense chlorite and chaotic carbonate. Whole-rock lithogeochemistry and short-wave infrared spectroscopy are useful in identifying key elements/element ratios and variations in white mica chemistry/mineralogy associated with each alteration assemblage and are useful vectors to mineralization.

Acknowledgements

This thesis has greatly improved through the help of many. First and foremost, I would like to thank my supervisor, Dr. Stephen J. Piercey for his endless support, guidance and mentorship over the years. His passion and excitement for teaching and research are infectious and played a large role in my development as a geologist and a person. I would also like to thank Dr. Luke Beranek for being on my committee, providing me with advice and reviewing my manuscript. I would also like to thank the following people for providing me with valuable advice and support: Jean-Luc Pilote, Stefanie Brueckner, Marie-Eve Lajoie, Jonathan Cloutier, John Jamieson, Michael Buschette, Steve Delgaudio, and Alex Hutter.

This project was made possible by Canadian Zinc Corp., who provided logistical support and allowed me to study the Hurricane zone. I would especially like to thank Gerry Squires, Andrew Hussey, Alexandria Marcotte, Mike Vande Gutche, and Dianne Fost for providing me with countless resources and support.

Financial support for this project was provided by the National Sciences and Engineering Research Council (NSERC) Discovery Grant and IRC to S.J. Piercey. Additional funding was provided by NSERC-Altius Industrial Research Chair in Mineral Deposits (supported by NSERC, Altius Resources Inc and the Research and Development Corporation of Newfoundland and Labrador), and an SEG Canada Graduate Fellowship to Michelle English.

Last but certainly not least, I would like to thank my friends and family back home and the numerous of amazing friends I've met during my time at MUN. Special thanks to my parents, Paul and Robin, and brothers, Alex and Kurtis, for constantly supporting me and providing me with motivation to pursue my graduate degree. I am incredibly thankful for the opportunities and experiences that moving to Newfoundland has brought me.

Table of Contents

List of Tables

Chapter 1

Chapter 2

List of Figures

Chapter 1

Chapter 2

List of Abbreviations

AI	Hashimoto Alteration Index
alt	Alteration, altered
Arg	Argillite
Carb	Carbonate
CC	Chaotic Carbonate
Ccp	Chalcopyrite
CCPI	Chlorite-carbonate-pyrite index
Chl	Chlorite
DH	Down Hole
Dis	Disseminated
E	Easting
Ep	Epidote
f.g, m.g, c.g	fine-grained, medium-grained, coarse-grained
Fe	Iron
Fig(s)	Figure(s)
Flow	Volcanic Flow
Fol	Foliation
Frags	Fragments
FW	Footwall
g/t	grams per ton
HFSE	High field strength elements
HREE	Heavy rare earth elements
HW	Hanging wall
ICP-ES	Inductively coupled emission-mass spectrometry
ICP-MS	Inductively coupled plasma-mass spectrometry
Int	Intrusion
Int	Intense
km	Kilometer
Lap	Lapilli
LC	Lower Contact
LREE	Light rare earth elements
LT	Lapilli Tuff
mm	millimeter
m	Meter
Mod	Moderate

MS	Massive Sulphide
Mud	Mudstone
N	Northing
Pheno(s)	Phenocryst(s)
ppb	parts per billion
ppm	parts per million
Py	Pyrite
Qtz	Quartz
REE	Rare earth element
RIL	Red Indian Line
Ser	Sericite
SMS	Semi-massive Sulphide
Sph	Spheralerite
Sul	Sulphide
SWIR	Short-wave infrared
TB	Tuff Breccia
UC	Upper Contact
UTM	Universal Transverse Mercator
VMS	Volcanogenic massive sulphide
xstals	Crystals
Zn	Zinc

List of Appendices

Chapter 1: Introduction to the Hurricane Zone of the Boomerang Volcanogenic Massive Sulphide Deposit, Central Newfoundland, Canada

1.1 Introduction and Purpose of Study

The Tulks volcanic belt (TVB) within the Victoria Lake supergroup (VLSG), central Newfoundland, is host to several volcanogenic massive sulphide (VMS) and epithermal/orogenic Au deposits (Fig. 1-1). Previous work by Hinchey (2007, 2011a) focused primarily on VMS deposits in the TVB (e.g., Boomerang, Tulks Hill, Tulks East) at the deposit-scale, using diamond-drill core for lithological, metallogenic, geochemical and alteration studies. The most recent discovery in the TVB is the Boomerang cluster (Boomerang-Domino-Hurricane sulphide lenses; referred to as the Boomerang deposit), a felsic siliciclastic VMS deposit located in the southern part of the belt (Hinchey, 2007). The Boomerang deposit is located approximately 3 km northeast of Pats Pond and 17.5 km southwest of the southern tip of Red Indian Lake (Fig. 1-2; Hinchey, 2007; 2011a). The Boomerang and Domino deposits were discovered by Messina Minerals Inc. (now a subsidiary of NorZinc Ltd.) in 2004 and 2006, respectively (De Mark and Dearin, 2007). Indicated resources at Boomerang are estimated at 1.36 Mt grading 7.09 wt. % Zn, 3.00 wt. % Pb, 0.51 wt. % Cu, 110.43 g/t Ag, and 1.66 g/t Au with inferred resources at 0.69 Mt grading 6.5 wt. % Zn, 2.8 wt. % Pb, 0.4 wt. % Cu, 95 g/t Ag, and 0.9 g/t Au (De Mark and Dearin, 2007). The inferred resources at Domino are estimated at 411,200 tonnes grading 6.3 wt. % Zn, 2.8 wt. % Pb, 0.4 wt. % Cu, 94 g/t Ag, and 0.6 g/t Au (De Mark and Dearin, 2007). While there has been extensive geological work on the Boomerang and Domino lenses, little research has been undertaken on the Hurricane zone (prospect), located 500 m to the east of the Boomerang lens (Hinchey, 2007). The Hurricane prospect is the smallest lens in the Boomerang-Domino deposit(s) with non-NI-43-101 compliant resources estimated at 55,100 tonnes grading 13.40 wt. % Zn, 7.0 wt. % Pb, 1.20 wt. % Cu, 159.0 g/t Ag and 2.90 g/t Au (A. Marcotte, personal communication, 2015).

The goals of this project are to conduct the first detailed study of the Hurricane zone by characterizing the lithostratigraphy, chemostratigraphy, and hydrothermal alteration of its host volcanic and sedimentary packages, and provide a potential genetic model for the Hurricane zone. This will expand on the work completed by Hinchey (2007, 2011a) and provide a more complete understanding of the Boomerang deposit.

This thesis consists of three chapters and supplementary appendices. Chapter 1 is an introductory chapter that presents the purpose of this thesis and provides background information on the regional and local geology, exploration history, previous work on the deposit and methods used during this study. Chapter 2 is the main body of the thesis and is a research manuscript that is intended for future publication in a scientific journal. This chapter presents detailed descriptions of the lithology and alteration assemblages, as well as lithogeochemistry and hyperspectral data, to reconstruct the volcanic and hydrothermal evolution of the Hurricane zone. Chapter 3 is a summary of the conclusions of the thesis and provides directions for future research.

1.2 Previous Studies and Exploration History

The VMS potential and mineralization in the Tulks volcanic belt have been investigated since the late 1950s. Riley (1957) and Williams (1970) conducted the first regional mapping in the belt. More detailed mapping was completed by the Newfoundland Department of Mines and Energy (Kean, 1977, 1979a, b, 1982, 1983; Kean and Jayasinghe, 1980, 1982; Kean and Mercer, 1981;

Evans et al., 1994a, b, c). Evans and Kean (2002) provided an in-depth regional synthesis of the area focusing on the geology, geochemistry, tectonic setting and mineralization of the VLSG. Hinchey (2007, 2011a) expanded the work of Evans and Kean (2002) and provided new information regarding the geology and mineralization of the VLSG and the northern and southern portions of the TVB, as well as providing new lithogeochemical and U-Pb geochronology data.

Numerous exploration projects have been conducted in the southern TVB. ASARCO led one of the first exploration programs in the belt, which consisted of prospecting and stream and soil sampling, and sequentially led to the discovery of the Tulks Hill deposit in 1961. Follow-up exploration by Abitibi-Price led to the discovery of the Tulks East prospect in 1977. Noranda Mining and Exploration continued to explore in the southern part of the belt from 1993-1998 utilizing geophysical surveys, mapping, surficial geochemistry and lithogeochemistry. The majority of their efforts were focused on additional diamond drilling on Tulks East and Curve Pond (an iron formation) prospects but also included examining a section of the Boomerang alteration zone, that is now interpreted to be part of the Domino lens (Hinchey, 2011a). Initial holes in the Boomerang alteration zone discovered hydrothermal alteration and sulphide stringers, and further drilling intersected massive Pb-Zn-rich sulphide grading 0.46 wt. % Cu, 2.63 wt. % Pb, 7.4 wt. % Zn, 76.5 g/t Ag and 0.67 g/t Au over 1.8 m (hole GA-97-05; Banville et al., 1998; Noranda, 1998). Since this discovery, several companies have explored the southern TVB, most notably Messina Minerals Inc., which discovered the Boomerang deposit in 2004. Further delineation of the Boomerang deposit led to the discovery of the Hurricane and Domino lenses in 2006. The Domino VMS zone is located 200 m northeast and approximately 100 m deeper than the Boomerang deposit, whereas the Hurricane zone is located 500 m east of the Boomerang zone, but is hosted by the same stratigraphic horizon (De Mark and Dearin, 2007). The Boomerang-

Domino deposit has been the main focus of exploration and research in this region with little work concentrated on the Hurricane zone. In 2012, Canadian Zinc Corporation acquired Paragon Minerals and their 10 base metal and precious metal VMS projects in the South Tally Pond area. In 2013, NorZinc Ltd., formally known as Canadian Zinc Corp, also acquired all Messina Minerals Inc. and are currently exploring the southern TVB including Tulks South, Long Lake and the Boomerang-Domino-Hurricane deposits.

1.3 Regional Geology and Tectonic Setting

In Newfoundland, the Appalachian orogenic belt is divided into four distinct tectonostratigraphic zones based upon lithology, age, geophysical signatures and metallogeny. From west to east these zones are: the Humber Zone, the Dunnage Zone, the Gander Zone and the Avalon Zone (Figs. 1-1 and 1-2; Williams, 1979; van Staal, 2007; van Staal and Barr, 2012). The Humber Zone represents part of the eastern Laurentian continental margin; the Dunnage Zone represents vestiges of the Iapetus Ocean and consists of arc, back-arc, and ophiolitic rocks of various affinities (Williams, 1978, 1979; Swinden et al., 1997; van Staal and Barr, 2012). The Gander and Avalon Zones are peri-Gondwanan microcontinental blocks that were sequentially accreted onto the margin of Laurentia during the mid-Paleozoic (450-380 Ma; Williams et al., 1988; van Staal, 2007; van Staal and Barr, 2012).

The Dunnage Zone (also known as the Central Mobile Belt) forms the central part of the Newfoundland Appalachians. It represents the vestiges of Cambrian-Ordovician continental and intra-oceanic arcs, back-arc basins and ophiolites that formed within the Iapetus Ocean and its peri-continental seaways (Kean et al., 1981; Swinden, 1990; Williams, 1995; Zagorevski et al., 2006; van Staal, 2007; van Staal and Barr, 2012). The Dunnage Zone can be further subdivided into the Notre Dame and Exploits subzones that consist of volcanic and sedimentary rocks that formed along the peri-Laurentian and peri-Gondwana margins, respectively (Williams, 1995; Zagorevski et al., 2006; Zagorevski et al., 2007; van Staal, 2007). The Notre Dame and Exploits subzones were accreted to the Laurentian and Gondwanan margins during the Taconic and Penobscot orogenies, respectively, in the Early to Middle Ordovician and subsequently to each other during the late stages of the Taconic orogeny in the Late Ordovician (van Staal, 2007; Zagorevski, 2007). The subzones are separated by a suture zone called the Red Indian Line (RIL; Williams, 1995). In addition to the separation of the RIL, these two sub-zones have very distinct stratigraphic, structural, faunal and isotopic characteristics (Williams et al., 1988; Zagorevski et al., 2007; Hinchey, 2011a).

The Victoria Lake supergroup (VLSG) is situated east of the Red Indian Line within the Exploits subzone (Fig. 1-3). It is bounded to the east by the Noel Pauls Line and is overlain by or is in fault contact with the Ordovician to Silurian sedimentary rocks of the Badger Group to the northeast (Kean and Jayasinghe, 1980; Rogers et al., 2005; Zagorevski et al., 2007). The VLSG was originally divided into two major volcanic belts: the Tally Pond and Tulks Hill volcanic belts (Kean and Jayasinghe, 1980, 1982; Kean et al., 1981; Rogers et al., 2006). Further lithological, geochronological, and geochemical studies resulted in the VLSG being subdivided into six distinct fault-bounded belts (Fig. 1-3). From east to west these include: the Tally Pond group (c. 513 Ma; Dunning et al., 1991; McNicoll et al., 2010), Long Lake group (c. 514-506 Ma; Zagorevski et al., 2007; Hinchey and McNicoll, 2016), Tulks group (c. 498 Ma; Evans et al., 1990; Evans and Kean, 2002; Zagorevski et al., 2007), Sutherlands Pond group (c. 462 Ma; Dunning et al, 1987), and the Pats Pond and Wigwam Brook groups (488 Ma and 453 Ma, respectively; Zagorevski et al., 2007). The TVB herein is used to delineate the broader VMS-hosting stratigraphy of the Tulks Valley area, and is not a stratigraphic entity per se, as the TVB is comprised of westward-younging tectonostratigraphic units that include the Tulks, the Pats Pond, the Sutherlands Pond, and the Wigwam Brook groups (Hinchey, 2011a).

1.4 Overview on Volcanogenic Massive Sulphide Deposits

Volcanogenic massive sulphide (VMS) deposits are strata-bound to stratiform lenses of polymetallic sulphide minerals that form by precipitation of metalliferous fluids on or just below the seafloor, and in spatial, temporal and genetic association with contemporaneous volcanism (Franklin et al., 2005). VMS deposits are the products of hydrothermal convection of seawater driven by magmatic heat flow, typically above subvolcanic intrusions in rift and arc environments (e.g., Franklin et al., 1981, 2005; Ohmoto, 1996; Galley et al., 2007). The deposit size, morphology and composition depends on the lithologies of the footwall and hanging wall host rocks, nature of synvolcanic faulting, basement rock composition, water depth, duration of hydrothermal circulation, temperature gradients, and degree of preservation (Galley et al., 2007). Several classification schemes have been suggested based on geological setting (i.e. tectonic regime; Sawkins, 1976; Eremin et al., 2000) and host-rock composition and stratigraphy (Morton and Franklin, 1987; Barrie and Hannington, 1999). These classifications will be discussed below and used mutually since host lithologies and assemblages are largely controlled by geodynamic processes (e.g., Barrie and Hannington, 1999). The lithological classification of VMS deposits includes a six-fold subdivision, including (Table 1.1): 1) bimodal-mafic; 2) mafic; 3) pelitic-mafic; 4) bimodal-felsic; 5) felsic-siliciclastic; and 6) hybrid bimodal-felsic. This six-fold classification is described in more detail by Barrie and Hannington (1999) and Franklin et al. (2005) with the addition of the high-sulfidation bimodal-felsic type by Galley et al. (2007), a hybrid between bimodal-felsic VMS deposits and high-sulfidation epithermal deposits. The lithological- and stratigraphic-based classification of deposits broadly defines the geological setting of VMS deposits and is the one most accepted by the geological community because it provides the best understanding of the geological characteristics of the VMS deposits, the processes and environment where it forms, and collectively this information can be used as an exploration tool (Franklin et al., 2005). Piercey (2011) summarized the various petrochemical signatures of VMS deposit environments.

Table 1.1. Classification of VMS deposits based on six lithotectonic settings (modified from Franklin et al., 2005 and Galley et al., 2007).

Type	Lithology	Tectonic Setting	Examples
Bimodal-Mafic	Dominantly mafic flows with up to 25% felsic volcanics	Oceanic rifted arc	Abitibi, Canada; Flin Flon, Canada
Mafic-Back Arc	Dominantly mafic flows with minor felsic flows or domes. Up to 50% synvolcanic mafic dykes and/or sills	Mature intra-oceanic back-arc	Central Newfoundland, Canada; Troodos, Cyprus
Pelitic-Mafic	Subequal basalt and pelites or pelites are dominant with up to 25% mafic sills. Felsic volcanics (volcaniclastics, sills, or flows) are typically absent	Juvenile and accreted back-arcs, oceanic mature back-arcs	Windy Craggy, BC, Canada; Besshi district, Japan
Bimodal-Felsic	Felsic volcanic rocks range from 30-75% of volcanic strata, basalts range from 20-50% and terrigenous sedimentary strata ~15%. Intermediate flows and sills are common	Continental margin arcs and related back-arcs, continental rifted arc	Eskay Creek, Canada; Dunnage Zone, Canada
Felsic-Siliciclastic	Siliciclastic rocks dominant ~80% with minor flows, domes, and extrusive equivalents making up the remainder 25% with minor mafic flows, sills and volcaniclastic rocks (~10%)	Mature epicontinental back-arcs	Iberian Pyrite Belt, Spain and Portugal; Bathurst, Canada
Hybrid Bimodal-Felsic	Felsic volcaniclastics and siliciclastic rocks	Combination of shallow water VMS and epithermal mineralization	Manus Basin, Pacific Ocean

Franklin et al. (2005) suggested a further subdivision of the lithostratigraphic types into three lithofacies end-members: flows, volcaniclastic rocks and sedimentary rocks. The lithofacies control the morphology of the deposit and the associated alteration distribution. Understanding lithofacies architecture allows for a better characterization of deposit architecture, the mechanisms of sulphide emplacement, and the nature and style of the hydrothermal alteration assemblages (Franklin et al., 2005).

There are two mechanisms by which sulphides are interpreted to have formed: precipitation directly on the seafloor (exhalation or exhalative mineralization) or via subseafloor replacement (Franklin et al., 2005). Exhalative sulphide formation is the classic model for VMS deposits (e.g. Fig. 1-4; Hutchinson, 1973; Lydon, 1984; Ohmoto, 1996; Franklin et al., 1981, 2005). Exhalation entails hydrothermal venting onto the seafloor producing growth of a sulphide chimney and sequential collapse, cementation and replacement of chimney debris (Lydon, 1984, 1988; Hannington et al., 1995; Ohmoto, 1996; Franklin et al., 2005). In long-lived exhalative systems there is often semi-continuous hydrothermal activity and multiple stages of chimney growth and evolution that often results in large chemical and mineralogically zoned sulphide mounds (Fig. 1-4; Franklin et al., 2005; Galley et al., 2007).

The process of subseafloor replacement occurs when metal-bearing hydrothermal fluids infiltrate and precipitate into porous volcanic and sedimentary rocks, infilling open spaces and replacing host material (Doyle and Allen, 2003; Franklin et al., 2005; Piercey, 2015). The Boomerang-Hurricane-Domino cluster deposit is interpreted to be a replacement-style siliciclastic felsic VMS deposit, as are most of the VMS deposits in the southern TVB, although local examples of bimodal-felsic and high-sulphidation bimodal felsic deposits are present (Hinchey, 2011a). These three types of felsic-hosted deposits are polymetallic and typically exhibit elevated base-metal grades, especially Zn and Pb (Barbour and Thurlow, 1982; Dearin, 2006).

Volcanogenic massive sulphide deposits are typically underlain by extensively hydrothermally-altered footwall volcanic rocks in pipe-like or discordant zones that contain sulphide-silicate stockwork mineralization (Riverin and Hodgson, 1980; Franklin et al., 1981, 2005; Gemmell and Large, 1992; Hannington, 2014). In some cases, hydrothermal alteration can be present in the immediate hanging wall (Gemmell and Fulton, 2001; Franklin et al., 2005; Piercey et al., 2014). Discordant stockwork zones can extend down to several hundreds of meters vertically below the massive sulphide. Hanging wall alteration, when present, can form as either semi-conformable halos tens of meters thick or extend several tens to hundreds of meters above the deposit as discordant alteration zones. Massive sulphide lenses can be stacked due to synchronous and/or sequential phases of ore formation during volcanic quiescence. In this case, proximal alteration halos and stockwork mineralization are connected (Knuckey et al., 1982; Gibson and Watkinson, 1990, Franklin et al., 2005).

Hydrothermal alteration in VMS deposits exhibits distinct mineralogical zoning related to the intensity of hydrothermal alteration in the upflow and recharge zones of the deposit (Fig. 1-4; Franklin et al., 2005; Galley et al., 2007; Hannington et al., 2014). Proximal alteration underlying the massive sulphide horizon is associated with high temperature mineral assemblages consisting of chlorite-quartz-sulphide ±sericite ± talc and are restricted to the core/upflow zone where fluids are rising and discharging (Zones 1 and 2; Fig. 1-5). Lower temperature alteration assemblages of chlorite-sericite ± phengite are associated with the envelope around the main upflow zone (e.g. Hellyer; Gemmell and Large, 1992; Gemmell and Fulton, 2001). Laterally continuous lower temperature fluids result in the formation of sericite, phengite, chlorite ± albite ± carbonate ± barite (Zones 3-4; Fig. 1-5; Galley et al., 2007). The lateral and spatial distribution of alteration assemblages can be used, if well defined, as vectors toward VMS mineralization (Franklin et al., 2005).

1.5 Geology of the Tulks Volcanic Belt

The Tulks volcanic belt is bounded to the north by the Red Indian Line and the sedimentary and volcaniclastic rocks of the Harbour Round belt, and to the south by the Roebuck's Intrusive Suite, which also separates it from the Long Lake belt (Fig 1-6 and 1-7; Hinchey, 2007, 2011a). The age of the TVB was originally constrained by a single age date of 498 ± 6 Ma from a subvolcanic porphyry located near the Tulks Hill VMS deposit (Hinchey, 2007, 2011a), but recent studies suggest a westward-younging of tectonostratigraphic units that make up the stratigraphy of the belt. These include the Tulks (ca. 498 Ma), the Pats Pond (ca. 487 Ma), the Sutherlands Pond (ca. 462 Ma; Dunning et al., 1987) and the Wigwam Brook groups (ca. 453 Ma; van Staal et al., 2005; Zagorevski et al., 2007). The TVB hosts seven significant zones of base-metal mineralization that are hosted within various stratigraphic elements (Figs. 1-6 and 1-7) these include: Bobbys Pond, Daniels Pond, Jacks Pond, Tulks Hill, Tulks East and the Boomerang-Domino-Hurricane deposits. The Hurricane zone is a satellite lens within the same stratigraphic horizon as the Boomerang deposit, which located in the southern part of the TVB within the Pats Pond group (De Mark and Dearin, 2007; Hinchey, 2011a).

The TVB deposits are further subdivided into southern and northern regions based on lithology (Figs. 1-6 and 1-7) and inferred depositional environment (see below; Fig. 1-8; Hinchey, 2011a). The main deposits in the southern TVB, particularly Boomerang, Tulks Hill and Tulks East, are bimodal-felsic to felsic-siliciclastic deposits. These deposits predominantly consist of felsic volcanic and volcaniclastic rocks, and lesser siliciclastic rocks; minor intermediate-mafic and intrusive rocks are also present. It should be noted that in some circumstances there are locally abundant siliciclastic sedimentary rocks (e.g., black shales, graphitic argillites and felsic to mafic lithic greywackes). The general stratigraphy for the southern TVB includes thick felsic volcaniclastic units intercalated with sedimentary rocks of varying thicknesses. These sedimentary and volcaniclastic rocks display fining-upwards turbiditic sequences, which are locally associated with mineralization (Hinchey, 2007; 2011a). This type of stratigraphic succession is conducive for the genesis of Zn-rich ore, which often forms via subseafloor replacement within the felsic volcaniclastic and sedimentary rocks (see discussion; e.g., Piercey, 2015).

The stratigraphy of the northern part of the TVB is dominated by rhyolite flows and breccias. This suggests a vent-proximal environment and shallow-water conditions (<1500m interpreted water depth) that transition into a deep-water (>1500m water depth), volcano-sedimentary-dominated environment in the southern TVB (Hinchey, 2007, 2011a). The northern TVB deposits, most notably Bobbys Pond and Daniels Pond, are bimodal felsic VMS deposits. However, they also have features similar to bimodal felsic VMS-high sulphidation (hybrid) deposits. The Jacks Pond deposit is interpreted to represent the transition from a deep-water VMS deposits (Boomerang-Domino-Hurricane, Tulks Hill) to the shallow water, vent-proximal, bimodal VMS-epithermal style deposit (Daniels Pond; Hinchey, 2011a). Bimodal volcanic sills occur synchronously with volcanic, volcaniclastic, and sedimentary rocks throughout the entire belt (Hinchey, 2011a). Many of the basaltic sills have amygdaloidal tops with chilled margins along the basal contact. Evidence of active volcanism and synchronous sedimentation indicate an extensional environment, most likely a rifted basin with back-arc affinities (Hinchey, 2011a). Such an environment is supported by previous lithogeochemical studies (e.g., Swinden et al., 1989; Swinden, 1991; Evans and Kean, 2002), which indicate a change in chemical signatures within the belt that suggests a transition from an active arc environment to a non-arc or back-arc rifting environment (extensional regime; Hinchey, 2011a).

1.6 Geology of the Boomerang-Domino-Hurricane Deposit

The Boomerang-Domino-Hurricane deposit cluster consists of three massive sulphide lenses: Boomerang, Domino and Hurricane. Although the focus of this project is on the Hurricane zone, the deposit geology is similar throughout the three lenses and will be discussed as one unit (i.e., the Boomerang deposit). The stratigraphy of the deposit is divided into three segments: hanging wall, mineralized horizon, and footwall.

The hanging wall rocks are comprised of undifferentiated, locally fining upwards, felsic to intermediate volcaniclastic and epiclastic rocks, predominantly quartz ± feldspar tuffs; fine-grained sedimentary rocks, such as black shales, argillite, greywacke, and chert; volcaniclastic conglomerates/breccias; and locally amygdaloidal, bimodal sills (Squires et al., 2005; Hinchey, 2007, 2011a). The fine-grained sedimentary rocks (shales and black argillites) typically cap the felsic tuffaceous rocks (Hinchey, 2011a). Most of the hanging wall has been affected by sericite-quartz-chlorite-carbonate alteration. Sericite, chlorite, and quartz occur as fine-grained laths in the groundmass of the volcaniclastic hanging wall rocks, whereas carbonate alteration occurs either as 0.5-1 mm glomeroporphyrocysts or as euhedral rhombohedral crystals (Hinchey, 2011a). The footwall sequence consists of felsic volcanic rocks, most commonly fine-grained, crystal-bearing tuffs, with base-metal stringer sulphides, local lapilli tuff, fine-grained sedimentary rocks and bimodal sills (Hinchey, 2007; 2011a). The tuffs are highly sericite altered and strongly foliated, locally displaying a crenulation cleavage (Hinchey, 2011a).

The mineralized horizon consists of several lenses in highly-altered felsic aphyric tuff and crystal tuffs, along with fine-grained sedimentary units, all which are intimately associated with massive sulphide mineralization. Sericite is the dominant alteration mineral with lesser chlorite, quartz and carbonate. The sulphides consist of fine- to medium-grained banded to wispy intergrowths of red and yellow sphalerite, chalcopyrite, galena and pyrite (Hinchey, 2011a).

The Boomerang deposit is interpreted to be a subseafloor replacement deposit (Squires, 2006; Hinchey, 2011a). This is evident from locally preserved original bedding within the massive sulphides, relict host rock clasts (i.e. felsic ash, crystal tuffs, quartz crystals) and hydrothermal alteration and stringer sulphides in hanging wall and footwall stratigraphy (Hinchey, 2011a). According to Hinchey (2011a), the fine-grained sedimentary packages that overlay the porous and permeable tuffaceous felsic rocks acted as a potential barrier that inhibited fluid migration and aided in the entrapment and replacement of the host rocks, thus enabling the precipitation of sulphides in the mineralized horizon.

1.7 Objectives

Since Messina's discovery of the Boomerang-Domino-Hurricane cluster of deposits between 2004 to 2006, the majority of the exploration efforts have been focused on delineating the Boomerang deposit with little research conducted on characterizing the architecture and genesis of the Hurricane zone. The Hurricane zone provides an excellent natural laboratory to study replacement-style mineralization and the controls on the associated alteration assemblages in a volcaniclastic rock dominated VMS deposit. This project will provide an in-depth study of the stratigraphy, the nature and distribution of alteration assemblages and the lithogeochemistry of the Hurricane zone in order to reconstruct its volcanic and hydrothermal architecture. The main objectives are as follows:

- build upon the stratigraphic framework proposed by Squires et al. (2005) and Hinchey (2007, 2011a) and evaluate the volcanic, plutonic, sedimentary, and alteration facies and mineralized horizons through core logging, stratigraphic sections and cross sections;

- characterize representative lithologies of the main stratigraphic units by core logging, petrography and lithogeochemistry;
- characterize alteration assemblages by petrography, lithogeochemistry and short-wave infrared (SWIR) spectroscopy. Specific attention will be placed on compositional and textural variations in micas, chlorite, silica and carbonates within the different alteration assemblages. This will in turn help to delineate and better understand the genesis of the alteration mineralogy;
- develop a chemostratigraphic framework for the deposit using lithogeochemistry. Mass balance calculations will be used to quantify elemental gains or losses associated with individual alteration assemblages;
- combine the lithostratigraphy and chemostratigraphy of the Hurricane zone to characterize the geodynamic environment, the nature of volcanism, and the genesis of mineralization; and
- combine primary geochemistry and stratigraphy to understand the tectonic setting of the deposit formation and the genesis of the volcanic host rocks within the Appalachians.

Overall, the results of this project will provide insight on ore-forming processes occurring by subseafloor replacement in volcaniclastic rock dominated domains. The project will also provide information on the controls on the associated alteration processes. The data should serve as an analogue for similar replacement-style deposits within the Appalachian orogenic belt and deposits worldwide.

1.8 Methodology

1.8.1 Drill Core logging and Sampling

Two and a half months of detailed core logging, lithogeochemical and petrographic sampling were completed in the Fall 2014 and Summer of 2015 using the Canadian Zinc Corporation exploration office in Buchans Junction, Newfoundland. In total, 22 of the 27 drill holes completed in the Hurricane zone were selected for logging based on the reconstruction of the stratigraphy and alteration of the deposit carried out by Canadian Zinc Corporation and Messina Minerals Inc.. Drill holes were selected to: a) provide the best representation of the stratigraphy within the entire study area; and b) to study the proximal and distal relationships of the alteration associated with the VMS mineralization. The company provided drill logs, a plan view map, and a long and cross sections that indicated holes that had anomalous base metal and precious metal, holes that had massive pyrite and holes that lacked anomalous base metals; these were also used in picking drill holes to log. A total of 445 samples were collected for alteration and lithological references. One hundred and forty-seven subsamples were selected for geochemical and petrographic analyses. These samples were selected to: a) provide representative geochemical signatures for each lithofacies and to aid in chemostratigraphic/lithological correlation between sections; and to b) provide geochemical signatures to characterize alteration assemblages and to determine elemental mass gains and losses for the various assemblages.

1.8.2 Major and Trace Lithogeochemistry

Samples were collected roughly every 20-25 m based on major lithological or alteration changes; sample lengths ranged from 20-30 cm. Samples that displayed characteristic hydrothermal alteration (e.g. sericite alteration, chlorite alteration and quartz alteration) were of primary interest. Alteration related to secondary hydrothermal overprinting or regional metamorphism were not sampled. One hundred and forty-seven core samples were collected from 22 drill holes for major and trace element analyses. Representative samples were cut in half and washed to avoid cross contamination before being individually bagged and sent to ActLabs in Ancaster, Ontario for analysis. The other half remained at Memorial University and were used as reference samples and for shortwave infrared spectral analysis.

Lithogeochemical samples were crushed and pulverized prior to analysis using mild steel at Actlabs. Samples were analyzed using lithium metaborate/tetraborate fusion, the resultant molten bead was rapidly digested in a weak nitric acid. Fusion ensures that the entire sample was digested. The digested sampled was then analyzed using inductively coupled plasma emission spectroscopy (ICP-ES). Mercury analysis was also undertaken at ActLabs using cold vapour flow injection mercury spectrometer (CV-FIMS) following digestion of the samples with aqua regia to leach out soluble compounds.

1.8.3 Petrography

Thirty-three samples were sent to Vancouver Petrographics in Winter 2014 and 2015 for polished thin sections (30 microns). The samples were chosen based on major lithofacies, textures and alteration assemblages (i.e., representative of host rock variability and alteration). Petrography involved utilization of both transmitted and reflected light microscopy.

1.8.4 Short Wave Infrared (SWIR) Spectroscopy

Short wave infrared (SWIR) spectrometry was used to map mineralogical variations in drill core samples and determine compositional variations in micas, chlorite and carbonate throughout the deposit. Spectral results from this study only proved to be effective for white micas. This data helped to define alteration assemblages associated with hydrothermal fluid alteration pathways and potentially allow targeting new prospects in the vicinity. Data points were collected approximately every 5 m to capture the spectral variation down hole. Every 20 samples, a duplicate point was taken and two reference materials (pyrophyllite and chlorite) were taken. A TerraSpec^{TM} 2 instrument was used and following the methodology of Buschette and Piercey (2015).

1.9 Thesis Presentation

This research project was designed by Dr. Stephen J. Piercey. The author conducted the primary research, which included core logging, sample collection, geochemical and hyperspectral analysis. The primary editor of this manuscript was Dr. Stephen J. Piercey with secondary editing by Dr. Luke Beranek.

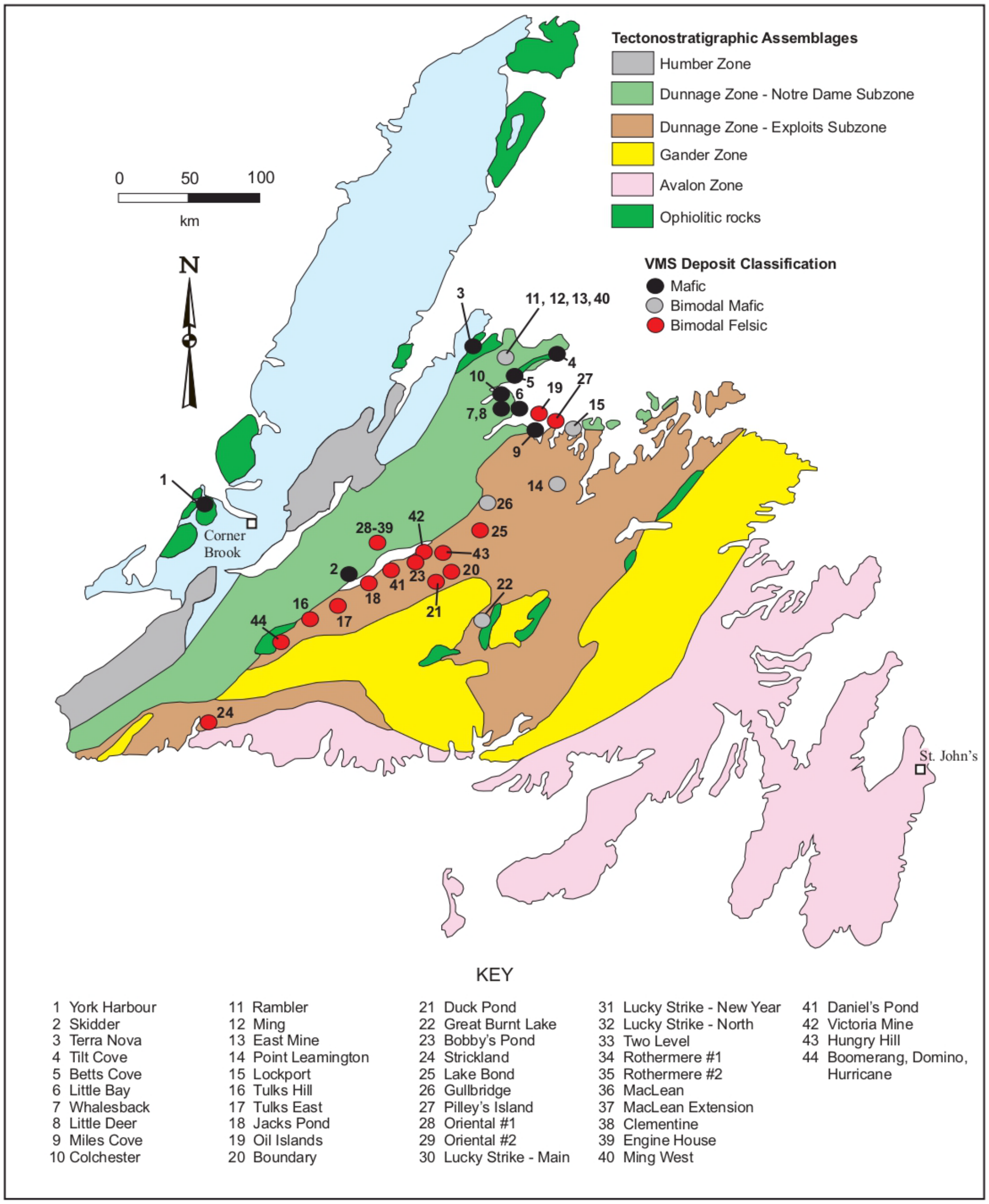

Figure 1-1. Simplified tectonostratigraphic map of Newfoundland Appalachians with peri-Laurentian (Notre Dame) and peri-Gondwana (Exploits) subzones based on Williams et al. (1988). VMS deposits classification based on lithotectonic settings after Barrie and Hanngington (1999) and Franklin et al. (2005) (modified from Piercey, 2007).

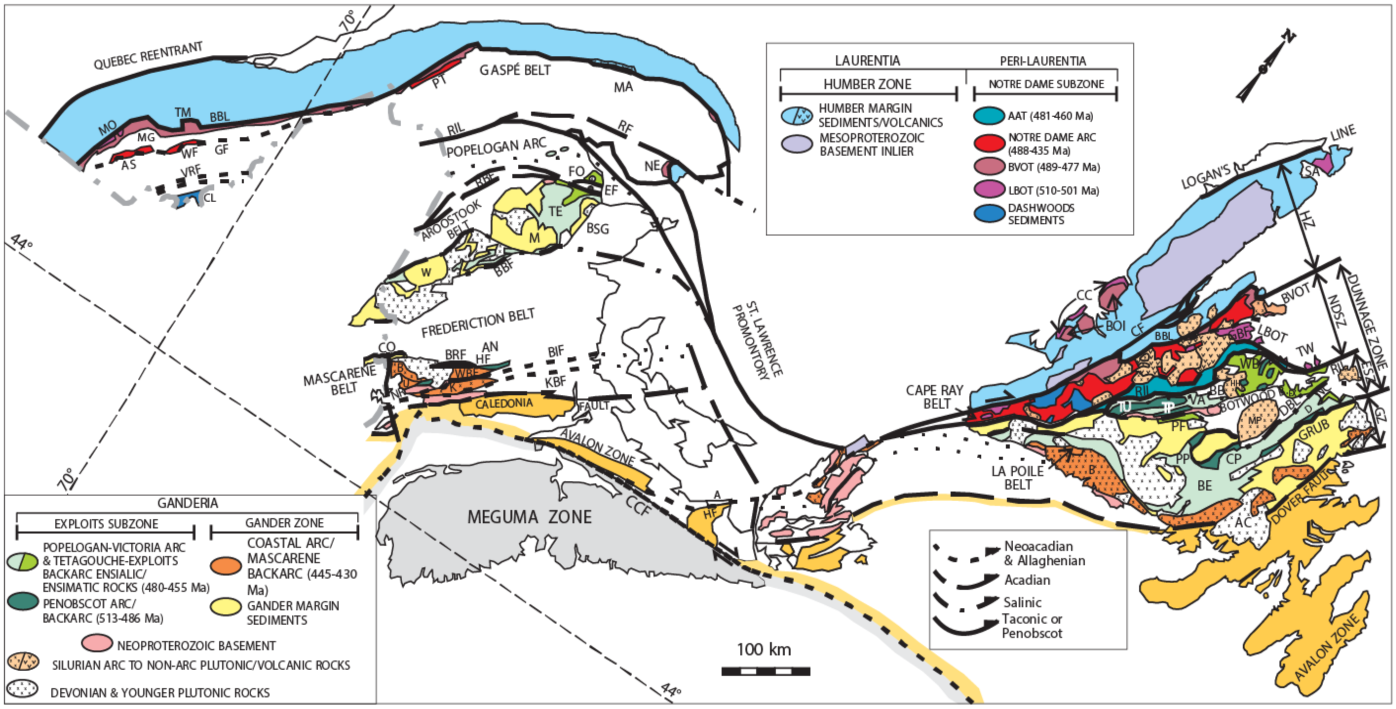

Figure 1-2. Detailed tectonostratigraphic map of the Canadian Appalachians (after van Staal, 2007) with distributions of Early Paleozoic tectonostratigraphic zones, subzones and other major tectonic elements (in color). Thick lines to the west of the Notre Dame Subzone represents the Red Indian Line (RIL).

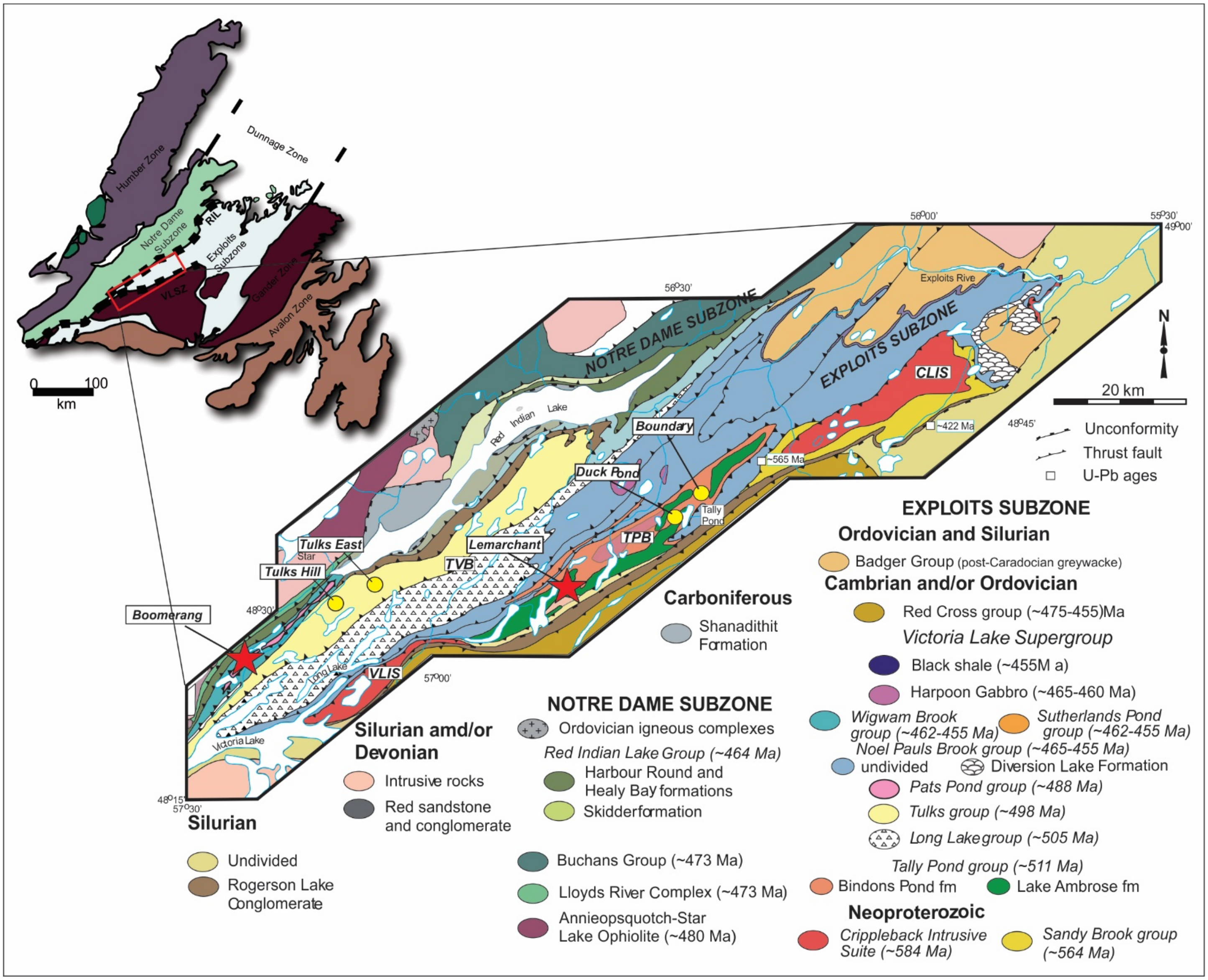

Figure 1-3. Location and geology of the area surrounding the Red Indian Lake, including the Victoria Lake Supergroup (VLSG). Relevant deposits indicated in northern and southern parts of the VLSG. TVB- Tulks volcanic belt, VLIS- Valentine Lake intrusive suite, TPB- Tally Pond belt, CLIS- Crippleback Lake intrusive suite (modified from Rogers et al., 2006).

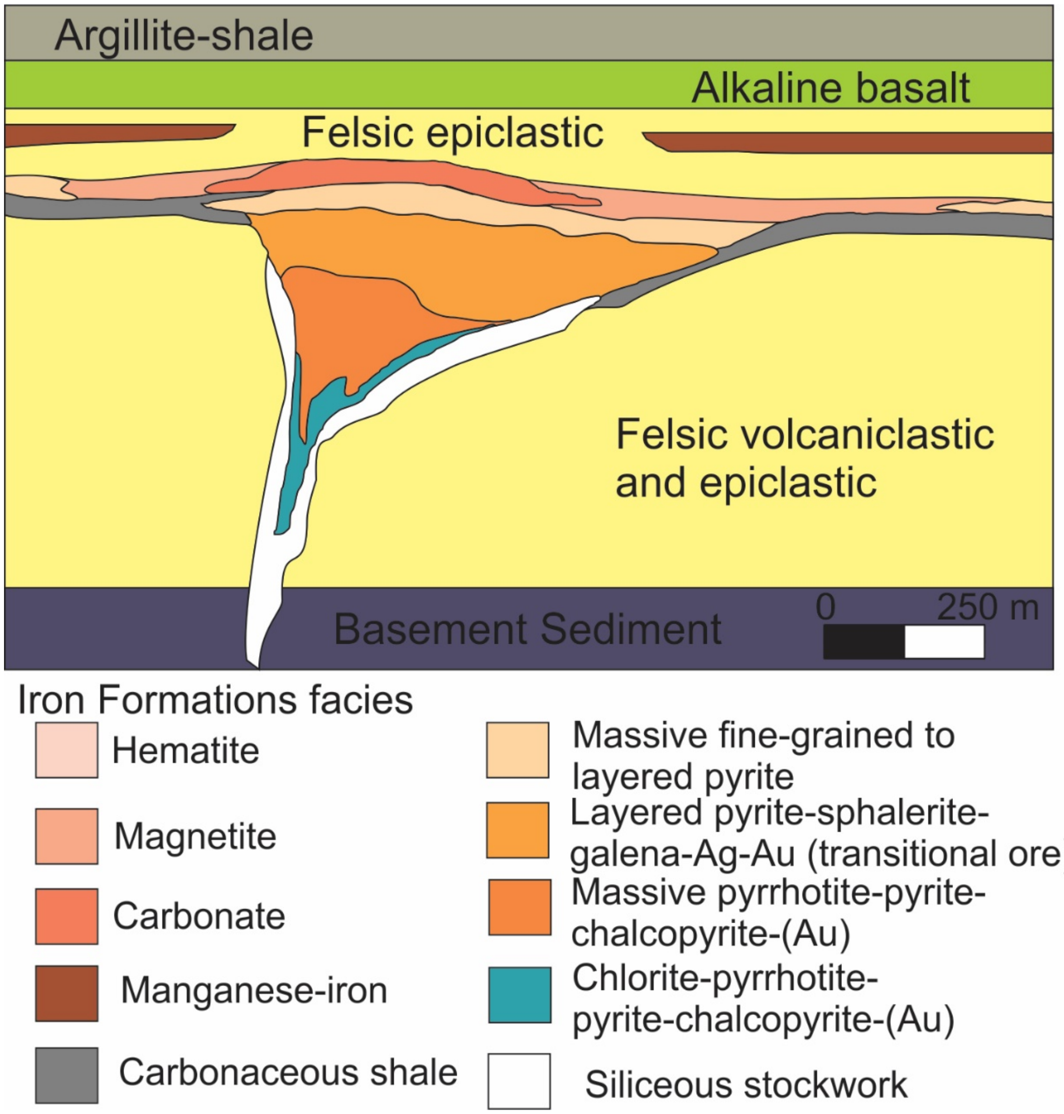

Figure 1-4. Idealized cross-section of felsic-siliciclastic volcanic massive sulphide deposit (modified from Galley et al., 2007).

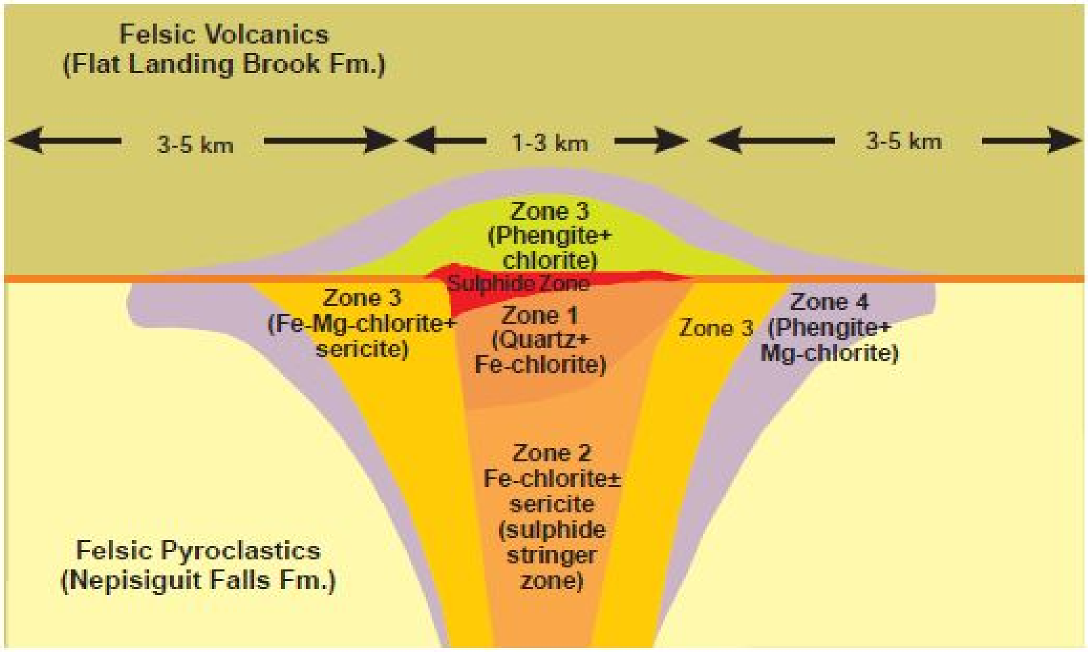

Figure 1-5. Cross section of idealized hydrothermal alteration assemblages from bimodal-felsic VMS deposit (from Galley et al., 2007).

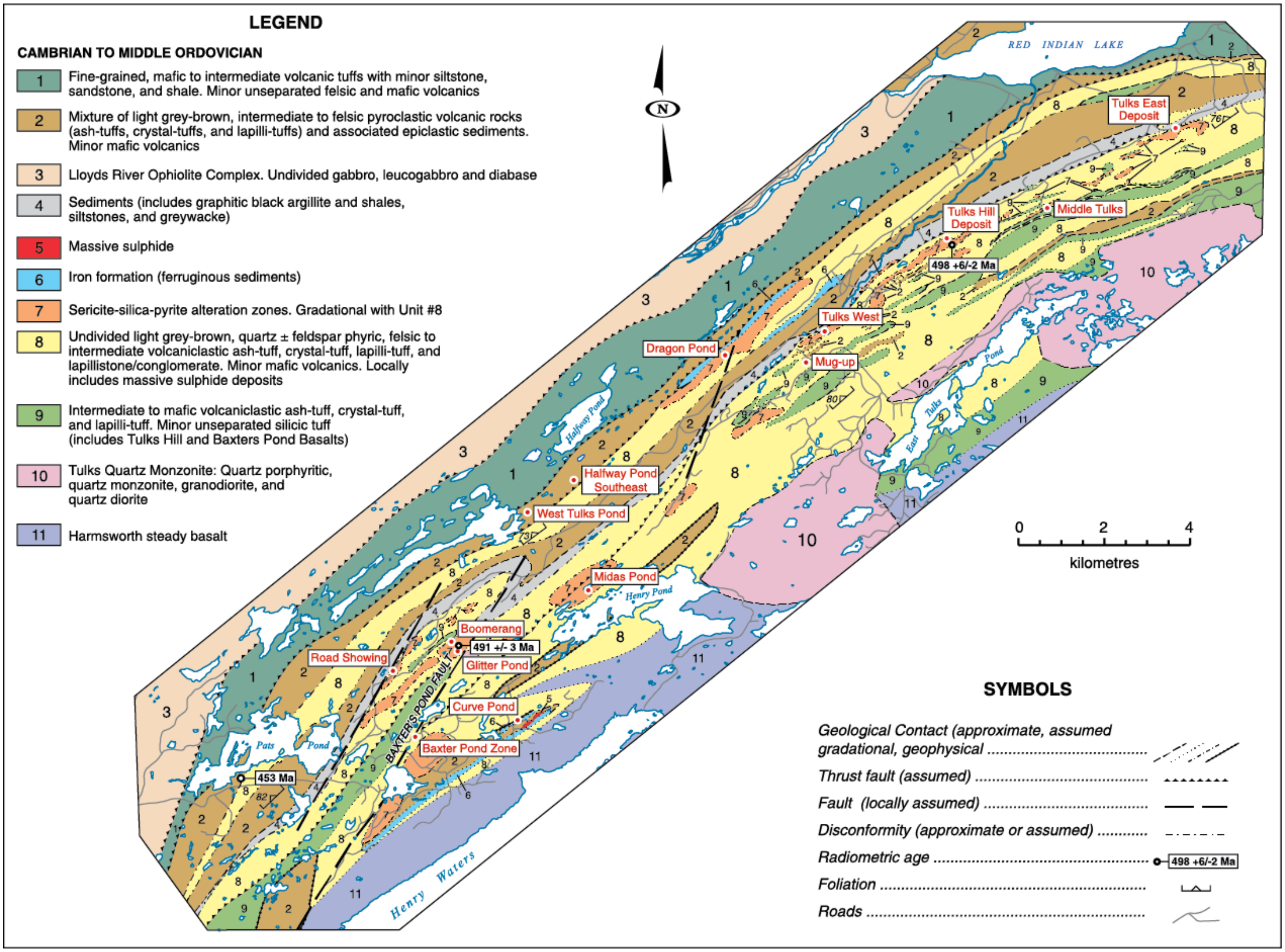

Figure 1-6. Geological map of the southern Tulks volcanic belt illustrating the various rock types with known base-metal and precious metal VMS deposits and prospects indicated (from Hinchey, 2011a).

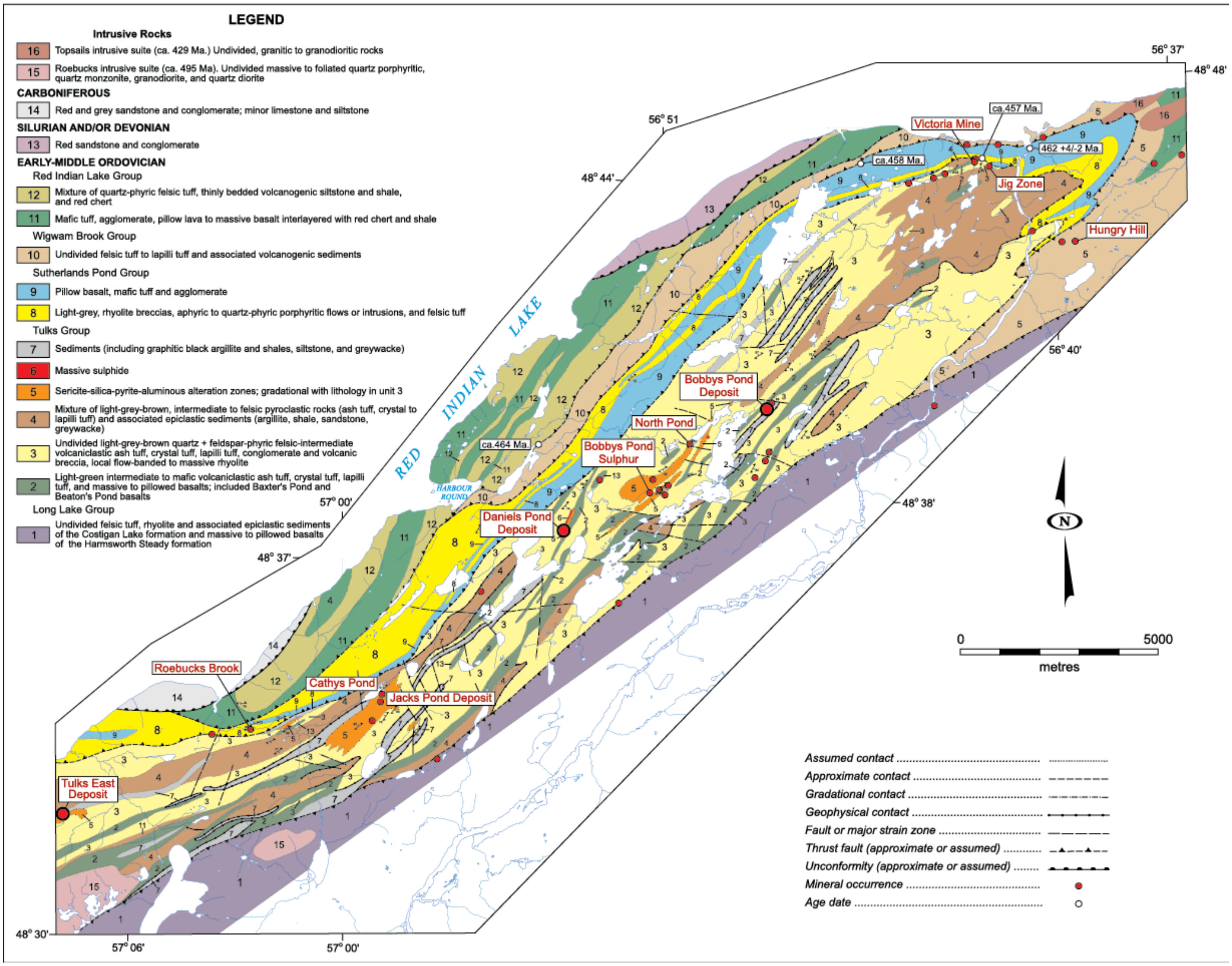

Figure 1-7. Geological map of the northern Tulks Volcanic Belt with known base-metal and precious metal VMS deposits indicated (from Hinchey, 2011a).

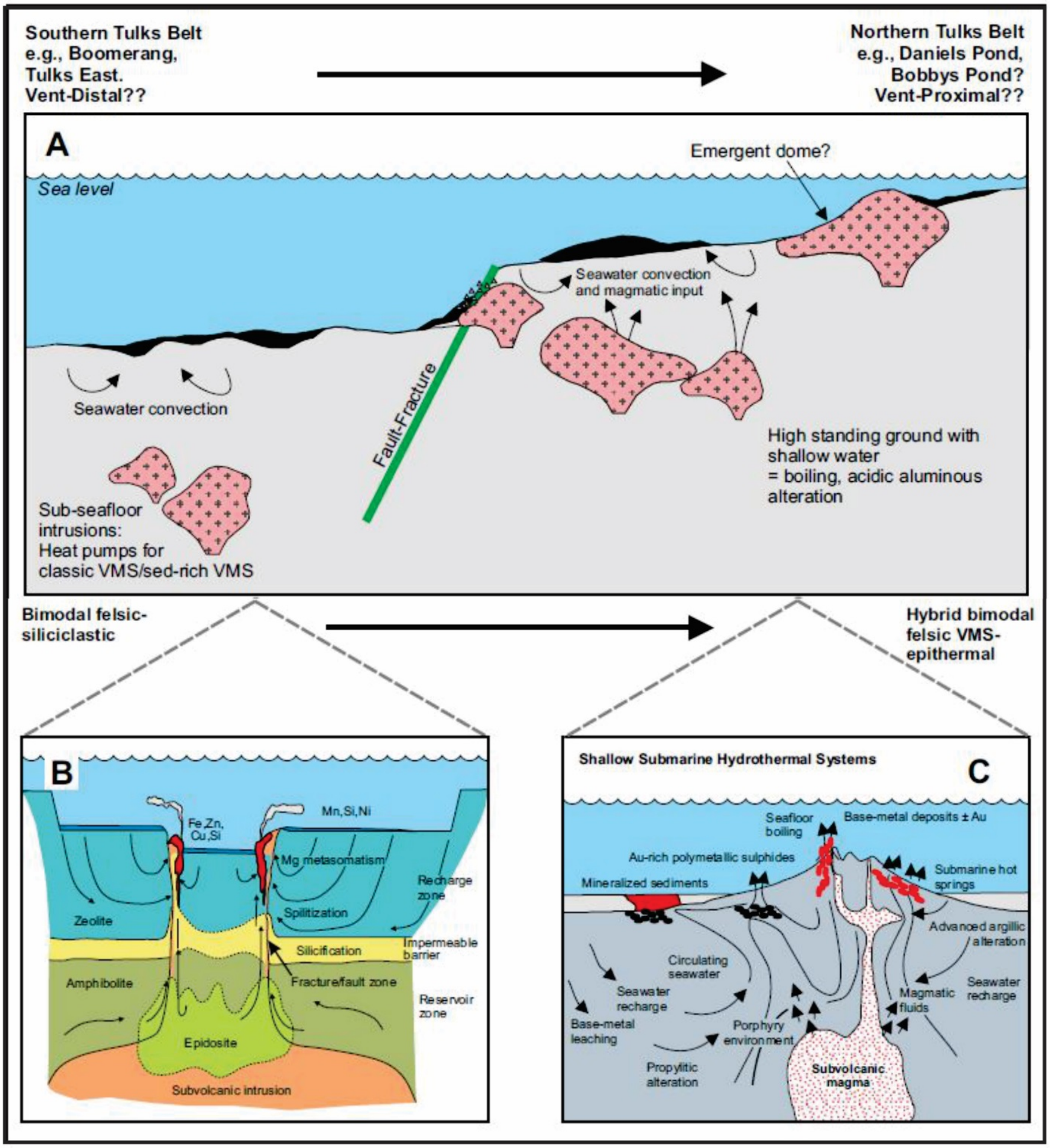

Figure 1-8. (A) Schematic model illustrating the two types environments VMS deposits form in the TVB (from Hinchey, 2011a). (B) Diagram of conventional model for VMS deposits in deep water (from Galley et al., 2007); (C) model for formation of shallow water VMS deposits TVB.

2. Lithofacies and Alteration of the Hurricane Zone, of the Boomerang volcanogenic massive sulphide deposit, Tulks Belt, Central Newfoundland, Canada

2.1 Abstract

The Hurricane zone of the Boomerang volcanogenic massive sulphide (VMS) deposit is part of the Cambro-Ordovician Tulks volcanic belt, in central Newfoundland. The Hurricane zone is one of three lenses in the deposit and consists of a sub-horizontal (semi-)massive sulphide lens, with combined resources of 55,100 tonnes @ 13.4% Zn, 7.0% Pb, 1.20% Cu, 159.0 g/t Ag, and 2.00 g/t Au. Mineralization is hosted in intermediate to felsic volcaniclastic rocks of the ca. 488 Ma Pats Pond group (Victoria Lake supergroup). The Hurricane zone consists of three distinct stratigraphic packages: the (1) hanging wall; (2) mineralized zone; and (3) footwall. The footwall consists of felsic to intermediate intercalated quartz-bearing crystal tuff and lapilli tuff. The hanging wall consists of felsic to intermediate volcaniclastic rocks, including aphyric to quartz/plagioclase-bearing tuff, lapilli tuff and breccias, locally intercalated and interbedded with sedimentary rocks. Two generations of mafic dykes and sills intrude the entire stratigraphic package. The mineralized zone occurs between the footwall-hanging wall interface and consists of (semi-)massive sulphide with fine- to medium-grained bands of red and yellow sphalerite, pyrite and galena with coarse blebs of chalcopyrite. The footwall rocks contain four dominant alteration assemblages, including: intense chlorite, chlorite-carbonate, sericite-quartz-chlorite ±pyrite, and intense sericite. Both the hanging wall and footwall have strong Na_2O depletions, enrichments in K_2O-Fe_2O_3-SiO_2-MgO-Ba, high alteration index values (chlorite-carbonate-pyrite index (CCPI), alteration index (AI), Ba/Sr), and enrichments in base (e.g., Zn, Pb, Cu) and volatile metals (e.g., Hg). Short-wave infrared spectral analyses conducted on white micas show systematic changes in AlOH wavelength with proximity to the mineralized horizon, with the hanging wall micas having phengitic compositions (> 2210 nm), whereas proximal to the hanging wall-footwall contact the mica species is paragonitic (<2195 nm).

The majority of the mineralization in the Hurricane zone shows evidence to have formed below the seafloor. This is indicated by relict quartz crystals and lapilli fragments in the bedded sulphides, rapidly emplaced volcaniclastic rocks, replacements fronts in the host lithofacies, and hydrothermal alteration in the lower hanging wall. The deposit likely formed as hot metal-laden fluids ascended towards the seafloor, percolating through permeable semi-consolidated volcaniclastic material and mixing with ambient seawater entrained in pore space until it reached an semi-impermeable mud boundary. The impermeable boundary played a crucial role in promoting subseafloor replacement, and in part may be a factor in the high Zn grades in the deposit.

Immobile element systematics of felsic to intermediate rocks within the entire stratigraphic package have subalkaline, tholeiitic to calc-alkaline ($2 \leq Zr/Y \leq 25$) affinities, and are characterized by slightly enriched LREE, flat HREE, and negative anomalies in Nb, Eu, and Ti on primitive normalized plots. The Hurricane zone is interpreted to represent a subseafloor replacement-style VMS lens that formed in a back-arc rift basin, adjacent to a volcanic arc, allowing synchronous deposition of volcanogenic sediments concurrent with hydrothermal activity. This study is a contribution to the understanding of replacement-style VMS mineralization environments rich in volcaniclastic rocks.

2.2 Introduction

Volcanogenic massive sulphide (VMS) deposits are an important source for base and precious metal mineralization both globally (Lydon, 1984; Ohmoto, 1996; Franklin et al., 2005; Hannington, 2014) and in the Newfoundland Appalachians (e.g., Piercey and Hinchey, 2012). These deposits form in some cases by exhalation on the seafloor (e.g., Lydon, 1988) and in other cases form by subseafloor replacement of permeable strata below the seafloor (Doyle and Huston, 1999; Doyle and Allan, 2003; Piercey, 2015). In the Newfoundland Appalachians there are numerous VMS deposits of varying styles and with varying formation mechanisms (e.g., Swinden et al., 1989; Hinchey, 2011a; Piercey et al., 2014), and is a natural laboratory for studying VMS deposits given this diversity of styles and types of deposits.

The Victoria Lake supergroup in central Newfoundland contains numerous deposits including past-producing (e.g., Duck Pond and Boundary) as well as deposits with advanced prospects with confirmed resources (e.g., Boomerang). The Tulks volcanic belt within the Victoria Lake supergroup hosts numerous deposits with varying styles (e.g., Hinchey, 2011a); however, the Boomerang deposit (and its associated lenses – Boomerang, Domino, and Hurricane) represent a type example of an Appalachian sediment- and volcaniclastic-hosted VMS deposit. Since the deposits discovery in 2004, the majority of exploration has been focused on delineating the Boomerang and Domino zones, with little research conducted on characterizing the architecture and genesis of the associated Hurricane zone. Although the area has experienced moderate deformation, the Hurricane stratigraphic sequence is largely intact, making it an ideal area to study VMS mineralization and the controls on associated alteration assemblages within a volcano-sedimentary-hosted VMS deposit. The objective of this paper is to build upon the previous stratigraphic framework of the Boomerang deposit (e.g., Squires et al., 2005; Hinchey 2007; 2011a) and expand it to include a detailed description of the lithofacies, hydrothermal alteration, and primary and secondary geochemical characteristics of host rocks to the Hurricane zone. This paper will thus: (1) document the stratigraphy, lithofacies, and alteration of the deposit; (2) use immobile element geochemistry to understand the chemostratigraphy and tectonic setting of the deposit; (3) characterize the alteration assemblages using petrography, lithogeochemistry and short-wave infrared spectroscopy (SWIR); and (4) combine the lithostratigraphy and chemostratigraphy to reconstruct the volcano-sedimentary history of the deposit, and the related VMS mineralization and alteration. Overall, the results from this project will provide insight to VMS-forming processes and controls associated with alteration occurring in volcaniclastic-rich basins and outline proximal and distal vectors to help explore for this style deposit within the Canadian Appalachians and worldwide.

2.3 Regional Geology and Metallogenic Framework

In Newfoundland, the Canadian Appalachians are divided into four tectonostratigraphic zones: the Humber, Dunnage, Gander and Avalon zones (Fig. 2-1; Williams, 1979; Williams et al., 1988; Van Staal, 2007; van Staal and Barr, 2012). The Hurricane zone is located within the Dunnage zone, which represents vestiges of Cambrian-Ordovician continental and intra-oceanic arcs, back-arcs and ophiolites that formed along the margins of Laurentia (Notre Dame subzone) and Gondwana (Exploits subzone), within the Iapetus ocean (Kean et al., 1981; Swinden, 1990; Williams, 1995; Zagorevski et al., 2006; van Staal, 2007; van Staal and Barr, 2012). The Notre Dame subzone was accreted to the Laurentian margin as a result of the initial closure of the Iapetus ocean during the Taconic orogeny (475-459 Ma; van Staal, 2007; van Staal and Barr, 2012), whereas the Exploits subzone was accreted to the Gondwana during the Penobscot orogeny (486-478 Ma; van Staal, 2007; Zagorevski et al., 2007, 2010). The two subzones were juxtaposed to each other during the final stages of the Taconic orogeny in the late Ordovician (455-450 Ma;), resulting in their juxtaposition along the Red Indian Line (RIL; van Staal, 2007; Zagorevski et al., 2007, 2010; van Staal and Barr, 2012).

The Hurricane zone is located southeast of the RIL in the Victoria Lake supergroup (VLSG), part of the Exploits subzone. The VLSG contains Neoproterozoic to Silurian volcanic and sedimentary rocks that was originally divided into two informal belts: the Tally Pond and Tulks volcanic belts (TPB and TVB, respectively; Kean and Jayasinghe, 1980; Kean et al., 1981; Evans and Kean, 2002; Rogers et al., 2006). Further lithological, geochronological and geochemical studies resulted in the subdivision of the VLSG into six fault-bounded packages (Fig. 2-1). With a general westward younging direction these groups include: the Tally Pond Group (~513-509 Ma; Dunning et al., 1991; McNicoll et al., 2010); the Long Lake Group (~514-506 Ma; Zagorevski et al., 2007; Hinchey and McNicoll, 2016); the Tulks Group (~498-487 Ma; Evans et al., 1990; Evans and Kean, 2002); the Sutherlands Pond Group (~462 Ma; Dunning et al., 1987); and the Pats Pond and Wigwam Brook groups (~488 and ~453 Ma, respectively; Zagorevski et al, 2007). Volcanogenic massive sulphide deposits are present in Tally Pond belt, the Long Lake belt and the informally defined Tulks volcanic belt, which comprises the Tulks, Pats Pond, the Sutherlands Pond, and the Wigwam Brook groups (Hinchey, 2007, 2011a).

2.4 Local and Deposit Geology

The Tulks volcanic belt (TVB) is a northeast-southwest trending bimodal belt dominated by felsic volcanic rocks with varying amounts of mafic volcanic, and mafic and felsic volcaniclastic rocks, which are all intruded by mafic and felsic intrusive rocks (Fig. 2-2; Hinchey, 2007; 2011a). The stratigraphy of the belt strikes northeast and dips steeply to the northwest and is transected by shear zones and faults (Hinchey and McNicoll, 2009). The TVB has undergone lower to middle greenschist facies metamorphism and shows moderate to strong deformation. Many primary textures are obliterated due to deformation and display well developed, bedding parallel regional foliations defined by the alignment of sericite and chlorite (Hinchey, 2007, 2011a). Despite this deformation, local low strain windows preserve primary lithostratigraphy, volcanic and sedimentary facies, and primary VMS-related hydrothermal alteration assemblages.

There are five VMS deposit clusters in the TVB, as well as numerous prospects and areas of alteration. The deposits are associated with sericite, quartz and pyrite with lesser chlorite and carbonate alteration, and formed by both exhalation on the seafloor and subseafloor replacement (e.g., Hinchey, 2007, 2011a). The environment these formed in trend from north to south from shallow water (<1500m water depth), vent proximal areas that display exhalative mineralization styles (e.g., Bobbys Pond and

Daniels Pond) to deeper (>1500m water depth), and distal replacement-style mineralization (e.g., Tulks East, Tulks Hill and Boomerang; Fig. 2-2; Hinchey, 2011a).

2.4.1 Deposit Geology

The Boomerang deposit is located in the southern tip of the TVB, 17 km southwest of the Red Indian Lake (Fig. 2-1). The Hurricane zone is one of three lenses within the Boomerang deposit, which also contains the Boomerang and Domino lenses. The Hurricane lens lies along strike and within the same stratigraphic panel as the Boomerang lens, whereas Domino lies down dip and stratigraphically below the other lenses. (Fig. 2-3). The Hurricane lens has a strike length of 250 m and a thickness of 15.3 m with a non-compliant 43-101 resources of 55,100t @ 13.4% Zn, 7% Pb, 1.2% Cu, 159g/t Ag, and 2g/t Au (Alexandra Marcotte, personal communication, 2015). Stratigraphically, the footwall of the lens is dominated by altered felsic to intermediate volcanic and sedimentary rocks, including quartz and feldspar crystal tuffs, lapilli tuffs, and lesser massive flows, siltstones, and shales (Figs. 2-3 to 2-8; Hinchey, 2011a). The mineralization occurs within the crystal and lapilli tuffs where the sulphides contain abundant fragments of host rocks, including relict quartz crystal and altered lapilli fragments. A similar volcaniclastic lithofacies overlies the footwall unit, but the package contains thin chert layers and no shale units. The latter package is further overlain by undifferentiated normally graded volcaniclastic and sedimentary rocks, crystal tuffs and massive aphyric to plagioclase-quartz phyric felsic flows. The entire stratigraphy is locally intruded by narrow, altered intermediate and mafic sills (Figs. 2-7 to 2-8).

2.5 Stratigraphy and Lithofacies

The stratigraphy, lithofacies, alteration and mineralization of the Hurricane zone were documented by logging drill core and creating graphic logs and stratigraphic sections.

2.5.1 General stratigraphy

The Hurricane zone stratigraphy can be divided into three distinct stratigraphic packages: (1) the hanging wall; (2) mineralized zone; and (3) footwall. Each of these packages has distinct lithological and geochemical lithofacies, which are described below.

2.5.2 Lithofacies

The Hurricane zone consists of five main lithofacies, including the massive sulphide horizon, all which are intruded by at least three generations of geochemically distinct intermediate and mafic dykes and sills. The lithofacies and their relationships are illustrated with representative photographs and photomicrographs in Figures 2-4 to 2-8 and in stratigraphic sections and drill core logs in Figures 2-9 to 2-11. The volcaniclastic lithofacies within the Hurricane zone are classified using the updated classification of Fisher (1966) by White and Houghton (2006). The updated classification focuses on naming volcaniclastic rocks based on their clast size, abundance and depositional process, rather than mode of fragmentation (i.e., descriptive and not process-oriented classification; White and Houghton, 2006). The basic rock type classification of the lithofacies is undertaken using the immobile element Zr/TiO_2-Nb/Y diagram of Pearce (1996; modified from Winchester and Floyd, 1976; Fig. 2-12a). Further details on the geochemistry of the lithofacies and analytical methods will be outlined in section 2.6.

2.5.2.1 Volcaniclastic lithofacies 1 (VCL1): intermediate lithic, crystal tuff to lapilli tuff. Volcaniclastic lithofacies 1 is found at the lowest part of the stratigraphy in the Hurricane zone and encompasses the entire footwall (Fig. 2.9). It falls within the andesite field on the Pearce (1996) diagram (Fig. 2-12a) and consists of normally graded crystal-lithic lapilli tuffs to crystal tuffs that are locally capped with silt and mudstone beds. Volcaniclastic lithofacies 1 is the host rock sequence to the massive sulphides, and the volcaniclastic rocks immediately underlying the massive sulphide have the highest degree of alteration, which often makes it difficult to discern primary volcanic/volcaniclastic features and textures. The semi-massive to massive sulphides progressively grade into or completely replace VCL1. The alteration in this unit ranges from moderate to strong sericite-quartz-pyrite-(±chlorite) alteration to localized areas of strong chlorite-carbonate alteration, particularly near massive sulphide mineralization. Fine-grained sericite, quartz, and lesser chlorite replaces the matrix of the lapilli and crystal tuffs and locally alter the lapilli fragments (Fig. 2-4a and Fig. 2-6a). Alteration assemblages and distribution are discussed further below.

2.5.2.2 Volcaniclastic lithofacies 2 (VCL2): felsic to intermediate lithic, crystal lapilli tuff to tuff.

Volcaniclastic lithofacies 2 falls within the rhyodacite/ rhyolite field on the Pearce (1996) diagram (Fig. 2-12a) and consists of volcaniclastic rocks dominated by lithic-crystal lapilli tuff to tuff with lesser silt and chert layers. This unit lies stratigraphically above VCL1 and is the lowest stratigraphic unit in the hanging wall (Fig. 2.9). This unit is similar to volcaniclastic lithofacies 3 (VCL3) and VCL1, with the exception that the clasts are monomictic, it contains chert layers, and lacks mudstone. The lapilli tuffs are light grey and contain rounded, elongated monomitic felsic clasts with 1-5 mm plagioclase, K-feldspar and quartz crystals that are hosted in a fine-grained matrix consisting predominantly of quartz and plagioclase (Fig. 2-4b and Fig. 2-6b); thin, 1-5 cm chlorite laths are abundant in VCL2 (Fig 2-6b). The tuffaceous layers are fine-grained with 10-25%, 1-5 mm subangular to rounded plagioclase crystals with lesser quartz and K-feldspar crystals and felsic lithic fragments. The lapilli tuff and tuff fine upwards into thinly laminated interbeds of very fine-grained tuff and chert. Chert is more dominant in the lower half of the stratigraphy and is commonly associated with thin bands of pyrite (Fig. 2-4b). The lapilli tuff and tuff display weak to moderate sericite, quartz and patchy chlorite alteration with local pyrite veins and/or clasts (Fig. 2-6b).

2.5.2.3 Volcaniclastic lithofacies 3 (VCL3): normally graded, heterolithic lapilli tuff to tuff.

Volcaniclastic lithofacies 3 ranges from andesite/basalt to the rhyolite/dacite fields on the Pearce (1996) diagram (Fig. 2-12a) and consists of a sequence of normally graded, heterolithic, lapilli tuffs (30-50%) and tuff (30-50%) with local thinly bedded mudstones (10%). Volcaniclastic lithofacies 3 lies between volcaniclastic lithofacies two and four (Fig. 2-9). The lapilli tuffs are light to medium grey in color and contain >50% subangular to subrounded, elongated heterolithic clasts. Clast composition ranges from felsic to intermediate with lesser mafic, chert, and mudstone rip up clasts, and plagioclase and quartz crystals (Fig. 2-4c and 2-4d). The matrix consists of fine-grained intermediate to felsic volcaniclastic rocks with <15% thin shards of chlorite and wispy sericite that are parallel to foliation (Fig. 2-6c and Fig. 2-6d). Rare block-sized fragments occur within the SW side of the Hurricane zone and consist of chlorite rimmed amygdaloidal basalt and altered intermediate volcanic rocks (Fig. 2-4c). The tuff is medium grey in color and consists of 65% matrix with small (1-2 mm) elongated felsic to intermediate clasts and lesser sub-rounded, 0.2-5 mm plagioclase and quartz crystals (Fig. 2-6c and Fig. 2-6d). This unit forms a repetitive, normally graded sequence from lapilli tuff to tuff with 1-10 cm thick units of thinly bedded silt and mudstones (Fig. 2-4d).

2.5.2.4 Volcaniclastic lithofacies 4 (VCL4): crystal-bearing felsic to intermediate tuff. Volcaniclastic lithofacies 4 consists of two crystal-rich end-members: a plagioclase-rich end member, which has a gradational relationship with the overlying quartz-rich end member (Fig. 2-4e and Fig. 2-4f). Volcaniclastic lithofacies 4 sits between volcaniclastic lithofacies three and five (Fig 2-9). They have signatures that range from basaltic-andesite to andesitic on the Pearce (1996) diagram (Fig. 2-12a), but the plagioclase dominated tuffs are more mafic in composition, whereas the quartz-rich tuffs are more intermediate in composition. Plagioclase- and quartz-bearing crystal tuffs are dark grey to blue-grey in color with 1-15 mm sized white to grey, glassy plagioclase and quartz crystals hosted in a fine-grained quartz and plagioclase matrix (Fig. 2-6e). Crystal content ranges from 5 to 20%, with localized areas of up to 40% to areas barren of crystals. The crystal content increases downhole with crystal-poor and -rich repetitive intervals occurring on the cm- to m-scale. The plagioclase-dominated intervals typically display weak to moderate chlorite alteration (Fig. 2-4e), whereas the quartz-dominated intervals are typically more sericite-quartz altered (Fig. 2-4f).

2.5.2.5 Coherent volcanic lithofacies 1a (CL1a): plagioclase and/or quartz phyric rhyolite flow. Coherent volcanic lithofacies 1 consists of two end members: aphyric rhyolitic flows and plagioclase-quartz phyric rhyolitic flows and breccias; all units are rhyolite/dacite (Fig. 2-12a). Coherent volcanic lithofacies 1a lies within the uppermost part of the stratigraphy at the top of the hanging wall sequence (Fig. 2-9). Coherent volcanic lithofacies 1a consists of a weakly to moderately foliated, plagioclase-quartz-K-feldspar phyric flows that are pale grey to beige in color with 10% to 25%, 1 to 8 mm plagioclase, quartz and lesser K-feldspar phenocrysts in a very fine-grained, siliceous matrix (Fig. 2-4g and Fig. 2-6f). Locally, towards their lower margins the massive flows are brecciated and grade into jigsaw-fit breccia with interstitial sericite and chlorite in the matrix. Typically, lower contacts are gradational with the underlying tuffaceous unit of VCL4 or in sharp, abrupt contacts with cross cutting mafic dykes. The matrix within the brecciated zones along the margins is typically infilled with sericite and lesser chlorite in thin wispy bands.

2.5.2.6 Coherent volcanic lithofacies 1b (CL1b) - massive aphyric rhyolite flow. Coherent volcanic lithofacies 1b is a relatively uncommon and thin unit and occurs in the uppermost part of the stratigraphic sequence. This unit is pale grey to pale pink in color, very fine-grained and siliceous with rare (1-3%) quartz-plagioclase phenocrysts (Fig. 2-4h and Fig. 2-6g). Locally it exhibits brecciation along margins with chlorite or sericite preferentially infilling the matrix. Typically, contacts are gradational with plagioclase-quartz phyric rhyolitic flows (CL1a), but locally are sharp and abrupt with cross-cutting mafic dykes. The unit is massive, with little to no foliations and displays strong quartz alteration, with lesser weak sericite and chlorite.

2.5.2.7 Intermediate to mafic intrusive dykes and sills

Two types of intrusions have been identified in the Hurricane zone, including: intermediate dykes and mafic intrusive rocks (IN1- IN2). The first intrusive unit (IN1) is intermediate in composition and falls within the andesite/basalt field on the Pearce (1996) diagram (Fig. 2-12a; IN1). IN1 cross-cuts the footwall volcaniclastic rocks (VCL1) and is beige, fine-grained, and massive with sharp upper and lower contacts displaying chilled margins (Fig 2-5a). The IN1 lacks primary textures due to strong sericite and pyrite alteration, which suggests emplacement prior to, or during, the hydrothermal alteration of the footwall.

The most common intrusive unit (IN2) are mafic dykes (IN2a) and sills (IN2b), which are fine- to medium-grained, dark green, and contain 5-15%, 1-25 mm carbonate filled amygdules. They typically have 5-10% thin (few mm) cross-cutting carbonate veins and within the lower parts of the stratigraphy contain 5-25%, 5-20 mm euhedral pyrite cubes (Fig. 2-5b and Fig. 2-6h). The mafic sills are locally strongly overprinted by 1-5 mm euhedral (rhombohedral) iron carbonate crystals. The mafic sills are the dominant intrusive unit, forming in thick 10-50 m sequences immediately above the footwall and hanging wall contact within VCL2. Lower contacts are usually sharp, whereas the upper contacts are can be diffuse or interfingered with overlying volcaniclastic rocks, indicating that the emplacement of the sills was likely synchronous with the deposition of volcaniclastic material. The mafic dykes are 0.5 to 10 cm thick, dark green in color, range in grain size from very fine-grained to coarse-grained, and have distinct chilled margins (Fig. 2-5c). They have 5-10%, 1-20 mm carbonate or epidote filled amygdules, <5%, 1-2 mm euhedral pyrite cubes and are cross-cut by thin to thick (0.5-5 cm) carbonate-chlorite veins (Fig. 2-5d). Mafic dykes occur in the upper part of the stratigraphy and crosscut volcaniclastic lithofacies 1 to 3 and typically occur within several clusters.

2.5.3. Mineralization and Alteration

2.5.3.1 Mineralization

Mineralization in the Hurricane zone is up to 15 m thick and consists of dominantly bedding parallel Zn-Pb ± Cu massive sulphide (Fig. 2-7a; Fig. 2-8a and Fig. 2-8b). The sulphides are in fine- to medium-grained bands and contain wispy intergrowths of red and yellow sphalerite, pyrite, and galena with coarse-grained chalcopyrite blebs (Fig. 2-8a and Fig. 2-8b); the massive sulphides contain abundant relict quartz crystals and intermediate altered volcaniclastic fragments or lapilli of VCL1 (Fig. 2-7a and Fig. 2-8c). The massive sulphide horizon displays metal zonation with thick lenses of bedded sphalerite, galena and pyrite that are usually flanked by semi-massive to massive pyrite dominated intersections. The semi-massive lenses directly underlie the massive sulphides for up to 10 m and occur as discontinuous 1-4 cm bands of yellow sphalerite, pyrite and galena associated with chlorite, sericite and/or quartz alteration

(Fig. 2-7b and Fig. 2-8c to Fig. 2-8g). Locally, semi-massive sulphides overlie the massive sulphide horizon indicating potentially stacked sulphide horizons or replacement zones (De Mark and Dearin, 2007; Hinchey, 2011a).

2.5.3.2 Alteration

Hydrothermal alteration is pervasive throughout the footwall of the Hurricane lens and within the lower 70- 100 m of the hanging wall rocks. Alteration intensity in the footwall increases proximal to the mineralized horizon and decreases stratigraphically upwards into the hanging wall.

There are four major alteration assemblages present within the Hurricane zone: intense sericite-quartz-pyrite, sericite-quartz-chlorite-pyrite, intense chlorite, and chlorite and chaotic carbonate (Fig. 2-7c to Fig. 2-7h). Intense sericite-quartz-pyrite alteration occurs within the lowest part of the stratigraphy and envelopes the deposit. This style of alteration occurs up to 350 m below the massive sulphide horizon and is laterally extensive for the entire strike length of the deposit (250 m; Fig. 2-10). It is beige to silver and is associated with disseminated pyrite and pyrite stringers and rarer base-metal/chlorite stringers (Fig. 2-7c and Fig. 2-8e).

Sericite-quartz-chlorite-pyrite alteration typically lies above the intense sericite-pyrite alteration and forms an envelope around the intense chlorite alteration (see below) a few meters below the massive sulphide horizon (Fig. 2-10). It ranges in thickness from 10-30 m thick directly below the massive sulphide horizon and thins laterally to less than 5 m, eventually transitioning into the sericite-quartz alteration assemblage. The sericite and quartz alteration is typically light to dark grey in color, and predominantly affects the volcaniclastic rocks, where the lapilli fragments are quartz and lesser sericite altered and surrounded by a matrix containing fine-grained, wispy bands of sericite and lesser chlorite (Fig. 2-7e and Fig. 2-8f to Fig. 2-8g). Within the finer-grained tuffaceous layers, fine-grained sericite and quartz are dominant, whereas chlorite manifests itself either as thin cross-cutting stockwork veins, locally associated with pyrite and base-metal (sphalerite-galena) stringers, or as centimeter-scale tabular laths in a sericite-quartz matrix (Fig. 2-7d and Fig. 2-7e).

Intense chlorite alteration typically underlies and/or is associated with the massive sulphides and, in most cases, completely replaces the original host rock (Fig. 2-7f). Chlorite alteration occurs as narrow, less than 10 m thick, strata-bound sheets, rather than cross-cutting pipes, similar to other volcaniclastic-rich deposits (Fig. 2-7; e.g., Large et al., 2001a; Piercey et al., 2014; Buschette and Piercey, 2015) and locally as isolated pods.

Chaotic carbonate alteration (e.g., Squires et a., 2001; Squires and Moore, 2004; Piercey et al., 2014) is dominated by dolomite and is milky white and associated with the intense chlorite alteration. It occurs 0.5 to 5 m below the intense chlorite zone and is laterally restricted to directly below the semi-massive to massive sulphides. Proximal to mineralization the carbonate occurs as clusters or elongated bulbous spheres that are typically barren of sulphides, whereas distally it manifests as more dendritic webs and is associated with semi-massive sulphide mineralization (Fig. 2-7g to 2-7h and Fig. 2-8h).

Weak to moderate sericite and quartz alteration is present within the hanging wall volcaniclastic rocks with localized patchy to lath-like chlorite alteration directly above the massive sulphide horizon (up to 60 m above; Fig. 2-4a and Fig. 2-8b). Fine-grained disseminated and bedded pyrite is present in siliceous chert and silt layers a few meters above the footwall.

Overprinting all other types of alteration are millimeter-scale iron-rich carbonate spots that are common throughout the Boomerang deposit and most other VMS deposits in the Victoria Lake Supergroup (e.g., Boundary). These spots have been interpreted to be associated with Silurian regional metamorphism (e.g., van Staal 2007; Piercey et al., 2014; Buschette et al., 2016). Changes in alteration types and intensities can be further demonstrated by lithogeochemistry in Section 2.6 below.

2.6 Lithogeochemistry

2.6.1 Sampling and Analytical Methods

A total of 147 drill core samples were collected for geochemical analysis from 22 representative drill holes in the Hurricane zone. Samples were collected every ~ 20 m or whenever there was a significant change in alteration or stratigraphy. Core samples that were faulted and fractured or exhibited widespread quartz and/or carbonate veining were avoided. Drill core samples were cut in half, with one half preserved at Memorial University of Newfoundland as a representative sample with the other having been analyzed. All samples were analyzed for major oxide elements (SiO_2, Al_2O_3, Fe_2O_3, MnO, MgO, CaO, Na_2O, K_2O, TiO_2, P_2O_5), base metals (Zn, Cu, Pb), transition metals (Sc, Ti, V, Cr, Mn, Co, Ni), high field strength elements (HFSE), low field strength elements (LFSE), REE, and volatiles (As, Bi, Hg, Cd, Sn, Sb, Tl) at Activation Laboratories Ltd (ActLabs) in Ancaster, Ontario. At Actlabs, all samples were crushed and pulverized in mild steel before undergoing a lithium metaborate/tetraborate fusion, followed by dissolution in a weak nitric acid. The samples were subsequently analysis by inductively coupled plasma atomic emission spectrometry (ICP-AES) and inductively coupled emission-mass spectroscopy (ICP-MS). The complete geochemical results can be found in Table 2.1a and 2.1b in Appendix B.

2.6.2 Primary Immobile Element Lithogeochemistry

2.6.2.1 Element mobility and magmatic affinity monitors.

The volcanic rocks of the Hurricane zone have been affected, to some degree, by seafloor hydrothermal alteration and subsequent regional greenschist-facies metamorphism. Due to the mobility of most major elements (except Al_2O_3 and TiO_2), LFSE, volatile elements and metals during hydrothermal alteration (Spitz and Darling, 1978; Saeki and Date, 1980; Barrett and MacLean, 1994; Jenner, 1996; Large et al., 2001a), it is essential to use elements that would be considered immobile under these conditions. Many studies of VMS deposits have determined the HFSE and REE (except Eu) to be immobile, except under intense hydrothermal alteration where they may become mobile (especially the LREE; e.g., MacLean, 1988). To determine the primary geochemical signatures of the volcanic rocks of the Hurricane zone Al_2O_3, TiO_2, HFSE, and some REE were used as immobile affinity monitors.

2.6.2.2 Footwall Geochemistry

Due to the highly-altered nature of the footwall volcanic rocks, it is difficult to distinguish different facies based on lithology and petrography alone, whereas immobile element ratios and binary plots can remove the effects of alteration and provide a useful method in distinguishing different chemical rock types (e.g., Barrett et al., 2001).

The footwall of the Hurricane zone has five geochemically distinct and correlative "andesitic" units based on immobile element ratios (Groups A-E; VCL1; Fig. 2-12a). Groups A to C are subalkaline and have La/Yb, Th/Yb, Th/Yb, and Zr/Y ratios that range from tholeiitic to transitional (Fig. 2-12b), accompanied by low Zr/Al_2O_3 (2.3-3.1) and Zr/TiO_2 (62-75) ratios (Fig. 2-12c). Group D is subalkaline, with transitional to calc-alkaline magmatic affinities, but has higher Zr/Al_2O_3 (6.6) ratios (Fig. 2-12c). Group E are anomalous samples that include a pyritic mudstone and strongly altered tuff that are not discussed further given their anomalous geochemistry. Immobile compatible vs. immobile incompatible plots of Zr vs Al_2O_3 and Th vs Al_2O_3 in Figure 2-16a and 2-16b show near-linear trends indicating that the various footwall lithogeochemical groups above had similar magma sources (e.g., MacLean and Barrett, 1993; Barrett et al., 2001).

2.6.2.3 Hanging wall felsic to intermediate geochemistry

The majority of the tuffaceous rocks fall within the intermediate (andesitic/basaltic) field on the Zr/ TiO_2 vs Nb/Y ratios, with the exception of volcaniclastic lithofacies 2 (VCL2), which is predominantly rhyolitic in composition. The coherent felsic volcanic rocks of lithofacies 5 (CL1a and b) tightly cluster within the rhyolite field and the mafic sills cluster within the basalt field (Fig. 2-12a). The Hurricane rocks are typically subalkaline and have La/Yb, Th/Yb, and Th/Yb ratios that range from tholeiitic to calc-alkaline (Fig. 2-12b; Barrett and MacLean, 1999; Ross and Bedard, 2009). The rocks from both the footwall (VCL1) and most of the hanging wall have low Nb and Y values and plot within the M-type field, with the exception of volcaniclastic lithofacies 2 and 3 (VCL2 and VCL3) that plot within the OR-field (Fig. 2-12c; Pearce, 1984). This suggests either, mixing of mafic material within the more felsic volcaniclastic rocks or that they were derived from melting of a mafic source (Fig. 2-12d; Piercey, 2009). Nearly all the samples fall with FIV field (Fig 2-12e), indicating that partial melting must have occurred at shallow levels in the crust (< 15 km) and implies derivation from potentially melting a juvenile or mafic source (Lesher et al, 1986; Hart et al., 2004; Piercey, 2011).

2.6.2.4 Primitive mantle normalized plots

Primitive mantle normalized plots from all the hanging wall rocks (VCL2-4 and CL1) are moderately LREE-enriched with relatively flat HREE profiles and negative Nb and Ti anomalies with low contents of Sc and V (Fig. 2-13). The footwall rocks (VCL1; Groups A to D) are similar to the hanging wall; however, they have lower REE concentrations and have negative Eu anomalies (Fig. 2-12b and 2-10d), with the exception of Group D, which has similar LREE values as the hanging wall samples (Fig. 2-12d). The large amount of scatter in the footwall samples is likely due to mobility of the LREE, or due to mass gains or loss during hydrothermal alteration (see below).

2.6.2.5 Mafic Intrusion Geochemistry

There are two groups of geochemically distinct intrusive mafic to intermediate units within the Hurricane zone: they consists of andesitic dykes (IN1) and a unit of basaltic dykes and sills (IN2a and b). IN1 plot within the andesitic field on the Pearce (1996) plot (Fig. 2-14a). They have subalkaline Nb/Y ratios and have transitional to calc-alkaline magmatic affinities (Fig. 2-12b). They plot within the alkaline and the arc basalt fields on the Ti-V discrimination diagram and the Th-Zr-Nb plot, respectively (Fig. 2-14b-c). IN1 is moderately enriched in LREE and MREE on primitive mantle normalized plots and have moderate Nb and Ti depletions and low contents of compatible elements (Al, V, Sc), which are characteristics of basaltic rocks with calc-alkaline to island-arc tholeiitic affinities (Fig. 2-13f).

IN2 mafic rocks are the most common intrusive unit and are subalkaline with tholeiitic magmatic affinities with primitive mantle-normalized patterns similar to island-arc tholeiites or back-arc basin basalts (BABB; Fig. 2-13b). The primitive mantle-normalized signatures of these mafic rocks have weak LREE enrichment with flat HREE, and are moderately depleted in Nb (Fig. 2-13f). On the Th-Zr-Nb diagram they plot within the arc-basalts field and on the Ti-V diagram they plot within the island-arc tholeiite (IAT), with one anomalous sample plotting in the MORB field (Fig. 2-14b-c)

2.6.3 Mobile Element Lithogeochemistry

2.6.3.1. Mobile element systematics

It has been well documented in numerous VMS deposits that hydrothermal alteration is responsible for the destruction of primary igneous phases and glass, resulting in replacement with secondary alteration minerals (e.g., Ohmoto, 1996; Riverin and Hodgson, 1980). The volcanic rocks of the Hurricane zone display strong to intense hydrothermal alteration within the footwall and lower hanging wall. At the footwall-hanging wall contact there is a distinct depletion in Na_2O (typically Na_2O < 0.94%) coupled with high Spitz-Darling index values (Al_2O_3/Na_2O > 25; Fig. 2-15a). The majority of the rocks have moderate to high Ishikawa alteration index (AI) and the chlorite-carbonate-pyrite index (CCPI) and plot towards the upper right-hand corner on the alteration box plot. The footwall rocks in the Hurricane zone follow four main trends on the alteration box plot (Fig. 2-15b): sericite-chlorite-pyrite, chlorite-pyrite-(sericite), chlorite-carbonate, and chlorite pyrite. Moreover, volcaniclastic rocks of volcaniclastic lithofacies 2 also trend along the chlorite-pyrite-(sericite) and sericite-chlorite-pyrite line, indicating the hanging wall rocks are hydrothermally altered (Fig. 2-15b; see below). The four alteration assemblages within the footwall and lower hanging wall are also clearly defined using bivariate plots of MgO-Al_2O_3 and K_2O-Al_2O_3 (Fig. 2-15c and 2-15d). All altered rocks have elevated concentrations of Hg, and high Hg/Na_2O and Ba/Sr ratios (Fig. 2-15e), typical of rocks found in the Tally Pond and Tulks volcanic belts (Collins, 1989; Buschette et al., 2016). However, they do not exhibit significant enrichments in Tl-Sb, like other volcaniclastic-hosted deposits globally (Fig. 2-15f; e.g., Rosebury; Large et al., 2001a,b).

2.6.3.2- Mass Balance

Mass balance calculations were used to quantify the absolute gains and losses associated with hydrothermal alteration for Groups A to D in the footwall (VCL1) and the lowest hanging wall unit

(VCL2), which are the units that experienced the most widespread hydrothermal alteration. Although there is evidence of hydrothermal alteration in VCL3, due to the heterogeneous nature of the lithic clasts, it makes it difficult to determine a precursor composition for the unit and calculations were not performed.

Least altered precursors from VCL1 and VCL2 were selected based on samples that displayed minimal Na_2O loss (2-5 wt%), low loss of ignition (LOI) and low base metal values (i.e., <100ppm, ideally). The single precursor method implies that rocks were from an originally homogenous volcanic unit and had a common homogenous parent that was variably altered. In single precursor systems when immobile, incompatible elements are plotted against one another the samples from a single precursor system will plot along a linear array that projects through the origin reflecting apparent elemental gains and losses due to mass losses and gains, respectively (Fig. 2-16a and 2-16b; e.g., Barrett and Maclean, 1991; MacLean and Barrett, 1993; Barrett and MacLean, 1994).

The three chemically distinct units that were identified based on immobile-incompatible diagrams and immobile binary plots are: Groups A to C, Group D and VCL2 (Fig. 2-16a and 2-16b). Groups A to C are grouped for mass balance calculations due to nearly linear trends in immobile-immobile and binary plots and have distinct tholeiitic to transitional magmatic affinities in comparison to the more calc-alkaline overlying Group D, which was group separately for mass balance calculations. Since the three groups display little variation in their immobile element ratios, the single precursor method (e.g., MacLean and Kranidiotis, 1987; MacLean, 1990; Barrett and MacLean, 1991; MacLean and Barrett, 1993) is appropriate to use to determine mass change.

2.6.3.3- Results of mass balance calculations

The major element oxides that are affected by hydrothermal alteration are SiO_2, Fe_2O_3, MgO, CaO, K_2O, and Na_2O, which express significant gains and losses relative to their proximity to the massive sulphide horizon. Intense sericite-pyrite alteration in the footwall is associated with K_2O (~2.5%) and SiO_2 (up to 26%) gains and losses of Na_2O (~ -2%), with some samples exhibiting gains in MgO (1-10%), with a loss of K_2O and SiO_2 (-0.5% and up to -60%), reflecting either a change in white mica composition or the formation of chlorite. Sericite-quartz-chlorite alteration exhibits mass gains in SiO_2 (up to 43%), Fe_2O_3 (1-14%), and MgO (up to 12%), coupled with relative losses of Na_2O and K_2O. The quartz-sericite alteration within both the hanging wall and footwall, display gains in SiO_2 (2-50%), K_2O (up to 2.6%), and locally has gains in Fe_2O_3 and MgO (up to 6% and 8%, respectively, if chlorite is present), and losses in Na_2O (approximately between -1% and -3%). The exception to these trends are samples from the volcaniclastic assemblage in the upward extent of the hanging wall alteration in volcaniclastic lithofacies 2 where there is a relative gain in Na_2O (up to ~1%). Rocks with intense chlorite alteration have mass gains in Fe_2O_3 (0.3 to 13%) and MgO (0.1 to 19%), with relative increases in CaO (up to 16%), depending on presence or absence of chaotic carbonate. This chlorite-chaotic carbonate assemblage typically has significant mass losses in SiO_2 (up to -39.5%), Na_2O (up to -2.5%), and K_2O (up to -1.5%). In additional to gains in Fe_2O_3, MgO and CaO, in the strongly altered chloritic zones in VLC1, this assemblage also displays gains in SiO_2 and K_2O, attributed to locally containing minor quartz-sericite alteration.

Certain LFSE elements, such as Ba, Sr, Rb, and trace elements, like Hg, Tl and Sb, that are related to alteration and mineralization also show significant gains associated with specific alteration assemblages. Barium and Rb are strongly elevated within the sericite-dominated altered footwall rocks (up to 2055 ppm and 61 ppm, respectively), with the exception of some of the intensely chlorite altered rocks. However, Rb is also elevated in the lower hanging wall (up to 25 ppm), whereas Ba displays significant losses above the mineralized zone. Mercury is elevated throughout the footwall within all alteration assemblages, proximal and distal to the deposit, and in lower hanging wall rocks directly above the massive sulphide horizon (up to 6305 ppb). Transition metals (Ni, V, Cr) are elevated in the footwall and display the greatest mass gains in the sericite-chlorite-quartz-pyrite alteration assemblage associated with chlorite stringers. Elevated Cu is associated with intense chlorite, chaotic carbonate and sericite-chlorite-pyrite stringer alteration. Zn and Pb are elevated in almost all alteration assemblages in both the footwall and lower hanging wall, with the exception of the intense sericite assemblage. Zinc is most strongly elevated in the intense chlorite alteration assemblage (up to 7796 ppm), whereas Pb has the greatest gains in sericite-chlorite-pyrite assemblage (up to 11,576 ppm). Both Zn and Pb have elevated values, up to 20 ppm, in the most distal lower hanging wall volcaniclastic rocks.

To better illustrate the relationship between elemental gains and losses associated with mineralization and alteration downhole profiles of drill cores GA-07-208 and GA-10-272 in Figures 2-17 and 2-18 were chosen to display the key elemental variations, including base metals, key mobile elements and alteration indexes. These holes were selected because they highlight the elemental gains and losses associated with each alteration assemblage and display how they changed downhole with varying proximity to the mineralization. Hole GA-07-208 illustrates common footwall alteration assemblages that are marked by low Na_2O contents at the footwall/hanging wall contact, coupled with high alteration indices, and elevated Hg-Cu-Pb-Zn contents. There are also elevated Fe_2O_3, MgO, which can be attributed to chlorite and pyrite alteration, and high K_2O further down hole attributed to shift from chlorite-pyrite to stronger sericite alteration. GA-10-272 has similar footwall alteration assemblages, with elevated CaO associated with Fe_2O_3, which can be attributed to the presence of chaotic carbonate alteration. Within both sections, there is evidence of alteration within the lower part of the hanging wall sequence with elevated levels of K_2O, Fe_2O_3, MgO, Hg, and high CCPI and AI.

2.7 Short Wave Infrared Spectroscopy

Short wave infrared spectroscopy (SWIR) data provides the ability to identify the presence and composition of some alteration minerals associated with mineral deposits in real time, and has been demonstrated to be very effective in characterizing alteration in VMS deposits (e.g., Herrmann et al., 2001; Jones et al., 2005). SWIR spectroscopy uses a light source to measure infrared wavelengths absorbed by certain bonds within the crystal structure of a mineral, such as the OH, H_2O, CO_3, NH_4, AlOH, FeOH, and MgOH molecular bonds (Thompson et al., 1999; AusSpec International, 2008). This method is particularly useful for identification of VMS alteration-associated hydrous minerals such as white micas and chlorite (Hermann et al., 2001; Hinchey, 2011b).

For the Hurricane zone, the most useful SWIR features are the AlOH absorption features between 2190 and 2225 nm, which, in the case of the Hurricane zone, correspond to variations in white mica compositions (AusSpec International, 2008). FeOH and MgOH bonds, corresponding to chlorite absorption features, show little systematic variations and are not a useful vector towards mineralization in the Hurricane zone, and therefore are not be discussed further. Sericite ([(K, Na)$_2$(Al, Fe,Mg)$_4$(Si, Al)$_8$(OH)$_2$]) has a deep absorption features that ranges from 2180 and 2228 nm (Herrmann et al., 2001). Compositional variations are caused by relative proportions of major cations, mainly in the octahedral site, and these produce differences in wavelengths and absorption features. The exact location of the wavelength is related to the compositional variation of the major cations in the octahedral site, mainly Al, Si, Fe and Mg, which are caused by Tschermark substitution (Al^{VI}+$Al^{IV}$$\leftrightarrow$ (Fe, Mg, Mn)^{VI} +Si^{IV}) or by the interlayer cation substitution between K and Na (e.g., Velde, 1978; Herrmann et al., 2001; Yang et al., 2011). Shorter wave lengths (2180-2195 nm) correspond to high Al contents in the octahedral site and are characteristic of sodic mica (paragonite), whereas longer wave lengths (2210-2228 nm) correspond to low Al levels and increases in Si and Fe+Mg characteristic of Fe-Mg mica (phengite; Herrmann et al., 2001; Yang et al., 2011). Potassic mica (muscovite) produces absorption features around 2200 and 2204 nm, and intermediate wavelengths are the result of mixed white micas or an intermediate composition (Herrmann et al., 2001).

Hyperspectral analysis were carried out at ~5 m intervals in each drill hole that was logged using a TerraSpec™ mineral spectrometer with a hand held Hi-Brite light wand. Samples were collected from each core box to get an accurate downhole representation of compositional variation with depth and proximity to mineralization. Samples required minimal preparation, as they were collected from dry, clean drill core. To ensure accuracy and avoid instrument drift, optimization, white reference and mineral references (e.g., pyrophyllite) were taken every 40 samples and at every hour. Analyses were completed in dark or naturally lit rooms to avoid interference from artificial lighting. Spectral data were collected using RS^3 spectral acquisition software and processed using “The Spectral Geologist Hotcore” v. 7.1.55 software. This program interprets and compares the analyzed spectra to a reference library of mineral standards to determine the exact location of the specific absorption feature to identify the mineral in the sample and allows for numerical extraction of various spectral information (e.g., absorption wavelengths, depths of absorption hulls).

2.7.1 SWIR Results

The SWIR data from the Hurricane zone illustrates a systematic variation in white mica spectral composition from 2189 nm to 2226 nm as a function to proximity to mineralization (Fig. 2-17 and Fig. 2-18). Within the Hurricane stratigraphy, downhole profiles indicate that phengitic micas (> 2210 nm) are the most common mineral species in the hanging wall volcaniclastic rocks. This likely partly reflects regional background micas associated with greenschist metamorphism and partly locally low temperature, distal hydrothermal alteration mica. The exception to this is directly above the mineralized horizon where the hanging wall exhibits strongly sericite-chlorite-pyrite alteration, which is associated with a decrease in wavelength to muscovite (<2195 nm). Within the mineralized zone and footwall, two mica species are present and reflect proximity to mineralization. Muscovite is associated with chlorite-sericite-pyrite alteration assemblage and directly underlies and extends laterally from the mineralized zone. Below this, paragonite is the dominant mica species, which is associated with the strong sericite-pyrite alteration that underlies the deposit.

2.8 Discussion

2.8.1 Tectonic and depositional setting of volcaniclastic rocks

The tectonic setting of the Tulks volcanic belt (TVB) has been the focus of previous studies (e.g., Evans and Kean, 2002, and references therein; Zagorevski et al., 2007, 2010). Most authors suggest that the TVB formed during development of the peri-Gondwanan Penobscot-Victoria arc-back-arc system on the leading edge of Ganderia during the Cambrian to early Ordovician (Zagorevski et al., 2007, 2010). The evolution of this arc-back-arc system was punctuated by multiple episodes of extension and/or incipient rifting accompanied by changes in magma compositions, volcanic and sedimentary facies, and VMS deposit formation (Evans and Kean, 2002; Zagorevski et al., 2010; Hinchey, 2007, 2011a). The results of this work are consistent with these previous models. For example, the textures in volcano-sedimentary facies present in the deposit, consist of well-defined, fining-upward turbiditic sequences of felsic to mafic volcaniclastic rocks intercalated with fine-grained sedimentary rocks, coupled with interfingered mafic and felsic sills. These textures are consistent with formation of sill-sediment complexes with high sedimentation rates coupled with coeval bimodal magmatism (Einsele et al., 1980; Einsele, 1986; Boulter, 2004). Further, the bimodal compositions of the sedimentary rocks suggest a mixed mafic and felsic provenance, likely from nearby arcs (e.g., Zagorevski et al., 2010; Hinchey, 2011a). The lithogeochemical signatures of these rocks are also partly supportive of a rifted arc origin, as well. For example, mafic sills and dykes show a transition in affinity upwards in the Hurricane stratigraphic sequence from transitional calc-alkaline basalts to island-arc tholeiites/back-arc basin basalts (Fig. 2-14b). The primitive mantle normalized patterns for IN1 and IN2 indicate an upward progression in host stratigraphy from island-arc-type to back-arc rift-type magmas (Fig. 2-13f), which would be consistent with shifts from magmatism derived from deeper sources (calc-alkalic) to shallower sources (e.g., tholeiites) associated with extension and back-arc asthenospheric upwelling. Similar geochemical results and progressions were observed regionally by Swinden et al. (1989) and Zagorevski et al. (2007).

The rifting of the Penobscot-Victoria arc was critical in the development of the volcano-sedimentary basin as periods of arc development and rifting are conducive for the formation of VMS deposits (e.g., Swinden, 1991; Lentz, 1998; Piercey, 2011). During extension, crustal thinning and asthenospheric mantle upwelling result in basaltic under plating of the overlying arc, leading to the production of bimodal magmatism, related elevated heat flow, and emplacement of a localized heat sources (i.e. magma chambers and/or intrusions) that could drive hydrothermal circulation (e.g., Lesher et al., 1986; Swinden, 1991; Lentz, 1998; Galley, 2003; Hart et al., 2004; Piercey 2009, 2011). While the Hurricane zone and Boomerang deposit do not have an exposed subvolcanic intrusion, the deposit contains abundant, multi-generational sills of mafic and felsic material, which were likely fed from an underlying magma chamber. This suggests that the deposit formed within a "thermal corridor" with elevated heat flow, and that this heat was responsible for driving the hydrothermal circulation that formed the deposit (e.g., Lentz, 1998; Galley, 2003; Piercey, 2011). Rifting would have also resulted in extensional faults and fractures that created porosity, permeability and conduits for fluid recharge and upwelling (Franklin et al., 1981, 2005; Lentz, 1998; Barrie and Hannington, 1999; Galley et al., 2007; Piercey 2009, 2011). The combination of these two features were critical in the formation of the Hurricane zone and the Boomerang deposit.

2.8.2. Characteristics and controls on hydrothermal alteration

Hydrothermal alteration in the Hurricane zone consists of proximal, pervasive stratabound alteration that transitions downward and laterally into broad, semi-pervasive alteration. The nature and geometry of alteration in the Hurricane zone was likely due to the original porosity and permeability present in the host rocks during formation of the deposit. For example, the volcaniclastic rocks were likely porous and unconsolidated to partially unconsolidated, which would have resulted not just in vertical hydrothermal fluid flow, but also lateral flow into the unconsolidated material (e.g., Piercey et al. 2014; Piercey, 2015). The interpreted high permeability of the volcaniclastic/volcano-sedimentary host rocks would have allowed for hydrothermal fluids to migrate along multiple paths resulting in alteration both discordant and also semi-concordant to stratigraphy, as fluids would have percolated through the permeable footwall rocks until they encountered a semi-permeable to impermeable boundary (e.g., Gibson et al., 1990; Franklin et al., 2005; Gibson, 2005). There are several lithostratigraphic units that could have acted as impermeable boundaries and influenced the distribution of alteration assemblages and replacement-style mineralization. For example, muddy or silty units at the top of the mineralized sequence likely had low porosities that would impede and trap ascending hydrothermal fluids, resulting in the downward and lateral growth of sulphide deposition and associated high temperature alteration in host rocks in the subseafloor. In addition, in areas where a mudstone cap is absent (i.e. from depositional erosion or lateral facies change) synchronous and rapid deposition of volcaniclastic material may have impeded venting of hydrothermal fluids onto the seafloor and would have resulted in pervasive and laterally extensive hydrothermal alteration into the lower hanging wall stratigraphy. This is similar to other replacement-style VMS deposits globally, such as the Rosebery and Mattabi deposits (Morton et al., 1991; Allen, 1994).

Despite the likely permeable control on the geometry of alteration, the mineralogical variations and elemental gains and losses of mobile elements are similar to global VMS deposits (Franklin et al., 2005; Galley et al., 2007). The Hurricane zone has four main alteration assemblages that systematically change with proximity to the mineralization. Intense chlorite and local chaotic carbonate directly underlie and are intimately associated with the mineralization (i.e., within 1-10 m of mineralization). Strong to moderate sericite-chlorite-pyrite alteration extends above and below the deposit into the hanging wall and footwall, with the strongest alteration occurring directly above (and below) the mineralization zone (within 0.5-5 m) and decreases in intensity laterally up to several 100 m transitioning into sericite-quartz-pyrite alteration that envelopes the deposit (Fig. 2-10).

These alteration assemblages are also associated with characteristic elemental gains and losses that can be explained by the modification of seawater and leaching of felsic/intermediate wall rock during hydrothermal alteration (e.g., Franklin et al., 2005; Hannington et al., 2005). There is strong Na_2O depletion throughout most of the footwall and within the lower half of the hanging wall indicating destruction of feldspars during hydrothermal alteration (Fig. 2-16c; e.g., Riverin and Hodgson, 1980; Date et al., 1983; Barrett and MacLean, 1994). The loss of Na (and Ca) and gains of K and Si (Fe and Mg) correlate with quartz-sericite alteration (Fig. 2-16d). Locally, this alteration assemblage has moderate gains in Fe and Mg, which are associated with either Mg-Fe chlorite laths and/or pyrite in the sericite matrix. The sericite in this alteration assemblage has a paragonitic composition with elevated Ba-Rb, and low base metal content (<150 ppm). The chlorite-sericite-pyrite and intense chlorite alteration assemblages have a net gain of Mg and Fe coupled with the loss of K (±Si and Na) that are attributed to the continual destruction of primary feldspars and previously formed micas with the addition of Mg and Fe to form chlorite (e.g., Riverin and Hodgson, 1980; Knuckey et al., 1982; Table 2.1b and Fig. 2-16c-f). However, the increase in chlorite content does not fully account for the mass gains of Fe and Mg (+Ca) alone, requiring additional Fe-Mg-Ca-rich phases. Such Fe-Mg-Ca-enrichment can be attributed to chaotic carbonate alteration associated within semi-massive sulphides, pyrite stringers, and intense chlorite alteration (Fig. 2-16c). Sericite within chlorite-sericite-pyrite zone is K-rich muscovite and the whole-rock samples exhibit gains in Ba-Rb and losses in Sr. The presence of Zn-Pb enrichment associated with the sericite-rich assemblages, and the occurrence of chlorite in the proximal alteration assemblage, reflects the evolution of the hydrothermal system, from lower temperature (~200ºC) Zn-Pb-Ba-rich mineralization associated with sericite to higher temperature (>300ºC) Cu-Hg-As-Sb-rich mineralization associated with chlorite and chaotic carbonate (e.g., Large et., 2001b; Franklin et al., 2005). Moreover, the stratabound geometry of some of the alteration illustrates that there was not only upward flow reflected by the presence of discordant chlorite alteration, but also lateral flow that was controlled by permeability of footwall strata.

In addition to footwall alteration, there is well-developed hanging wall alteration in the Hurricane zone. The presence of sericite-quartz (±chlorite) alteration in the hanging wall illustrates that the hydrothermal system continued to operate while the hanging wall was deposited (e.g., Gemmell and Fulton, 2001; Shanks, 2011). Furthermore, the phengitic mica composition in the hanging wall, coupled with gains of Si, Na, Pb, Rb, and Sr (±Fe-Mg, if chlorite is present), and losses of K, Ba directly above the mineralized horizon, are consistent with sericite-quartz alteration that is more Na-rich compared to footwall muscovite alteration. This likely represents a distal signature and potentially a lower temperature alteration associated with the potential waning of the Hurricane hydrothermal system (e.g., Gemmell and Fulton, 2001).

Alteration assemblages in both the hanging wall and footwall have distinctive geochemical signatures that can be used as potential exploration vectors in determining proximity to ore. The most useful proximal vectors are enrichments in Zn, Pb, Cu, Hg, and transition metals; high AI, CCPI, Al_2O_3/Na_2O, Hg/ Na_2O, and Ba/Sr indexes; and the presence of K-rich muscovite or paragonite. These vectors are useful for at least 100 m along strike and 10-60 m into the footwall. Distal vectors include Zn, Pb, Hg enrichments; losses in Ba and K; and phengitic mica, and are detectable along strike for 250 m from mineralization.

2.8.3 Implications for subseafloor replacement

Many modern and ancient seafloor hydrothermal systems form from the exhalation and accumulation of sulphides on the seafloor (e.g. Ohmoto, 1996; Franklin et al., 2005; Galley, 2007; Hannington, 2014). In the ancient geological record; however, there are a sub-set of deposits that formed via replacement in the subseafloor environment, and these deposits are often large and/or high grade (e.g., Galley et al., 1995; Doyle and Allen, 2003; Piercey, 2015). Modern seafloor systems are remarkably inefficient and only 5-10% of metals are precipitated at the seawater interface (Converse et al., 1984), leading to deposits that are generally small (Hannington et al., 2005 and references therein). In contrast, replacement-style systems are much larger and often exhibit higher grades due to the efficiency of precipitation and the enhancement of zone refining processes (e.g., Doyle and Allen, 2003; Piercey, 2015). The Hurricane zone displays well preserved textures and features that suggest formation by subseafloor replacement processes, including many of the criteria outlined by Doyle and Allen (2003). The five features that Doyle and Allen (2003) used to distinguish subseafloor replacement-type VMS deposits, include: (1) the massive sulphides are enclosed in rapidly emplaced lithofacies (i.e. mass-flow deposits, volcaniclastic rocks); (2) relicts of the host lithofacies (i.e. sedimentary, volcaniclastic, or coherent volcanic rocks) are preserved within the massive sulphides; (3) replacements fronts can be identified between the massive sulphide and the host rock; (4) evidence of similar types of hydrothermal alteration and intensity is present in the overlying hanging wall succession; and (5) discordant alteration with enclosing lithofacies.

The first three criteria are diagnostic of replacement-style mineralization, whereas criteria 4 and 5 are considered supportive but not diagnostic.

Within the Hurricane zone the first four of these characteristics are present. For example, the Hurricane zone is hosted in and overlain by normally graded, lithic crystal tuffs and lapilli tuffs with local, thin beds of chert and/or mudstone. The rounded nature of the lithic fragments implies that these are most likely reworked volcaniclastic debris and the fining-upward turbiditic sequence indicates that these were likely emplaced rapidly by subaqueous sediment gravity flows (e.g. McPhie et al., 1993; criteria 1). Evidence of hydrothermal alteration in the overlying hanging wall volcaniclastic rocks and locally within the mafic sills provides further evidence for synchronous high temperature hydrothermal fluids, mafic volcanism coupled with rapid emplacement of volcaniclastic rocks (criteria 1 and 4). Textural and stratigraphic relationships also support formation of the Hurricane zone by subseafloor replacement, including the presence of clasts having similar alteration and textures as the surrounding footwall lapilli tuffs, along with relict quartz crystals in bedded sulphides (Fig. 2-19a; criteria 2). There are also replacement fronts that vary from sharp to gradational with the graded volcaniclastic rocks depending on the presence or absence of a cap rock (i.e. mud), as well as occurrences of sulphides lenses at different stratigraphic levels (Fig. 2-19b; criteria 3). In addition, pervasive sericite-quartz-chlorite-(+/- pyrite) alteration, similar to the footwall alteration, occurs in the hanging wall volcaniclastic rocks directly above the massive sulphide horizon which extends up to 10-40 m above mineralization and continues laterally for several 10s of meters (criteria 4; Fig. 2-19c). This is also geochemically evident as there are elevated alteration index values, anomalous base metal enrichments, and mobile elements proportional to the alteration mineral assemblages (Figs. 2-17 and 2-18). This alteration clearly suggests that the hanging wall volcaniclastic rocks were emplaced prior to and/or synchronous with the hydrothermal system that formed the Hurricane zone. Collectively, the criteria above are strong indicators that the Hurricane zone formed predominantly by subseafloor replacement processes.

The style of mineralization and alteration of the Hurricane zone is a function of the semi-consolidated to unconsolidated nature of the volcaniclastic, sedimentary rocks and overlying mudstone unit. It is interpreted that hot, metalliferous fluids initially flowed along synvolcanic structures and permeated through the relatively porous and permeable, fluid-saturated footwall volcaniclastic rocks until it encountered an impermeable mud unit, resulting in mixing of cooler seawater and inter-pore fluids which ultimately lead to the progressive precipitation of sulphides in a subseafloor setting (e.g., Piercey, 2015). Multiple sulphide horizons and alteration in the hanging wall are supportive of this hypothesis and suggest that there was variable permeability in both the footwall and hanging wall volcaniclastic rocks that was controlled by lithology (i.e. normally graded or massive volcaniclastics). In particular, within the normally graded sequences, the massive sulphide preferentially replaced the coarser beds with lesser sulphides in the finer grained beds (i.e., mudstone or siltstone; Fig. 2-8a, Fig. 2-8d and Fig. 2-16a). This was accompanied by an increase in alteration and mineralization upwards in stratigraphy proximal to mineralization and in more permeable units (e.g., Fig. 2-7b and Fig 2-19d). A similar case is observed in the hanging wall where coarser beds are more strongly altered, suggesting that the coarser units were more permeable, allowed greater fluid flow, and provided a nucleation site for sulphide and hydrothermal alteration (e.g., Piercey, 2015).

Even though there is strong evidence for subseafloor replacement, the Hurricane zone, like other similar volcaniclastic-hosted replacement style VMS deposits, the deposit shows evidence for local mineralization that occurred on the seafloor. For example, the presence of thinly bedded fine-grained sedimentary rocks interbedded with fine-grained pyrite suggests potential exhalative seafloor mineralization during a decline in volcaniclastic input (Fig. 2-4). Also, there are regional iron formations that are interpreted to have been formed contemporaneous with the Boomerang deposit (e.g., Curve Pond, Dragon Pond occurrences; Hinchey, 2011a); these units are generally considered to form from exhalative processes (Peter, 2003).

Despite the Hurricane zone and Boomerang deposit being relatively small, it has excellent grades, particularly for Zn. This is partly due to the subseafloor replacement processes, coupled with zone refining. Numerous workers have illustrated that zone refining can lead to increased grade if done within a semi-permeable cap rock or semi-permeable interface at the seawater interface (Hodgson and Lydon, 1977; Campbell et al., 1984; Barriga and Fyfe. 1988; Large, 1992; Schardt and Large, 2009; Piercey, 2015). A semi-permeable cap of mud or volcaniclastic rocks, like in the Hurricane zone, would have hindered the dissipation of hydrothermal fluids into the overlying water column, which would have provided a thermal and chemical gradient, and would have allowed cold seawater to ingress into the subseafloor into permeable volcaniclastic and sedimentary rocks. This would have created a thermal and chemical gradient with upwelling hydrothermal fluids (i.e., it would be cold, high fO_2, fluid-rich), thereby inducing sulphide precipitation both upon and beneath the seafloor as hydrothermal fluids mixed at the seawater interface with seawater, and beneath the seafloor with cool fluids trapped in the pore spaces within volcaniclastic and sedimentary material (e.g., Campbell et al. 1984, Lydon, 1988, Piercey, 2015). Moreover, this type of environment would have resulted in a semi-permeable interface that would have facilitated zone refining, coarsening of sulphides, and metal upgrading beneath the semi-permeable interface, leading to the observed metal zoning and Zn-enrichment found in the deposit (e.g. Large, 1992; Ohmoto, 1996; Dearin and DeMark, 2007; Hinchey, 2011a; Piercey, 2015)

2.8.4 Comparison between Boomerang zone and Hurricane Zone

There are many similarities in lithology, mineralization styles, whole-rock geochemistry and SWIR data between the Hurricane zone and Boomerang zone. There have been several studies completed outlining the lithological, geochemical and spectral characteristics of the Boomerang zone (Hinchey, 2007; 2011a and 2011b; Hinchey and McNicoll, 2009), and outlined below are comparisons between the various geological, mineralogical, and lithogeochemical attributes between the Hurricane and Boomerang zones.

The Hurricane zone is located 500 m north east of and along strike with the Boomerang zone and has been interpreted to lie within the same stratigraphic horizon as Boomerang zone (DeMark and Dearin, 2007). For example, the hanging wall stratigraphy of the Boomerang zone with undifferentiated, locally fining upwards felsic to intermediate volcaniclastic and epiclastic rocks that are dominated by ash- and quartz-feldspar crystal tuff (i.e., VCL4), black shale, argillite, greywacke, chert and volcaniclastic conglomerate/breccia and bimodal, locally amygdaloidal sills (i.e., IN2a; Hinchey, 2011a) are identical to the VCL2, VCL3, VCL4 and IN2 facies present at Hurricane. Similarly, the footwall fine-grained crystal-ash tuffs and local lapilli tuff and fine-grained sedimentary rocks are similar to VCL1 in the Hurricane zone (i.e., VCL1). Alteration and mineralization styles are also similar between the two zones. The intense sericite alteration with local moderate to strong chlorite-silica-carbonate alteration and "chaotic" carbonate in the Boomerang zone are similar to that present in the Hurricane zone; both zones also contain similar hanging wall alteration (Hinchey, 2011a). Furthermore, the subseafloor replacement style mineralization in both zones are similar.

In addition to stratigraphy, mineralization, and alteration similarities, the Hurricane and Boomerang zones have similar lithogeochemical and hyperspectral attributes. For example, the volcaniclastic host rocks have HFSE and REE signatures that are identical with volcanic-arc to ocean-ridge type (or mixed-type) signatures, and similar primitive mantle normalized patterns (e.g., Hinchey, 2011a). Likewise, the primitive-mantle-normalized plots for the mafic sills in the Boomerang are identical to the mafic sills within the Hurricane zone (Hinchey, 2011a). Lastly, short-wave infrared spectroscopy data from the Boomerang zone shows the same systematic decrease in wavelength of the Al-OH absorption features in footwall white micas from phengite ranging to muscovite (>2000 nm) distal to mineralization and paragonite (< 2000 nm) proximal to the ore, and with a significant drop in wavelength from >2000 nm to <2000 nm occuring at, or just above, the hanging wall-footwall contact (Hinchey, 2011a), similar to the downhole profiles in the Hurricane zone (Fig. 2-17 and Fig. 2-18).

Taken together, various geological, geochemical, and spectral elements suggest that the Boomerang and Hurricane zones represent stratigraphic and mineralized equivalents within the broader Boomerang deposit.

2.9 Conclusions

The Hurricane zone is a subseafloor replacement-style VMS deposit hosted in thick packages of turbiditic felsic to intermediate volcaniclastic rocks, thinly interbedded with fine-grained sedimentary rocks and locally intruded by felsic and mafic sills. The nature of the volcaniclastic rocks and sills implies synchronous sedimentation and magmatism in a rifted arc to back-arc formed on the leading edge of Ganderia. The mineralized zone consists of massive to semi-massive bedded sphalerite-galena-chalcopyrite-pyrite lenses enveloped by strongly altered volcaniclastic rocks in both the footwall and hanging wall. Four main alteration assemblages are present in the Hurricane zone that correspond to increases in alteration intensity towards the massive sulphide horizon. They consist of widespread sericite-quartz alteration and sericite-chlorite-pyrite underlying the semi-massive to massive sulphide horizon and intense chlorite and chaotic carbonate alteration intimately associated with the massive sulphides (i.e., within meters). The alteration styles and their geometry reflect the permeability of host rock lithologies and physicochemical attributes of the hydrothermal fluids during deposit formation. Results from whole-rock lithogeochemistry and mass balance calculations indicate that net gains and losses of major mobile elements (e.g. SiO_2, MgO, Na_2O, Fe_2O_3, K_2O), base metals, and LFSE (e.g. Ba) vary within each alteration assemblage. Results from SWIR analysis of white micas indicate a systematic change from phengite (Mg-rich) in the weakly altered hanging wall rocks to muscovite (K-rich) in the strongly altered volcanic rocks proximal to mineralization, progressing to more Na-rich paragonite in the sericite-quartz alteration assemblage immediately below the mineralized horizon. The combination of mass balance calculations of major and trace elements, coupled with alteration indices, such as CCPI, AI and the Collins index (Hg/Na_2O-Ba/Sr), can be used as vectors towards mineralization.

The Hurricane zone is interpreted to have formed via subseafloor replacement. Four diagnostic features of replacement style mineralization are apparent in the Hurricane stratigraphy (see Doyle and Allen, 2003), including: relicts of the host lithofacies (i.e. crystals and lapilli fragments) in the bedded massive sulphides; replacement fronts with the host lithofacies and the massive sulphide; rapid emplacement of the host lithofacies; and evidence of strong alteration in the hanging wall. It is interpreted that replacement was important for both the geometry of the deposit and likely influenced the high Zn-grades found within the mineralization. The Hurricane zone shows similar characteristics to other volcaniclastic hosted replacement-style VMS deposits globally (e.g. Rosebery, Hercules, Scuddles). Results from this study provide further insight to understanding the processes associated with subseafloor replacement in volcano-sedimentary basins and outlines the characteristics and controls of the alteration assemblages associated with these types of deposits. The multi-technique approach (i.e. lithostratigraphy, geochemistry, hyperspectral) provide valuable exploration techniques and results to better explore for VMS deposits in the Victoria Lake supergroup and in similar volcano-sedimentary belts globally.

2.10 Acknowledgements

Financial support for this project was provided by the National Sciences and Engineering Research Council of Canada (NSERC) Collaborative Research and Development Grant to S.J. Piercey. Additional funding was provided by NSERC-Altius Industrial Research Chair in Mineral Deposits (supported by NSERC, Altius Resources Inc and the Research and Development Corporation of Newfoundland and Labrador), and SEG Canada Graduate Fellowship to English. Logistics and support provided by Canadian Zinc Corporation, with special thanks to Diane Fost, Alexandria Marcotte, Andrew Hussey and Gerry Squires for their field and technical support.

2.11 References

Allen, R.L. 1994. Synvolcanic, subseafloor replacement model for Rosebery and other massive sulfide ores. In: Cook, D.R., Kitto, P.A. (Eds.), Contentious Issues in Tasmania Geology. *Geological Society of Australia Abstracts*, v. 39. p. 107-108.

AusSpec International, 2008. Spectral Interpretation Field Manual: GMEX, Edition 3, Volumes 1-10.

Banville, R., Huard, A., Sheppard, D., Woods, G., and Drolet, B., 1998. Assessment report on geological, geochemical, geophysical and diamond drilling exploration for 1997 submission for the Anglo-Newfoundland Development Limited Charter, Reid Lots 227, 229, 234 and 247 and fee simple grants. Volume 1 folio 61 and volume 2 folio 29 in the Victoria Lake-Red Indian Lake areas, central Newfoundland, 10 reports. [012A/1015]

Barbour, D.M., and Thurlow, J.G., 1982. Case histories of two massive sulphide discoveries in central Newfoundland. *In* Prospecting in Areas of Glaciated Terrain. Canadian Institute of Mining and Metallurgy, p. 300-320.

Barrett, T.J., and MacLean, W.H., 1991. Chemical, mass, and oxygen isotope changes during extreme hydrothermal alteration of an Archean rhyolite, Noranda, Quebec: *Economic Geology*, v. 86, p. 406-414.

Barrett, T.J., and MacLean, W.H., 1994. Chemostratigraphy and hydrothermal alteration in exploration for VHMS deposits in greenstones and younger rocks: in Lentz, D. R., ed., Alteration and Alteration Processes Associated with Ore-Forming Systems: Geological Association of Canada, Short Course Notes, v. 11, p. 433-467.

Barrett, T.J. & MacLean, W.H. 1999. Volcanic sequences, lithogeochemistry, and hydrothermal alteration in some bimodal volcanic-associated massive sulfide systems: *Reviews in Economic Geology,* 8, p. 101–131.

Barrett, T. J., MacLean, W. H., & Tennant, S. C. 2001. Volcanic sequence and alteration at the Parys Mountain volcanic-hosted massive sulfide deposit, Wales, United Kingdom: Applications of immobile element lithogeochemistry. *Economic Geology*, v. 96, p. 1279-1305.

Barrie, C.T., and Hannington, M.D., 1999. Introduction: classification of VMS deposits based on host rock composition, in volcanic-associated massive sulfide deposits: *Reviews in Economic Geology,* v. 8, p. 2-10.

Barrie, C.T., and Hannington, M.D., 1999. Classification of volcanic-associated massive sulphide deposits based on host-rock composition: *Reviews in Economic Geology*, v. 8, p. 1–11.

Barriga, F.J.A.S., and Fyfe, W.S., 1988. Giant pyritic base-metal deposits: The example of Feitais (Aljustrel, Portugal): Chemical Geology, v. 69, p. 331-343.

Boulter, C. A., Hopkinson, L. J., Ineson, M. G., & Brockwell, J. S. 2004. Provenance and geochemistry of sedimentary components in the Volcano-Sedimentary Complex, Iberian Pyrite Belt: discrimination between the sill–sediment-complex and volcanic-pile models. *Journal of the Geological Society*, v. 161, p. 103-115.

Buschette, M.J. and Piercey, S.J., 2016. Hydrothermal alteration and lithogeochemistry of the Boundary volcanogenic massive sulphide deposit, central Newfoundland, Canada. *Canadian Journal of Earth Sciences*, v. 53, p. 506-527.

Bradshaw, G. D., Rowins, S. M., Peter, J. M., & Taylor, B. E., 2008. Genesis of the Wolverine volcanic sediment-hosted massive sulfide deposit, Finlayson Lake district, Yukon, Canada: mineralogical, mineral chemical, fluid inclusion, and sulfur isotope evidence: *Economic Geology*, v. 103, p. 35-60.

Campbell, I.H., McDougall, T.J., and Turner, J.S., 1984. A note on fluid dynamic processes which can influence the deposition of massive sulfides: *Economic Geology*, v. 79, p. 1905-1913.

Collins, C.J., 1989. Report on lithogeochemical study of the Tally Pond Volcanics and associated alteration and mineralization, Unpublished Report for Noranda Exploration Company Limited (Assessment File 012A/1033 Newfoundland Department of Mines and Energy, Mineral Lands Division): St. John's, Newfoundland, p. 87.

Converse, D.R., Holland, H.D. and Edmond, J.M., 1984. Flow rates in the axial hot springs of the East Pacific Rise (21 N): Implications for the heat budget and the formation of massive sulfide deposits. *Earth and Planetary Science Letters*, v. 69, pp.159-175.

Date, J., Watanabe, Y., and Saeki, Y., 1983. Zonal alteration around the Fukazawa Kuroko deposits, Akita Prefecture, northern Japan: *Economic Geology Monograph,* v. 5, p. 365-386.

De Mark, P., and Dearin, C., 2007. Technical report on Tulks South Property. Map stake licenses: 11924 M and 11925 M and Ried Lot 228. Red Indian Lake area, central Newfoundland, Canada. NTS 12A/06 and 12A/11, p. 97.

Dearin, C., 2006. Technical report on the Tulks South Property. Map stake licenses: 11924M, 1925M and Ried Lot 228. Red Indian Lake area, central Newfoundland, Canada. NTS 12A/06 and 12A/11, p. 158.

Doyle, M.G., and Allen, R.L., 2003. Subsea-floor replacement in volcanic hosted massive sulfidedeposits: *Ore Geology Reviews*, v. 23, p. 183–222.

Doyle, M. G., & Huston, D. L. 1999. The subsea-floor replacement origin of the Ordovician Highway-Reward VMS deposit, Mount Windsor Subprovince, northern Queensland: *Economic Geology*, vol. 94, p. 825-844.

Dunning, G.R., Kean, B.F., Thurlow, J.G., Swinden, H.S., 1987. Geochronology of the Buchans, Roberts Arm, and Victoria Lake Supergroups and Mansfield Cove Complex, Newfoundland: *Canadian Journal of Earth Sciences*, v. 24, p. 1175-1184.

Dunning, G.R., Swinden, H.S., Kean, B.F., Evans, D.T.W., and Jenner, G.A., 1991. A Cambrian island arc in Iapetus: Geochronology and geochemistry of the Lake Ambrose volcanic belt, Newfoundland Appalachians: *Geological Magazine*, v. 128, p. 1–17.

Einsele, G., 1986. Interaction between sediments and basalt injections in young Gulf of California-type spreading centers: *Geologische Rundschau*, v. 75, p.197-208.

Einsele, G., Gieskes, J.M., Curray, J., Moore, D.M., Aguayo, E., Aubry, M.P., Fornari, D., Guerrero, J., Kastner, M., Kelts, K. and Lyle, M., 1980: Intrusion of basaltic sills into highly porous sediments, and resulting hydrothermal activity. *Nature*, v. 283, p. 441.

Evans, D.T.W., and Kean, B.F., 2002. The Victoria Lake Supergroup, central Newfoundland: its definition, setting and volcanogenic massive sulfide mineralization: Newfoundland and Labrador Department of Mines and Energy, Geological Survey, Open File NFLD/2790, p. 1-68.

Evans, D.T.W, Kean, B.F., and Jayasinghe, N.R., 1994a. Geology and mineral occurrences of Noel Paul's Brook. Map 94-222. Scale: 1:50 000. Newfoundland Department of Mines and Energy, Geological Survey Branch, Open File 012A/09/0685.

Evans, D.T.W, Kean, B.F., and Jayasinghe, N.R., 1994b. Geology and mineral occurrences of Badger. Map 94-224. Scale: 1:50 000. Newfoundland Department of Mines and Energy, Geological Survey Branch, Open File 012A/16/0687.

Evans, D.T.W., Kean, B.F., and Mercer, N.L., 1994. Geology and mineral occurrences of Lake Ambrose. Map 94-223. Scale: 1:50 000. Newfoundland Department of Mines and Energy, Geological Survey Branch, Open File 012A/10/0686. Blueline paper. GS# 012A/10/0686.

Eremin, N.I., Dergachev, A.L., Sergeeva, N.E., and Pozdnyakova, N.V., 2000. Types of volcanic-hosted massive sulphide deposits: *Geology of Ore Deposits*, v. 42, p. 160–171.

Fisher, R.V., 1966, Rocks composed of volcanic fragments and their classification: *Earth-Science Reviews*, v. 1, p. 287-298.

Franklin, J.M., Lydon, J.W., and Sangster, D.F., 1981. Volcanic-associated massive sulfide deposits: *Economic Geology 75th Anniversary Volume*, p. 485–627.

Franklin, J.M., Gibson, H.L., Jonasson, I.R., and Galley, A.G., 2005. Volcanogenic massive sulphide deposits. *In* 100th Anniversary volume, 1905-2005: *Economic Geology*, v. 100, p. 523-560.

Galley, A. G. 1993. Characteristics of semi-conformable alteration zones associated with volcanogenic massive sulphide districts: *Journal of Geochemical Exploration*, v. 48, p. 175-200.

Galley, A.G. 1995. The subsea-floor formation of volcanic-hosted massive sulfide: Evidence from Ansil Deposit, Royun-Noranda, Canada. *Economic Geology*, v. 90, pp. 2006-2017.

Galley, A. G., Hannington, M. D., & Jonasson, I. R., 2007. Volcanogenic massive sulphide deposits. Mineral deposits of Canada: A synthesis of major deposit-types, district metallogeny, the evolution of geological provinces, and exploration methods: Geological Association of Canada, Mineral Deposits Division, Special Publication, v. 5, p. 141-161.

Gemmell, J.B., and Fulton, R., 2001. Geology, genesis, and exploration implications of the footwall and hanging-wall alteration associated with the Hellyer volcanic-hosted massive sulphide deposit, Tasmania, Australia: *Economic Geology*, v. 96, p. 1003–1035.

Gemmell, J.B., and Large, R.R., 1992. Stringer system and alteration zones underlying the Hellyer volcanogenic massive sulphide deposit, Tasmania, Australia: *Economic Geology*, v. 87, p. 620–649.

Gibson, H.L., and D.H. Watkinson, 1990. Volcanogenic massive sulphide deposits of the Noranda cauldron and shield volcano, Quebec, in M. Rive, P. Verpaelst, Y. Gagnon, J.-M. Lulin, G. Riverin, A. Simard, eds., The Northwestern Quebec polymetallic belt: a summary of 60 years of mining exploration: Canadian Institute of Mining and Metallurgy Special Volume 43, v. 43, p. 119-132.

Hannington, M. D., 2014. Volcanogenic massive sulphide deposits, *In* Holland HD, Turekian KK (ed), Treatise on Geochemistry, 2nd ed.: Oxford, Elsevier, p. 463-488.

Hannington, M.D., Jonasson, I.R., Herzig, P.M., and Peterson, S., 1995. Physical and chemical processes of sea floor mineralization at mid-ocean ridges. Seafloor hydrothermal systems: Physical, chemical, biological, and geological interactions: *American Geophysical Union*, v. 91, p. 115-157.

Hannington M.D., Poulsen K.H., Thompson J.F.H., and Sillitoe R.H., 1999. Volcanogenic gold in the massive sulphide environment: *Reviews in Economic Geology*, v. 8, p. 325-356.

Hannington, M.D., de Ronde, C.D. and Petersen, S., 2005. Sea-floor tectonics and submarine hydrothermal systems: *Economic Geology, 100th Anniversary Volume*, v. 100, p. 111-142.

Hart, T.R., Gibson, H.L., and Lesher, C.M., 2004. Trace element geochemistry and petrogenesis of felsic volcanic rocks associated with volcanogenic massive Cu-Zn-Pb sulphide deposits: *Economic Geology*, v. 99, p. 1003–1013.

Herrmann, W., Blake, M., Doyle, M., Huston, D., Kamprad, J., Merry, N. and Pontual, S., 2001. Short wavelength infrared (SWIR) spectral analysis of hydrothermal alteration zones associated with base metal sulfide deposits at Rosebery and Western Tharsis, Tasmania, and Highway-Reward, Queensland: *Economic Geology*: v. 96, p. 939–955.

Hinchey, J.G., 2007. Volcanogenic massive sulphides of the southern Tulks volcanic belt, central Newfoundland: Preliminary findings, overview of styles and environments of mineralization, *in* Pereira, C.P.G., and Walsh, D.C., eds., St. John's, Newfoundland, Geological Survey Branch: *Current Research Report 2007-1,* p. 117-142.

Hinchey, J.G., 2011a. The Tulks volcanic belt, Victoria Lake Supergroup, central Newfoundland: Geology, tectonic setting, and volcanogenic massive sulfide mineralization, St. John's, NL, Canada, Newfoundland and Labrador Department of Natural Resources, Geological Survey: *Current Research Report 2011-02*, p. 167.

Hinchey, J.G., 2011b. Visible/infrared spectroscopy (VIRS) of volcanogenic massive sulphide hydrothermal alteration products, Tulks volcanic belt, Central Newfoundland: An additional exploration technique? Newfoundland and Labrador Department of Natural Resources, Geological Survey: *Current Research Report 2011-1*, p. 97-108.

Hinchey, J.G., McNicoll, V., Pereira, C.P.G. and Walsh, D.G., 2009. Tectonostratigraphic architecture and VMS mineralization of the southern Tulks Volcanic Belt: new insights from U-Pb geochronology and lithogeochemistry. Newfoundland and Labrador Department of Natural Resources, Geological Survey: *Current Research Report 2009-1*, p. 13-42.

Hinchey, J.G., McNicoll, V. 2016. The Long Lake group: an update on U-Pb geochronological studies. Current Research. Newfoundland and Labrador Department of Natural Resources Geological Survey: *Current Research Report 2016-1*, p. 27-38.

Hodgson, C.J. and Lydon, J.W., 1977. Geological setting of volcanogenic massive sulphide deposits and active hydrothermal systems: some implications for exploration. *Canadian Institute of Mining and Metallurgy Bulletin*, v. 70, pp.95-106.

Hutchinson, R.W., 1973. Volcanogenic sulphide deposits and their metallogenic significance: *Economic Geology*, v. 68, p. 1223-1246.

Jenner, G.A., 1996. Trace element geochemistry of igneous rocks: Geochemical nomenclature and analytical geochemistry: *in* Wyman, D.A., ed., Trace Element Geochemistry of Volcanic Rocks: Applications for Massive Sulfide Exploration: Geological Association of Canada, Short Course Notes, v. 12, p. 51–77.

Jones, S., 2005. Short wavelength infrared spectral characteristics of the HW horizon: Implications for exploration in Myra Falls volcanic-hosted massive sulfide camp, Vancouver Island, British Columbia, Canada: *Economic Geology*, v. 100, p. 273-94.

Kean, B.F., 1977. Geology of the Victoria Lake map area (12A/06), Newfoundland. Newfoundland Department of Mines and Energy, Mineral Development Division: *Current Research Report 1977-4*, p. 11.

Kean, B.F., 1979a. Star Lake, Newfoundland. Map 79-001. Scale 1:50,000. Newfoundland Department of Mines and Energy, Mineral Development Division (with descriptive notes).

Kean, B.F., 1979b. Buchans, Newfoundland. Map 79-125. Scale 1:50,000. Newfoundland Department of Mines and Energy, Mineral Development Division (with descriptive notes).

Kean, B.F., 1982. Victoria Lake, Newfoundland. Map 82-009. Scale: 1:50,000. Government of Newfoundland and Labrador, Department of Mines and Energy, Mineral Development Division.

Kean, B.F., 1983. King George IV Lake, Grand Falls district, Newfoundland. Map 82-051. Scale 1:50,000. *In* Geology of the King George IV Lake map area (12A/4). Newfoundland Department of Mines and Energy, Mineral Development Division: Report 1983-04, p. 1-74.

Kean, B.F., Dean, P.L., and Strong, D.F., 1981. Regional geology of the Central Volcanic Belt of Newfoundland: Geological Association of Canada Special Paper, v. 22, p. 65-78.

Kean, B.F., and Jayasinghe, N.R., 1980. Noel Pauls Brook, Newfoundland. Map 80-019. Scale: 1:50,000. Geology of the Lake Ambrose (12-A/10) – Noel Pauls Brook (12-A/9) map areas, central Newfoundland: Newfoundland Department of Mines and Energy, Mineral Development Division, Report v. 80-02, p. 33. 2 maps.

Kean, B.F., and Jayasinghe, N.R., 1982. Geology of the Badger map area (12-A/16), Newfoundland. Newfoundland Department of Mines and Energy, Mineral Development Division: *Current Research Report 1981-2*, p. 42.

Kean, B.F., and Mercer, N.L., 1981. Grand Falls, Newfoundland. Map 81-099. Scale 1:50,000 Newfoundland Department of Mines and Energy, Mineral Development Division.

Knuckey, M.J., Comba, C.D.A., and Riverin, G., 1982. Structure, metal zoning and alteration at the Millenbach deposit, Noranda, Quebec: Geological Association of Canada Special Paper 25, v. 25, p. 255–295.

Large, R.R., 1992. Australian volcanic-hosted massive sulphide deposits: features, styles and genetic models: *Economic Geology*, v. 87, p. 471-510.

Large, R. R., McPhie, J., Gemmell, J. B., Herrmann, W., & Davidson, G. J. 2001a. The spectrum of ore deposit types, volcanic environments, alteration halos, and related exploration vectors in submarine volcanic successions: some examples from Australia: *Economic Geology*, v. 96, p. 913-938.

Large, R. R., Allen, R. L., Blake, M. D., & Herrmann, W. 2001b. Hydrothermal alteration and volatile element halos for the Rosebery K lens volcanic-hosted massive sulfide deposit, western Tasmania: *Economic Geology*, v. 96, p. 1055-1072.

Lentz, D.R., 1998. Petrogenetic evolution of felsic volcanic sequences associated with Phanerozoic volcanic-hosted massive sulphide systems: The role of extensional geodynamics: *Ore Geology Reviews*, v. 12, p. 289–327.

Lesher, C.M., Goodwin, A.M., Campbell, I.H., and Gorton, M.P., 1986. Trace-element geochemistry of ore-associated and barren, felsic metavolcanics rocks in the Superior province, Canada: *Canadian Journal of Earth Sciences*, v. 23, p. 222–237.

Lydon, J.W., 1984. Ore deposits models: Volcanogenic massive sulfide deposits. Part 1: A descriptive model: *Geoscience Canada*, v. 11, p. 195-202.

Lydon, J.W., 1988. Volcanogenic sulphide deposits. Part 2: Genetic models: *Geoscience Canada,* v. 15, p. 43-65.

MacLean, W.H., 1988. Rare earth element mobility at constant inter-REE ratios in the alteration zone at the Phelps Dodge massive sulphide deposit, Matagami, Quebec: *Mineralium Deposita*, v. 23, p. 231–38.

MacLean, W, H., 1990. Mass change calculations in altered rock series: *Mineralium Deposita*, v. 25, p. 44-49.

MacLean, W. H., and Barrett, T. J., 1993. Lithogeochemical techniques using immobile elements: *Journal of geochemical exploration*, v. 48-2, p. 109-133.

MacLean, W.H., and Kranidiotis, P., 1987. Immobile elements as monitors of mass transfer in hydrothermal alteration: Phelps Dodge massive sulfide deposit, Matagami, Quebec: *Economic Geology*, v. 82, p. 951-962.

McNicoll, V., Squires, G., Kerr, A., and Moore, P.J., 2010. The Duck Pond and Boundary Cu–Zn deposits, Newfoundland: New insights into the ages of host rocks and the timing of VHMS mineralization: *Canadian Journal of Earth Sciences*, v. 47, p. 1481–1506.

McPhie, J., Doyle, M., and Allen, R.L., 1993. Volcanic textures: A guide to the interpretation of textures in volcanic rocks: Centre for Ore Deposit and Exploration Studies, University of Tasmania, Hobart, Australia, p. 198.

Morton, R.L., and Franklin, J.M., 1987. Two-fold classification of Archean volcanic-associated massive sulphide deposits: *Economic Geology*, v. 82, p. 1057–1063.

Ohmoto, H., 1996. Formation of volcanogenic massive sulfide deposits: The Kuroko perspective: *Ore Geology Reviews*, v. 10, p. 135-177.

Pearce, J., 1996. A users guide to basalt discrimination diagrams. *In* Wyman, D.A., ed., Trace element geochemistry of volcanic rocks: applications for massive sulphide exploration: Geological Association of Canada, Short Course Notes: v. 12, p. 79-113.

Pearce, J.A., Harris, N.B. and Tindle, A.G., 1984. Trace element discrimination diagrams for the tectonic interpretation of granitic rocks: *Journal of petrology*, v. *25* p. 956-983.

Piercey, S.J. 2007. Volcanogenic Massive Sulphide (VMS) Deposits of the Newfoundland Appalachians, Canada: An Overview of their Setting, Classification, Grade-Tonnage Data, and Unresolved Questions. Newfoundland and Labrador Department of Natural Resources Geological Survey: *Current Research Report 2007-1*, p.169–178.

Piercey, S.J., 2009. Lithogeochemistry of volcanic rocks associated with volcanogenic massive sulfide deposits and applications to exploration, *in* Submarine Volcanism and Mineralization: Modern through ancient, (eds.) B. Cousens and S.J. Piercey: Geological Association of Canada, Short Course, p. 15-40.

Piercey, S., 2011. The setting, style, and role of magmatism in the formation of volcanogenic massive sulfide deposits: *Mineralium Deposita*, v. 46, p. 449–471

Piercey, S. J. (2015). A semipermeable interface model for the genesis of subseafloor replacement-type volcanogenic massive sulfide (VMS) deposits: *Economic Geology*, v. 110, p. 1655-1660.

Piercey, S.J., Squires, G.C., and Brace, T.D., 2014. Lithostratigraphic, hydrothermal, and tectonic setting of the Boundary volcanogenic massive sulfide deposit, Newfoundland Appalachians, Canada: Formation by subseafloor replacement in a Cambrian rifted arc: *Economic Geology*, v. 109, p. 661–687.

Piercey, S. J., and J. Hinchey., 2012. Volcanogenic massive sulphide (VMS) deposits of the Central Mineral Belt, Newfoundland. *In* Geological Association of Canada–Mineralogical Association of Canada Joint Annual Meeting, Field Trip Guidebook B4. Newfoundland and Labrador Department of Natural Resources, Geological Survey, Open File NFLD/3173.

Peter, J. M., 2003. Ancient iron formations: their genesis and use in the exploration for stratiform base metal sulphide deposits, with examples from the Bathurst Mining Camp, *in* Lentz, D. R., ed., Geochemistry of Sediments and Sedimentary Rocks: Secular Evolutionary Considerations to Mineral Deposit-Forming Environments, Geological Association of Canada, GEOtext v. 4, p. 145-176.

Riley, G.C., 1957. Red Indian Lake (west half), Map 8-1957. Scale: 1: 125,000. Newfoundland. Geological Survey of Canada, (with descriptive notes).

Riverin, G., and Hodgson, C.J., 1980. Wall-rock alteration at the Millenbach Cu-Zn mine, Noranda, Quebec: *Economic Geology*, v. 75, p. 424-444.

Rogers, N., van Staal, C. R., Pollock, J., and Zagorevski, A., 2005. Map NTS 12-A/10 and part of 12-A/15. Scale 1:50,000. Geology, Lake Ambrose and part of Buchans, Newfoundland.

Rogers, N., van Staal, C., McNicoll, V., Pollock, J., Zagorevski, A., & Whalen, J., 2006. Neoproterozoic and Cambrian arc magmatism along the eastern margin of the Victoria Lake Supergroup: A remnant of Ganderian basement in central Newfoundland?: Precambrian Research, v. 147, p. 320-341.

Ross, P.S., and Bédard, J.H., 2009. Magmatic affinity of modern and ancient subalkaline volcanic rocks determined from trace-element discriminat diagrams: Canadian Journal of Earth Science, v. 46, p. 823-839.

Ruks, T.W., Piercey, S.J., Ryan, J.J., Villeneuve, M.E. and Creaser, R.A., 2006. Mid-to late Paleozoic K-feldspar augen granitoids of the Yukon-Tanana terrane, Yukon, Canada: Implications for crustal growth and tectonic evolution of the northern Cordillera: *Geological Society of America Bulletin*, v. 118 p. 1212-1231.

Saeki, Y., and Date, J., 1980. Computer application to the alteration data of the footwall dacite lava at the Ezuri Kuroko deposits, Akito Prefecture: *Mining Geology*, v. 30, p. 241–250.

Sawkins, F.J., 1976. Massive sulphide deposits in relation to geotectonics: *Geological Association of Canada Special Paper 14*, p. 222–240.

Schardt, C., and Large, R.R., 2009. New insights into the genesis of volcanic-hosted massive sulfide deposits on the seafloor from numerical modeling studies: *Ore Geology Reviews*, v. 35, p. 333-351.

Shanks, W.,C. 2001. Stable isotopes in seafloor hydrothermal systems: vent fluids, hydrothermal deposits, hydrothermal alteration, and microbial processes: *Reviews in Mineralogy and Geochemistry*, v. 43, p. 469-525.

Shervais, J.W., 1982. Ti-V plots and the petrogenesis of modern and ophiolitic lavas: *Earth and planetary science letters*, *v. 59*, p. 101-118.

Spitz, G., and Darling, R., 1978. Major and minor element lithogeochemical anomalies surrounding the Louvem copper deposit, Val d'Or, Quebec: *Canadian Journal of Earth Sciences*, v. 15, p. 1161–1169.

Squires, G.C., and Moore, P.J., 2004. Volcanogenic massive sulphide environments of the Tally Pond Volcanics and adjacent area: Geological, lithogeochemical and geochronological results, *in* Pereira, C.P.G., Walsh, D.G., and Kean, B.F., eds., St. John's, Newfoundland, Geological Survey Branch: *Current Research Report 2004-1,* p. 63-91.

Squires, G.C., Brace, T.D., and Hussey, A.M., 2001. Newfoundland's polymetallic Duck Pond deposit: Earliest Iapetan VMS mineralization formed within a sub-seafloor, carbonate-rich alteration system, *in* Evans, D.T.W., and Kerr, A., eds., Geology and mineral deposits of the northern Dunnage zone, Newfoundland Appalachians: St. John's, Newfoundland, Geological Association of Canada-Mineralogical Association of Canada: *Field Trip Guide A2*, p. 167–187.

Squires, G., Tallman, P., Sparkes, K., Hyde, D., House, F, .and Regular, K., 2005. Messina Minerals' new Boomerang VMS discovery: Preliminary evaluation of a sub-seafloor replacement-style massive sulphide deposit. CIMM Newfoundland Branch Meeting: Program with Abstracts p. 15.

Squires, G., Sparkes, K., House, F., Lodge, R., 2008. Ninth year assessment report on prospecting, metallurgical testing, resource estimation and geochemical, geophysical, and diamond drilling exploration for licenses 11924M-11925M on claims Tulks River area, central Newfoundland, 5 reports, N.T.S. 12A/06 for Messina Minerals Incorporated, Newfound and Labrador Geological Survey, p. 1-1149.

Swinden, H.S., 1990. Regional geology and metallogeny of central Newfoundland. *In* Metallogenic Framework of Base and Precious Metal Deposits, Central and Western Newfoundland. *Edited by* H.S. Swinden, D.T.W. Evans and B.F. Kean. Eighth IAGOD Symposium Field Trip Guidebook. Geological Survey of Canada: Open File 2156, p. 1-27.

Swinden, H.S., Jenner, G.A., Kean, B.F., and Evans, D.T.W., 1989. Volcanic rock geochemistry as a guide for massive sulfide exploration in central Newfoundland: Newfoundland Department of Mines: *Current Research Report 1989-1*, p. 201–219.

Swinden, H.S. 1991. Paleotectonic settings of volcanogenic massive sulphide deposits in the Dunnage Zone, Newfoundland Appalachians: *Canadian Institute of Mining and Metallurgy Bulletin*, v. 84, p. 59–89.

Swinden, H. S., Jenner, G. A., and Szybinski, Z. A., 1997, Magmatic and tectonic evolution of the Cambrian-Ordovician Laurentian margin of Iapetus: Geochemical and isotopic constraints from the Notre Dame subzone, Newfoundland, *in* Sinha, A. K., Whalen, J. B., and Hogan, J. P., eds., The Nature of Magmatism in the Appalachian Orogen: Boulder, Colorado: *Geological Society of America Memoir*, v. 191, p. 337-365.

Tallman, P., 2006. Block modeling and grade variance of Messina Minerals' Boomerang massive sulphide deposit, central Newfoundland. Canadian Institute of Mining, Metallurgy and Petroleum, Newfoundland Branch. 53rd Annual Conference and Trade Show, Abstract volume, p. 18.

Thompson, A. J., Hauff, P. L., & Robitaille, A. J. 1999. Alteration mapping in exploration: application of short-wave infrared (SWIR) spectroscopy. *SEG Newsletter*, v. 39, p. 16-27.

van Staal, C.R., 2007, Pre-Caroniferous tectonic evolution and metallogeny of the Canadian Appalachians, *in* Goodfellow, W.D., ed., Mineral Deposits of Canada: A Synthesis of Major Deposit-Types, District Metallogeny, the Evolution of Geological Provinces, and Exploration Methods: Geological Association of Canada, Mineral Deposits Division, Special Publication No. 5, p. 793-818.

van Staal, C.R. and Barr, S.M. 2012. Lithospheric architecture and tectonic evolution of the Canadian Appalachians and associated Atlantic margin. Chapter 2 *In* Tectonic Styles in Canada: the LITHOPROBE Perspective. *Edited by* J.A. Percival, F.A. Cook, and R.M. Clowes. Geological Association of Canada, Special Paper 49, v. 49, p. 41-96.

Velde, B., 1978. Infrared spectra of synthetic micas in the series muscovite-MgAl celadonite: *American Mineralogist*, v. 63, p. 341-349.

White, J.D.L., and Houghton, B.F., 2006, Primary volcaniclastic rocks: *Geology*, v. 34, p. 677-680.

Williams, H., 1970, Red Indian Lake (east half), Newfoundland. Geological Survey of Canada, Map 1196A

Williams, H. 1979. Appalachian Orogen in Canada: *Canadian Journal of Earth Sciences*, v. 16: p. 792–807.

Williams, H., 1995, Geology of the Appalachian-Caledonian Orogen in Canada and Greenland. Geological Survey of Canada: *Temporal and Spatial Divisions*; Chapter 2, v. 6, p. 21-44.

Williams, H., Colman-Sadd, S.P., and Swinden, H.S., 1988., Tectonicstratigraphic subdivisions of central Newfoundland. *In Current Research*, Part B. Geological Survey of Canada, Paper 88-1B, p. 91–98.

Winchester, J.A. and Floyd, P.A., 1976. Geochemical magma type discrimination: application to altered and metamorphosed basic igneous rocks: *Earth and Planetary Science Letters*, v. 28, p. 459-469.

Yang, K., Huntington, J.F., Gemmell, J.B., Scott, K.M., 2011. Variations in composition and abundance of white mica in the hydrothermal alteration system at Hellyer, Tasmania, as revealed by infrared reflectance spectroscopy: *Journal of Geochemical Exploration*, v. 108, p. 143-156.

Zagorevski, A., Rogers, N., van Staal, C.R., McNicoll, V., Lissenberg, C.J., and Valverde-Vaquero, P., 2006, Lower to Middle Ordovician evolution of peri-Laurentian arc and back-arc complexes in the Iapetus: constraints from the Annieopsquotch Accretionary Tract, Central Newfoundland: *Geological Society of America Bulletin*, v. 118, p. 324–362.

Zagorevski, A., van Staal, C.R., McNicoll, V.J., and Rogers, N., 2007, Upper Cambrian to Upper Ordovician peri-Gondwanan island arc activity in the Victoria Lake Supergroup, central Newfoundland: Tectonic development of the northern Ganderian margin: *American Journal of Science*, v. 307, p. 339–370.

Zagorevski, A., van Staal, C.R., Rogers, N., McNicoll, V.J. and Pollock, J., 2010. Middle Cambrian to Ordovician arc-backarc development on the leading edge of Ganderia, Newfoundland Appalachians: *Geological Society of America Memoirs*, v. 206, p. 367-396.

Table 2.1a. Representative Whole-Rock Geochemistry of the HW Samples in the Hurricane Zone

Sample ID:	32178	32177	14521	25424	14535	14496
Hole ID:	GA-14-278	GA-14-278	GA-07-208	GA-07-254	GA-07-208	GA-06-147
Depth (m):	60.9	42.91	59.95	157.1	169.1	125.35
Deposit Location:	Hanging wall	Hanging wall	Hanging wall	Hanging wall	Hanging wall	Hanging wall
Lithology:	Coherent Felsic Flow	Porphyritic Felsic Flow	Crystal Tuff	Heterolithic Tuff	Crystal Lithic Tuff	Mafic Sill
SiO_2 (wt %)	83.72	67.16	49.62	64.17	61.16	50.27
Al_2O_3 (wt %)	9.62	13.27	19.13	15.67	16.67	16.19
Fe_2O_3 (wt %)	0.71	5.99	9.65	5.51	5.67	10.97
MnO (wt %)	0.01	0.04	0.12	0.05	0.06	0.17
MgO (wt %)	0.07	4.5	7.17	6.31	5.23	6.3
CaO (wt %)	0.13	0.3	2.08	0.19	0.61	3.1
Na_2O (wt %)	5.03	3.39	4.72	0.48	2.33	5.36
K_2O (wt %)	0.27	1.2	1.41	3.32	3.2	0.03
TiO_2 (wt %)	0.23	0.53	0.74	0.57	0.85	0.99
P_2O_5 (wt %)	0.04	0.06	0.06	0.07	0.11	0.09
LOI	0.22	3.54	5.87	4.6	4.12	7.21
Total	100	99.98	100.6	100.9	100.0	100.7
Hg (ppb)	2.5	6.0	2.5	2.5	2.5	2.5
Sc (ppm)	3	22	27	18	18	37
Be (ppm)	0.5	0.5	1	2	2	1
V (ppm)	15	164	223	45	50	380
Cr (ppm)	50	40	30	< 20	< 20	30
Co (ppm)	2	18	21	6	4	25
Ni (ppm)	10	10	< 20	< 20	< 20	< 20
Cu (ppm)	5	5	20	5	5	50
Zn (ppm)	15	90	90	60	110	90
Ga (ppm)	5	13	19	19	19	15
Ge (ppm)	0.25	0.25	1	1	1	1.3
As (ppm)	2.5	29	< 5	< 5	5	8
Rb (ppm)	3	15	24	51	54	< 1
Sr (ppm)	27	28	46	10	33	188
Y (ppm)	15.3	10.7	24.6	54.6	48.3	13.7
Zr (ppm)	88	59	104	212	171	42
Nb (ppm)	1.3	0.6	1.2	1.6	1.4	0.6
Mo (ppm)	3	1	< 2	< 2	< 2	< 2
Ag (ppm)	0.25	0.25	< 0.5	< 0.5	< 0.5	< 0.5
In (ppm)	0.05	0.05	< 0.1	< 0.1	< 0.1	< 0.1
Sn (ppm)	0.5	0.5	< 1	1	< 1	< 1
Sb (ppm)	0.1	0.1	< 0.2	< 0.2	0.4	0.7
Cs (ppm)	0.05	0.1	0.2	0.4	0.4	< 0.1
Ba (ppm)	173	227	538	1390	414	33
La (ppm)	7.44	4.7	8.6	20.3	17.9	4.36
Ce (ppm)	15.8	9.12	18.8	48.6	43.4	8.87
Pr (ppm)	1.75	1.00	2.32	6.47	5.85	1.16

Nd (ppm)	6.66	4.32	9.88	29.9	27.1	5.97
Sm (ppm)	1.69	1.1	2.82	8.08	7.16	1.7
Eu (ppm)	0.35	0.32	0.91	1.96	2.28	0.59
Gd (ppm)	1.84	1.33	3.67	9.05	8.53	2.08
Tb (ppm)	0.34	0.27	0.69	1.62	1.5	0.4
Dy (ppm)	2.41	1.89	4.5	10.3	9.25	2.57
Ho (ppm)	0.56	0.39	0.97	2.15	1.91	0.56
Er (ppm)	1.73	1.19	2.85	6.5	5.67	1.66
Tm (ppm)	0.29	0.20	0.44	0.99	0.85	0.24
Yb (ppm)	2.04	1.53	3.11	6.66	5.59	1.58
Lu (ppm)	0.34	0.26	0.52	1.06	0.91	0.25
Hf (ppm)	2.4	1.4	2.1	4.1	3.5	1
Ta (ppm)	0.03	0.005	0.18	0.18	0.18	0.1
W (ppm)	0.9	0.25	0.5	< 0.5	< 0.5	1.2
Tl (ppm)	0.025	0.06	< 0.05	0.12	0.09	< 0.05
Pb (ppm)	2.5	12	< 5	2.5	9	2.5
Bi (ppm)	0.05	0.05	< 0.1	< 0.1	< 0.1	< 0.1
Th (ppm)	5.2	3.07	4.63	4.6	3.75	0.77
U (ppm)	1.3	0.79	1.25	1.59	1.58	0.23

Table 2.1b. Representative Whole-Rock Geochemistry Samples in the FW of the Hurricane Zone

Sample ID:	14547	31769	14544	32200	14800
Hole ID:	GA-07-208	GA-10-273	GA-07-208	GA-14-278	GA-14-276
Depth (m):	328.3	267.8	273.6	309.3	311.6
Deposit Location:	Footwall	Footwall	Footwall	Footwall	Footwall
Lithology:	Crystal tuff	Tuff	Tuff	Tuff	Lapilli tuff
Alteration Type:	Least Altered	Sericite-quartz-chlorite-pyrite	Sericite-pyrite	Chlorite	Chaotic carbonate-chlorite
SiO_2 (wt %)	61.09	49.67	69.15	31.9	25.42
Al_2O_3 (wt %)	14.87	11.71	10.90	16.15	11.87
Fe_2O_3 (wt %)	5.64	14.42	7.12	12.31	4.39
MnO (wt %)	0.43	0.18	0.03	0.41	0.75
MgO (wt %)	3.89	7.31	0.31	18.6	12.86
CaO (wt %)	2.41	0.35	0.42	3.05	15.29
Na_2O (wt %)	2.56	0.13	0.52	0.63	0.25
K_2O (wt %)	1.49	1.61	2.52	0.53	2.43
TiO_2 (wt %)	0.57	0.49	0.40	0.75	0.46
P_2O_5 (wt %)	0.13	0.05	0.03	0.12	0.19
LOI	7.07	10.47	6.13	14.14	24.25
Total	100.20	96.37	97.52	98.60	98.16
Hg (ppb)	12	5010	479	454	23
Sc (ppm)	11	11	15	17	11
Be (ppm)	< 1	< 1	0.5	< 1	< 1
V (ppm)	91	133	108	142	79
Cr (ppm)	< 20	< 20	40	< 20	< 20
Co (ppm)	10	13	8	20	5
Ni (ppm)	< 20	< 20	10	< 20	< 20
Cu (ppm)	30	930	640	30	< 10
Zn (ppm)	400	> 10000	7680	3580	200
Ga (ppm)	14	16	11	21	13
Ge (ppm)	0.7	0.6	1.3	< 0.5	< 0.5
As (ppm)	21	335	136	55	19
Rb (ppm)	35	29	55	11	45
Sr (ppm)	39	9	28	35	138
Y (ppm)	19.9	24.7	20	16.9	24
Zr (ppm)	85	25	32	106	76
Nb (ppm)	2.3	< 0.2	0.1	3.1	1.8
Mo (ppm)	< 2	24	< 2	12	6
Ag (ppm)	< 0.5	7.5	1.7	0.6	< 0.5
In (ppm)	0.2	0.4	0.2	0.3	< 0.1
Sn (ppm)	< 1	10	1	2	5
Sb (ppm)	1.2	12.2	10	4.2	< 0.2
Cs (ppm)	0.30	0.20	0.30	0.10	0.30
Ba (ppm)	201	833	425	383	4466
La (ppm)	8.46	4.34	4.98	3.9	4.8
Ce (ppm)	18.00	10.80	10.50	11.50	13.30
Pr (ppm)	2.29	1.56	1.32	1.65	1.98

Nd (ppm)	9.51	7.44	5.7	8.12	9.74
Sm (ppm)	2.63	2.42	1.71	2.01	3.33
Eu (ppm)	0.79	0.29	0.35	0.25	0.74
Gd (ppm)	2.81	3.25	2.2	2.5	4.19
Tb (ppm)	0.54	0.66	0.45	0.45	0.7
Dy (ppm)	3.41	4.33	3.21	2.85	4.22
Ho (ppm)	0.74	0.92	0.69	0.62	0.85
Er (ppm)	2.22	2.55	2.08	1.96	2.51
Tm (ppm)	0.36	0.38	0.33	0.32	0.39
Yb (ppm)	2.51	2.42	2.14	2.38	2.54
Lu (ppm)	0.42	0.36	0.34	0.40	0.39
Hf (ppm)	1.8	< 0.1	0.7	2.9	2
Ta (ppm)	0.22	< 0.01	0.06	0.32	0.1
W (ppm)	1.1	15	2.3	3.5	1.1
Tl (ppm)	0.24	1.62	0.82	1.08	1.94
Pb (ppm)	19	9300	3990	2340	17
Bi (ppm)	< 0.1	9.6	< 0.1	0.3	0.4
Th (ppm)	2.45	1.48	0.4	2.36	1.93
U (ppm)	0.7	6.76	0.97	6.34	0.72

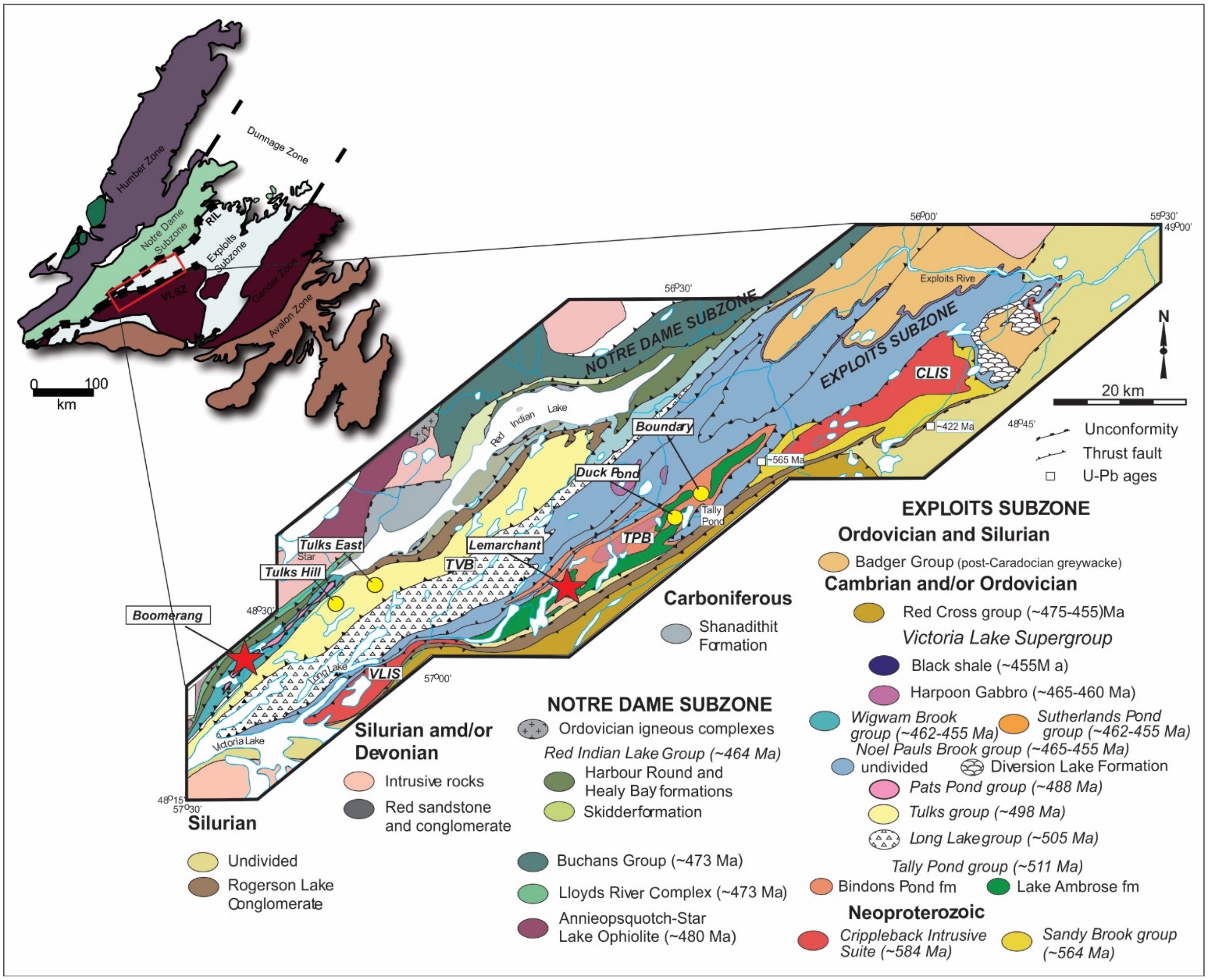

Figure 2-1. Location and geology of the area surrounding the Red Indian Lake, including the Victoria Lake supergroup (VLSG). Relevant deposits indicated in northern and southern parts of the VLSG. TVB- Tulks volcanic belt, VLIS- Valentine Lake intrusive suite, TPB- Tally Pond belt, CLIS- Crippleback Lake intrusive suite (modified from Rogers et al., 2006).

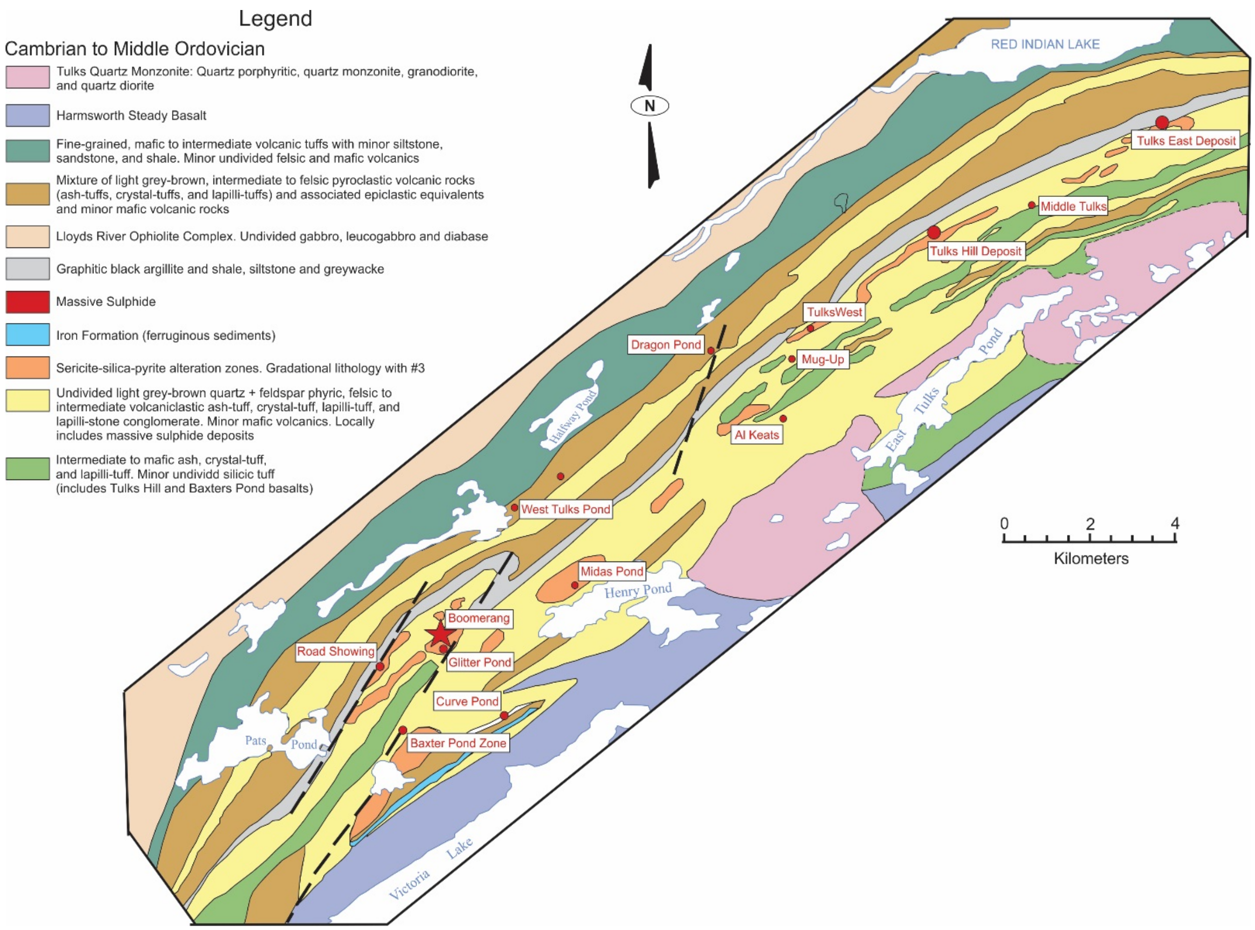

Figure 2-2. Geological map of the southern Tulks volcanic belt with known base-metal and precious metal VMS deposits indicated (modified from Hinchey, 2011a).

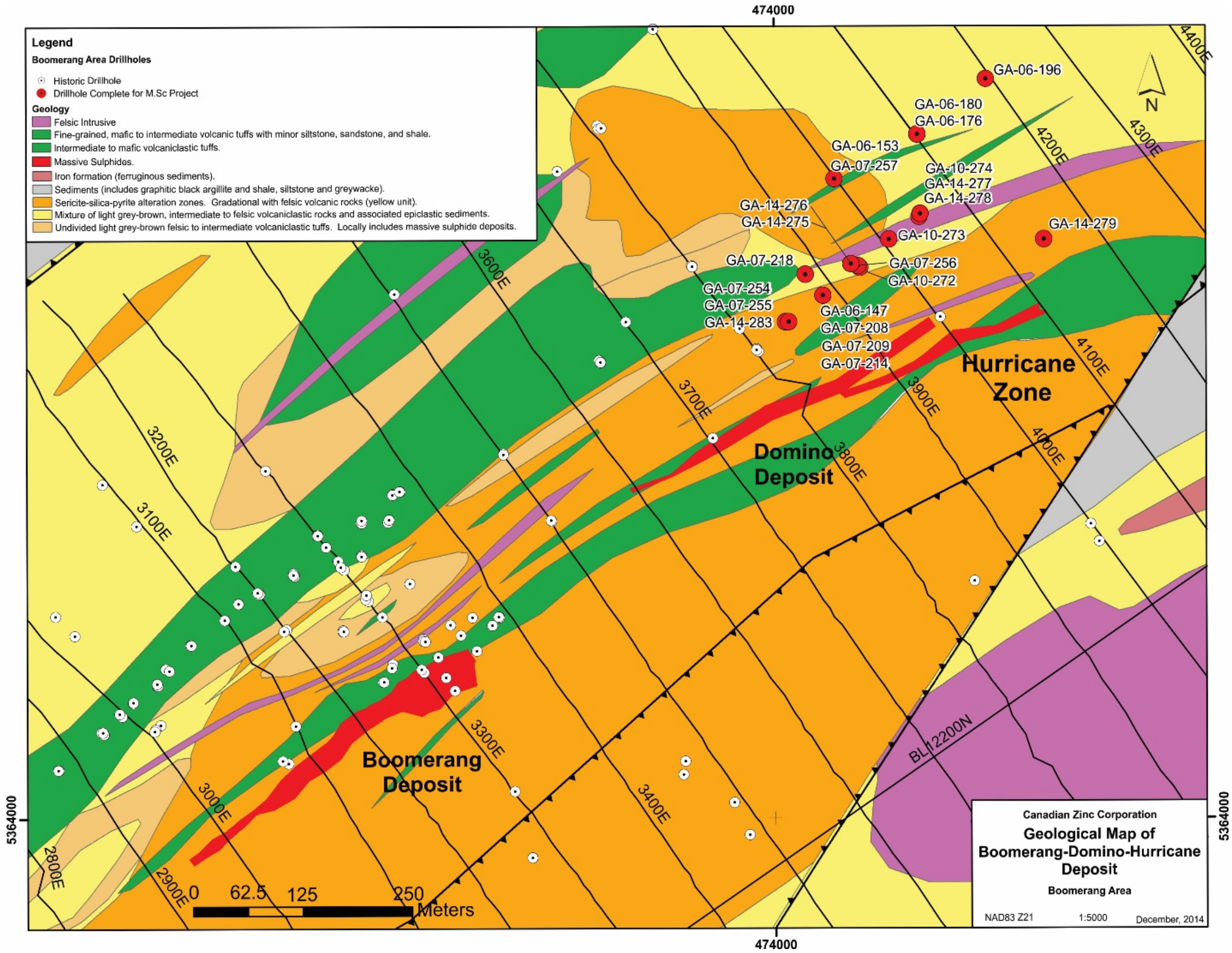

Figure 2-3. Geological map of the Boomerang-Domino-Hurricane deposit from surface mapping completed by Canadian Zinc Corporation. Ore zones of the Boomerang and Domino deposits and Hurricane zone are projected to surface (D. Copeland, personal communication, 2019).

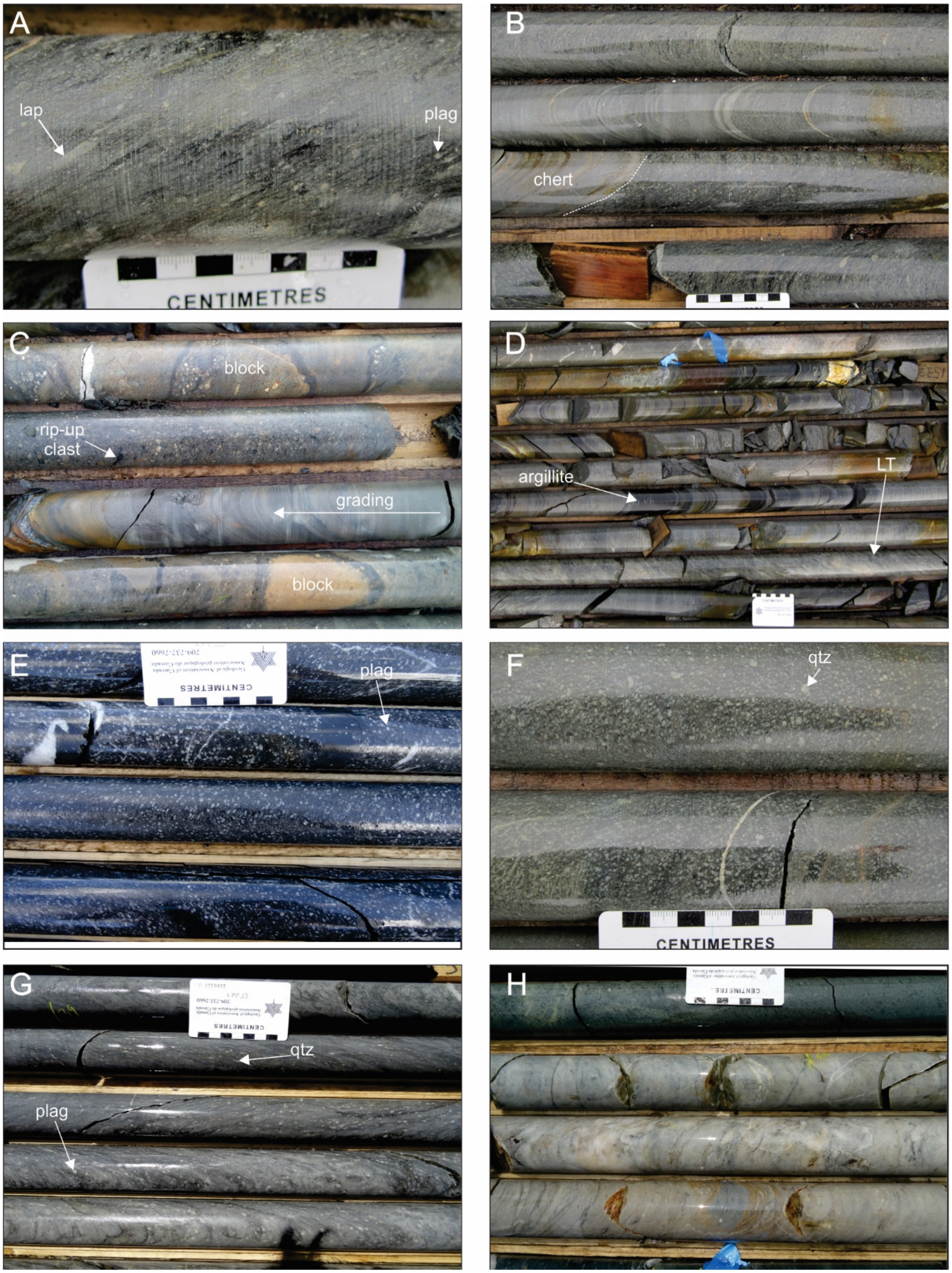

Figure 2-4. Major lithofacies that comprise the footwall and hanging wall stratigraphy in the Hurricane zone. (A) VCL1: weak to moderately sericite-silica-chlorite altered medium-grained, plagioclase-bearing crystal tuff. (B) VCL2: normally graded, medium-grained crystal-bearing tuff to lapilli tuff with thin chert interbeds. (C) VCL3: bedded fine- to coarse-grained lapilli tuffs with block-sized fragments. (D) VCL3:

normally graded, heterolithic, coarse-grained lapilli tuff to thinly bedded argillite. (E) VCL4: plagioclase-bearing crystal tuffs. (F) VCL4: quartz ± plagioclase crystal-bearing tuffs. (G) CL1a: plagioclase-quartz porphyritic felsic volcanic rocks (H) CL1b: aphyric felsic (rhyolite) volcanics. Abbreviations: plag- plagioclase crystals, lap- lapilli fragment, LT- lapilli tuff, qtz- quartz crystal.

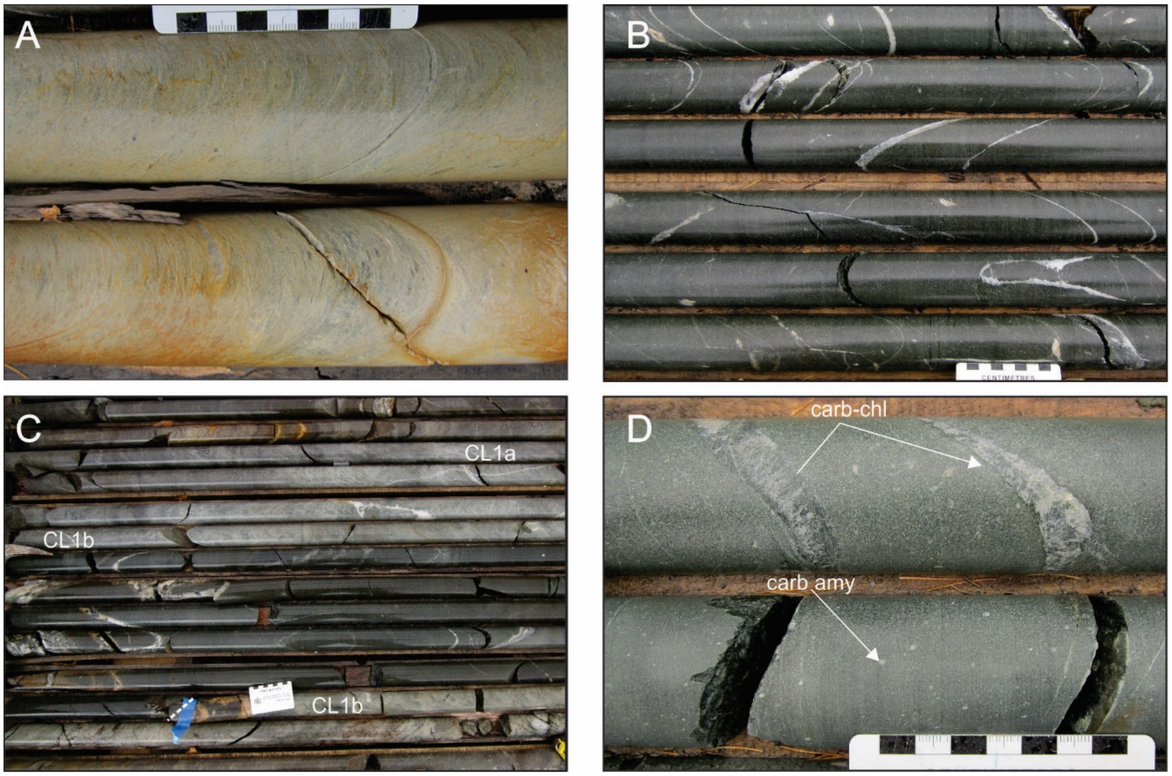

Figure 2-4. Intermediate to mafic intrusive rocks in the Hurricane zone. (A) Strongly sericite-quartz altered intermediate dyke within footwall. (B) Fine- to medium-grained mafic sills overlying footwall volcaniclastics with 0.5 to 2 cm thick carbonate-quartz veins. (C) Fine-grained, dark green-grey mafic dykes with sharp chilled margins along contact with CL1a and CL1b. (D) Close-up of mafic dyke with mm-scale carbonate amygdules and 1 cm calcite-chlorite veins. Abbreviations: carb-chl- carbonate-chlorite veins, carb amy- carbonate amygdules.

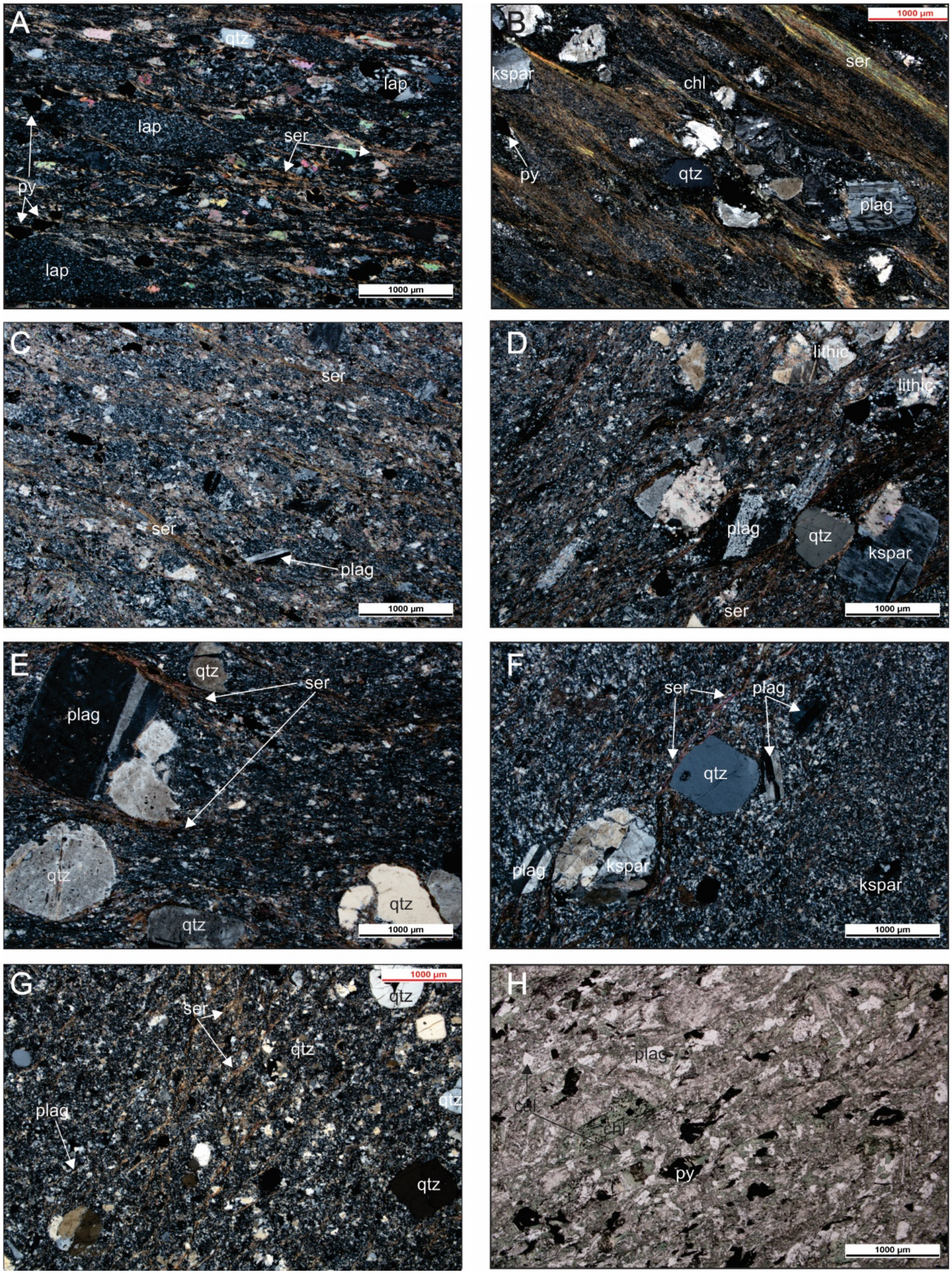

Figure 2-5. Photomicrographs of the volcaniclastic and volcanic lithofacies in the Hurricane zone. (A) Weakly altered footwall volcaniclastic (VCL1). Lapilli fragments and lesser quartz crystals within a fine-grained groundmass consisting of quartz-sericite alteration and rare medium-grained anhedral pyrite. (B) Moderately altered lithic, crystal tuff (VCL2) in the hanging wall above the mineralized horizon. The

sample contains wispy, banded sericite-chlorite-quartz alteration with rare anhedral pyrite. (C) Fine- to medium-grained crystal tuff with weak sericite alteration in the hanging wall (VCL3). (D) Medium- to coarse-grained crystal, lithic tuff (VCL3) with weak sericite alteration. (E) Plagioclase-quartz-bearing crystal tuff (VCL4). Weak sericite alteration is present in wispy thin bands parallel to foliation. (F) Quartz-plagioclase-phyric felsic volcanic rocks with fine-grained sericite within the matrix (CL1a). (G) Fine-grained felsic volcanic with rare fine-grained plagioclase and quartz phenocrysts (1CLb). (F) Medium-grained mafic dyke. All photomicrographs are in cross-polarized light except Fig. 2-6H, which is in plane-polarized light.

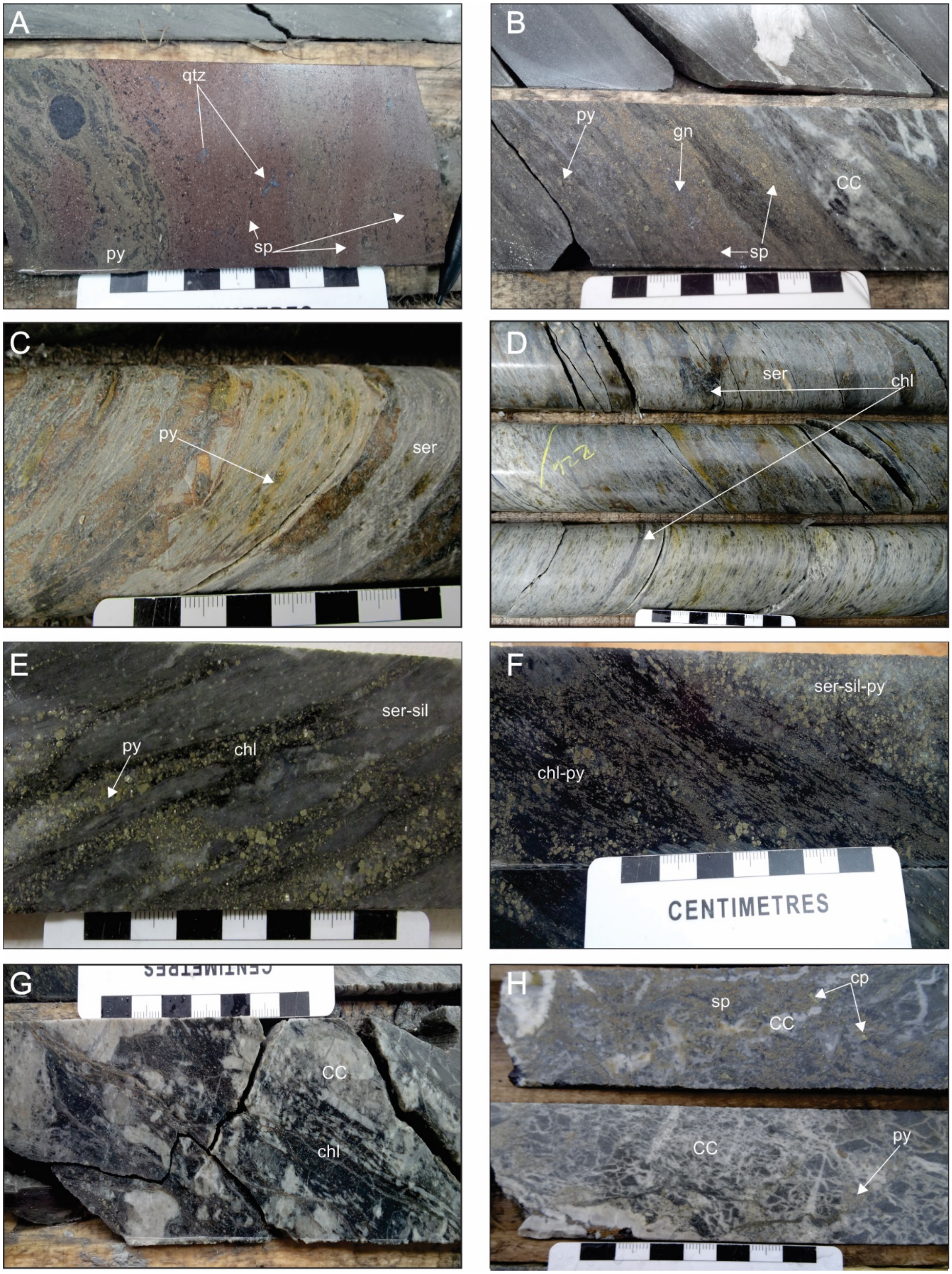

Figure 2-6. Mineralization and alteration from the Hurricane zone. (A) Banded pyrite with yellow and red sphalerite and lesser galena; note relict quartz grains in sulphide matrix. (B) Weakly banded pyrite, yellow and red sphalerite, and galena in strongly sericite and chlorite altered matrix with moderate chaotic carbonate and chlorite alteration. (C) Intense sericite-pyrite alteration. (D) Strong sericite-quartz alteration

with patchy-lath-like and stockwork chlorite. (E) Strong sericite and quartz alteration with chlorite-pyrite stockwork veins. (F) Intense chlorite and pyrite alteration. (G) Intense chaotic carbonate and chlorite alteration. (H) Dentritic chaotic carbonate alteration with disseminated pyrite, yellow and red sphalerite in chlorite-sericite matrix. Abbreviations: qtz- quartz, py- pyrite, sp- sphalerite, gn- galena, ser- sericite, chl- chlorite, CC- chaotic carbonate, cp- chalcopyrite.

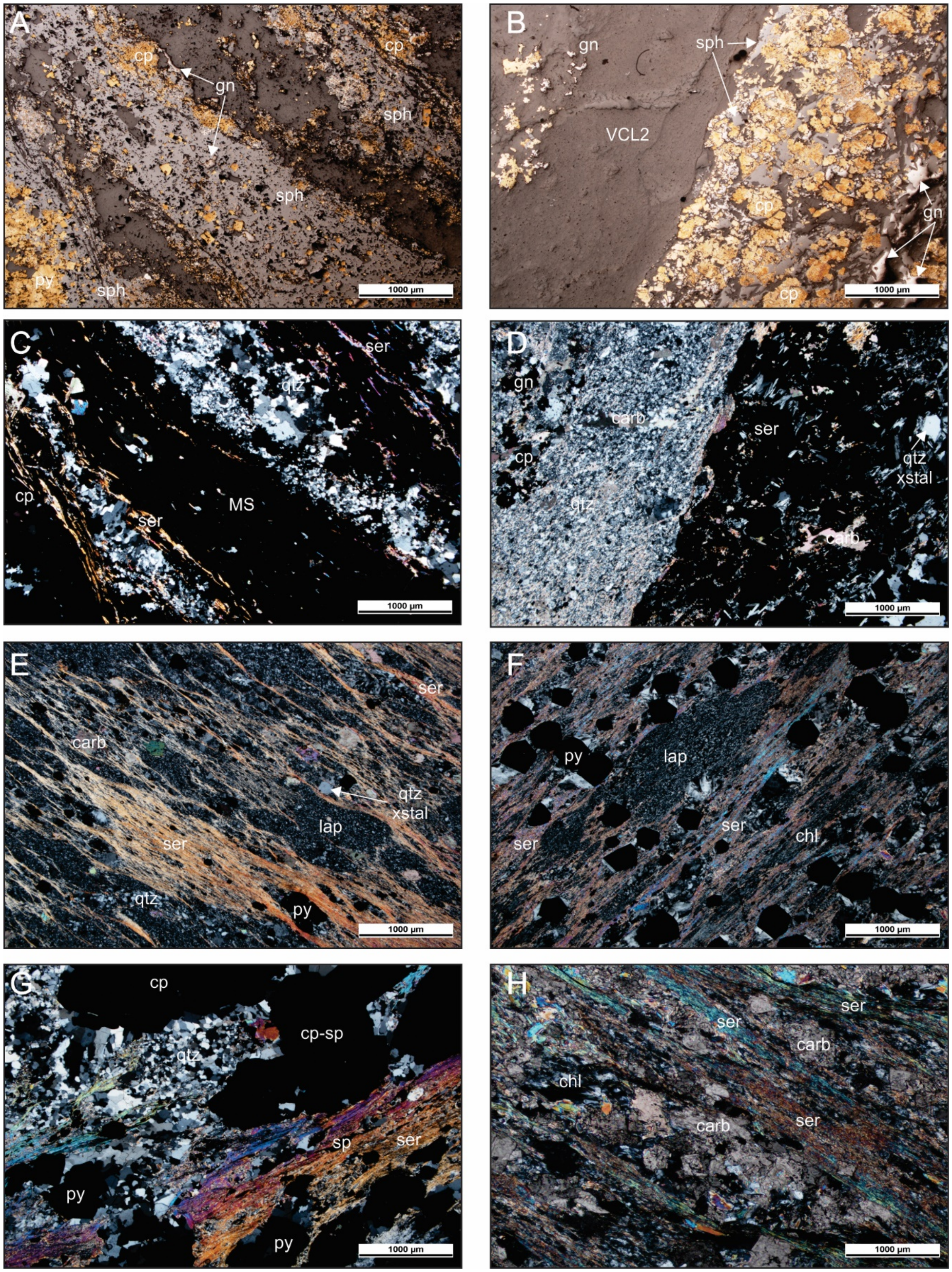

Figure 2-7. Photomicrographs of the footwall mineralization and alteration at the Hurricane zone. (A) Banded sphalerite, chalcopyrite, pyrite and lesser galena. (B) Sharp contact between bedded massive sulphide (chalcopyrite, sphalerite, pyrite and lesser galena) and VCL1 with rare massive sulphides in fine-grained volcaniclastic matrix. (C) Cross-polarized photomicrograph of Fig. 2-8a highlighting quartz-

sericite alteration associated with massive sulphide. (D) Cross-polarized photomicrograph of Fig. 2-8b illustrating sharp contact between massive sulphide and fine-grained volcaniclastic rock (VCL2), as well as sericite-carbonate-quartz alteration and relict quartz crystals in massive sulphide. (E) Moderately sericite-quartz-pyrite altered fine-grained lapilli tuff with rare carbonate alteration. (F) Moderate to strong sericite-chlorite-quartz-pyrite altered lapilli tuff. (G) Strong sericite-quartz-pyrite altered tuff with medium-grained chalcopyrite and sphalerite. (H) Distal chaotic carbonate and sericite alteration.

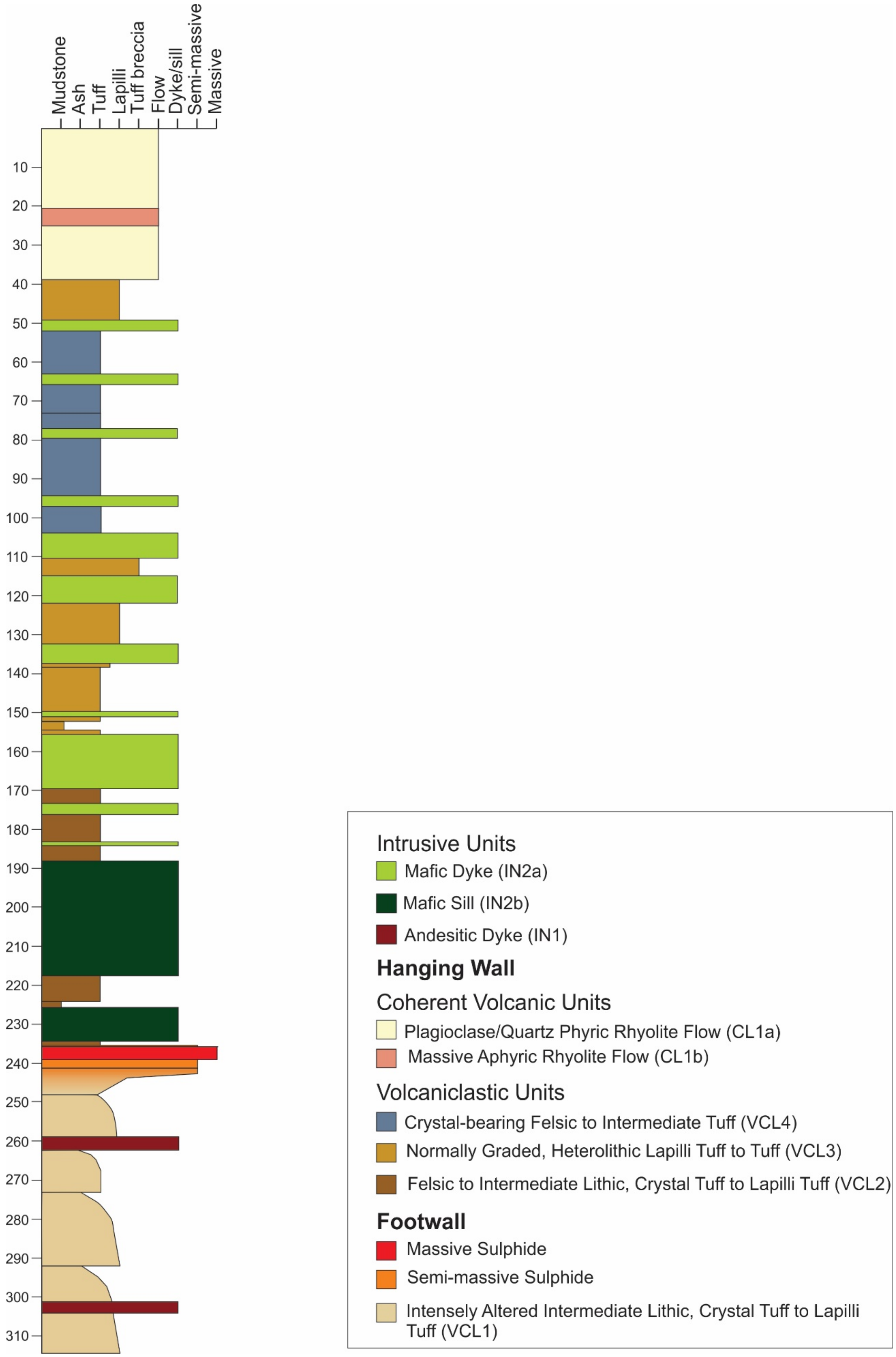
Mudstone
Ash
Tuff
Lapilli
Tuff breccia
Flow
Dyke/sill
Semi-massive
Massive
10
20
30
40
50
60
70
80
90
100
110
120
130
140
150
160
170
180
190
200
210
220
230
240
250
260
270
280
290
300
310
Intrusive Units
Mafic Dyke (IN2a)
Mafic Sill (IN2b)
Andesitic Dyke (IN1)
Hanging Wall
Coherent Volcanic Units
Plagioclase/Quartz Phyric Rhyolite Flow (CL1a)
Massive Aphyric Rhyolite Flow (CL1b)
Volcaniclastic Units
Crystal-bearing Felsic to Intermediate Tuff (VCL4)
Normally Graded, Heterolithic Lapilli Tuff to Tuff (VCL3)
Felsic to Intermediate Lithic, Crystal Tuff to Lapilli Tuff (VCL2)
Footwall
Massive Sulphide
Semi-massive Sulphide
Intensely Altered Intermediate Lithic, Crystal Tuff to Lapilli Tuff (VCL1)

Figure 2-8. Simplified stratigraphic section illustrating the relationship between the five lithofacies, intrusive units and the mineralized horizon in the Hurricane zone.

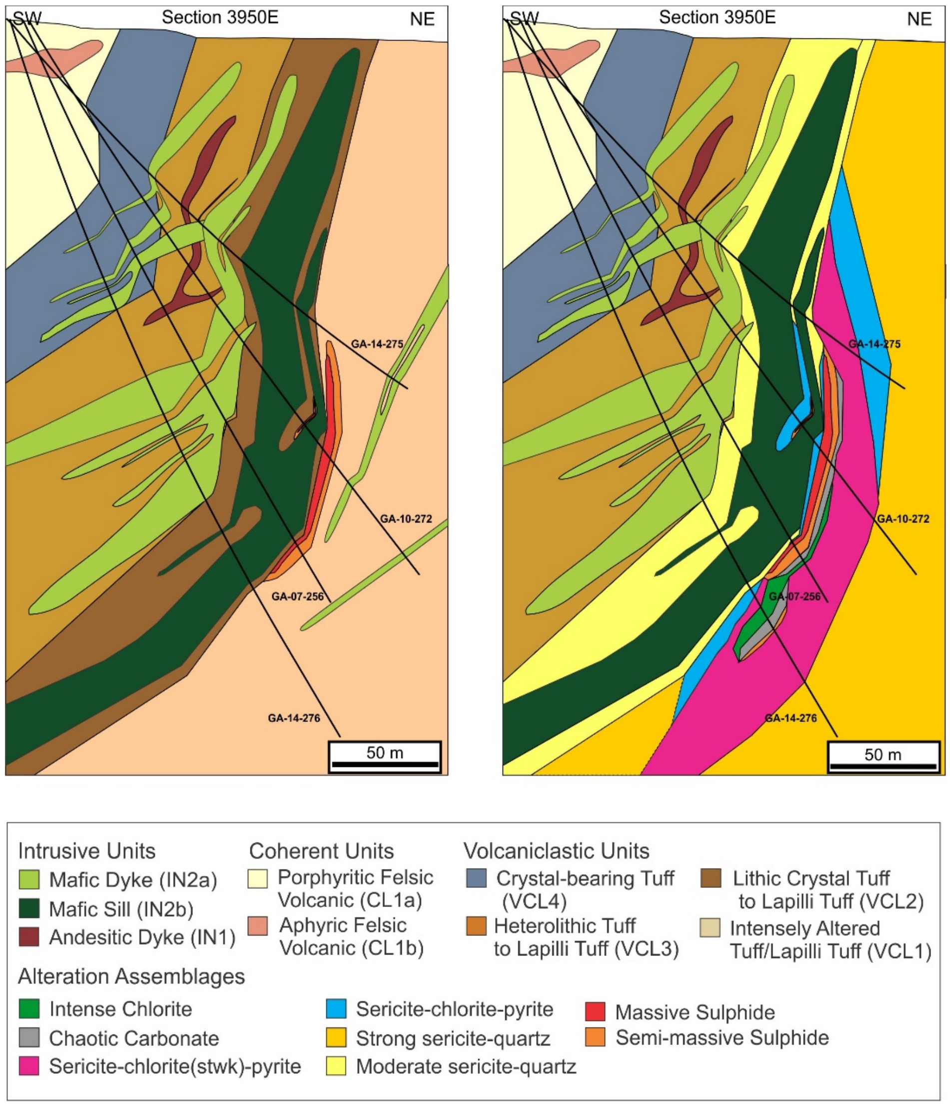

Figure 2-9. Simplified cross section illustrating the relationship between lithofacies and the alteration assemblages in the Hurricane zone.

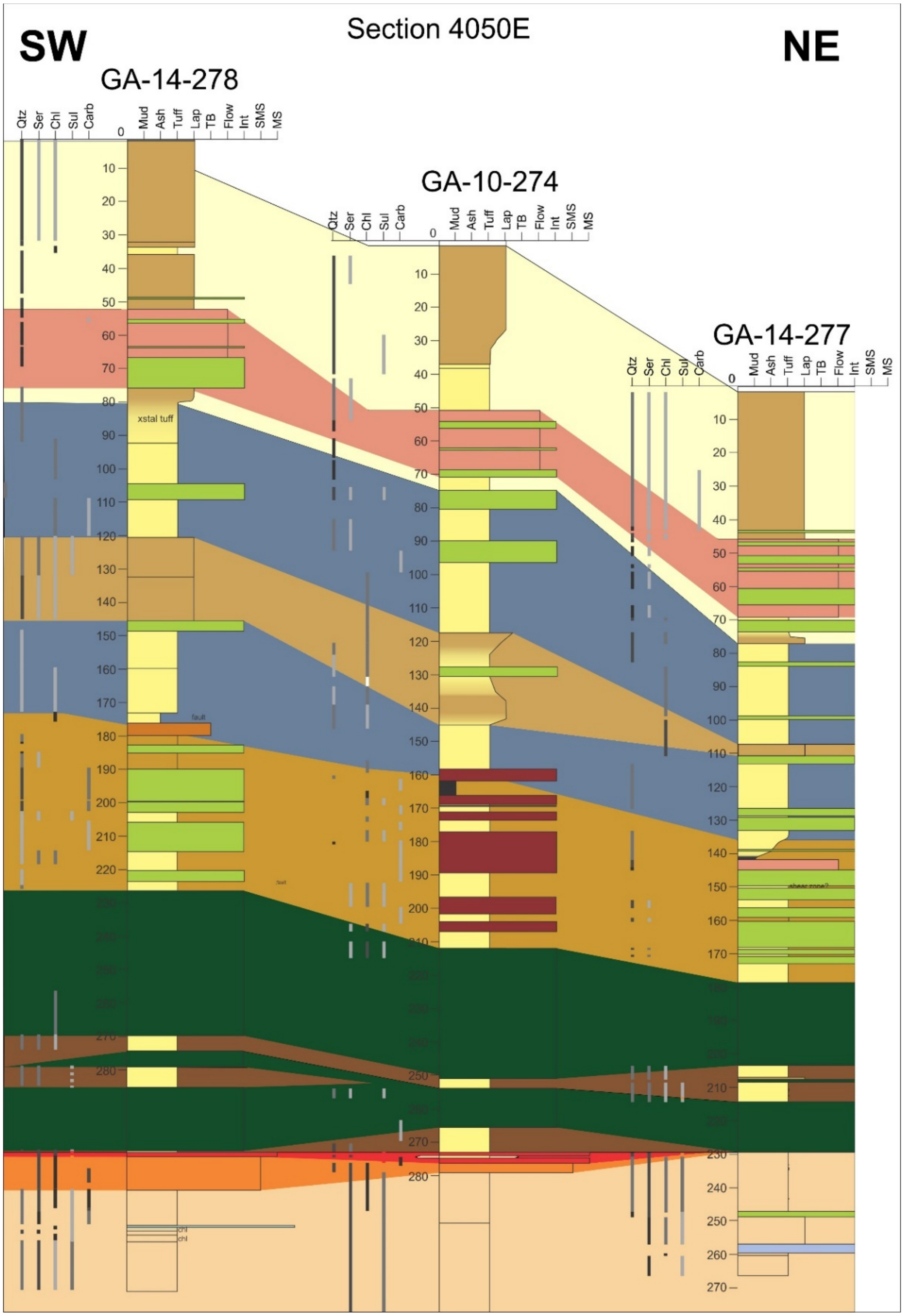

Figure 2-10. Simplified stratigraphic cross section of section 4050 with alteration intensities indicated. Legend is shown in Figure 2-7. Abbreviations Qtz- quartz; Ser- sericite; Chl- chlorite; Sul- sulphide; carb- carbonate; mud-mudstone; Lap- lapilli tuff; TB- tuff breccia; Int- Intrusive; SMS- semi-massive sulphide; MS- massive sulphide.

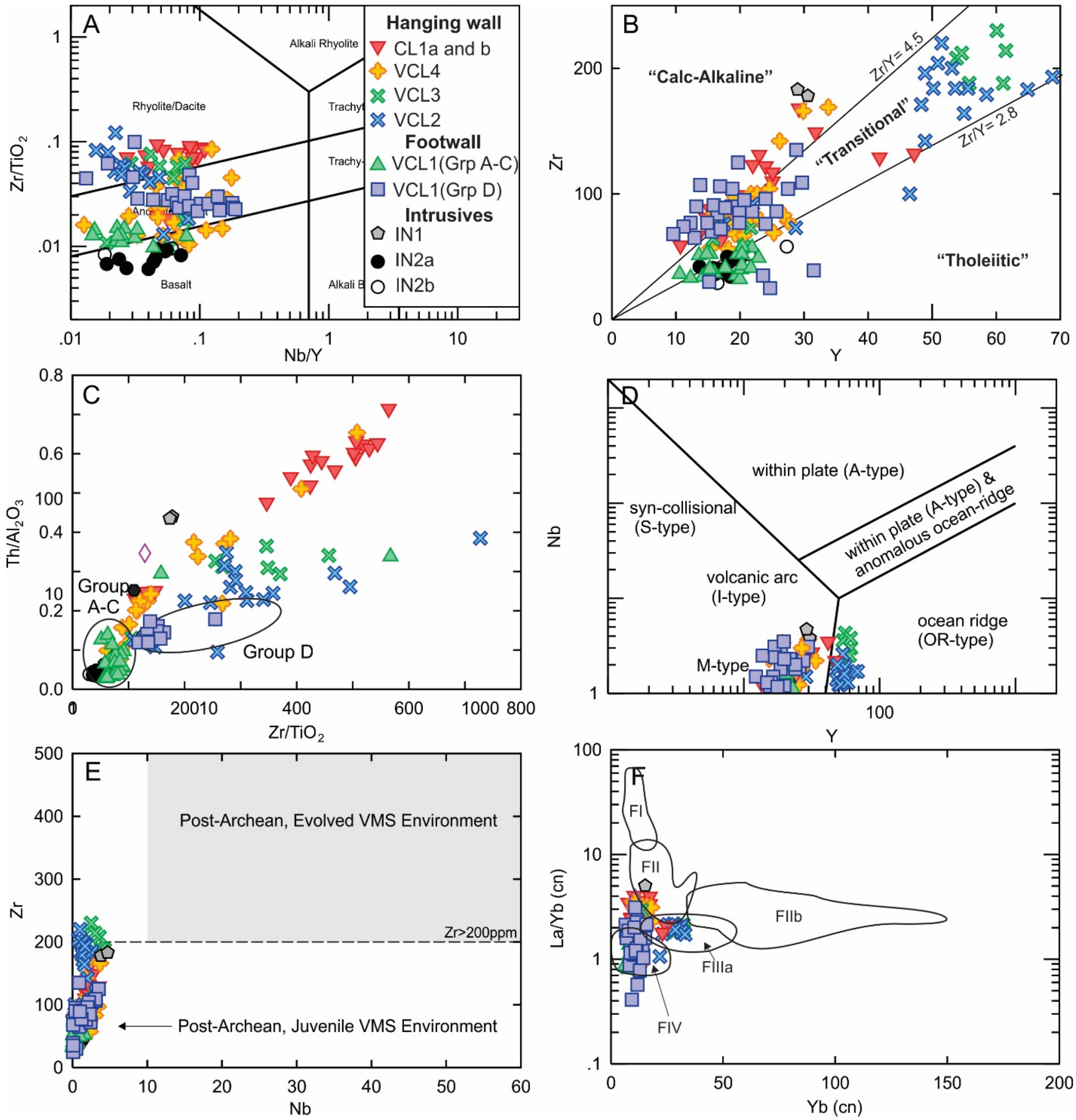

Figure 2-11. Immobile element discrimination diagrams of the volcanic and intrusive rocks from the Hurricane zone. (A) Modified Winchester and Floyd (1977) Zr/TiO_2 vs. Nb/Y discrimination diagram for rock type classification (from Pearce, 1996). (B) Zr vs. Y magmatic affinity discrimination diagram (from Ross and Bedard, 2009). (C) Immobile element ratio plot Th/Al_2O_3 vs. Zr/TiO_2 highlighting the geochemical group distinction for Group A-C and Group D in VCL1 in the Hurricane zone. (D) Nb vs. Y discrimination diagram for determining tectonic environments (from Pearce 1984). (E) Zr vs. Nb discrimination diagram for determining juvenile environments from evolved environments (from Piercey, 2009). (F) La/Yb_{cn}-Yb_{cn} FI-FIV rhyolite discrimination diagram (chondrite-normalization (CN) values from McDonough and Sun (1995); diagram from Lesher et al., 1986 and Hart et al., 2004).

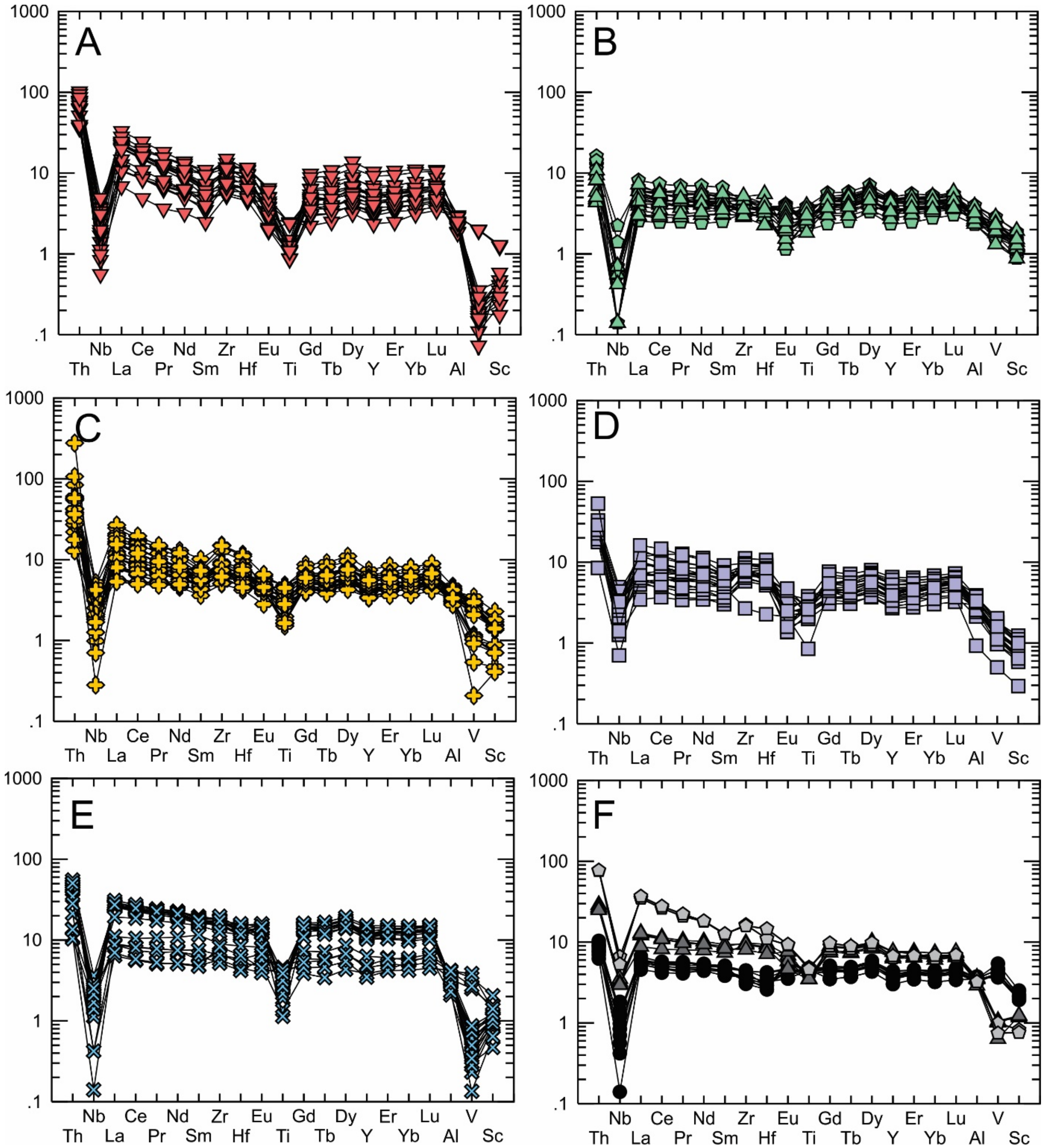

Figure 2-12. Primitive mantle normalized multi-element plots for the major lithofacies and geochemical units of the Hurricane zone (primitive mantle-normalized to the values of McDonough and Sun 1995). (A) Coherent lithofacies 1a and 1b (Cl1a and Cl1b). (B) Volcaniclastic lithofacies 1 (VCL1; Group A to C). (C) Volcaniclastic lithofacies 4 (VCL4). (D) Volcaniclastic lithofacies 1 (VCL1; Group D). (E) Volcaniclastic lithofacies 2 and 3 (VCL2 and VCL3). (F) Mafic intrusives (IN1 and IN2a and IN2b). Legend indicated in Figure 2-12.

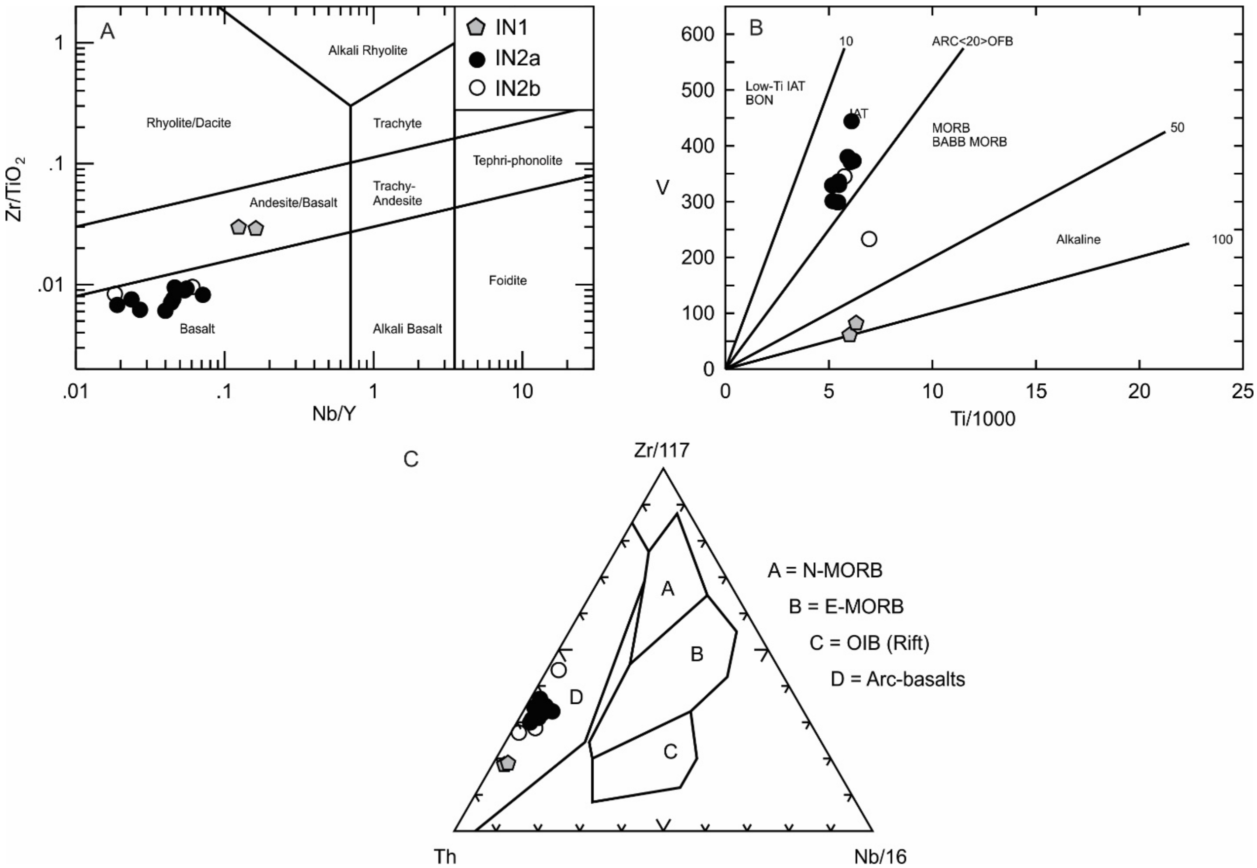

Figure 2-13. Immobile element discrimination diagrams for mafic intrusive volcanic rocks of the Hurricane zone. (A) Zr/TiO_2 vs. Nb/Y discrimination diagram modified from Winchester and Floyd (1977) to determine rock type (from Pearce, 1996). (B) Ti/1000 vs. V diagram (from Shervais, 1982). (C) Th-Zr-Nb plot (from Wood 1980). Abbreviations: ARC- arc-related basalts; BABB- back-arc basin basalts; IAT- island-arc tholeiite; OIB- ocean island basalt; N -MORB- normal mid-ocean ridge basalt; E-MORB- enriched mid-ocean ridge basalt; BON- boninite.

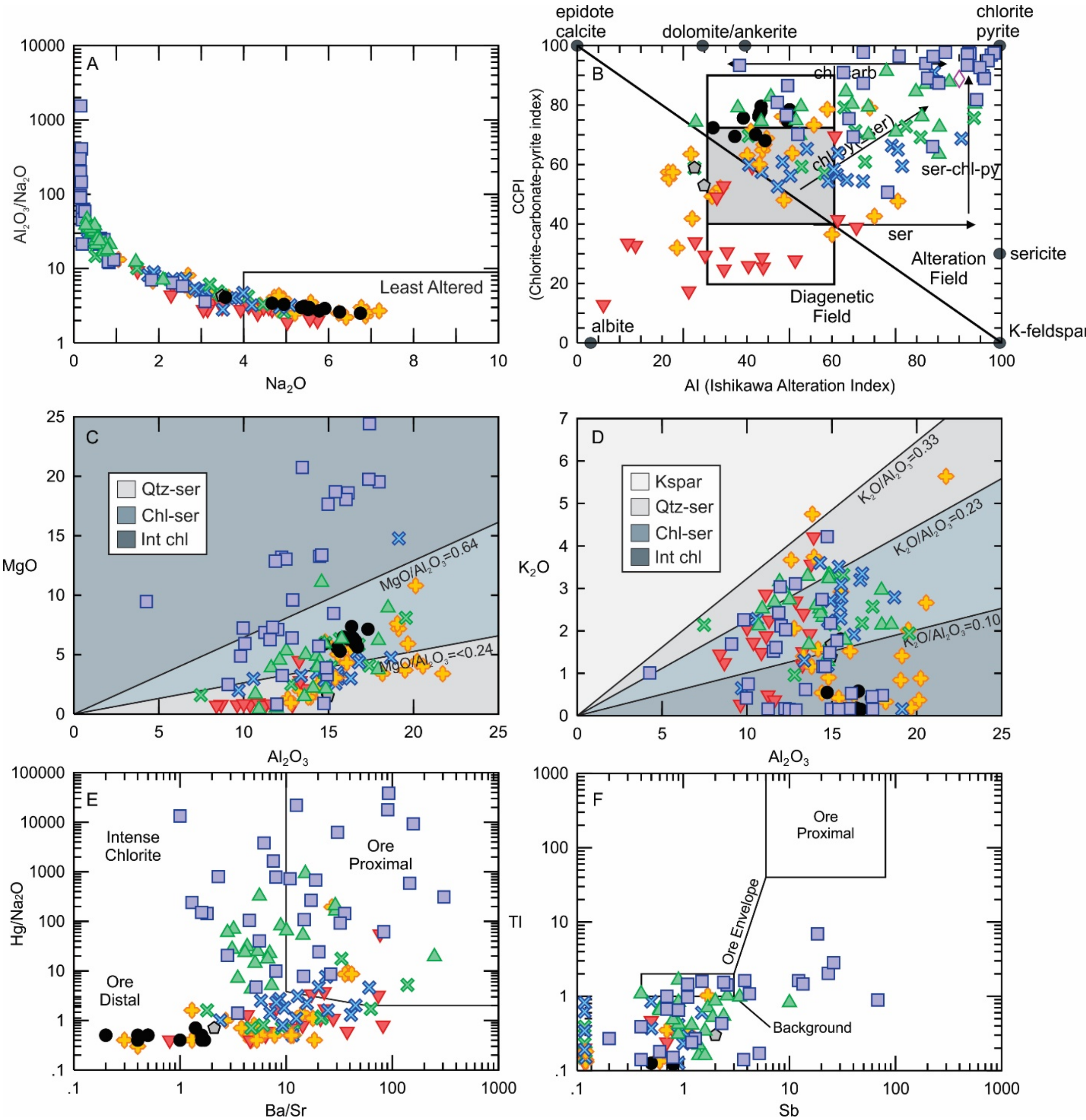

Figure 2-14. Mobile element plots for hanging wall, footwall and intrusive rocks of the Hurricane zone. (A) Splitz-Darling (Spitz and Darling, 1978) index vs. Na_2O (modified from Ruks et al., 2006). (B) Alteration box plot (from Large et al., 2001a). (C) Diagram of MgO vs. Al_2O_3 defining main alteration assemblages in Hurricane zone (from Buschette et al., 2016). (D) Diagram of K_2O vs. Al_2O_3 defing alteration assemblages in the Hurricane zone (from Buschette et al., 2016). (E) Diagram of Hg/Na_2O vs. Ba/Sr indicating the “Duck Pond alteration signature” in the ore proximal field (from Collins, 1989; Buschette et al., 2016). (F) Diagram of Tl vs. Sb (from Large et al., 2001a). Abbreviations: Qtz- quartz; Ser- sericite; Chl- chlorite; Kspar– K-feldspar; Carb- carbonate; Py- pyrite.

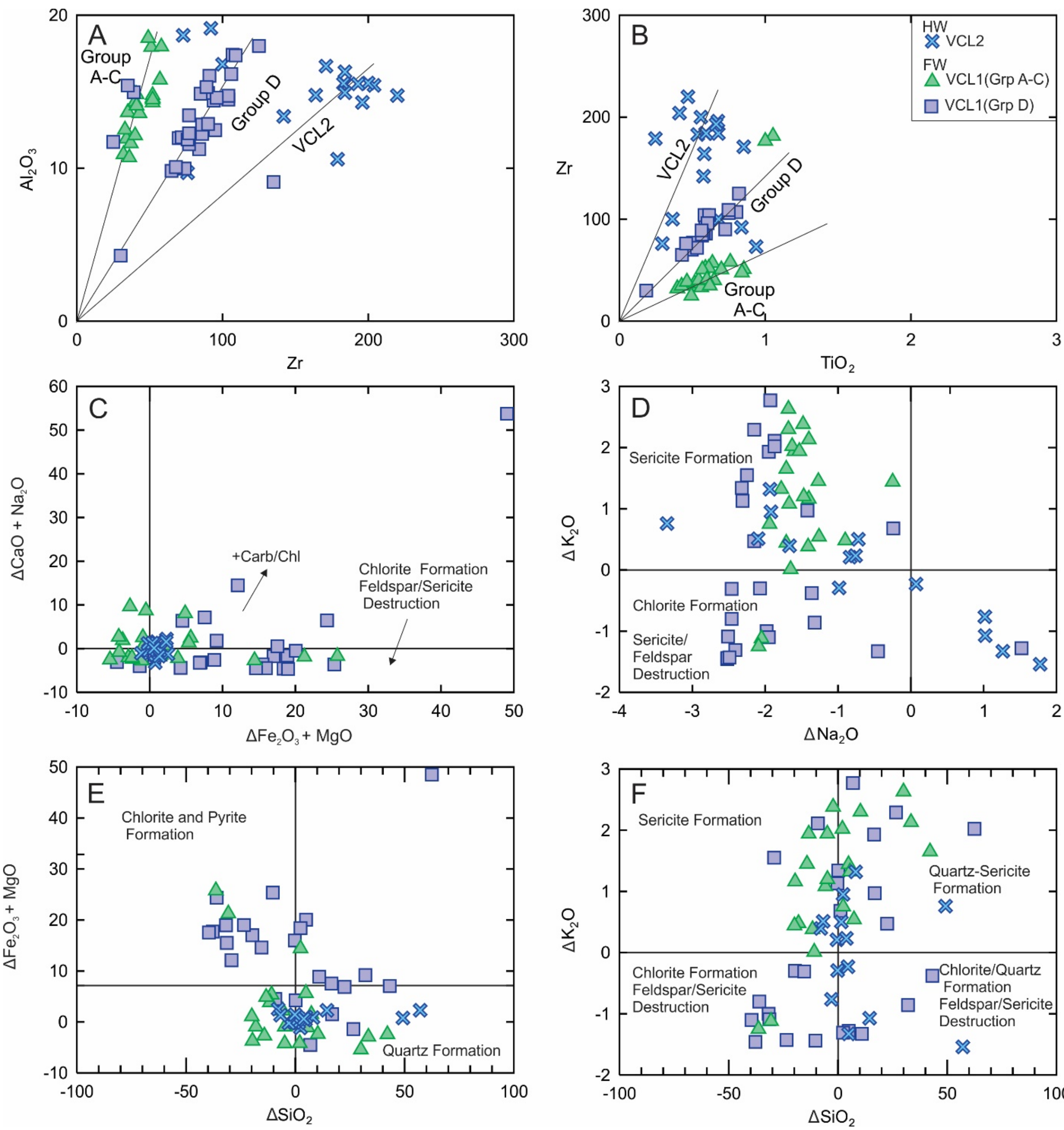

Figure 2-15. Mass balance plots showing the gains and losses of key alteration influenced elements. (A) Immobile element plot Al_2O_3 vs. Zr. (B) Zr vs. TiO_2 highlighting the linear relationship between groups A-C, D (VCL1) and VCL2 suggesting derivation from single precursors. (C) Mass change plot of CaO + Na_2O vs. Fe_2O_3 + MgO showing the association between the destruction of feldspars and the formation of hydrothermal mica and chlorite. (D) Mass change plot of K_2O vs. Na_2O indicating the development of sericite alteration associated with the destruction of feldspars. (E) Mass change plot of Fe_2O_3 + MgO vs. SiO_2 showing the development of chlorite, pyrite and quartz. (F) Mass change plot of K_2O vs. Si_2O showing the development of sericite, quartz and chlorite.

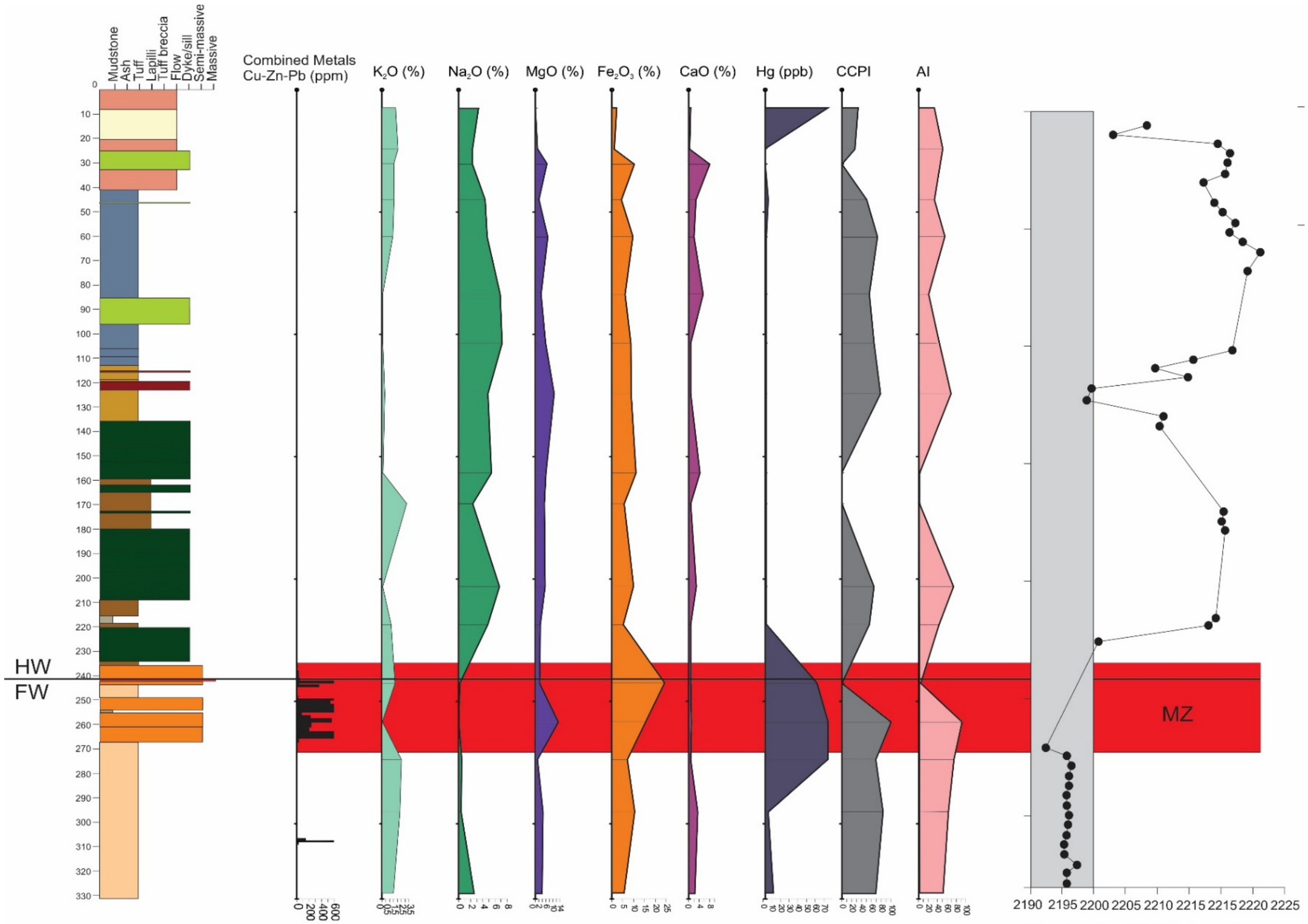

Figure 2-16. Geochemical strip log of GA-07-208 indicating the elemental gains and losses related to mineralization and alteration in the hanging wall and footwall. Short-wave infrared spectroscopy results for Al-OH wave-length shows systematic change downhole towards the mineralized horizon and in footwall volcaniclastic rocks. Abbreviations: HW- hanging wall; FW- footwall, MZ- mineralized zone.

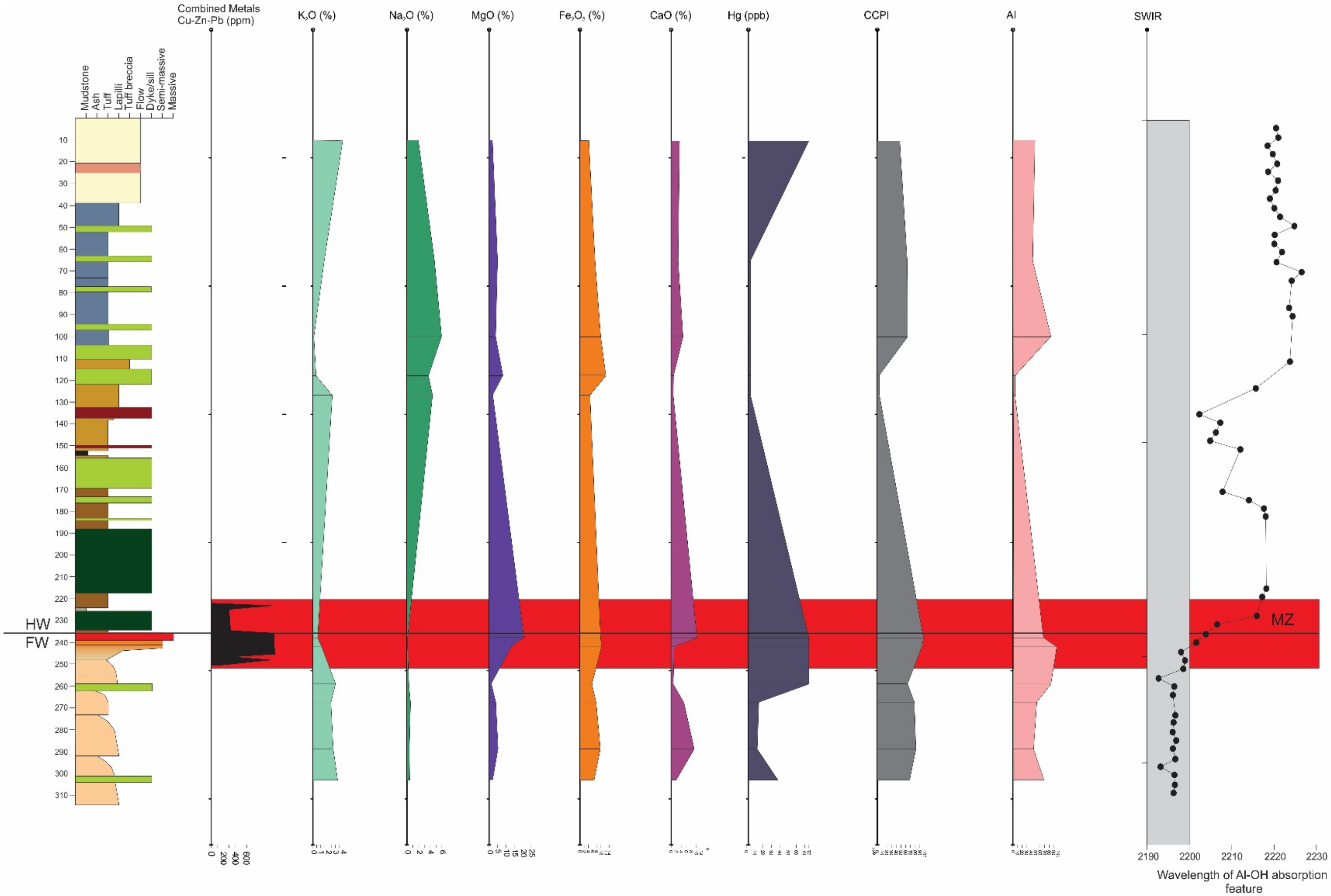

Figure 2-17. Geochemical strip log of GA-10-272 indicating the elemental gains and losses related to mineralization and alteration in the hanging wall and footwall. Short-wave infrared spectroscopy results for Al-OH wave-length shows systematic change downhole towards mineralized horizon and in footwall volcaniclastic rocks. Abbreviations: HW- hanging wall; FW- footwall, MZ- mineralized zone.

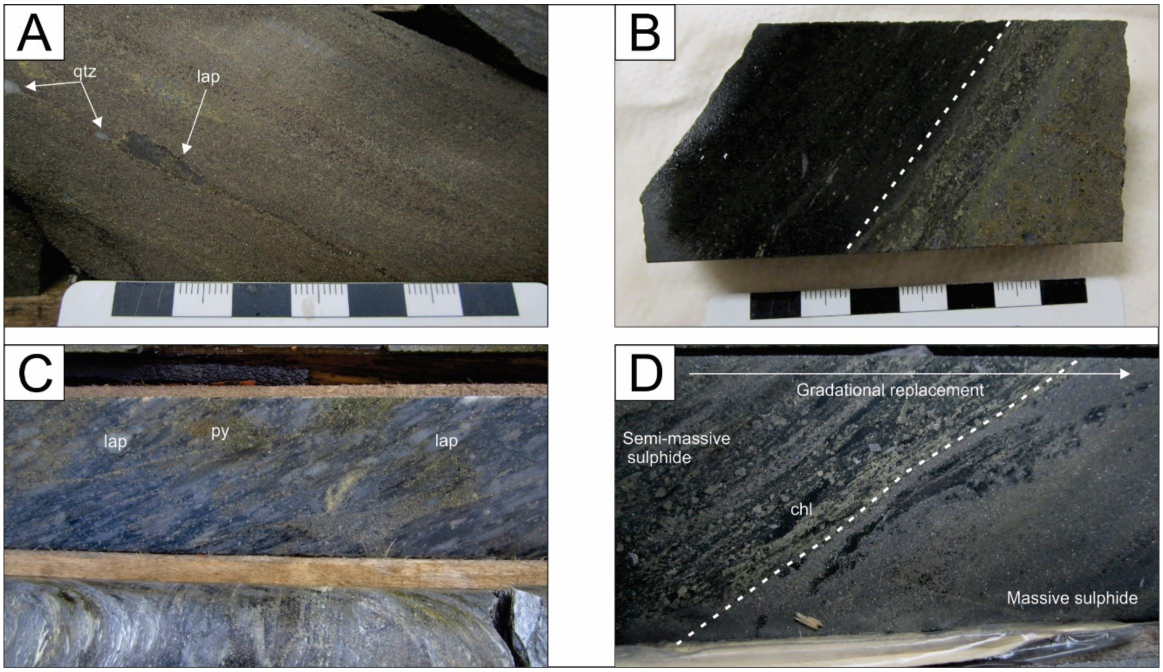

Figure 2-18. Evidence for replacement style VMS mineralization in the Hurricane zone. (A) Relict host lapilli fragments and quartz crystals from volcaniclastic lithofacies 1 in massive (sphalerite-pyrite-galena-chalcopyrite) sulphides. (B) Replacement fronts between the host lithofacies (VCL1) and the massive sulphide horizon. (C) Moderate sericite-quartz-chlorite-pyrite alteration in volcaniclastic lithofacies 2 displays evidence for alteration in the hanging wall. (D) Gradational replacement front between strongly chlorite altered semi-massive sulphide and the bedded massive sulphide.

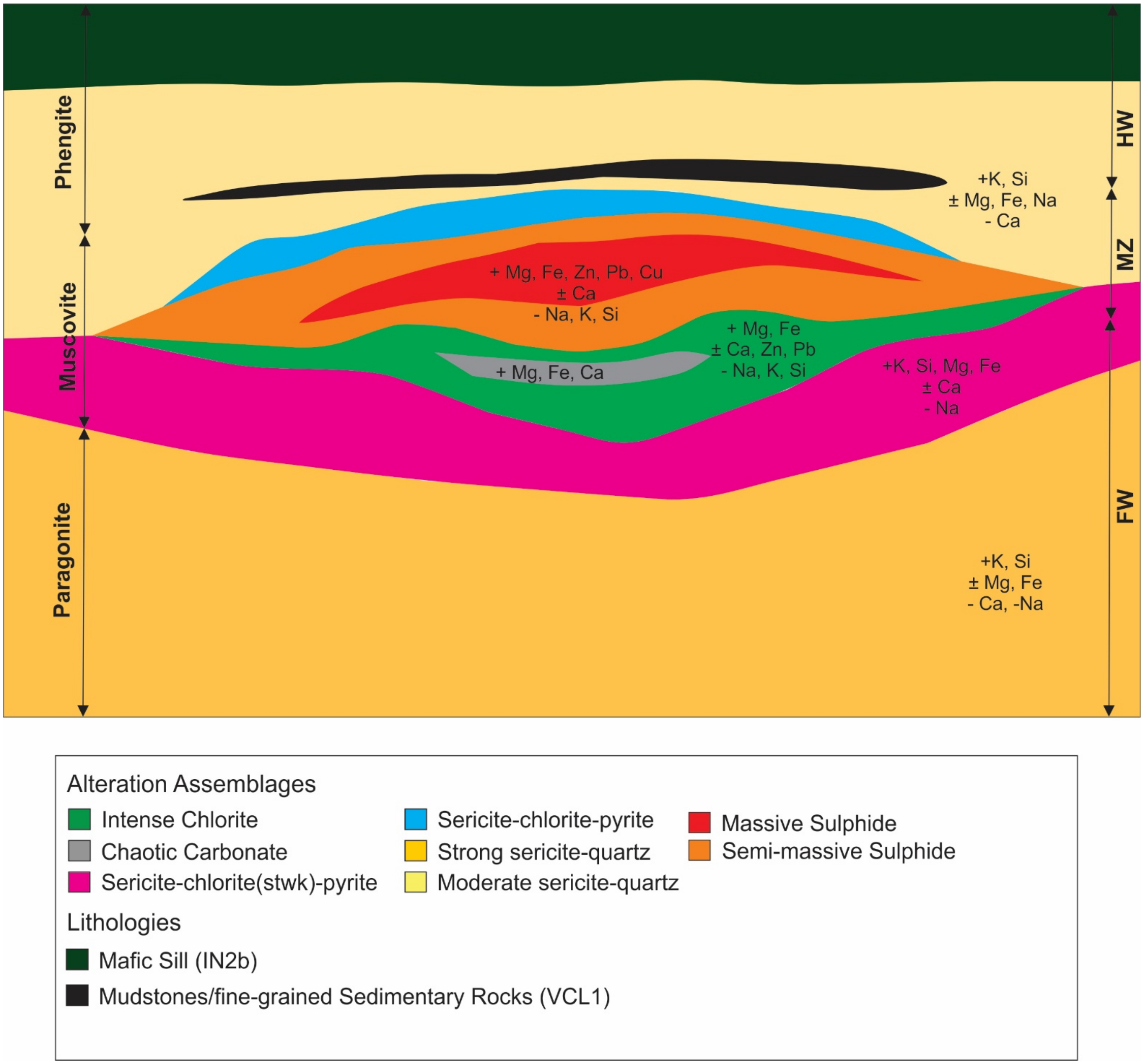

Figure 2-19. Schematic diagram illustrating the alteration assemblages, mass gains and losses and hyperspectral data in the Hurricane zone. Lithology in hanging wall (HW) is VCL2 and in mineralized zone (MZ) and footwall is VCL1.

Chapter 3: Conclusion

3.1 Summary

The Hurricane zone consists of Zn-Pb-Cu (± Au and Ag) felsic siliciclastic replacement-style VMS mineralization within the Boomerang deposit hosted within the Pats Pond group Newfoundland, Canada. The Hurricane zone is an ideal location to study the controls and distribution of mineralization and alteration of a replacement-style VMS deposit, as it experienced moderate deformation, with the majority of the deposit's stratigraphy and alteration distribution intact. Furthermore, lithogeochemical and hyperspectral data provide insight into the deposition and evolution of the hydrothermal alteration system. The major conclusions from this study are:

1. The Hurricane zone formed on the leading edge of Ganderia within a volcano-sedimentary basin formed during Ordovician back-arc rifting. This is supported by lithological relationships in drill core and furthered supported by immobile element lithogeochemistry and previous studies undertaken in the Tulks volcanic belt.
2. The Hurricane zone contains four alteration assemblages: intense sericite-quartz-pyrite, sericite-quartz-chlorite-pyrite, intense chlorite and chaotic carbonate, each which have distinct geochemical signatures and hyperspectral signatures. The alteration assemblages and their distributions are controlled by the porosity and permeability of the host volcanic rocks, host rock composition, and past hydrothermal fluid conditions.
3. Useful vectors that indicate proximity to mineralization include enrichments in Zn, Pb, Cu, Hg and transition metals, coupled with elevated alteration indices, such as the Hashimoto alteration index (AI), chlorite-carbonate-pyrite index (CCPI), Al_2O_3/Na_2O, Hg/ Na_2O, and Ba/Sr indexes, and K-rich muscovite or paragonite. Distal vectors include weak Zn, Pb, Hg (50-100 ppm) enrichments; losses in Ba and K; and phengitic mica.

4. Quantitative mass change calculations illustrate that major oxides (e.g., SiO_2, K_2O, Fe_2O_3, MgO, CaO), base metals, transition metals (e.g., V, Ni), and alkaline earth (e.g., Ba, Sr) vary between each alteration assemblage. Proximal alteration assemblages which include intense chlorite, chlorite-chaotic carbonate and sericite-chlorite-pyrite have relative increases in major oxides such as K_2O, Fe_2O_3, CaO and MgO coupled with gains in transition metals such as Ni, V, and Cr and base metals including Cu, Zn, Pb. Distal alteration assemblages which include sericite-quartz-pyrite and intense sericite-pyrite display gains in major oxides such as: K_2O, SiO_2, and locally Fe_2O_3. These assemblages also display gains in LFSE elements including Ba, Sr and Rb and in base metals including Zb and Pb. All alteration assemblages display losses of Na_2O and gains in Hg.
5. The genesis and evolution of the volcano-sedimentary basin and hydrothermal system lead to development of the replacement-style mineralization present at the Hurricane zone. Initial large-scale faulting associated with back-arc rifting created a primary pathway for hydrothermal fluids to travel through lower footwall lapilli tuffs. The highly permeable volcaniclastic host rocks allowed both vertical and lateral fluid flow creating multiple pathways for fluid movement and subsequent alteration and mineralization. This resulted in mineralization and alteration that is both discordant and semi-concordant to stratigraphy. The impermeable boundary (e.g., fluid-saturated mud) initiated replacement-style mineralization by capping the hydrothermal system, which resulted in the downward and lateral movement of sulphide mineralization and high temperature alteration below the seafloor. Synchronous deposition of volcaniclastic material with hydrothermal activity likely prevented venting of hydrothermal fluids on the seafloor and would have resulted in the pervasive and laterally extensive alteration into the lower hanging wall.

3.2 Future Research

Research completed on the Hurricane provides a framework for exploring for similar VMS systems within the Tulks volcanic belt, but there are still several unanswered questions that would greatly benefit the understanding of the Hurricane zone. Potential future research could include: (1) refined U-Pb dating within the Tulks volcanic belt to better define the evolution of the belt, including a better understanding of the stratigraphy, timing and longevity of the hydrothermal activity, which in turn would provide a better chronostratigraphic framework for mineralization within the overall tectonostratigraphic framework of the Victoria Lake supergroup; (2) a comphensive study of the mineralization including detailed microscopy and scanning electron microscopy, and other microbeam methods, to determine the mineralogy, paragenesis of sulphide minerals, and sulfur and lead isotope composition of the sulfide minerals to determine the source of metals and fluids in the deposit; (3) related to (2) detailed mineral chemistry, mineralogy, stable isotopes and physiochemical modeling of the sulphides and associated hydrothermal fluids to determine temperature, conditions of formations and metal and fluid origins; and 4) electron microprobe analysis of the sericite and chlorite compositions to compare with compositions from Terraspec measurements to determine variation in compositions and to their relationship to infrared spectral wavelengths.

A.1- Graphic Logs

Fieldwork at the Hurricane deposit consisted of detailed logging and sampling of hanging wall, mineralization zone, and footwall rocks of the deposit in diamond drill core. Logging of drill core focused mainly on lithology, alteration assemblages and mineralization at the Hurricane deposit. Drill core logging took place during September to October 2014 and June to July 2015 at the Canadian Zinc field office in Buchan's Junction, Newfoundland. A total of 22 drill holes were logged and 445 samples were collected and 147 representative samples were analyzed for whole-rock lithogeochemistry. Samples denoted by (S) on the stratigraphic logs represent where samples were taken for lithogeochemistry. A complete sample list is available in Appendix F including sample intervals, lengths and descriptions. A total of 33 thin sections were made of representative lithologies and alteration facies.

A Legend (fig. A.2.1) and Abbreviation Key (table A.2.1) in Appendix A.2 is below for the 22 graphic logs completed (Appendix A.3). Drill holes are labeled using the following nomenclature: GA-XX-YYY, where GA stands for Glitter Anomaly, XX stands for the last two digits of the year the hole was drilled, and YYY represents the hole number drilled in the overall drill program (i.e. GA-07-214 was drilled at the Hurricane deposit in 2007 and is the 214th hole drilled at the deposit).

A.2- Abbreviation Key and Legend for Graphic Logs

Table A.2.1- Abbreviation Key for Graphic Logs

General	
E	Easting
m	Meter
N	Northing
UTM	Universal Transverse Mercator
Alteration Types	
Ep	Epidote
Qtz	Quartz
Ser	Sericite
Chl	Chlorite
Sul	Sulphide

Carb	Carbonate
Host Rocks	
Arg	Argillite
Mud	Mudstone
Flow	Volcanic Flow
Int	Intrusion
LT	Lapilli Tuff
TB	Tuff Breccia
SMS	Semi-massive Sulphide
MS	Massive Sulphide
Other (in description)	
alt	Alteration, altered
CC	Chaotic Carbonate
Ccp	Chalcopyrite
DH	Downhole
Dis	Disseminated
Int	Intense
Fe	Iron
f.g, m.g, c.g	fine-grained, medium-grained, coarse-grained
Frags	Fragments
FW	Footwall
HW	Hanging wall
LC	Lower Contact
UC	Upper Contact
Fol	Foliation
Lap	Lapilli
Mod	Moderate
Pheno(s)	Phenocryst(s)
Py	Pyrite
Sph	Sphalerite
xstals	Crystals
Zn	Zinc

Figure A.1.2 Legend for Graphic Logs

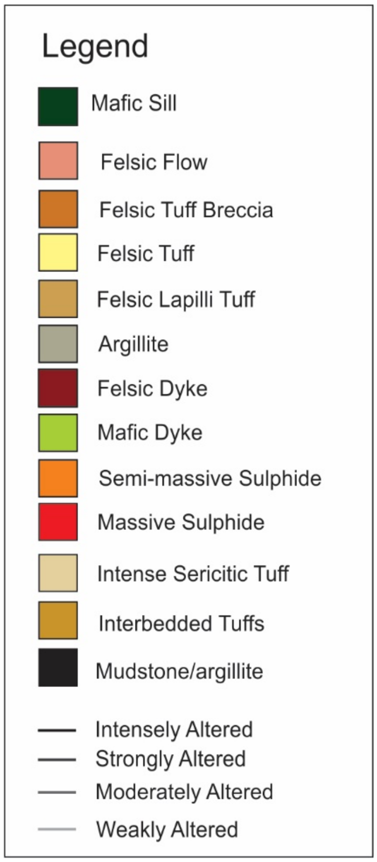

Project: Hurricane Drill Hole: GA-06-147 Date: Oct 27th, 2014		UTM 474055E 5364696N	Azimuth: 141.0 Dip: -51.0 Depth: 413.3 m

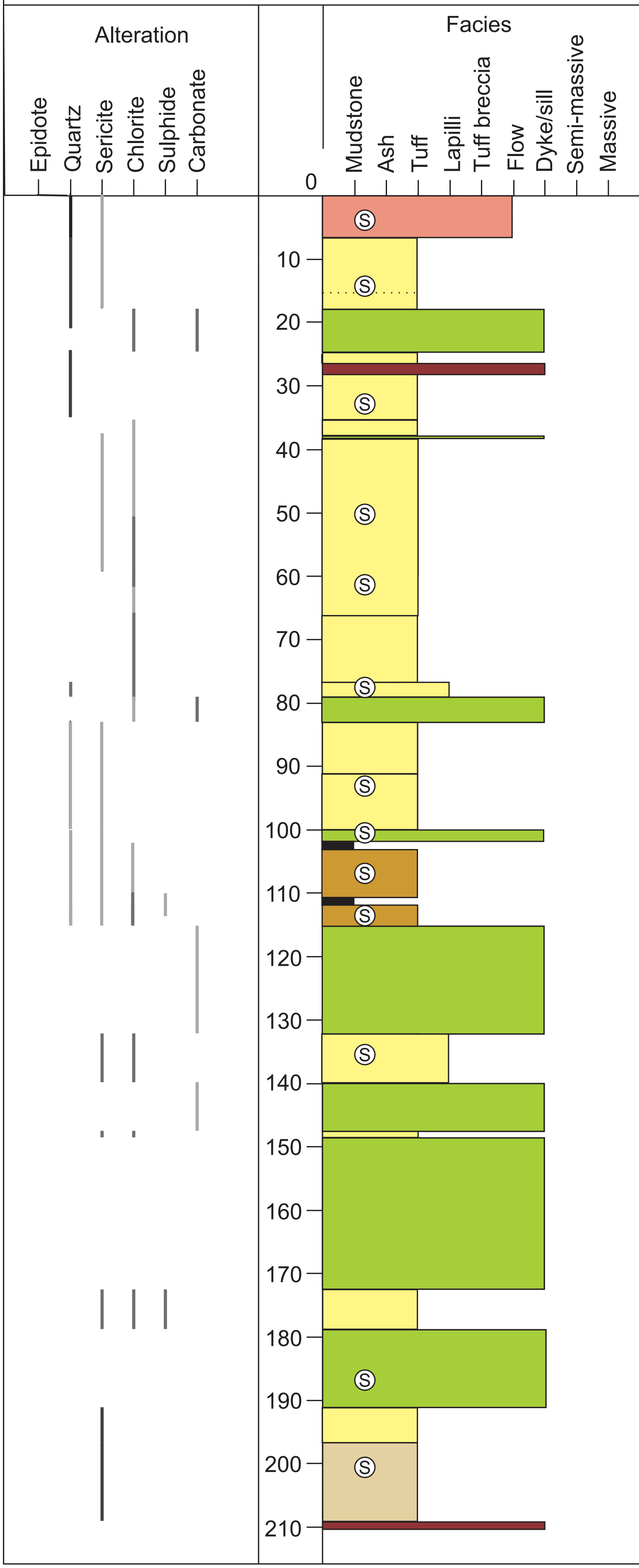

Descriptions

0 to 5.1: ash tuff or felsic flow?; v.sil alt, beige, py; white x-cutting+ concordant qtz veinlets
5.1 to 18.9: xstal tuff >20% xtals but xtasl are lap. M-coarse-gr tuff w/ some lap sized frags. Some fe-carb over print "infilling" between lap, almost L.T w/ some lap clasts, more sandy than sil; mod-wk sil ± ser.
18.9 to 23.4:

Project: Hurricane
Drill Hole: GA-06-147
Date: Oct 27th, 2014

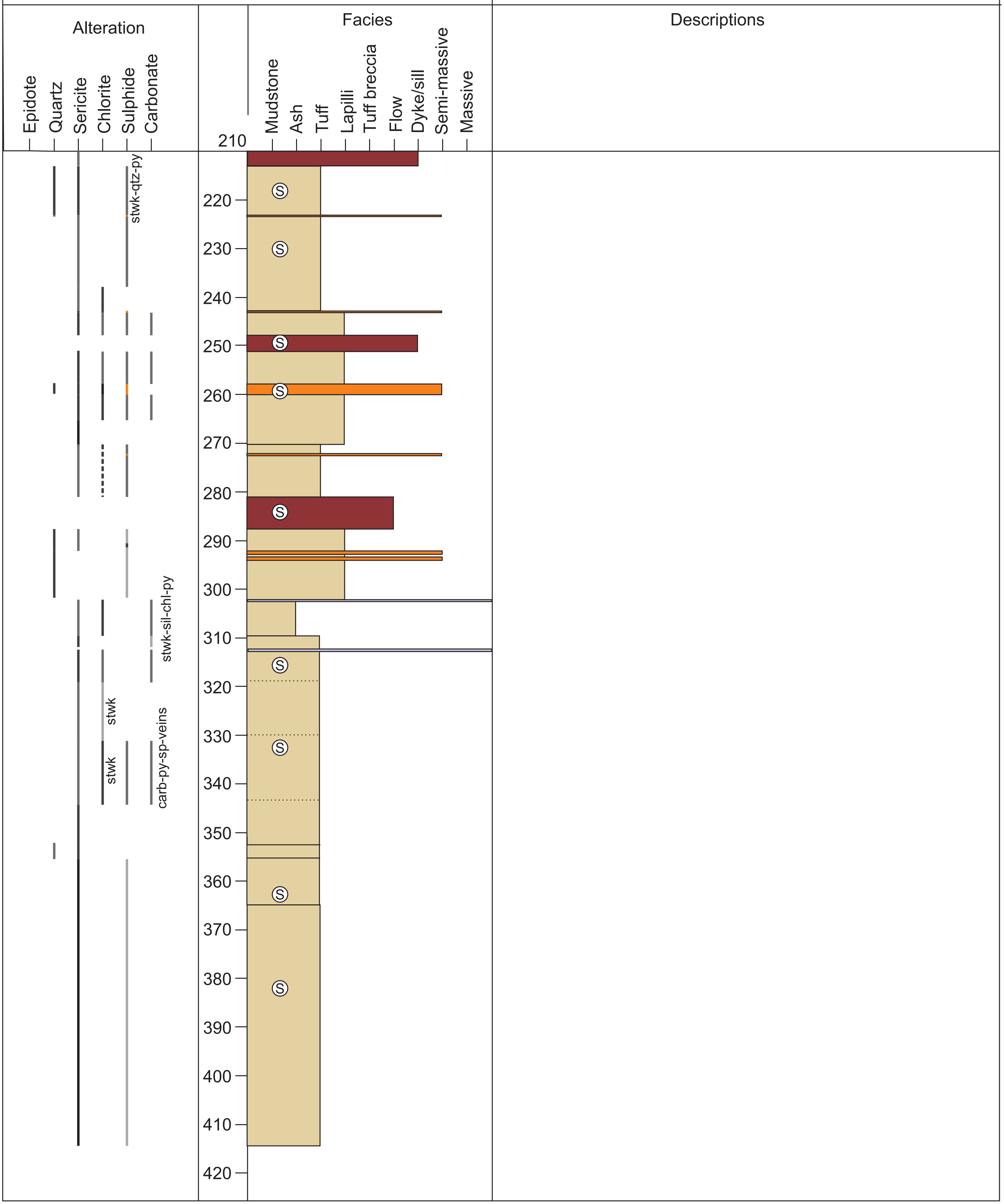

Project: Hurricane Drill Hole: GA-06-153 Date: June 14, 2015		UTM 474068E 5364729N	Azimuth: 140.6 Dip: -51.0 Depth: 487.4 M

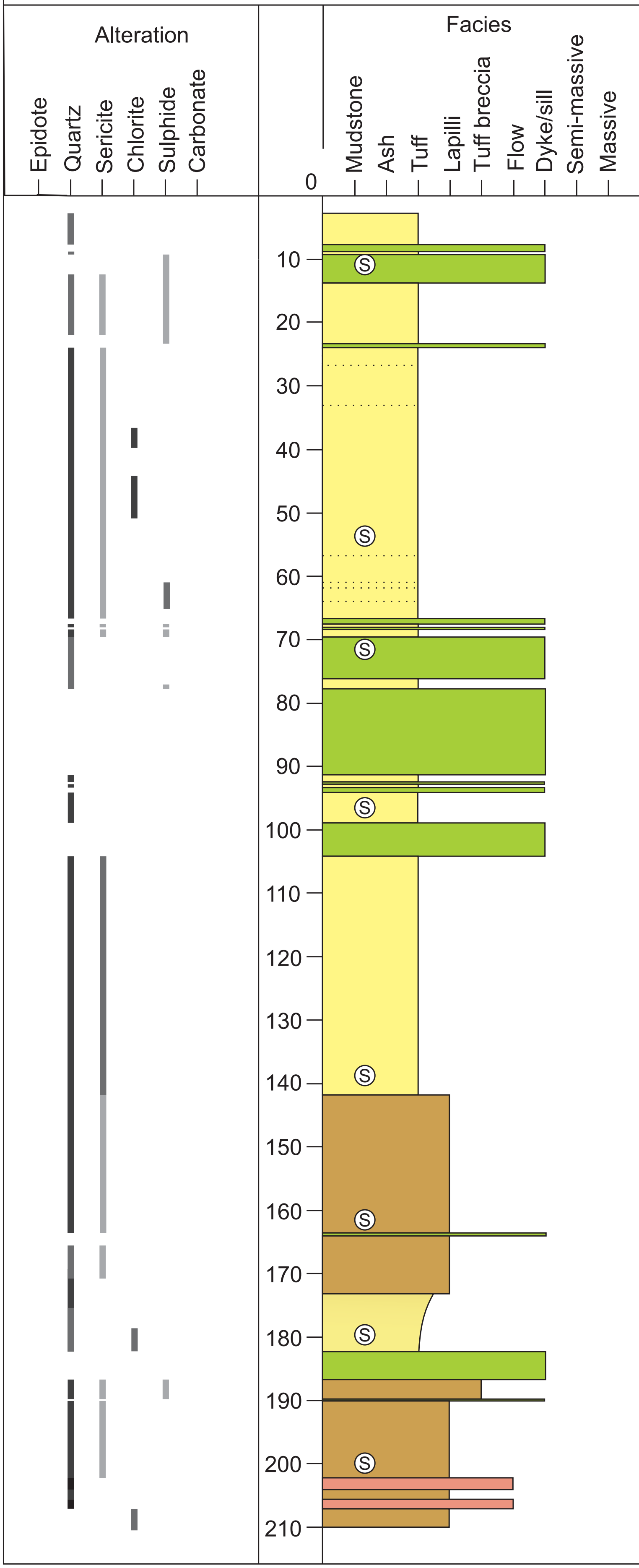

Descriptions

2-7.94: Xstal tuff: fine-grained, pale grey to pink with 1-3 mm white feldspars xstals. Mod to strong ser/sil. Mod fol.
7.94 to 9.04: Mafic dyke: fine-grained, dark green, sharp upper and lower contacts with chilled margins, carb overprint. 2-5 cm thick qtz-carb veins.
9.04 to 10.5: Crystal tuff: same as above
10.65 to 14.01: Mafic dyke: same as above, tr fine- to med-grained py.
14.01 to 23.58 m: Xstal tuff: same as above
23.58 to 24.19 m: Mafic dyke: same as above
24.19 to 66.91 m: Xstal tuff: same as above, feldspar xstals increase down hole, mod to strong fol. Mod to strong sil, with wk ser and wk chl veinlets. From 27 to 33- broken core (fault?).

From 44.9 to 52.9 get 5-10 beds that are chloritic w/ patchy fe-carb.

From 57.03 to 61.24 — fault?
From 62.12 to 64.18 — increase sil, 1% cp in veinlets.

66.91 to 70.78 m: Mafic dyke interleaved with xstal tuff.

70.78 to 79.03 m: Mafic dyke: pepperite? same MD as above, but with abundant fe-carb overprinting and clasts of xstal tuff. 3-5% py along margins.
79.03 to 92.59: Mafic dyke. sharp, chilled margins. Coarsens inwards and becomes locally plag-phyric. From 80.2-80.3 and 86.75 to 86.98 m 5% qtz-carb veining, locally with 1-2% py.

92.59 to 100.18: Mafic dyke interleaved with xstal tuff.

100.18 to 105.43m: Mafic dyke: dark grey-green, fine to med-grained, 1-2% qtz-carb veins, rare py.

105.43 to143.07: Crystal-bearing tuff: beige to light grey, 1-5 m feldspar xstals (5-10%). Strongly sil alt, decreasing downhole, strongly foliated. 1-2% concordant qtz veins. 1-2% py along proximal to lower contact.

143.07 to 164.83: Lapilli tuff: normally graded, fine- to coarse-grained, 1-5% feldspar crystals in fine-grained matrix. Mod to str sil-ser alt and strongly foliated.

164.83 to 165.3: Mafic dyke, same as above.
165.3 to 183.55: Heterolithic coarse-grained lapilli tuff, similar to above. Locally beds contain up to 15-20% feldpsars and quartz crystals. Increase chl alt around 174 m.

183.55 to 187.95: mafic dyke: same as above
187.95 to 191.03: Tuff breccia/lapilli tuff: heterolithic fragments consisting of pale and dark grey (felsic and mafic) with medium grey, fine-grained matrix. Moderately foliated with fine to coarse-grained py in matrix.
191.03 to 191.36: amygdaloidal mafic dyke. 0.5 to 1.5 cm round amygdules in fine-grained dark green-grey matrix.
191.36 to 208.37: normally graded tuff to lapilli tuff interbedded with felsic flows. Felsic flows may be bomb sized felsic fragments. Very strongly sil altered with minor ser veinlets.

Project: Hurricane
Drill Hole: GA-06-153
Date:

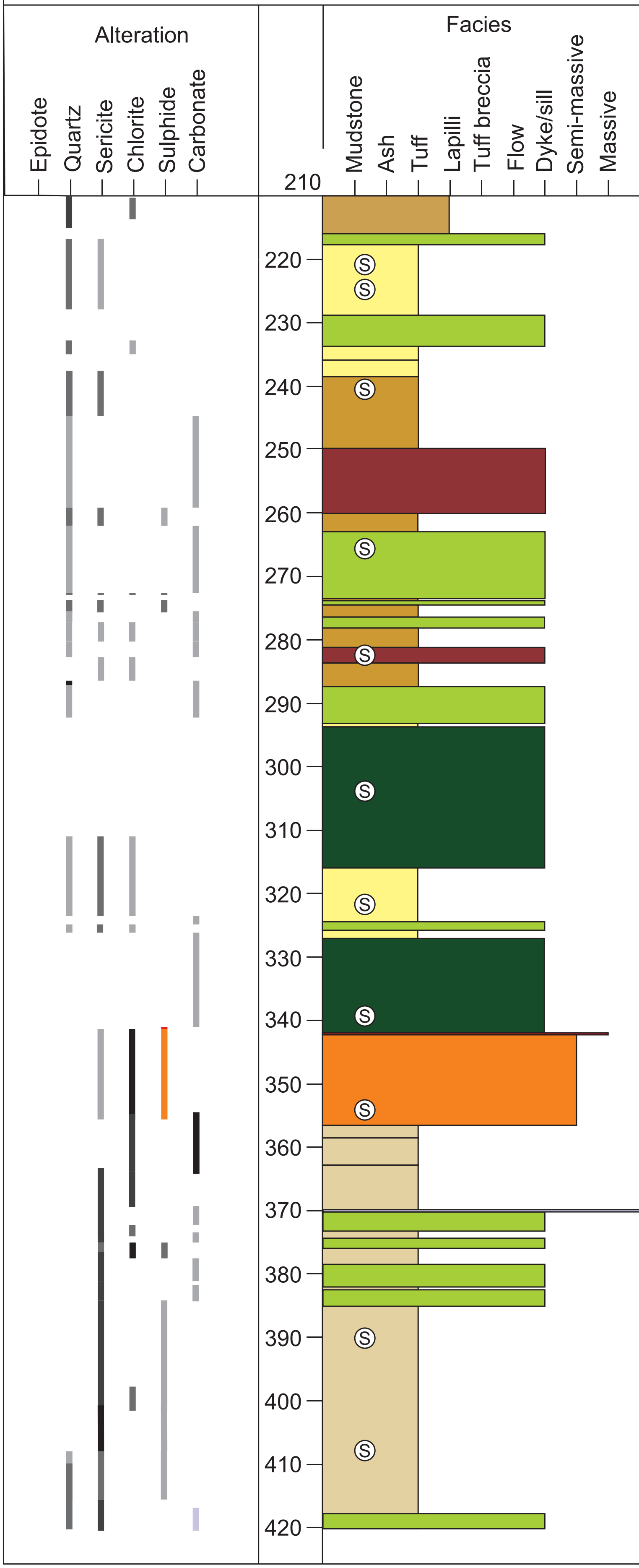

Descriptions

208.37 to 215.95: Normally graded tuff: pale grey to dark grey, strongly sil alt fine to coarse-grained with local interbeds of heterolithic lapilli tuff.
215.95 to 217.7: Mafic dyke: dark green-grey, fine to med-grained (coarsens inwards) with 5% carb concordant to discordant veinlets near lower contact.
217.7 to 229.88: Normally graded tuff: dark grey to creamy beige, ash to fine-grained tuff (10%) grading into med- to coarse-grained tuff and locally heterolithic lapilli tuff. Locally in ash tuffs there is fine-grained py and po veinlets.
229.88 to 234.78: Mafic dyke: similar to above, 10 cm chilled margin, coarsens inwards, 1-3 cm carb veinlets and rare carb amygdules.
234.78 to 240.84: Normally graded tuff: dominantly by ash to fine-grained tuff, bleached/sil lower contact. Clusters of med to coarse-grained py in thin bands parallel to fol.
240.84 to 250.52: Normally graded heterolithic (10%)tuff to tuff (80%). Similar to above, but first appearance of thinly bedded argillites, typically associated with fine- to coarse-grained banded py (parallel to fol). Arg are locally sheared.
250.84 to 265.0: Altered amygdaloidal mafic dyke or felsic dyke: pale grey/beige, 1-3 cm qtz-carb amy, 15% fe-carb veins.
265.0 to 267.87: Normally graded heterolithic tuff to tuff: similar to above, but tuffaceous layers are more qtz-felds-rich and loss of argillite units.
267.87 to 278.41: Intermediate to mafic dyke?: Brownish grey, vfg white xstals. sharp contacts.
278.41 to 278.73: package of vfg tuff/ash tuff interbedded with thin argillites. 5% disem py in associated with arg-tuff interbeds.
278.73 to 288.57: Interleaved grade tuffs and mafic dykes. Locally, faulted zone along lower contact and into lower unit, characterized by broken core and thick qtz veins
288.57 to 292.27: Mafic dyke: light grey-beige/olive green (altered?). Chilled margins, coarsens inwards. 1-2% carb amy.
292.27 to 298.63: med-grained tuff with local xstal-rich layers.
298.63 to 316.82: Mafic sill: light grey-green to dark grey-green. Fines down hole. Likely multiple intrusions. From 306-311 feldspar-rich layer.

316.82 to 324.47: Normally graded felsic lapilli tuff: pale grey, locally heterolithic, but dominantly felsic, plag-rich xstal-bearing with thin 5-20 cm thick chert intervals. fine-grained banded py is associated with chert layering.
324.47 to 326.11: amygdaloidal mafic sill: fine-grained, beige-grey with 8% carb amy, 1-3 cm, oval and elongated, moderately foliated, 4% carb veinlets.

Project: Hurricane
Drill Hole: GA-06-153
Date:

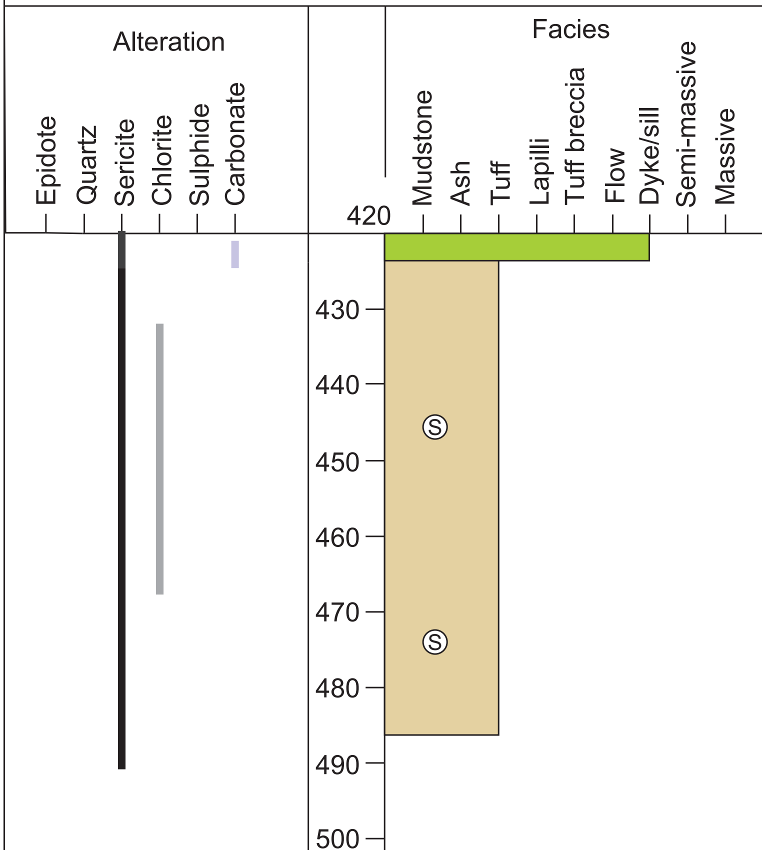

Descriptions

Project: Hurricane Drill Hole: GA-06-176 Date:	UTM 474163E 5364780N	Azimuth: 140.6 Dip: -46.0 Depth: 383.1 m

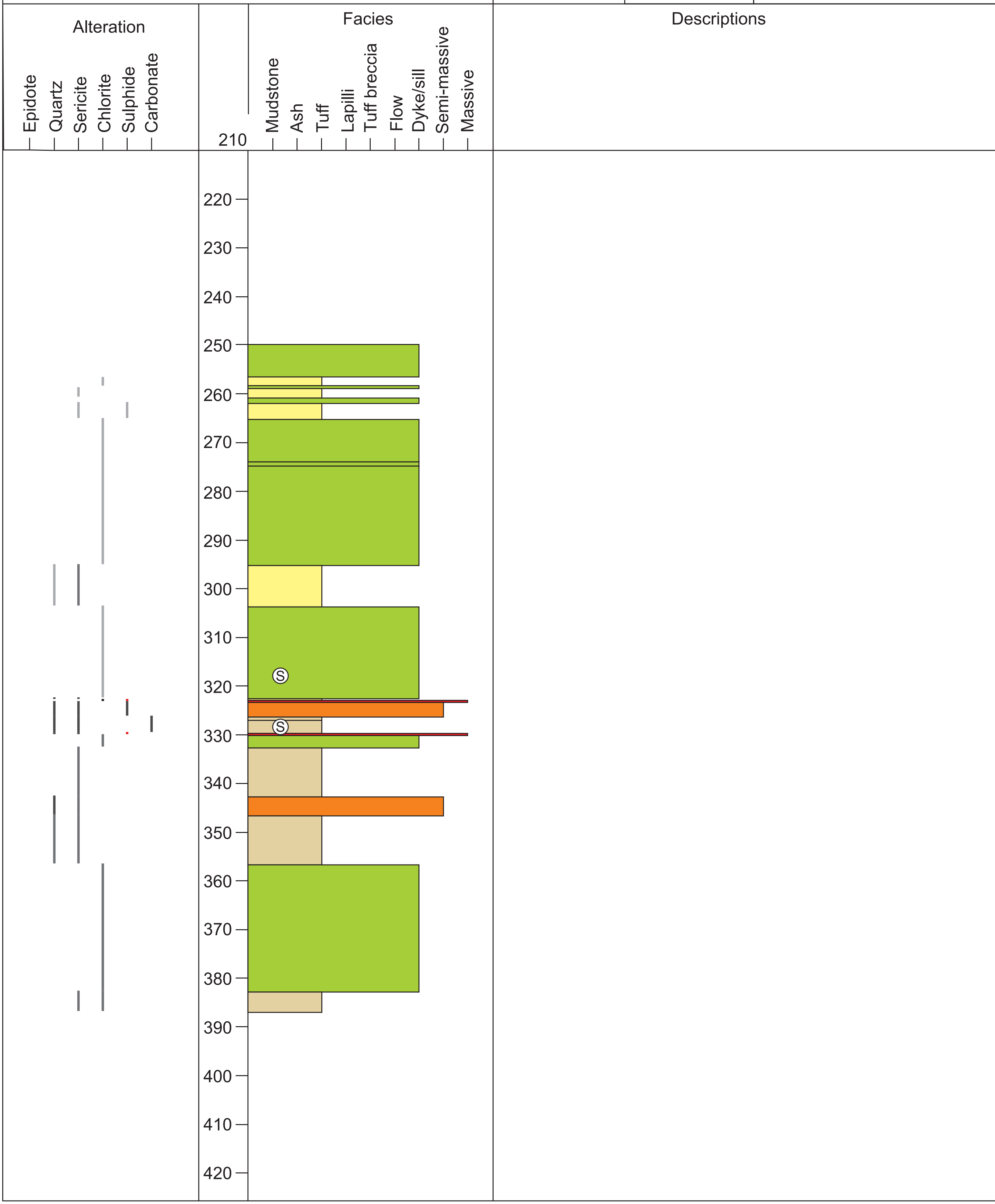

Project: Hurricane Drill Hole: GA-06-180 Date:		UTM E N	Azimuth: Dip: Depth:

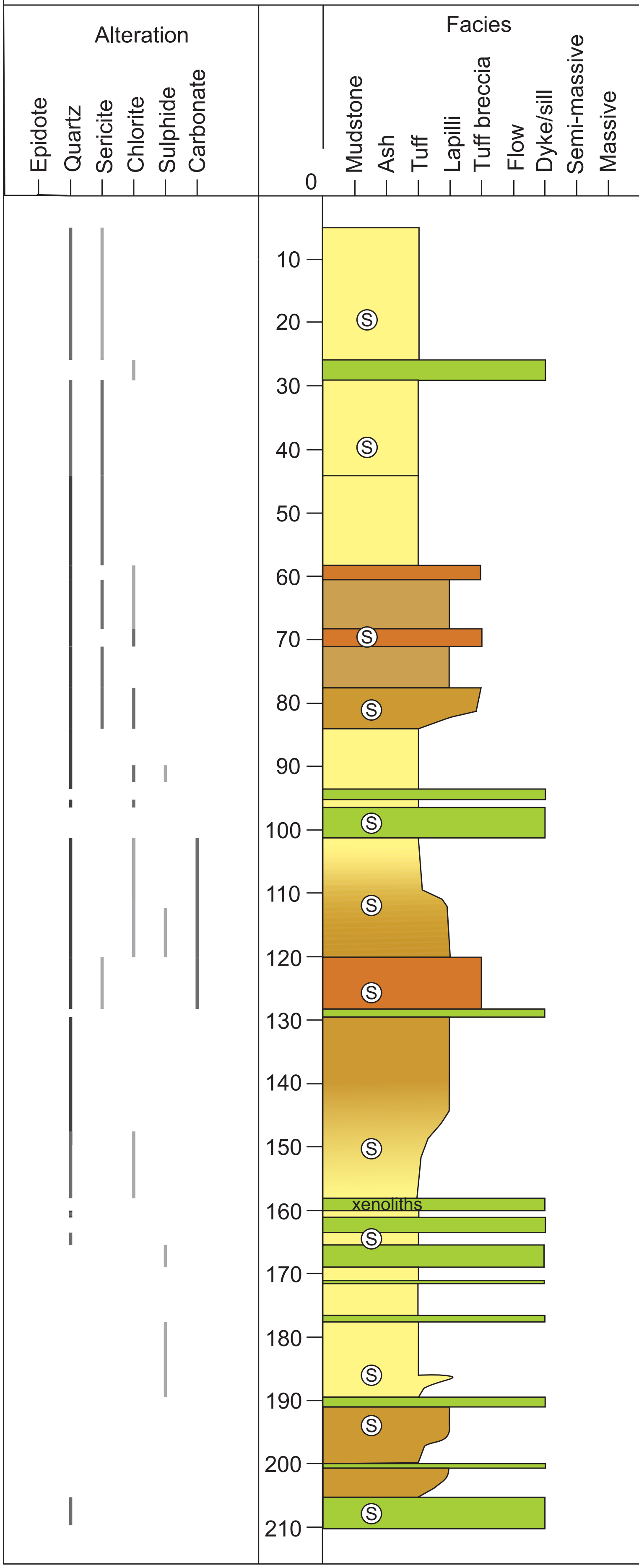

Descriptions

Project: Hurricane
Drill Hole: GA-06-180
Date:

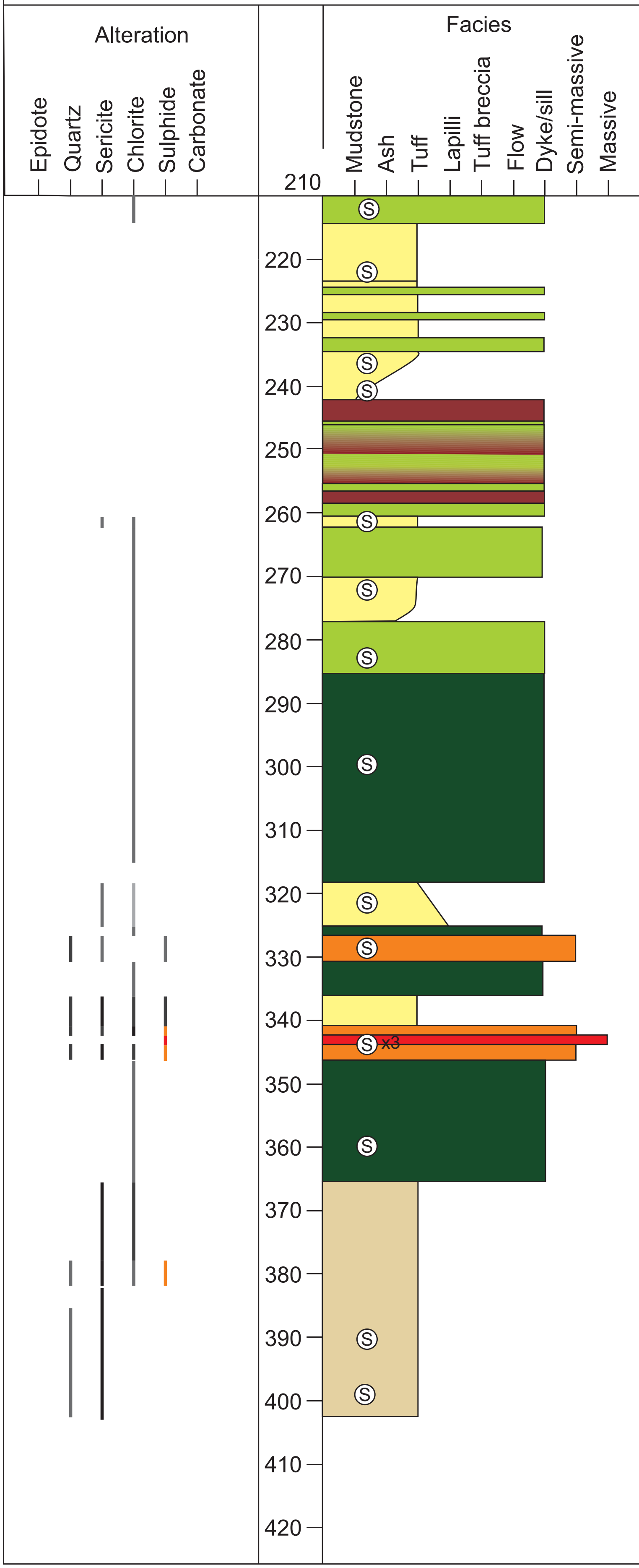

Descriptions

Project: Hurricane Drill Hole: GA-07-208 Date: Oct 17th to 18th, 2014	UTM E: 474055 N: 5364596	Azimuth: 141.0 Dip: -53.0 Depth: 330.7 m

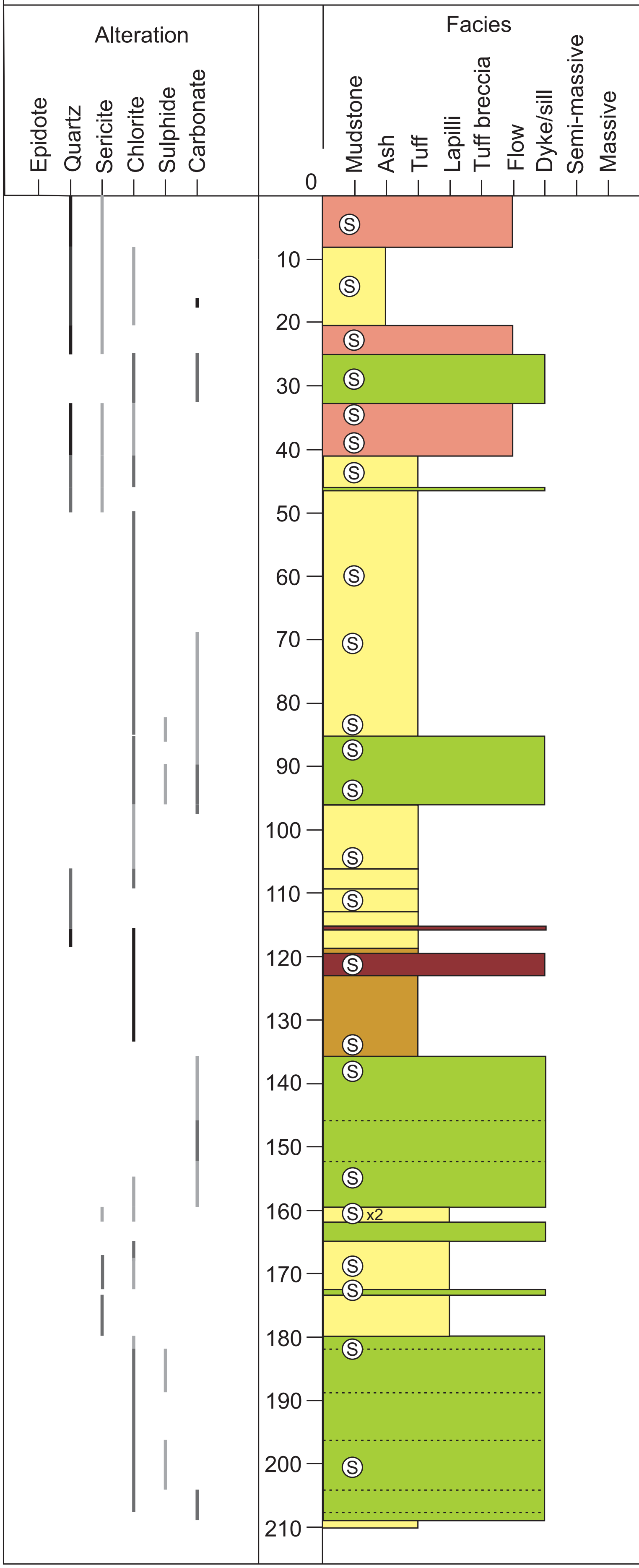

Descriptions

0 to 8.1: Felsic flow; v.sil alt; light bright grey, v.f.g with 1-4 cm thick discont and discordant qtz veins (can appear almost brecciated-looking); thin med-gr py veins, some 1-4% dis py (f-med-grained), trace gn; 1-3% round white qtz xtstals.

8.1 to 20.5: F.g tuff; med grey; fl with fu clear, glassy qtz xtals (20%); mu (could have been plag, now carb overprinted) white-beige (5%), subangular; vuggy, has dark brown weathering

20.5 to 24.5:Light grey, v.f.g sil alt felsic flow with thin (1mm) discordant and irregular chl (black) veins; 7-10% qtz xstals (fu-cl)± plag (rare).; wk ser alt in thin spider-like veins; minor carb overprint (1%).

24.5 to 31.6: mafic dyke; v.f.g dark grey green dyke with spotted fe-carb

31.6 to 40.3: Same plag-porphyritic, str sil felsic flow.

40.3 to 89.9: medium to bluish-grey, fine to medium-grained, quartz- to plagioclase-bearing tuffs. Mod chl alt, mod to str fol. Locally graded and xstal-poor zones.

from 80 to 85 1-3% euhedral py.

89.9 to 96.21 : Dark grey to green with fine-grained carb amy (5-7%). Sharp upper and lower margins.

96.21 to 136.1: Interbedded fine- to coarse-grained tuff to local lapilli tuff. Local zones of quartz-bearing crystal tuffs graded into fine-grained to ash tuff layers with thin mudstones interbeds.

Locally strongly sil altered and bleached associated with fault zone.

136.1 to 159.9: Dark grey-green mafic sill, fine to med-grained, 2-5% carb amy.

159.9 to 162.24: Med-grained tuff with coarse-grained lap fragments. 10% white, round plag xstals, thin cherty interbeds.

162.24 to 165.47: Sharp upper and lower contacts, dark grey-green, mafic dyke.

165.47 to 180.23: Same tuff as above, cherty layers have fine-grained, banded py. weak to moderate ser-sil alt, with wk chl laths.

180.23 to 209.34: Dark green-grey, fine- to med-grained, 2-3% carb amy, local 1-3 mm, 5% euhedral py along lower margin.

Project: Hurricane
Drill Hole: GA-07-208
Date: Oct 17th to 18th, 2014

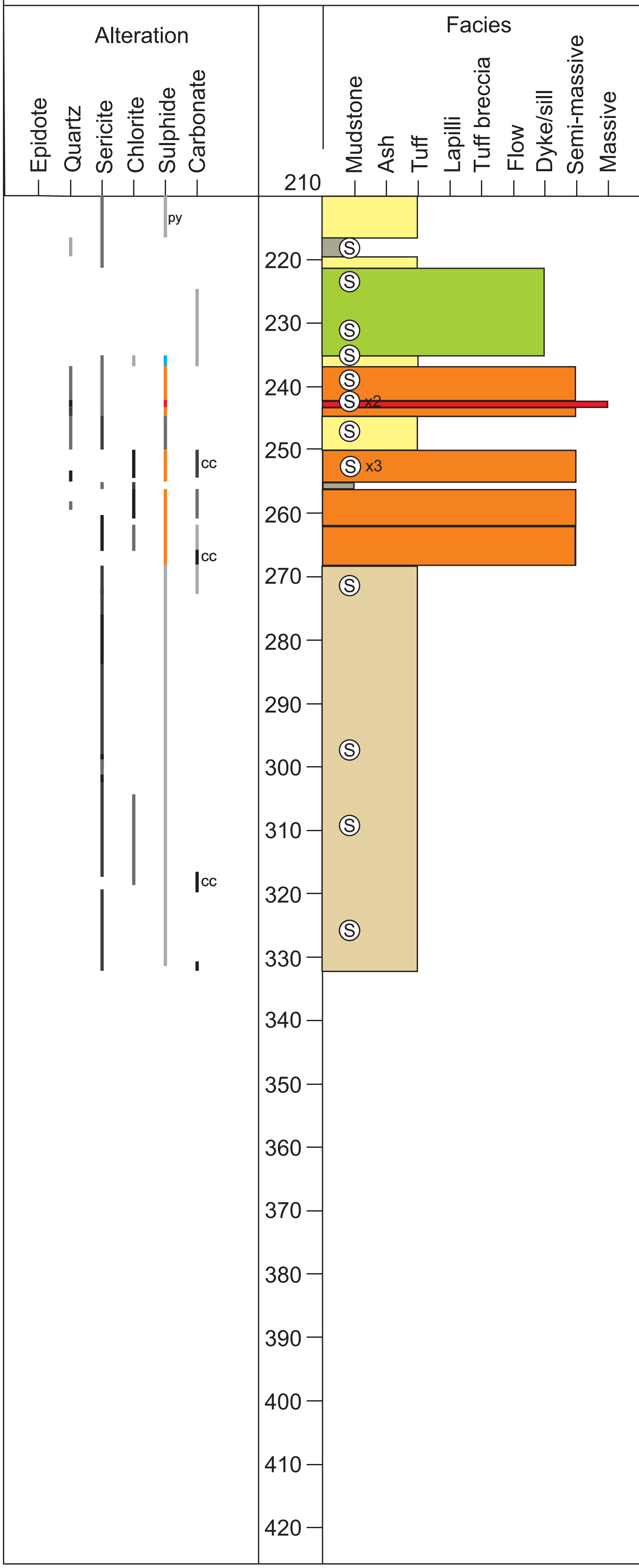

Descriptions

209.34 to 221.6: med grey, fine to med-grained tuff with white, rounded plag xstals Local cherty intervals with fine-grained banded py. Two fautls from 211.1 to 211.37 and 219.2 to 221.6

221.6 to 233.3: Mafic dyke

223.3 to 236.18: fine to med-grained, ser-sil tuff with local chl laths and 7-10% py.
236.81 to 241.51: Strongly fol, discont bands of py with chl stwk veins in ser-sil alt matrix. Qtz xstals in altered matrix. Tr BM.
241.51 to 242.44: Undulating/banded cp-red sp-gn-py in chl-ser matrix.
242.44 to 243.8: Same as semi-massive above
243.8 to 249.11: thin to medium banding (1-5cm) of light grey v.f.l (appears more si-rich, thin bands, appears on tops? Of beds, some loading structures (flames) with lower dark grey fl unit). Med-grey beds (thickest) that are v.f.l-fl with disem py(f.g; 2%), in between med-grey beds are dark-grey fl-fu more sandy looking thin-med bedded, could be base and grade into lighter grey, but not always; mod to strong ser alt.
249.11 to 254.11: v.chl alt (VMS?); v.black, v.f.g (no grains in black can be seen, chl replacing original tuff) w/ small bleds (1-2mm) of qtz (white, or carb??); 2-3% carb veins with py, trace ccp and possible sp. (<5%)
254.11 to 255.06: thinly interbedded siltstone to chert.
255.06 to 266.8: ser/sil tuff ± py ± thin chl bed; light grey a.t with thin dark (chl alt?) blebs; thin layers of darker of (chl alt?) with fine-med-gr py; v.f.g py is disseminated throughout the sample; 4% of randomly distributed qtz fragments, typically subrounded.
266.08 to 332.6: ser alt tuff + mineralized. Strong to intensely ser alt L.T (f-coarse?); disseminated bands of med-gr py with rare ccp; possible fucshite? Some green rounded-tabular mineral.

Project: Hurricane
Drill Hole: GA-07-209
Date: Oct 4th to 5th, 2014

UTM	Azimuth: 141.0
474055E	Dip: -66.0
5364596N	Depth: 297.2

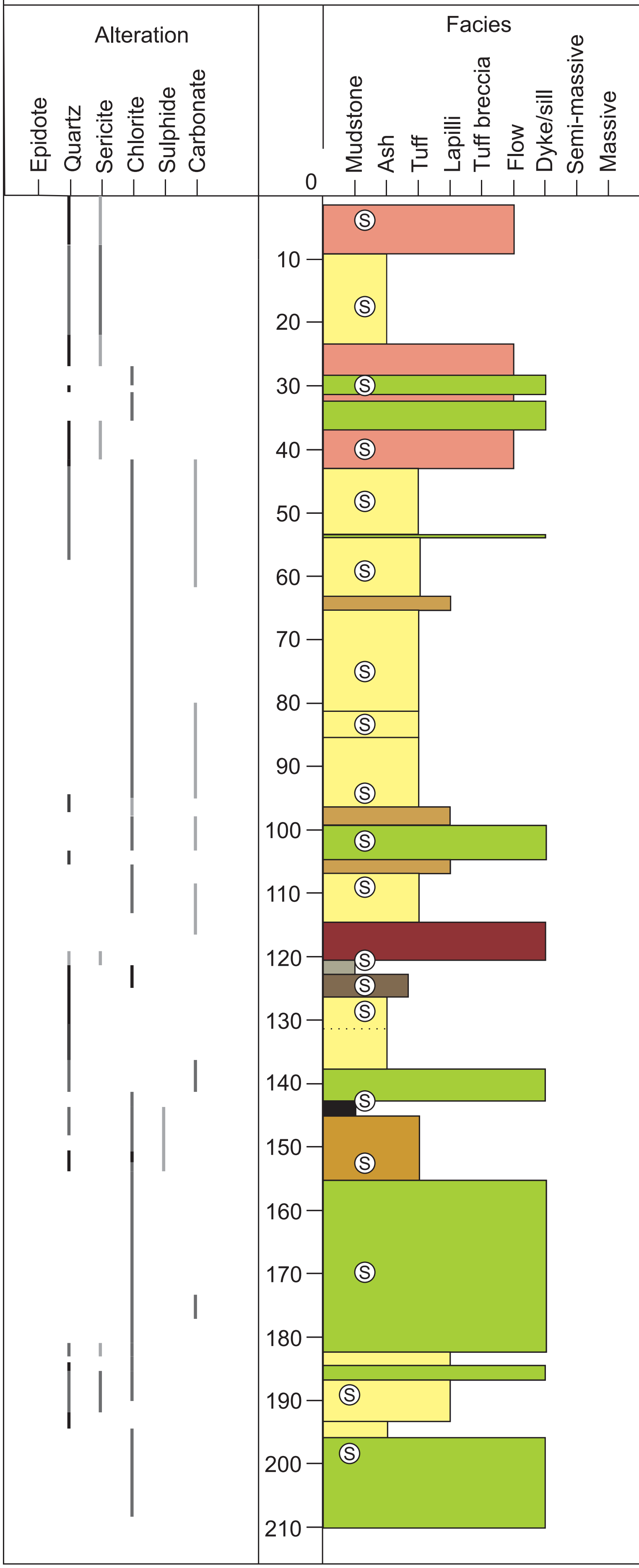

Descriptions

1.5 to 9.2: Felsic flow, v.f.g; light grey/ beige with irregular white qtz veins (5%); v.sil alt; 3% dis py; few minor sericite veins.

9.2 to 19.68: f-m.gr L.T w/ strong sil ± ser/chl; light to med grey in color. Lapilli are light to dark grey in color with finer matrix. Qtz and plag xtals in interstitial space, some chl infilling interstitial space, appear as dark grey elongated fragments (rare). Lapilli are subangular and slight elongated looking. mod fol.
19.68 to 41.2: porphyritic felsic flow. mix of white and light grey; worm like texture; both have mu-sized qtz xtals; white is sil alt, whereas grey is more ser alt; strong sil, wk ser. Intruded by two, fine-grained, dark green-grey mafic dykes.

41.2 to 63.0: xstal tuff; med-grey fl with m-cu white-glassy qtz xtals (40%); rare carb clast/amygdule; rare disem py; strong sil. down hole matrix is dark grey and more plag-rich; there is more red/brown staining (fe-carb) which is kind of replacing xtals (maybe some plag then) still mod-strongly sil alt w/ wk-med chl alt.
63.0 to 65.2: Med-gr LT, 10% glassy xstals, irregular calcite filled amys,

65.2 to 97.3: xstal tuff; dark grey- almost black fl-v.f.u matrix with fl-mu qtz and plag xstals (15%). Not an obvious xstal tuff. More sandy in apperance. 5% carb over print; mod chl alt.

97.3 to 99.3: sil tuff breccia; clasts are subangular. Some large rhyolite clasts are fractures with carb infilling interstitial space. Most clasts are sil alt light grey fine-gr rhyolite piece (I think?), some chert/qtz fragments and some thicker carb veins, few darker grey blebs. strong sil alt.
99.3 to 104.7: amygdaloidal dyke; med-grey green; oval 0.5-1 cm carb amygdule; possibly elongated, seems to wk-mod fol; cluster of amygdules, few thin discordant carb veinlets.
104.7 to 105.7: Same LT/tuff breccia as above
105.7 to 114.5: fu-ml tuff, well fol,; fe-carb overprint pervasive, rare carb concordant veinlet; least alt? Or wk chl alt
114.5 to 115.1: Altered dyke??
4
115.1 to 137.9: Heterolithic tuff. Local fault from 120.9 to 122 m, black with many quartz veins. Normally graded, tuff to xstal tuff with local lap fragments and mudstone units.

137.9 to 143.07: Mafic dyke
143.07 to 144.7: v.chl alt mud; thin bands of py in very alt part; also diseminated py in v.black, f.g chl.
144.7 to 155.3: Normally graded heterolithic tuff. Lapilli are locally cholotized and matrix is mod sil alt with 5% disem py, unit is mod fol. Grades locally to mudstone.

155.3 to 182.9: Mafic sill

182.9 to 195.75: light grey tuff with 5-10% white, round plagioclase xstals, mod ser-sil alt, locally mod chl as laths. Local sulphide staining.

195.75 to 229.45: dark green/black mafic dyke; f.g wk fol, rare carb vein; v.f carb over print

Project: Hurricane
Drill Hole: GA-07-209
Date: Oct 4th to 5th, 2014

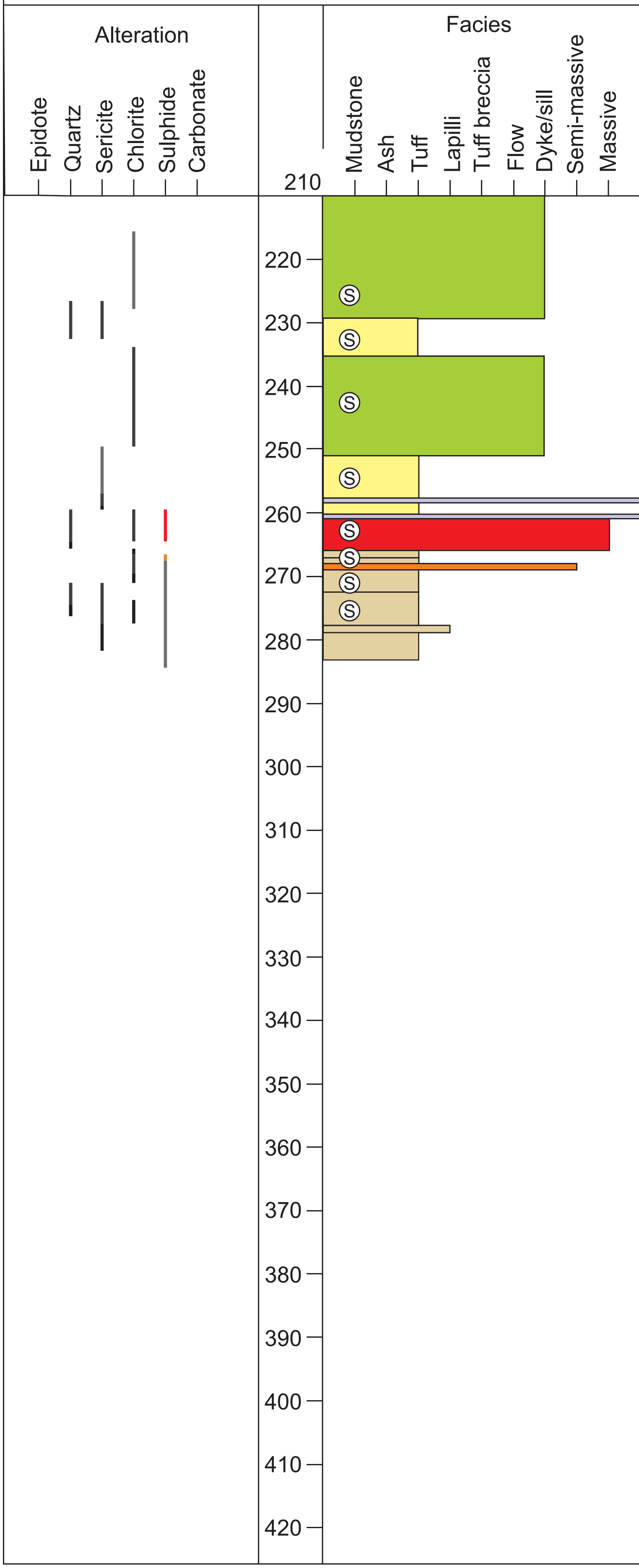

Descriptions

229.45 to 235.0: ser alt fu tuff with few fl plag xstals (white).

235.0 to 250.8: Dyke (grey/brown); f.g; few fe-carb filled amyguldes, some round qtz xstals, mod fol, wl chl alt. Could be tuff?

250.8 to 261.25: tuff (ser); light-med grey, med-gr tuff with few white xtals, finer version of above, sandy-ish. Not really fol.

261.25 to 266.55: Banded red sp,py,gn, cp with str chl alt and chaotic carb- can see py replacing xstals (qtz?)
266.55 to 269.8: super mineralized, banded red sp, py, ccp, few qtz blebs
269.8 to 272.3: chl matrix with sulphides, py, patches of gn, bands of qtz (or carb?)
272.3 to 283.4: Dominantly mod to str sil-ser-py alt with localized zones of chl stwk.

Project: Hurricane
Drill Hole: GA-07-214
Date: Sept 15th, 2018

UTM	
474055 E	Azimuth: 141
5364596 N	Dip: -69.0
	Depth: 340.8 m

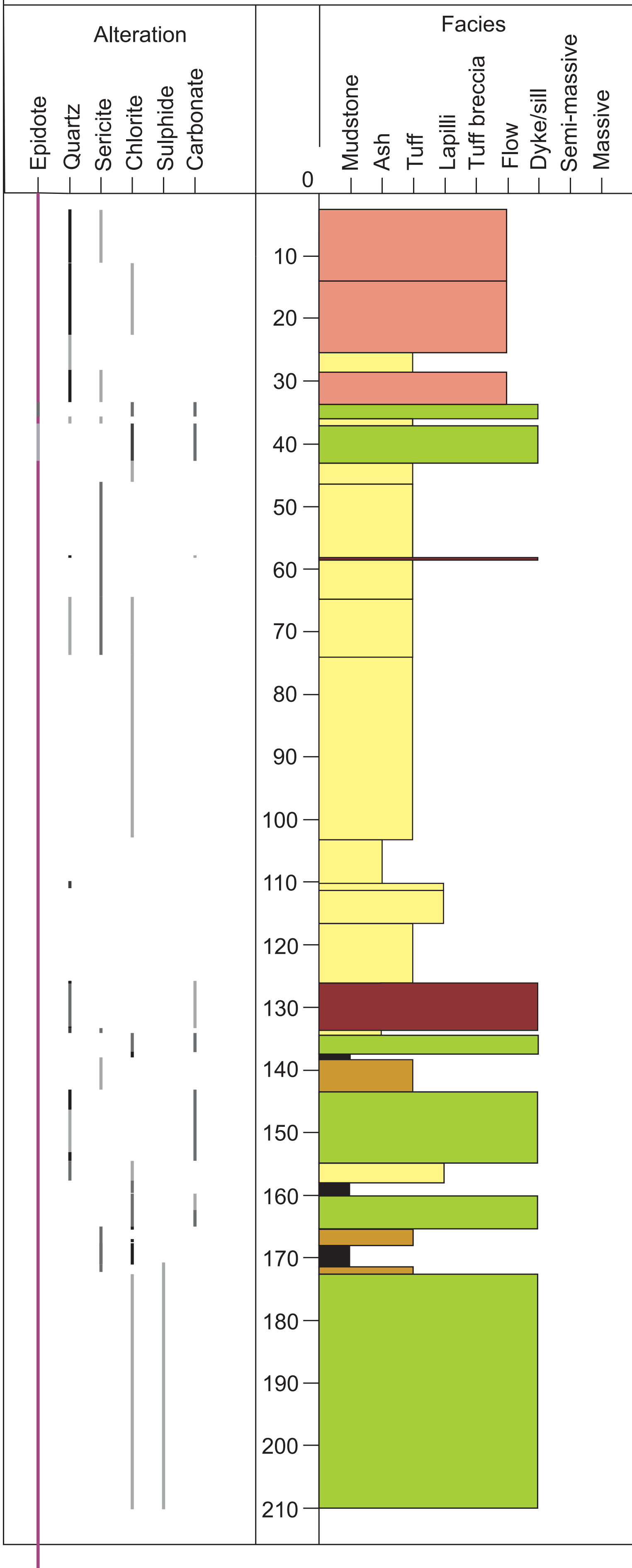

Descriptions

2 to 33.06: Felsic porphyritic flow locally interbedded with cg tuff to fg LT. f.g med-grey tuff with white round to subround white qtz xtals; appears to be discont banded or web-like with light grey (v.sil alt) and med-dark grey (w/ vein-like more chl rich zones, v.thin, ropey looking); strong sil alt, wk chl.

33.06 to 42.2: mafic dyke; fu/ml-gr dark grey-green dyke; somewhat granular looking; black specs, some carb-over print, v.g.f golden yellow flecks; few carb amygdules (round to rod-like), thick qtz-carb vein, rare qtz discordant qtz veins; rare disem py
42.2 to 102: felsic tuff; med-dark grey fl tuff with fu-m white qtz xtals (rounded-subrounded); 1-2% subangular carb lap; patches of v.f.g py, wk carb overprint (5%); few lap sized qtz fragments; wk-mod chl alt; mod fol.

102 to 109.9: felsic flow? Or fl tuff? Dark-grey f-gr with few (5%) qtz xtals, rare rod-like carb amygdules, 3% carb veinlets, mod chl alt.

109.9 to 125.78: ash tuff ± some lapilli; or felsic dyke? Light grey, fl-gr, well fol, 15% reddish-dark brown flecks (prob py), orange sulphide staining, few quartz frags; mod-strong ser

125.78 to 133.35: altered dyke?
133.35 to 136.9: fine-grained ash tuff.
136.9 to 142.59: normally graded, heterolithic tuff.

142.59 to 153.95: mafic dyke

153.95 to 160: mudstone/siltstone; black v.f.g w/ thin concondrant veinlets of carb; thin interbeds of sil-grey light grey ash tuff (1-3cm) down hole. Mod chl, small patches (<5mm) of v.f.g py. Locally grades into LT.
160 to 164.1: mafic dyke
164.1 to 167.1: Normally graded heterolithic tuff
167.1 to 171.2: Thick mudstone, potentially faulted?
171.2 to 172: Normally graded heterolithic tuff
172 to 215: Mafic sill

Project: Hurricane
Drill Hole: GA-07-214
Date: Sept 15th, 2018

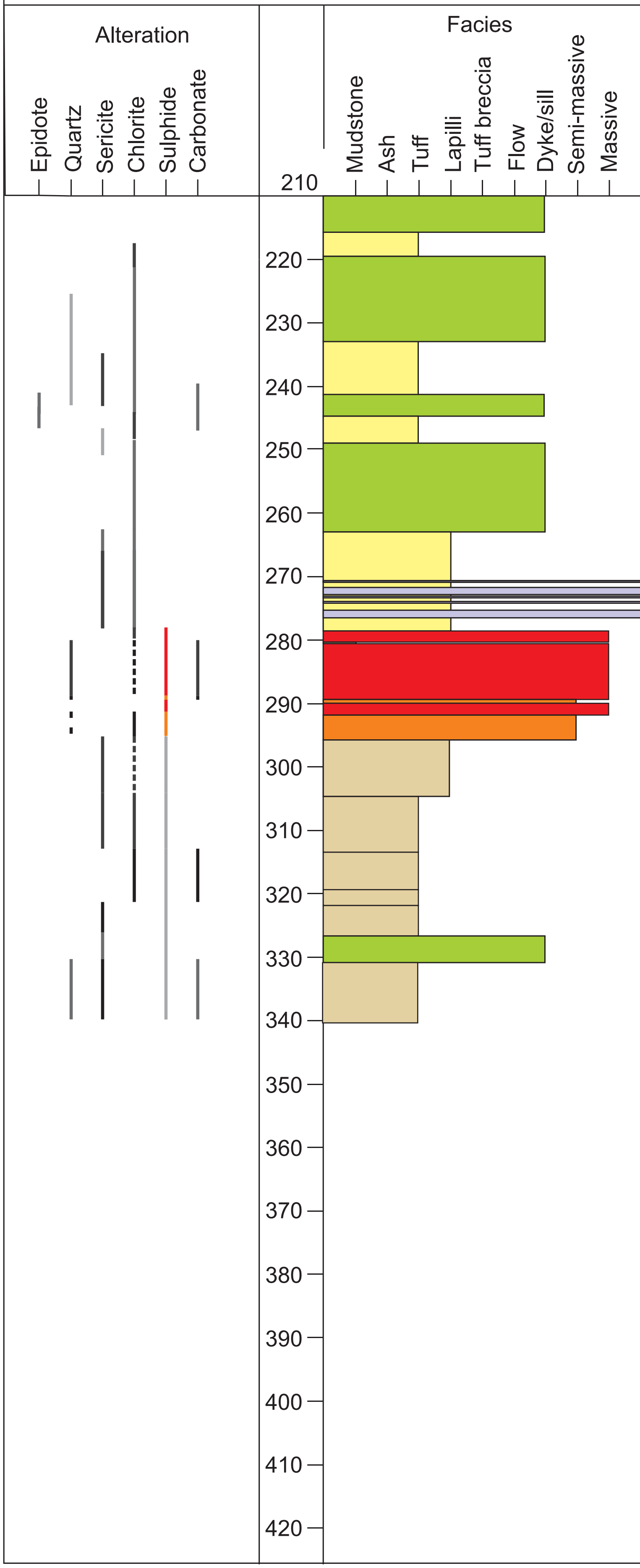

Descriptions

215 to 219.8: light grey, normally graded tuff with fine to med, white, round plag xstals.
219.8 to 232.2: Mafic dyke

232.2 to 241.1: same tuff as before mod to str ser, wk sil.

241.1 to 243.6: mafic dyke
143.6 to 249.6: same tuff as before
249.6 to 263: Mafic dyke

263 to 277.1: mod to str ser-chl alt tuff with 10% quartz veining.

280 to 291: banded red and yellow sp, py, gn. cp.

291 to 327.2: str to int ser alt tuff with localized chl alt.

295.2-295.42: py-chl alt f-gr tuff ± cp outside massive sulphide zone; fine-coarse gr-py in clusters and disem bands in chl alt tuff. Fragments of light grey mu-gr sil alt tuff ranging in size from 1-7cm x 0.5-2cm. Rare ccp with py. Py is rarely euhedral.
309.71-309.90: felsic graded med tuff ± lapilli --> v.fine-grained tuff; fu/ml light grey felsic tuff with thin (1-2cm) discont bands of med-gr black chl alt tuff with white subrounded qtz grains; rare dis py. Elongate black clasts in light grey tuff. Grey could be elongated lapilli; strong ser alt.

322.2-322.41: chaotic carbonate+vein contact+v.f.g chl alt tuff; with disem f.g p; rare red sp near veins, blebs of qtz/ chaotic carb fragments in matrix, larger clusters of coarse qtz fragments milky white to clear white in color; wk to mod fol; strong chl alt.

Project: Hurricane
Drill Hole: GA-07-218
Date: Oct 19th to 22nd, 2014

UTM
474035E
5364620N

Azimuth: 141.0
Dip: -67.0
Depth: 400.5 m

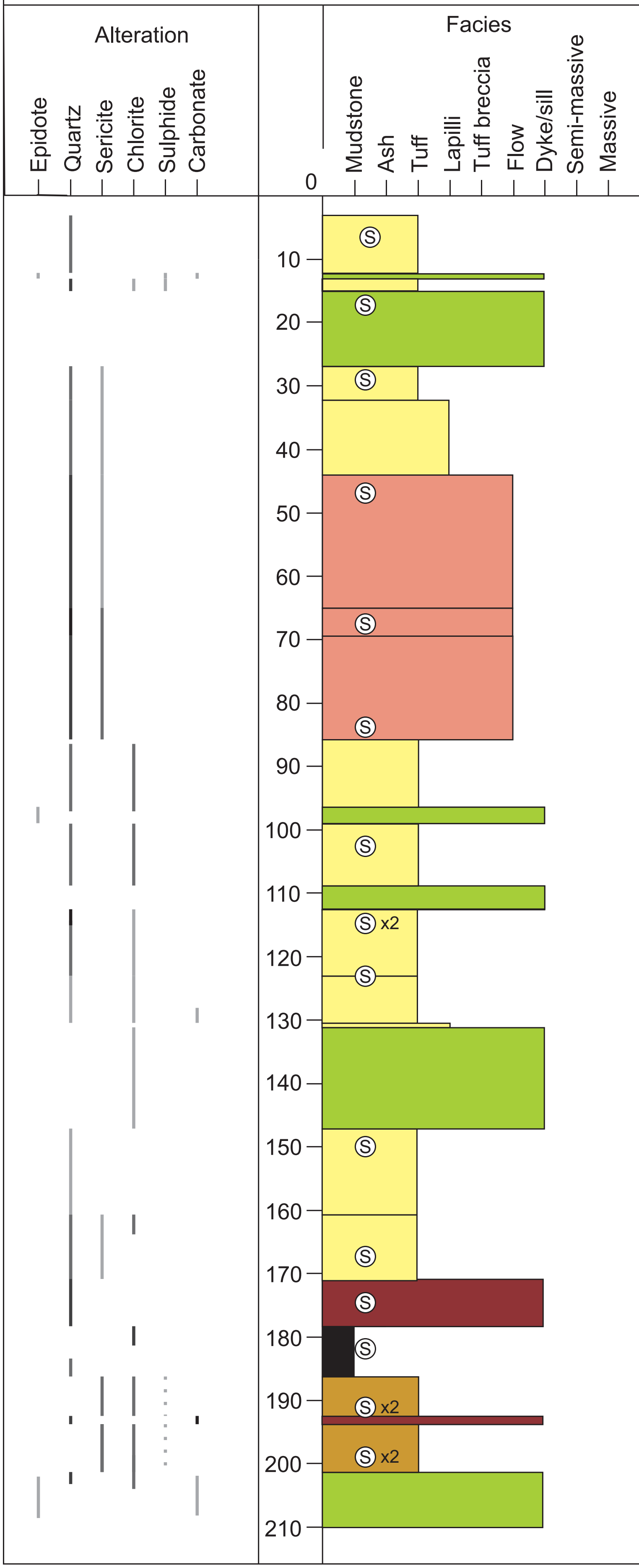

Descriptions

2.3 to 11.62: felsic tuff? ± py, sil alt, carb overprint

11.62 to 12.4: Fine-grained mafic dyke, tr py.
12.4 to 14.3: med gr, med-grained tuff with 5% plag-qtz xstals. Local lap frags
14.3 to 26.12: med-grained mafic dyke; chl alt green in color

26.12 to 45.7: f.g tuff with grey pheno (qtz?) or chl alt clast; thin py veinlets, wk sil alt. Grades down hole into lapilli tuff.

45.7 to 85.5: Intebedded plag- porphyritic felsic flow and aphyric felsic flow. locally brecciated with ser-chl in margins.

85.5 to 95.5: dark bluish grey, fine to medium-grained quartz/plag xstal tuff with fine-grained matrix. Local zones of wk to mod sil alt.

95.5 to 98.1: Mafic dyje
98.1 to 107.9: fine/med-grained (fl/ml), graded grey tuff, mod sil alt

107.9 to 111.5: Mafic dyke
111.5 to 130.4: f.g xstal tuff pale white qtz, some plag, some pulled qtz veins, shear zone? +wk-mod chl alt

130.4 to 146.5: Mafic dyke, chilled margins, coarsens inwards, 1-5% amy.

146.5 to 170.24: xstal tuff, massive? Pale white qtz xstals (<1mm-7mm), locally graded with chl-rich thin beds.

170.24: 177.1: v. sil alt xstal ash tuff or felsic dyke, likely tuff affected by underlying fault, increased fluid movement.
177.1 to 185.1: mm interbeds of chl alt silt? + ash tuff. Fault zone.

185.1 to 200.5: Normally graded heterolithic tuff. mm interbeds of chl alt silt? + ash tuff + py, med-grained tuff with local sandy zones and mudstone clasts.

200.5 to 234.8: Mafic dyke

Project: Hurricane
Drill Hole: GA-07-218
Date: Oct 19th to 22nd, 2014

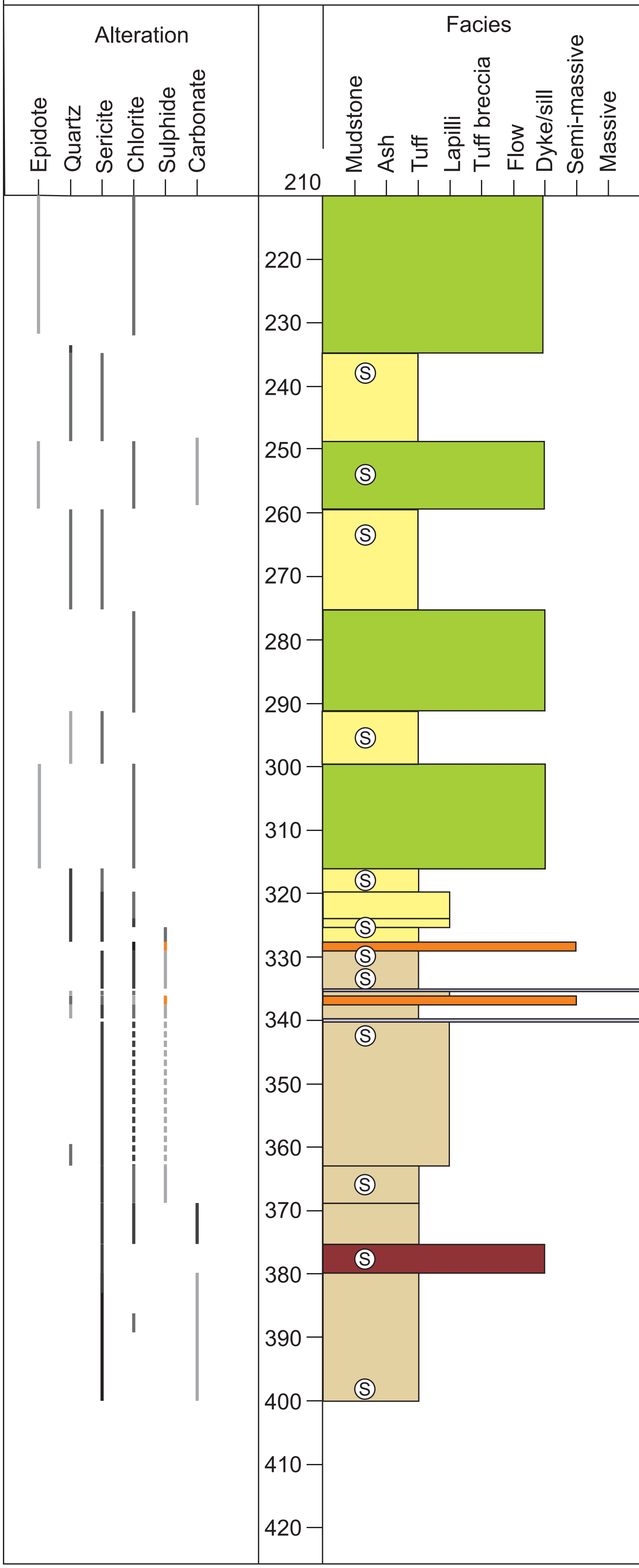

Descriptions

234. 4 to 248.8: graded tuff (mu/cl-->f.g);py in thin bands; mod ser alt, chl bands

248.8 to 259.4: med-grey f.g tuff, vuggy? Could be dyke, thin carb veins

259.4 to 275.2: sil alt tuff f.g ± few qtz xstals

275.2 to 291.1: wkly foliated mafic dyke.

291.1 to 299.4: sil alt/ ser alt tuff f.g ± few qtz xstals; well fol

299.4 to 315.9: Dark grey-green mafic sill. fine-grained, only slightly coarsening inward. Local spotty fe-carb spotting up to 30-40%.

315.9 to 319.9: ash tuff with sil and ser alt
319.9 to 328.6: tuff with chl alt >sil+ser

328.6 to 329.2: Semi-massive sulphides, banded and spotty red and yellow sp, cp. py, gn with chl-ser matrix.
329.9 to 335.4: mod-strong ser< chl; thin bands of py (10-15%) in chl + disem py, trace sp?
335.5 to 337.1: semi-massive sulphide with alt chl and "un-alt" patches; ser alt too, chl > ser, 2% py, tr sp.
337.1 to 362.5: ser-sil alt tuff with chl stwk and local bands of fine- to med-grained py.

362.5 to 371.6: stwk alt; f.g tuff w/ chl and ser alt; patches of more chl alt w/ py.
371.6 to 374.5: str chl and CC alt tuff

374.5 to 380: Ser-sil alt intermediate dyke
380 to 400.5: v.ser alt tuff; f-m-gr w/ some thin black clasts

Project: Hurricane
Drill Hole: GA-07-254
Date: September 19th to 20th, 2014

UTM	
474012E	Azimuth: 141.0
5364566N	Dip: -69.0
	Depth: 322.2

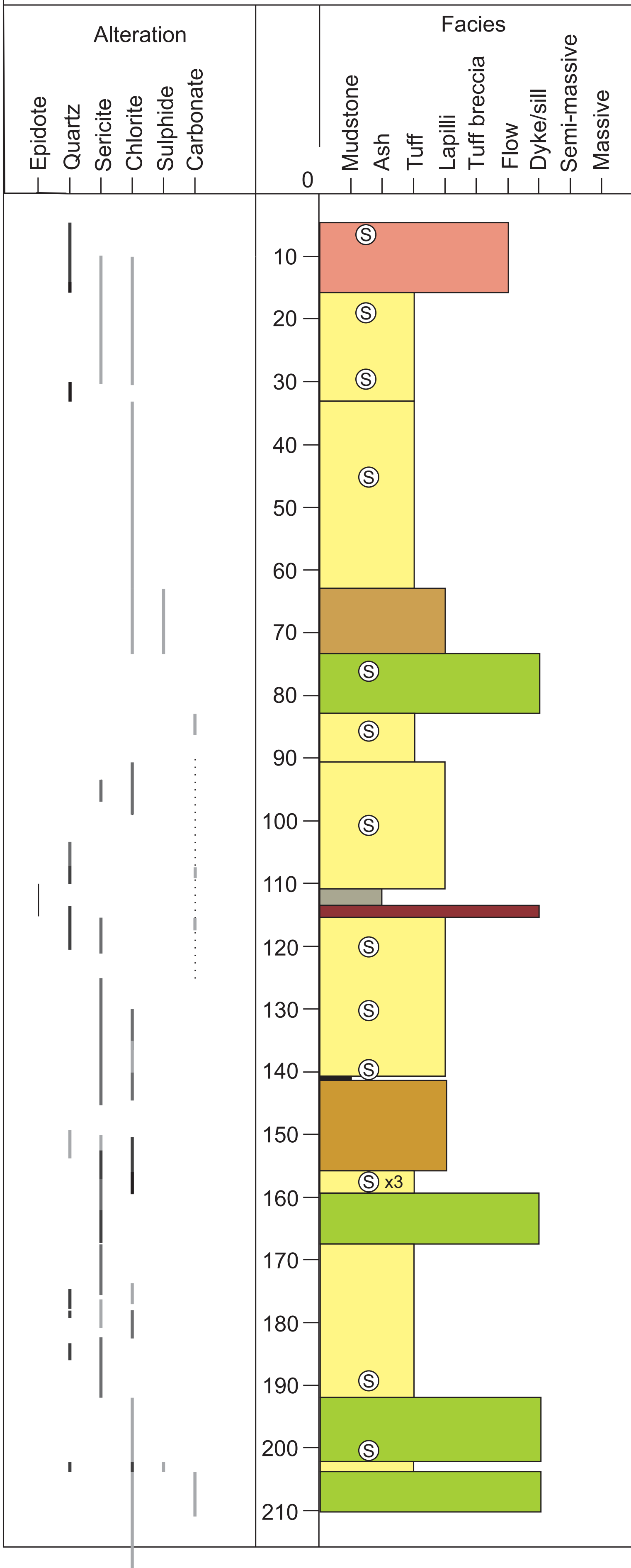

Descriptions

3.5 to 15.66: Beige to grey plag-qtz phyric rhyolitic felsic flow. First 7 m is quartz-phyric which transitions into qtz-plag phyric DH with Pheno size increasing to 1 mm to 5 mm. Unit is brecciated from 9.8 to 15.7 m (LC). Clasts are angular and range from 1-5 cm and appear to be jigsaw-fit. Strong qtz, wk-mod foliation. LC is gradational with tuff.

15.66 to 68.25: Grey to brown/dark grey in color. Contact is gradational v.f.g ash tuff (xstal ~3%) almost interfingers w/ med-coarse xstal tuff (matrix is vfu/fl) w/ xstals ~1-2 mm. Moderately foliated. xstals are white and rounded-subrounded; they increase in size DH to ~2-4 mm and increase in abundance from 5-12% to 10-20%. Fol decreases DH. @ 30.96-32.6 m get pale grey c.g. tuff; matrix is fu w/ dark grey and glassy clasts ranging from 0.5-1cm (common 2-5 mm). Local large clasts (rare lap) are milky white and subrounded to subangular. common clasts are subrounded.
(2) 30.96-45.4: dark grey±green vfl-vfu matrix with 1-3cm xstals white rounded to subrounded. @ top 15-20% increase to 20-30% DH. ~10% has 0.5-2 cm±(4 cm) calcite filled amygdules. Locally rimmed with fe-carb. Unit also has 5-7% qtz/carb veins from 0.1-5 cm thick; locally 18 cm thick. Fol decreases DH. Matrix coarsens DH to ~fl. @ 51.96-64.75 get interbeds where dramatic decrease in white xstals vs tuff (65:35). tuff is fu/fl w/ ml xstals (~2%). Fg unit can range from 20 cm-1 m thick.

64.75- 73.20 m--> graded xstal tuff tol LT (sub-rounded; locally clast-supported). Matrix is ml-fl w/ large distribution of clast sizes from 0.5- 23cm (avg. 2-4 cm). Lap frags composition range from: qtz xstals, rhyolite, chert, porphyritic felsic frags, py (1%). contact is v. abrupt and sharp either capped by f.g. ash tuff some sulphide staining near contact.

68.25 to 82.63: Dark grey-green f. to m.g. mafic dyke. UC and LC have chilled margins. 3-10 % 1-5 mm rounded to subrouded amy, 5% thin (1-2 mm) x-cutting carb veinlets. Amy and veinlet concentration increases DH. Local breccation infilled with calcite.

82.63 to 90.43: Plag and quartz-rich crystal-bearing tuff. Qtz and plag xstals are 1-5 mm, rounded in fine-grained, dark blue-grey matrix. Xstals 20-30% dominantly quartz-rich.
90.43 to 110.6: Interbedded, normally graded, heterolithic tuff to lapilli tuff. Beige to grey in color. Tuffaceous units are mg to vcg with rare mudstone clasts. Locally, grade into ash tuff and/or siltstone.

110.6 to 113.3: Thinly laminated, light grey siltstone.
113.3 to 114.9: Beige to grey, fine-grained, massive, altered mafic dyke

114.9 to 158.8: Similar normally graded heterolithic tuff as above. However, first appearance of mudstone interval associated with thinly banded py. Fault from 153.1 to 153.6m.

158.8 to 167: Grey to greenish-grey, massive to weakly fol, fine-grained mafic dyke. 3% discordant carb veining, trace calcite amy, sharp upper and lower contacts.

167 to 191.46: grey to light grey, normally graded, ash tuff to LT. Fine- to coarse-grained tuffaceous layers contain 5-10% white, round plag xstals. Local sulphide staining is visible. Wk to mod sil-ser, mod fol.

191.46 to 260.81: Overall, unit consits of mutiple mafic intrusives. They are dark green grey, fine- to med-grained, with 1-10%, 1-5 cm concordant qtz-carb veins, 2-3% carb amy. Locally. thin intervals of light grey tuffaceous unit is seen, contacts are sharp, appears to concordant contact.

Project: Hurricane
Drill Hole: GA-07-254
Date:

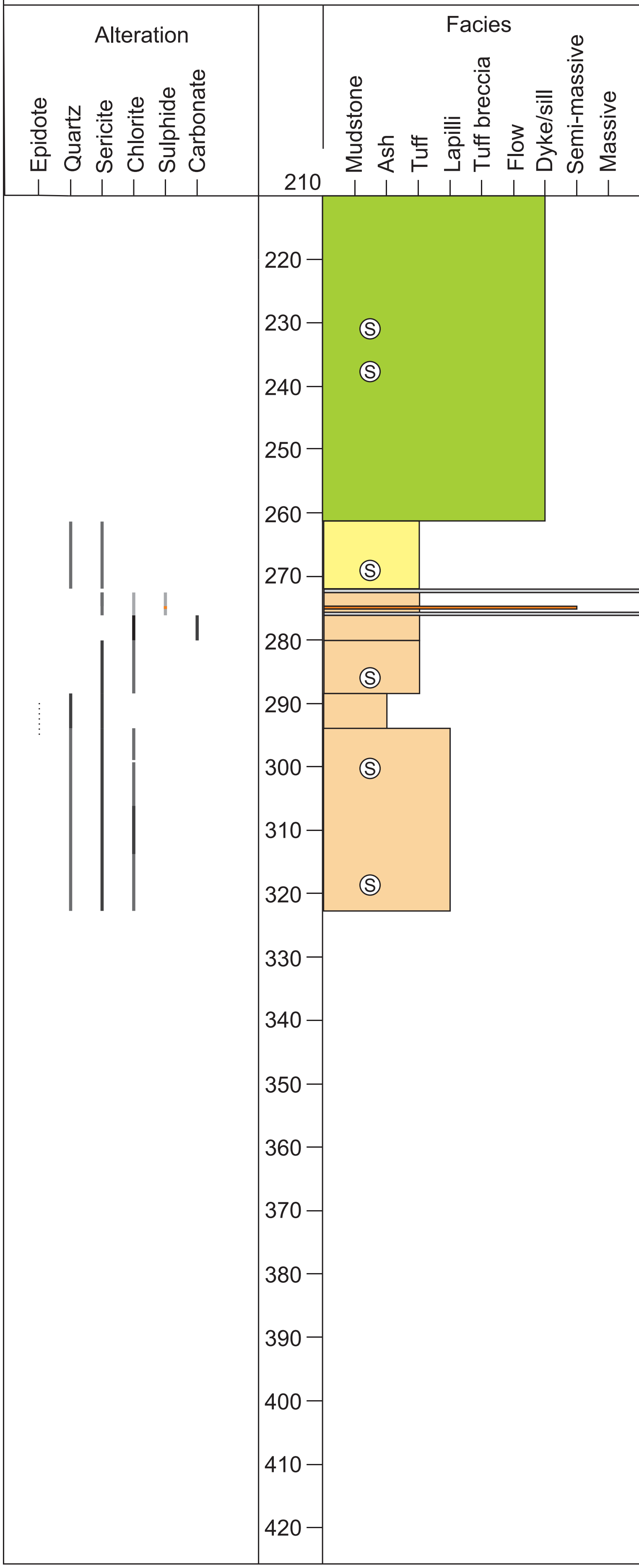

Descriptions

260.81 to 271.53: Contact is fractured, but appears to be abrupt with overlying sill. Light to med grey, fine to med-grained, plag-bearing tuff. Local chert and ash intervals. Ser-sil alt increases downhole.
271.53 tp 274: Upper contact is highly veined and weakly fractured. Normally graded, siltstone to fine-grained tuff. Mod-str ser-sil alt with thin blk chl laths with diseminated py.
274 to 274.5: Semi-massive sulphide, fine-grained py with lesser sp, cp, and gn
274.5 to 287.9: Similar to above, with stwk py-chl. From 275 to 279.5 intensely chl alt (black) related to qtz-carb veining (CC).
287.9 to 293.4: light grey with white bands, rare 1 cm qtz, bands of py (10%) and rare cp.
293.4 to 322.2 m: strongly sericite altered tuff with chl stwk associated with py and lesser BM stringers.

Project: Hurricane
Drill Hole: GA-07-255
Date: Sept 11th to Sept 12th, 2014

UTM	
474012E	Azimuth: 141.0
5364566N	Dip: -68.0
	Depth: 287.1 m

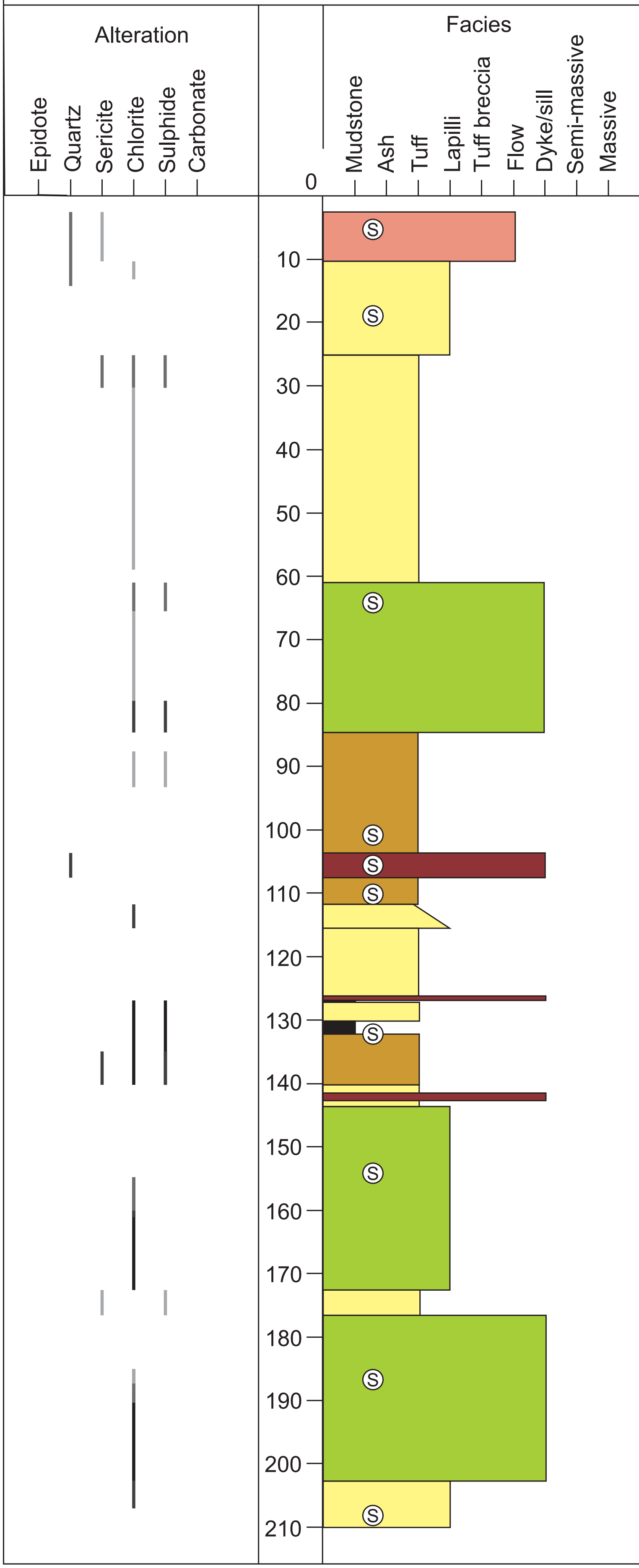

Descriptions

1 to 10.81: White to light beige in color that transitions DH to more grey-brown. 10-20% 0.1-0.5 cm plag and qtz phenocrysts in vfg matrix. Phenocrysts increase in size DH to 0.5-0.8 cm. Thin, wispy, discontinous bands of chlorite and/or sericite parallel to wk to mod foliation. Brecciated lower contact.
10.81 to 25.19: Bottom of unit is brecciated with clasts ranging from bombs/blocks to lapilli. Larger fragments are anuglar and irregular fragment size is heterogenous. Grades upwards from breccia to lapilli tuff. Clasts are chlorotized. Cholo decreases down hole, some sericite alt down hole. lapilli size is consistent through unit. grey-brown in color. well foliated.

25.19 to 61.5: Generally, unit is fg, massive phenocrysts ~0.2-5 cm in size.
61.5 to 84: Amygdaloidal mafic dyke, unit is fg, massive w/ homogenous amygdules ~0.2-5 cm in size. Some rare large amygdules range from 1-10cm and are more common in top 25m, only ~3% of core. Appear to be later also. White amygdules either qtz or carb. Could have carbonate over-printing or replacement (orange).

84 to 111.78: Overall, gradational sequence (grading can be abrupt) of med-coarse grained volcaniclastic into finer grained lapilli. This sequence repeats itself every 0.5-1m. Fine portion is typically associated with sulphide staining and alt (minor chlorite). moderately foliated. 103.9-108.0--> highly veined unit +k-alt- grey to light beige, speckled (lapilli) rusty orange (on weathered surface). Minor visible py <1%. matrix of tuff is pink/beige. After this resumes to typical grey lapilli tuff that grades into finer tops.
111.78 to 115.5: Very fine-grained ash tuff- black highly chlorotized. Grades into chlorotoid tuff then qtz vein then fault which goes though v.f.g tuff.
115.5 to 172.5: Same graded lapilli tuff. Alteration predominately in fine-grained portions. With some exceptions. (a) v.f.g elongated clasts in lapilli tuff. Some with pyrite; range in size from 1x3--> 5x30 cm parallel to foliation. Not restricted to coarse or fine. typically sulphide staining around them. (B) alteration goes from red/black/orange/yellow; TOP--> coarser grained units have disseminate py/sulphide staining +chl alt. whereas fine-grained are heavily chl alt--> black, some sulphide staining. v.f.g pyrite. Moving downhole f.g still heavily chlorotized but med-grained lapilli becomes more sericitized± sulphide. Top 30 cm is silicified. (A) massive lapilli tuff--> less clasts then previous unit. Light grey to dark grey in color. disseminated qtz veins throughout ~0.5-6cm thick and randomly oriented. some rare granule size lapilli/phenocrysts (or amygdules) that are white. minor grading but not as defined as previous unit.

172.5 to 176.5: Top is coarse-grained lapilli w/ some minor brecciation; grades into fine-grained lapilli. Sequence repeats itself w/o brecciated unit throughout. Pyrite increases towards alt horizon at base. Mod fol.
176.5 to 202.75: massive to weakly graded med lapilli tuff. Lapilli at top are mu/cl grades gradually into fine lapilli. Massive (non-foliated I guess) and very chlorotized . Rare amygdules filled with calcite or qtz

Project: Hurricane
Drill Hole: GA-07-255
Date: Sept 11th to Sept 12th, 2014

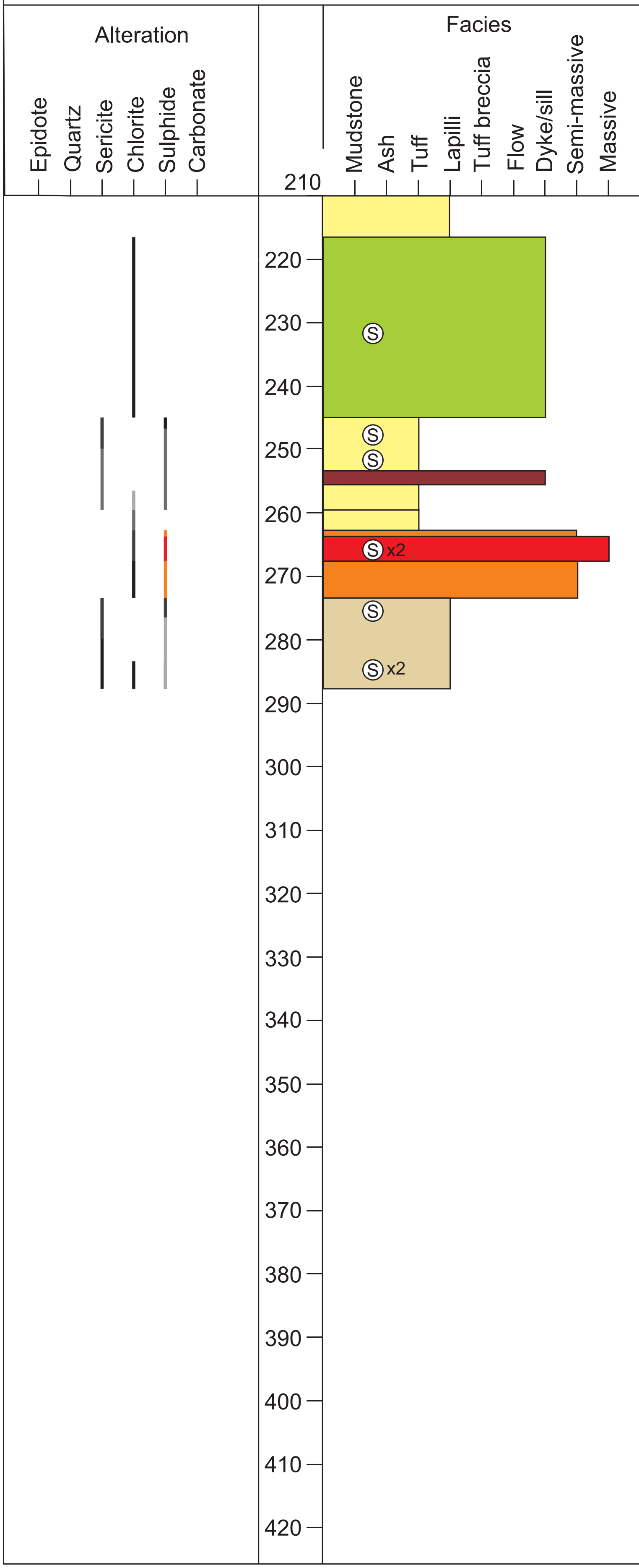

Descriptions

202.75 to 216.55: erosional contact b/t units. Cl/cu lapilli tuff (massive) minor grading. ~1-2% euhedral pyrite. "foliated". Minor 1-3cm chlorotized clasts. Top of unit chlorotized (dark grey) transitions into more epidote/sericite rich alt (greeny/yellow color).
216.55 to 245.0: gradational contact; small euhedral 0.5 pyrite in coarser grained upper unit. Unit is typically mu-ml ± fu and massive + highly chlorite alt (90%). Few 10-30 cm cu-->vcl ± mu matrix that abruptly grades into mu/ml unit (1%). Dark grey-green in color. coarser unit grey with white lapilli. @228.3-231.85 (qtz veined zone?)- euhedral py above and below qtz veins in mu-fu lapilli tuff. some smaller qtz veins above red horizon (on strat log?). rare chalco on margins of large qtz lapilli. @239.9 qtz-carb veining increase till end of unit. all f.g (ml-fu± m) chlorotized lapilli tuff.
245 to 263.7: Contact has lots of qtz veins, almost looks erosional. Repetitive graded sequence of cu/cl w/ ml matrix ± vcl grains into vfu--> ash or fl. Grading appears to be very abrupt. Fl units have pale green mineral associated with it (also highly sericitized). Fine-grained units more alt then coarse-grained (or appears to be) sulphide staining in c.g where has f.g=sericite and/or chl silic. upper part of unit is coarse-grained (~4m; sulphide staining+fe-carb) which grades into ~1m of v.f.g--> fine-grained unit is moderately fissile and sericitized. Thickness of "beds" of coarse vs fine decreases moving downhole where f.g units become thicker then c.g. Top of unit is "c.g" lapilli tuff with some f.g chlorotized clasts. @ 260.98m disseminated+ clusters <0.1mm-1cm pyrite grains, clusters up to 4cm long. Galena in elongated clusters (1x7cm). Sulphides within bedding of volcaniclastics. @261.66m--> qtz vein (4cm thick)+ multiple <1cm qtz veins interbedded w/ highly chlorotized v.f.g tuff + small disseminated veinlets of pyrite/sulphides. Sulphides are interbedded with fu/fl±mu l.t (or maybe just tuff; can be as fine as ash). Fine unit grades abruptly into ml--> mu/cu w/ coarse clusters of pyrite (0.5-.3cm) some are elongated w/ bedding. all are parallel with bedding/foliation. (15% py;1-3% honey sp; <1% ccp)
263.7 to 268: massive sulphide is typically composed of vfu, fl of py and red sp. They are typically intermingle in clusters of elongated wispy bands. The bands are 1mm-1.5 cm thick. @ top of unit, they increase in thickness moving down the hole. There is an increase in py grains moving down hole. few elongated clasts of f.g chlorotized L.Y(1%; could be mudclasts). @266.52-266.88 qtz vein w/ coarse ccp+gn+copper colored mineral--> massive py till end of unit.
268 to 274: General--> v.f.u-->ash w/ mu elongated lapilli? With 15-20% pyrite grains (relatively euhedral; 0.5-1mm) incorporated within the bedding. Typically associated with finer grained chlorotized units but not exclusively. Near contact much finer v.f.l and speckled. elongated wispy qtz bands. foliated? dark grey to med grey in color. coarser lapilli appear elongated.
274 to 287.1: ml-mu matrix w/ cu-vcl lapilli that are elongated up to 3cm. Grades into ml+mu lapilli tuff. Lower portion is typically ml/mu but with large elongated clasts, matrix is just slightly finer then before. @ 277.85 disseminated py (1%) incorporated into sediment gets progressively more clustered (5%). @279 ~15-20% py clusters parallel with foliation ± gn (1%); honey sp (7%); cp (1%). sulphides are associated with finer matrix. at 282 clusters decrease but disseminated py still present (<5%).

Project: Hurricane Drill Hole: GA-07-156 Date:		UTM 474095E 5364630N	Azimuth: 140.0 Dip: -66.0 Depth: 308.5

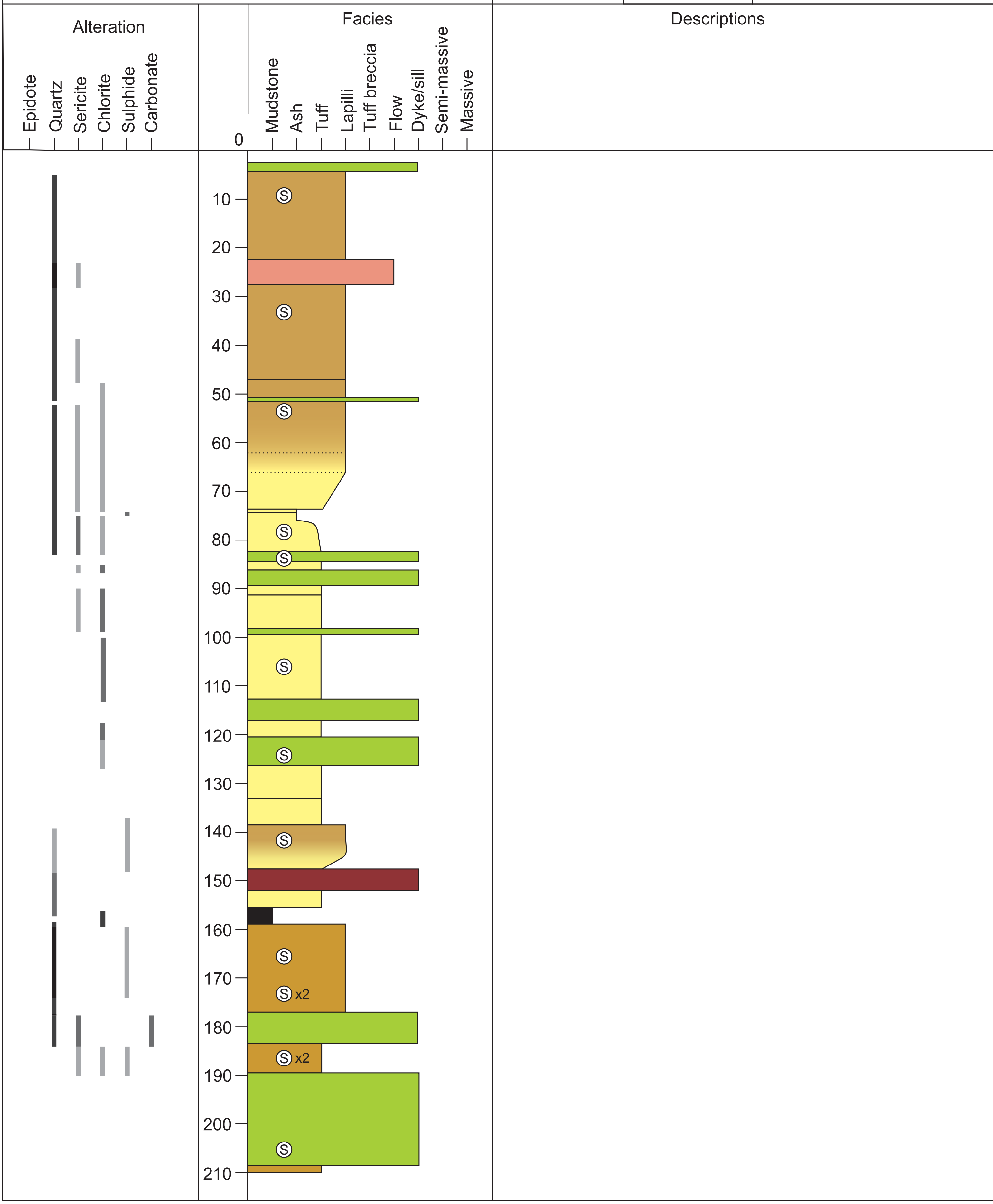

Project: Hurricane
Drill Hole: GA-07-256
Date:

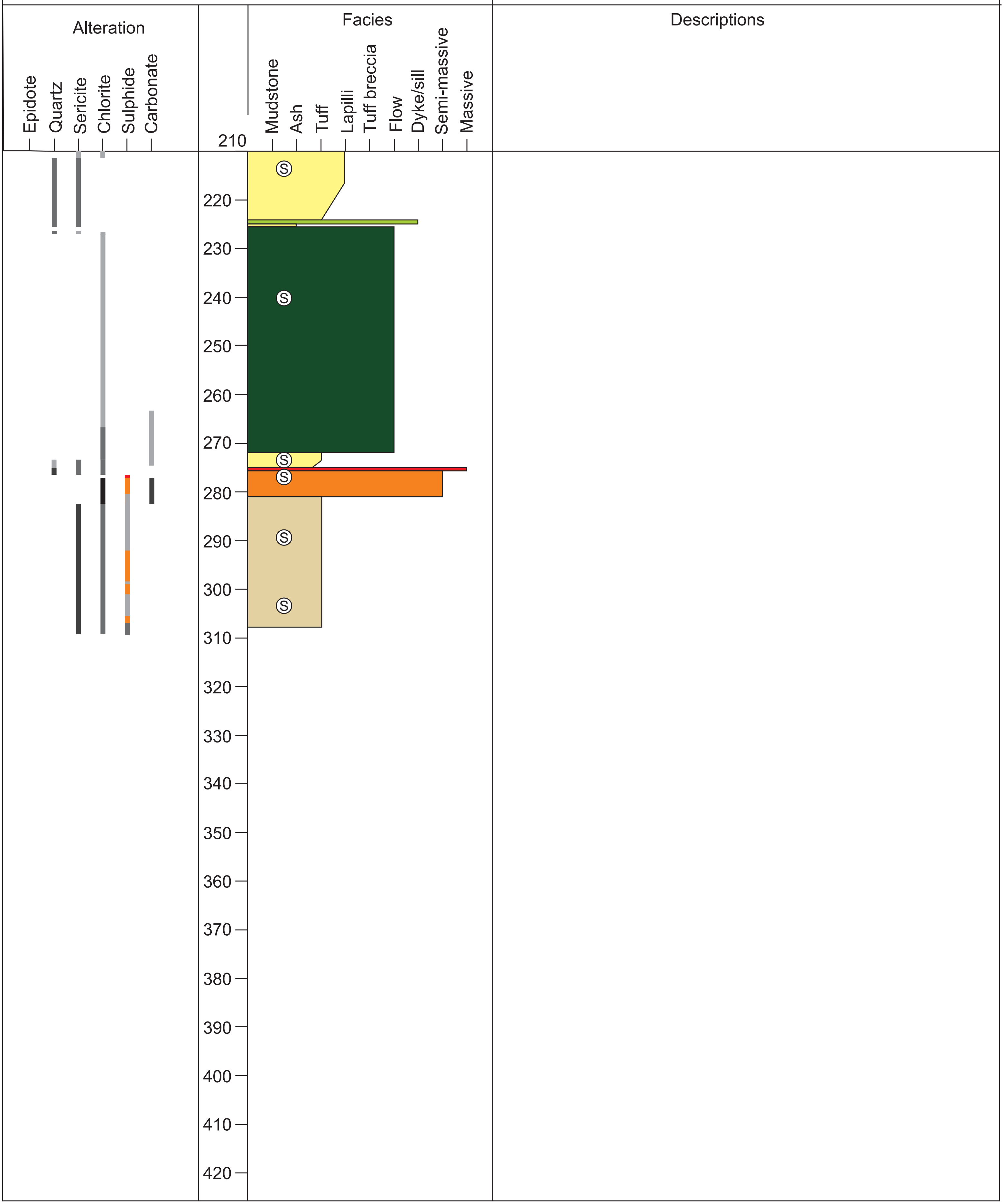

Project: Hurricane
Drill Hole:GA-07-257
Date:

UTM	Azimuth: 140.0	
474092E	Dip: -66.0	
5364630N	Depth: 308.5 m	

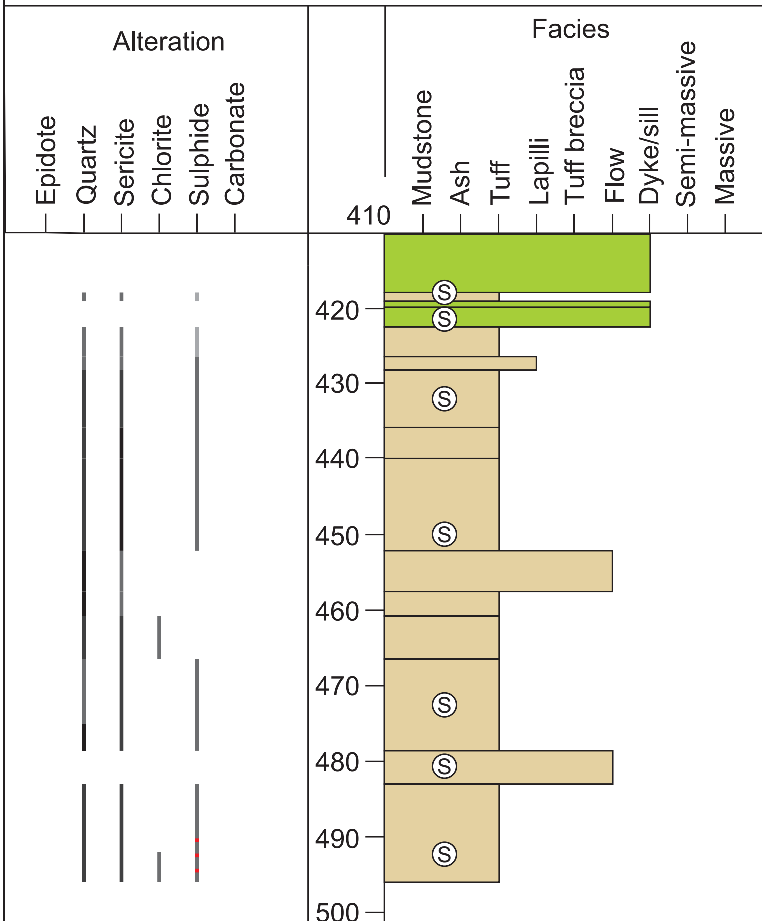

Descriptions

Project: Hurricane Drill Hole: GA-10-272 Date:	UTM 474097E 5364628N	Azimuth: 141.0 Dip: -60.0 Depth: 317.9 m

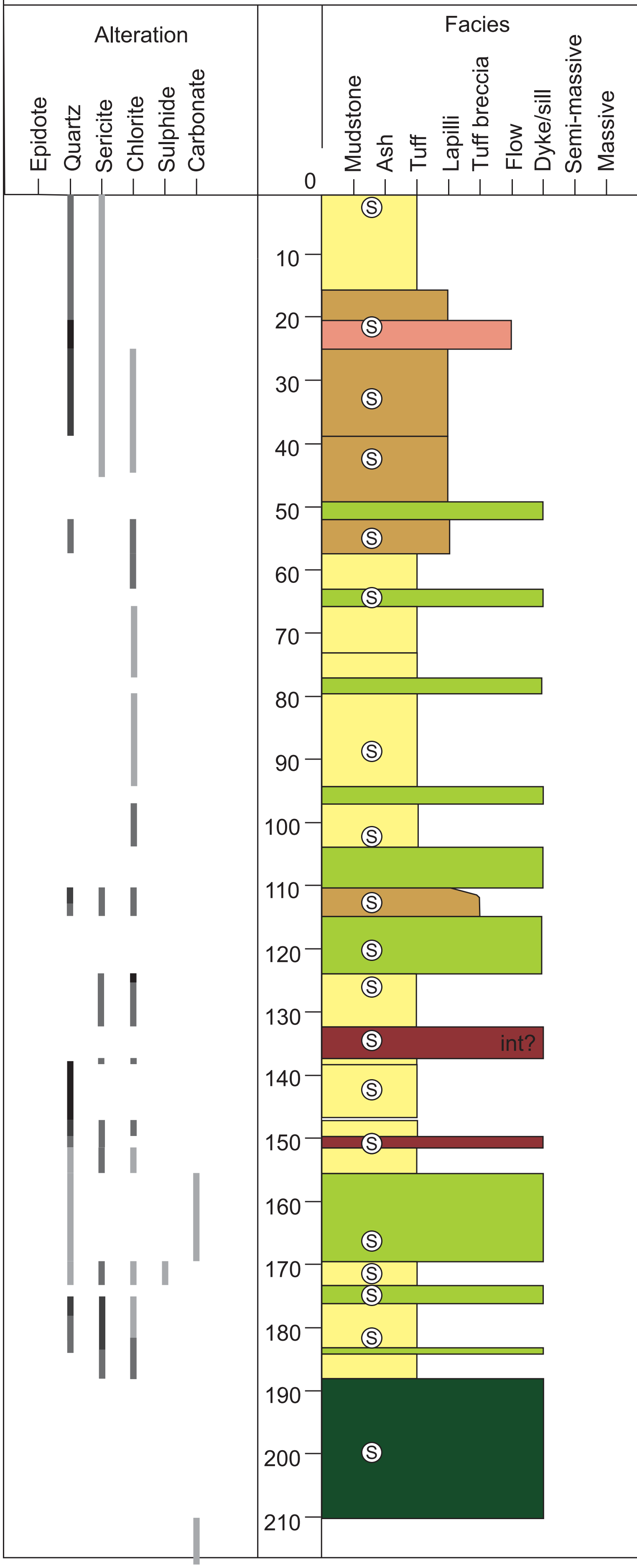

Descriptions

Project: Hurricane
Drill Hole:
Date:

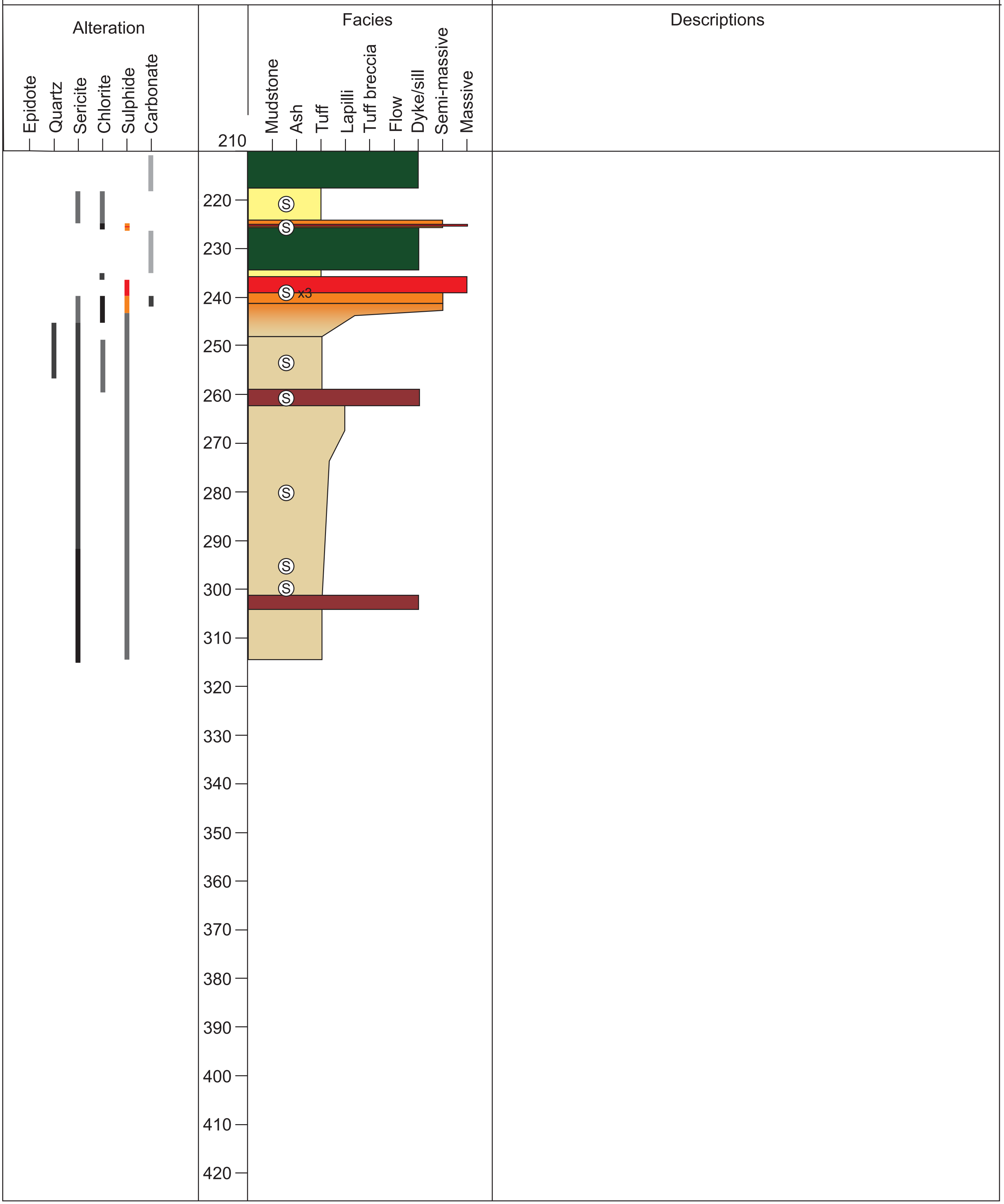

Project: Hurricane Drill Hole: GA-10-273 Date: October 11, 2015		UTM 474130E 5364660N	Azimuth: 141.0 Dip: -61.0 Depth: 309.1 m

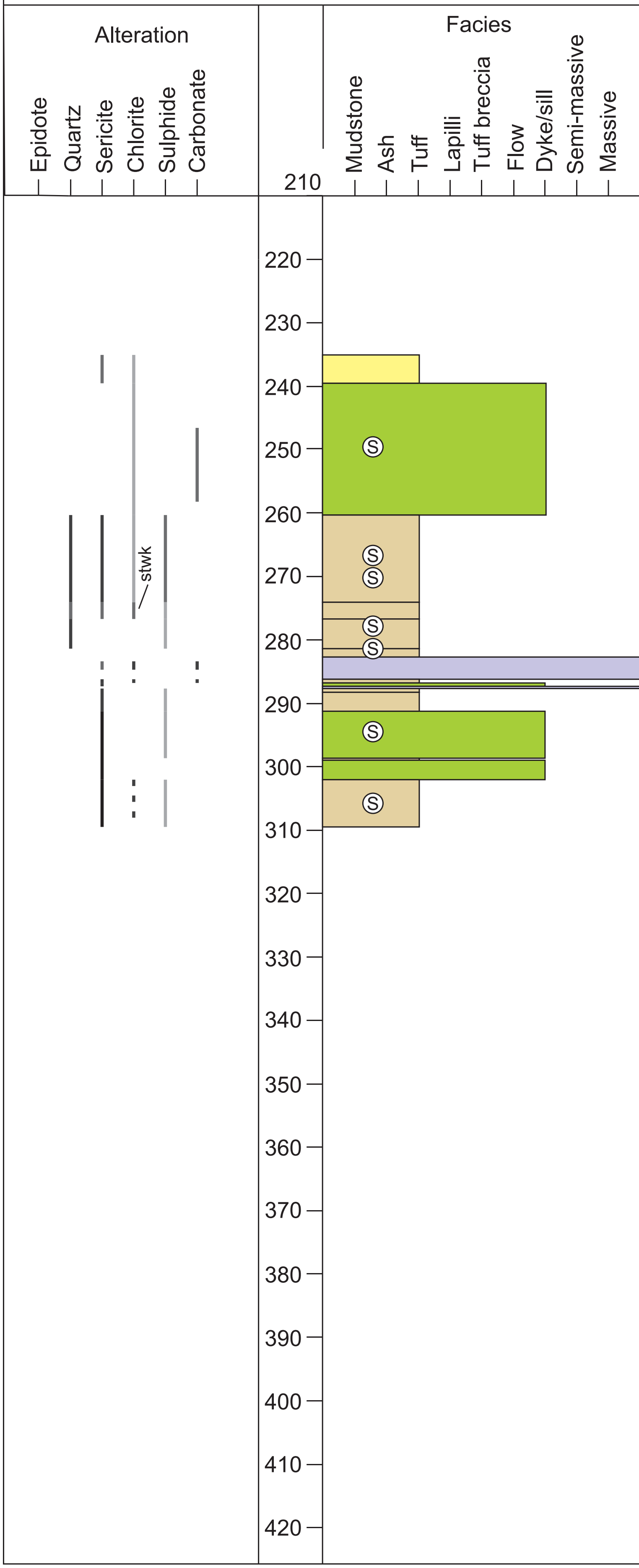

Descriptions

235 to 239.47: Graded tuff: med grey, med- to coarse-grained tuff with 10% white, round plagioclase xstals. and 5% felsic lap; mod ser, wk-mod chl. Local vgf to ash tops.

239.47 to 260.25: dark grey-green, massive, mafic sill. <1% euhedral 2 cm py near UC. 5-15% carb overprint and 1% disaggregated qv-carb veins.

260.25 to 276.64: strongly altered tuff; mod to str with chl stwk veins with py. py is fg-mg. stwk veins are 1-5 cm thick (15% of unit). locally stwk veins have 10% gn-sp
276.64 to 281.32: same as above, except dominated by str ser- py only. Locally chaotic carbonate.
281.32 to 282.64: same as above, chaotic carbonate more is thicker and more pervasive. Increase f to mg py mineralization (up to 30%) in thin bands near LC.
282.64 to 286.14: Quartz vein with 30% altered tuff xenoliths.
286.14 to 286.33: finely laminated tuff with chaotic carb alt.
286.33 to 286.86: sericite altered dyke
286.86 to 290.9: sericite altered tuff. local chevron folding and fault gouge.
290.9 to 298.3: sericite altered dyke
298.3 to 298.58: sericite altered tuff with 10% thin bands of f to mg py.
298.58 to 301.65: same altered dyke as above with disem clusters of py
301.65 to 309.1: altered graded tuff to lapilli tuff. str to locally int ser with local fuchsite. Thin chl-carb alteration; mod to str fol and 15-20% thin py bands.

Project: Hurricane Drill Hole: GA-10-274 Date:	UTM 474155E 5364686N	Azimuth: 141.0 Dip: -59.0 Depth: 320.6

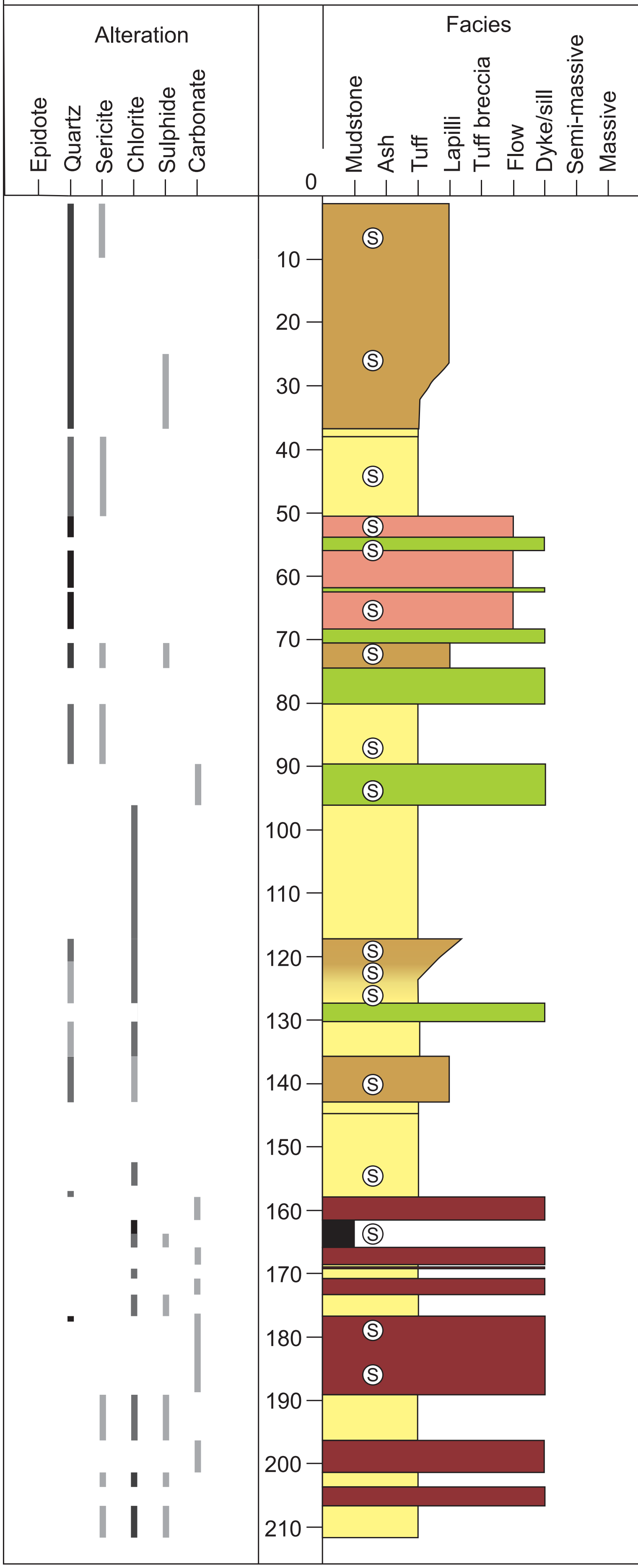

Descriptions

1.5 to 37: Beige grey to grey in color with 10-15% white plag xstals/phenocrysts. Mod to str sil alt. Phenocrystas increase in size downhole from 1-2 mm to 2-5 mm. Locally zone are aphyric. Multiple Qvs from 22.4 to 22.8 and 24.7 to 25.3, they range in size from 10-15 cm. Local dis py (6%) starting at 22 m. Mod to str sil, mod fol. This unit consists of interbedded porphyritic felsic flows and lapilli tuffs.

37 to 38.25: Fault gouge
38.25 to 50.78: Same as 1.5 to 37 m. From 48 to 48.8 fine-grained, creamy white-grey vuggy LT/ or porphyritic felsic flow.

50.78 to 70.78: Overall, unit consists of plag porphyritic to aphyric felsic flows interleaved with 0.5 to 2 m mafic dykes. Felsic units are pale grey to pinkish-white with 5-15% white plag phenocrysts or are aphryic. Locally, they have 1-3% 1-2 cm thick Qvs. They are strongly sil alt and have wk ser alt within weak brecciation. Mafic dykes are dark green-grey, fine-grained and have sharp contacts with felsic flows.

70.78 to 74.73: Med grey, med to str sil alt, wk ser. Fine-grained LT or coarse-grained tuff, felsic to intermediate.
74.73 to 80.4: Mafic dyke, dark green -grey, sharp contacts, but appears to locally e pepperitic with tufaceous fragments.
80.4 to 89.86: Med grey, med- to coarse-grained, str fol, 30-35% plag-qtz xstals, fines downhole slightly. Downhole xstals become more qtz-rich.

89.86 to 96.35:Dark green-grey mafic dyke. Coarsen inwards from margins. Local erratic veining.
96.35 to 117.43: Dark grey, str fol with 3-10% plag>qtz xstals. 5-15% sheared/ripped up carb veins. Could be sheared amy or boudinage carb veins.

117.43 to 144.98: Locally tuff breccia, grades down hole into normally graded tuff to LT. Lapilli fragments are mafic to intermediate in composition. Matrix is fg, dark grey. Locally grades into thin mudstone layers and mud clasts in coarser tuffaceous. Locally intruded by mafic dyke.

144.98 to 158.13: Same tuff as above. Tuffcaeous layers are qtz crystal-rich and sandy.

158.13 to 161.78: Felsic dyke or altered mafic dyke? Sharp upper and lower margins.
161.78 to 162.4: Fault gouge? black argillite? Strongly qtz-veined.
162.4 to 207.71: Overall this unit consists of interleaved altered mafic dykes (or felsic dykes?) and normally graded tuffs to locally LT. Similar to tuff unit above, it consists of fine to coarse-grained, qtz-rich, sandy normally graded tuffs that locally grade into mudstones. These mudstones typically have fine-grained banded py associated with them. Shear within the mudstones is also locally apparent.
The altered dykes are beige to greenish beige in color, they have sharp upper and lower contacts and are fine-grained. They have 1-5% carb amy that range in 1-3 mm in size. Locally contacts appear to be interfingering with tuffaceous units. Could be pepperitic contacts?

Project: Hurricane
Drill Hole:GA-10-274
Date:

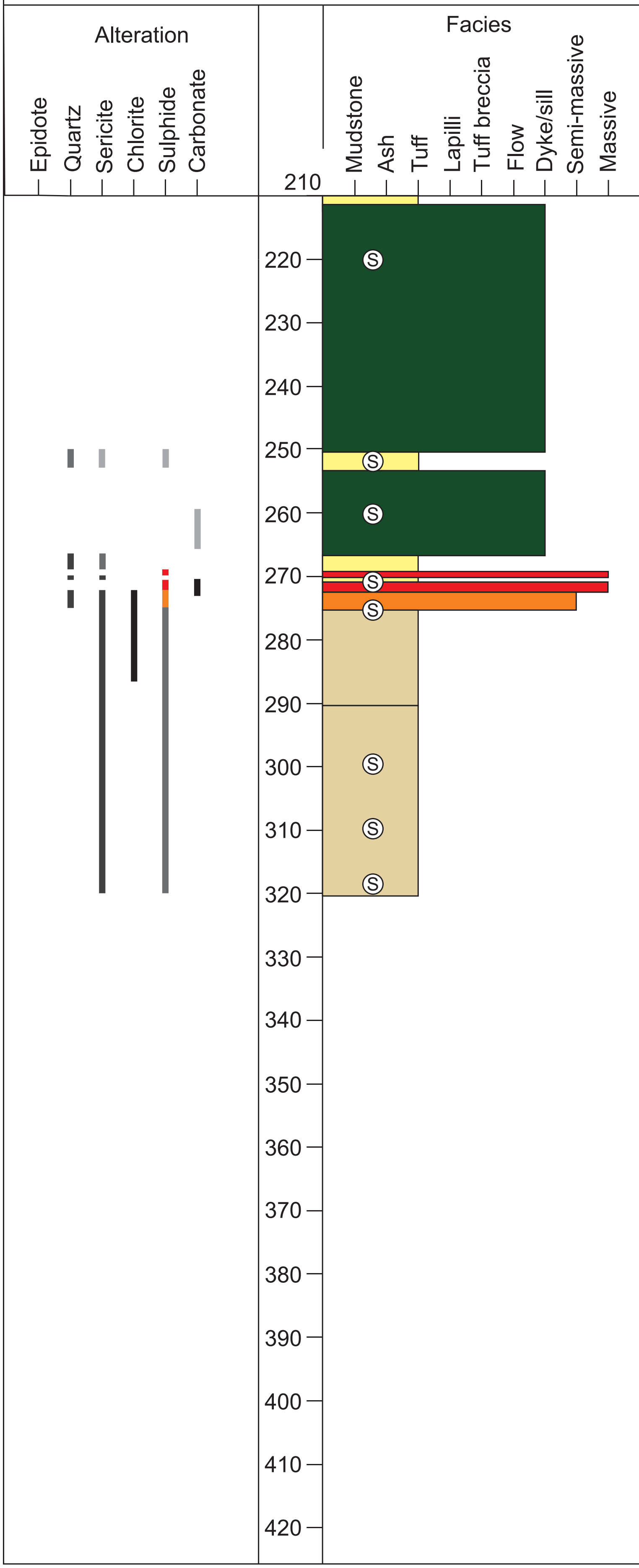

Descriptions

207.7 to 246.75: Mafic sill, dark green-grey, fine-grained, rare amy, cg py along lower margin. 15% concordant carb veining.

246.75 to 249.68: fine to med-grained tuff with 20% round plag xstals with thin silt and chert interbeds, normally graded.
249.68 to 266.33: Mafic sill, same as above

266.33 to 268.84: light grey with pale grey, white, dark grey lap, few mc stringers, med-str ser with wk-mod chl laths, str fol. Two Qvs (1.5 and 3.5 cm thick).
268.84 to 269: banded MS with blebs of ser alt tuff and some qtz xstals. f.g bands of red sp (25%), py (20%) and honey sp(5%), gn (10%) and coarse-grained cp. Contacts are gradational, showing sulphides replacing tuff.
269 to 270: Mod ser/mod chl alt tuff, 10% qtz veins, dis py along contacts
270 to 270.52: Banded MS, same as above. str ser and mod chl in stwk veins.
270.52 to 273.34: Semi massive sulphides with very str chl alt, bands of fine- to med-grained, py with lesser honey sp and 3% cp in veinlets. chl alt decreases down hole changing to ser alt.
273.34 to 320.6: Top 10 m is str chl alt, down hole transitions into mod-str ser with chl stwk associated with py stringers.

Project: Hurricane Drill Hole: GA-14-275 Date: June 18th, 2015	UTM 474097E 5364628N	Azimuth: 141.0
		Dip: -50.0
		Depth: 254.0 M

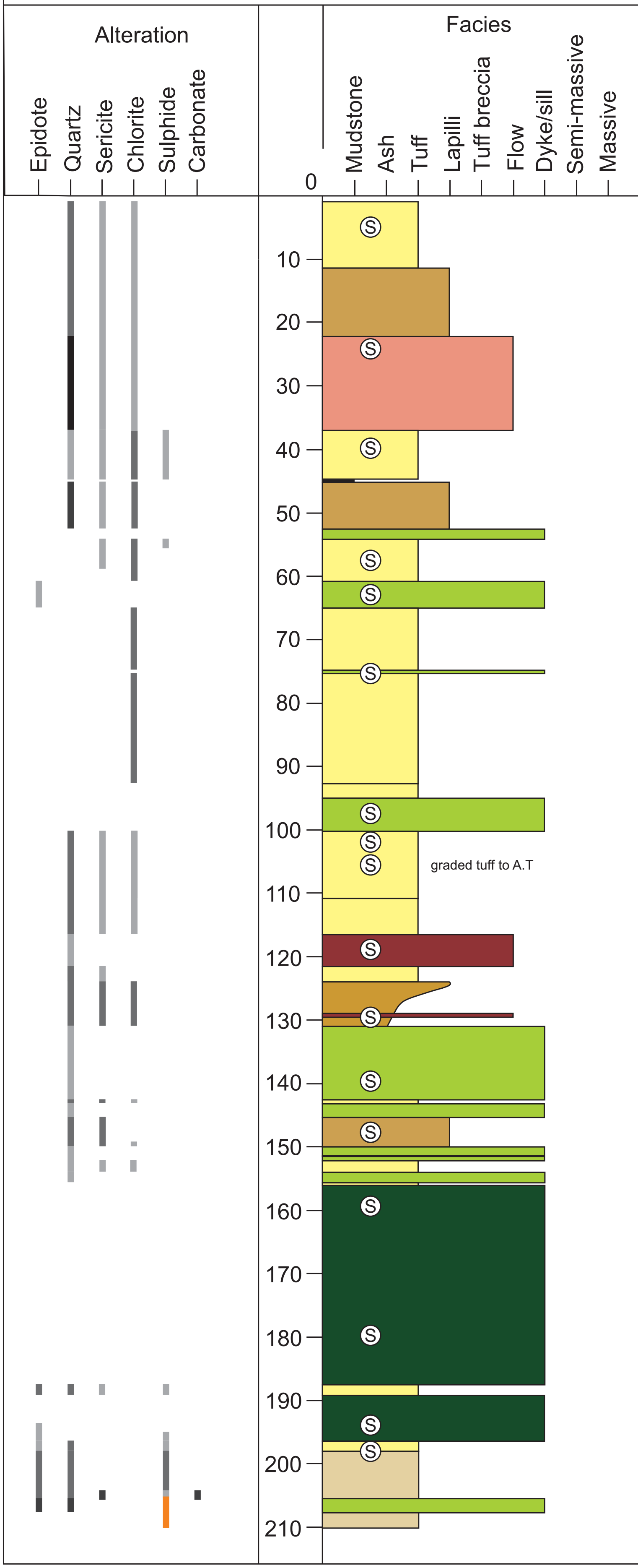

Descriptions

0.5 to 11.1: Sil alt tuff with plag xstals

11.1 to 22.3: Pale to creamy grey-white, plag-phyric, LT interbedded with porphyritic felsic flow. Ser alt in selvages of weak brecciation in felsic flow

22.3 to 37.8: Aphyric coherent felsic flow with localized zones with 1-5% plagio phenocrysts. Contacts are brecciated.

37.8 to 45.1: Heterolithic tuff to LT, mod sil and chl.

45.1 to 52.3: Heterolithic LT, similar to above.
52.3 to 54: Mafic dyke, dark green-grey, fine-grained.
54 to 92.3: Quartz-feldspar xstal tuff. Fine-grained matrix, blue-grey with 20-35% qtz-felds xstals. Tuffs become more qtz-dominant down hole.

92.3 to 94.7: Heterolithic, normally graded tuff.
94.7 to 100.6: Mafic dyke, dark green-grey, fine-grained, massive, sharp upper and lower contacts.
100.6 to 116.8: Normally graded, heterolithic tuff. Grades from locally ash tuff to coarse-grained and sandy, locally granule sized.

116.8 to 121.3: Beige to grey, fine-grained, plag-phyric, sharp upper and lower margins.
121.3 to 124.2: Same tuff as above
124.3 to 131.5: Interbedded argillite and normally graded tuff. 5% dis py.

131.5 to 145.5: Overall, several mafic dykes, greenish-grey, fine-grained, fine-grained plag xsals, 1-3% concordant carb veinlets. Thin tuffaceous xenolith, similar to above.

145.5 to 150.1: Heterolithic tuff, pale grey, locally thin lap fragments, 1-5% rounded, white plag xstals, mod ser with chl laths.
150.1 to 156.4: Overall, this unit consists of several, 0.5 to 2 m mafic dykes with interleaved graded tuffs.
156.4 to 188.8: Mafic sill, dark green-grey, fine to med-grained, massive.

188.8 to 189.2: Normally graded xstal tuff. Pale grey, white, round plag xtals. Mod ser alt, wk chl laths.
189.2 to 195.2: Same mafic sill as above

195.2 to 196.2: same tuff as 188.8 to 189.2 with thin chert interbeds.
196.2 to 207.3: Ser-sil alt tuff. 5% py stringers
207.3 to 208.1: Sericite altered mafic dyke

Project: Hurricane
Drill Hole: GA-14-275
Date:

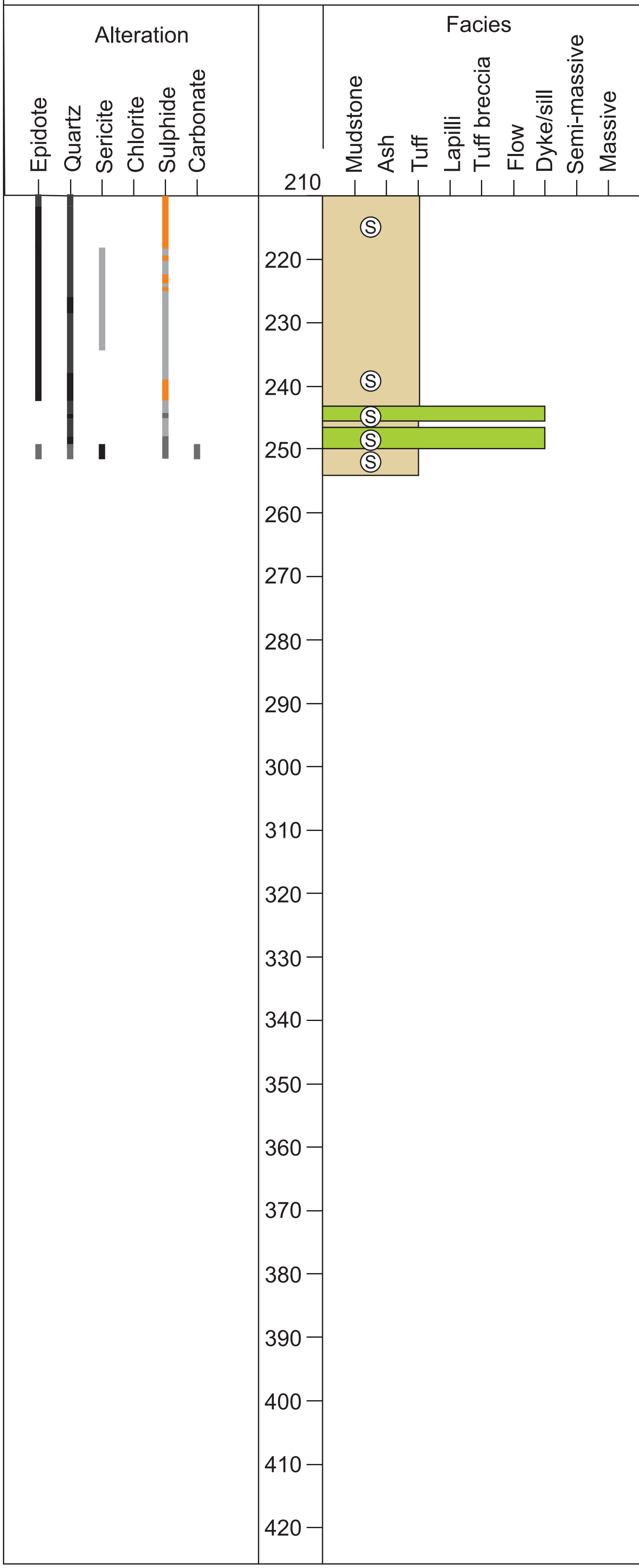

Descriptions

208.1 to 243.6: pale grey to beige, intensely ser-sil alt tuff with discont py stringers.

243.6 to 249.9: Two strongly sericite altered mafic dykes
249.9 to 254.0: Intensely sericite-sil altered tuffs with BM-stringers

Project: Hurricane
Drill Hole: GA-14-276
Date: June 19th to 20th, 2015

UTM	
474087E	Azimuth: 141.0
536632N	Dip: -73.0
	Depth: 371.0 M

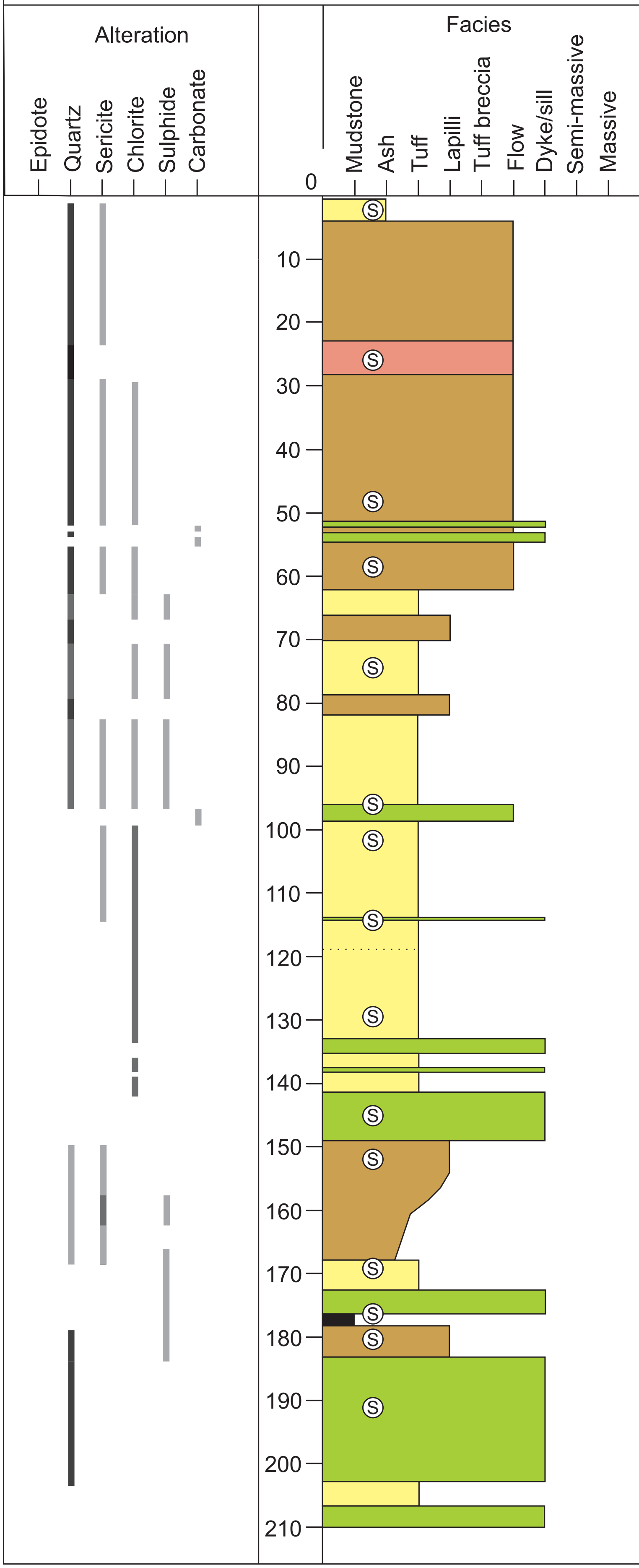

Descriptions

0 to 4: light to med grey, fine-grained, ash tuff.
4 to 22.3: light to med grey, x-stal-bearing lapilli tuff. 5-10% plag xstals (1-2% qtz), str sil and mod fol; local chl and/or ser veinlets. locally, clasts of fine-grained tuff, med-grey with fine-grained disem py. Clasts become more abundant downhole. 8% Qvs throughout unit 3-10 cm thick.

22.3 to 26.2: porphyritic felsic flow, white to beige with 5% plag phenocrysts.

26.2 to 62.12: Overall, unit consists of interbedded porphyritic felsic flows and felsic lapilli tuffs. Local concordant Qvs (8%) and 3-10% dis py throughout (increasing downhole). Locally, appears to be clast-rich with felsic to intermediate clast composition. Two 0.5 to 1 m mafic dykes.

62.12 to 66.12: Heterolithic tuff to LT. Lap frags are 2-8 cm, matrix is fine-grained, dark grey, locally contains qtz-xstals and dis py. Some lap frags look armoured, range in composition from felsic to intermediate and contained plag-qtz xstals. str sil alt, mod-wk chl-ser.
66.12 to 70.13: Fine to med-grained tuff with 10% qtz crystals. 1% dis py.
70.13 to 78.68: same as 62.12 to 66.12
78.68 to 81.85: same as 66.12 to 70.13
81.85 to 95.95: Normally graded tuff. Appears to be the finer portion of the lapilli tuff from above.

95.95 to 98.6: Mafic dyke
98.6 to 141.27: Xstal-bearing tuff. 10-25% xtals, either plag or qtz. Weakly graded with intervals which was xstal poor. Top part of unit is more plag rich and lower half is more qtz-rich.

0.5 to 2 m mafic dykes are common.

141.27 to 148.92: Dark green-grey mafic dyke, fine to med-grained, pervasive carb OP. 5% x-cutting carb veinlets. Thick Qv from 141.55 to 142.2 that has xenoliths of dyke and ash tuff.

148.92 to 167.74: Normally graded heterolithic tuff to lapilli tuff. Locally grades into

167.74 to 172.45: Thinly interbedded arg and med-grained tuff. Arg shows local evidence of weak shearing and deformation and has bedded fg py.
172.45 to 176.21: Mafic dyke, pepperitic contacts
176.21 to 178.1: Similar arg unit as before except increase shearing, local fault gouge. Recrystallized py in fault gouge.
178.1 to 180.89: Str sil alt normally graded LT, 1-2% py.
189.89 to 202.65: Pale beige to grey alt mafic dyke. Upper contact looks intermingled but sharp. 5-7% carb amy, locally bleached.

202.65 to 206.43: Same arg interbedded tuff unit as before. Weakly deformed arg.
206.43 to 212.39: Same dyke as above.

Project: Hurricane
Drill Hole: GA-14-276
Date: June 19, 2015

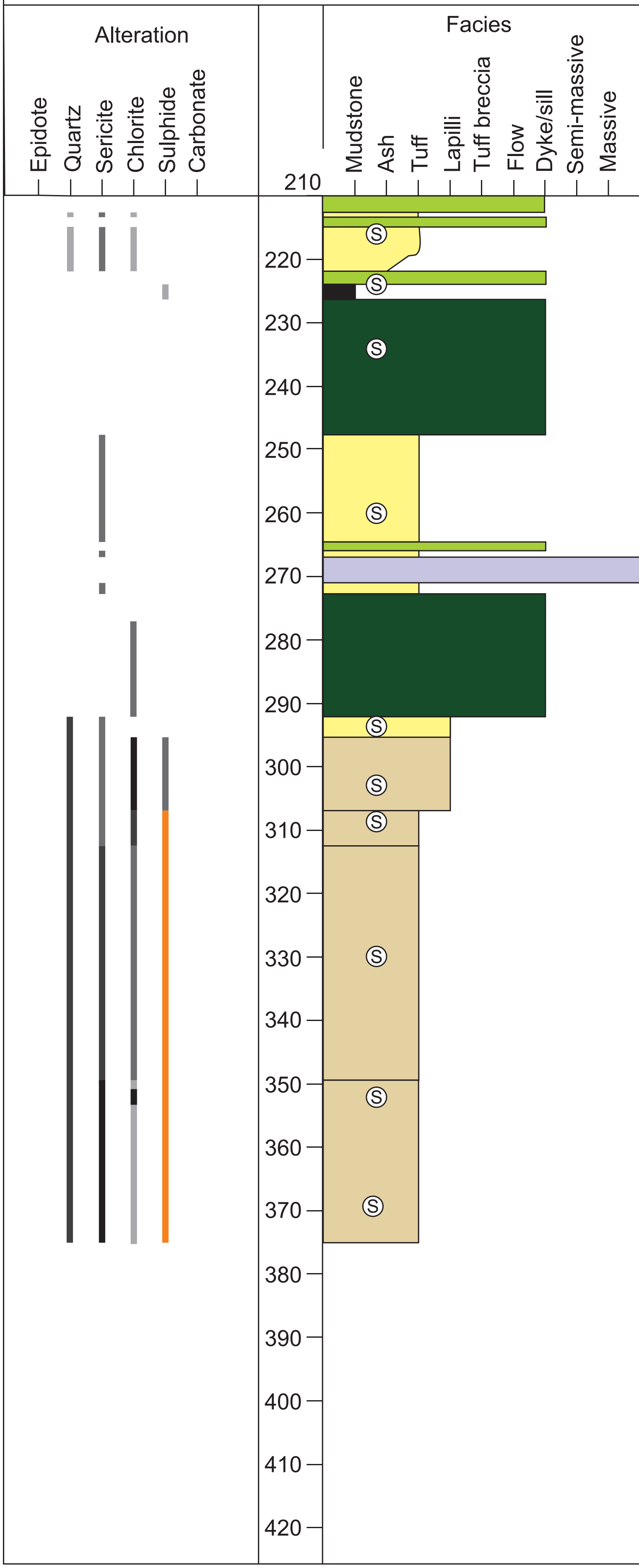

Descriptions

212.39 to 221: pale grey, normally graded med-grained tuff to fine-grained LT, heterolithic, round plag xstals, localy py stringers.

221 to 223.6. Beige-grey mafic dyke. Lower contact appears faulted.

223.6 to 226.03: Graded arg and tuff unit. First 1.5 m of arg has abundant deformed Qvs and 2% py veinlets. Tuff has white, round plag xstals.
226.03 to 247.38: Mafic sill, dark green-grey, fine-grained, massive. 4% carb veinlets, 1-3% amy.

247.38 to 264.28: Pale grey normally graded tuff with 1-2 mm white, round plag xstals, 5-7% py stringers, matrix is mod ser alt.

264.28 to 265.66: Same dyke as before
265.66 to 272.46: Same tuff as above with 5 cm thick Qvs.

272.46 to 291.84: Mafic sill, same as above.

291.84 to 295.7: Shear zone?
295.7 to 306.6: pale grey, normally graded, fine to coarse-grained with local lap fragments. At 299 start to see chert/ash intervals (~20 cm thick). Increase chl alt down hole with mod-str ser.
306.6 to 312.16: Intensely chl alt tuff, ~10% py stringers and local CC around lower contact.

312.6 to 349.52: Str ser alt tuff with chl stwk associated with py stringers,

349.52 to 375: Str ser-sil alt tuff with abundant qtz veining and folding.

Project: Hurricane Drill Hole: GA-10-277 Date: July 9th-10th, 2015		UTM 474166E 5364689N	Azimuth: 141.0 Dip: -47.0 Depth: 266.0 m

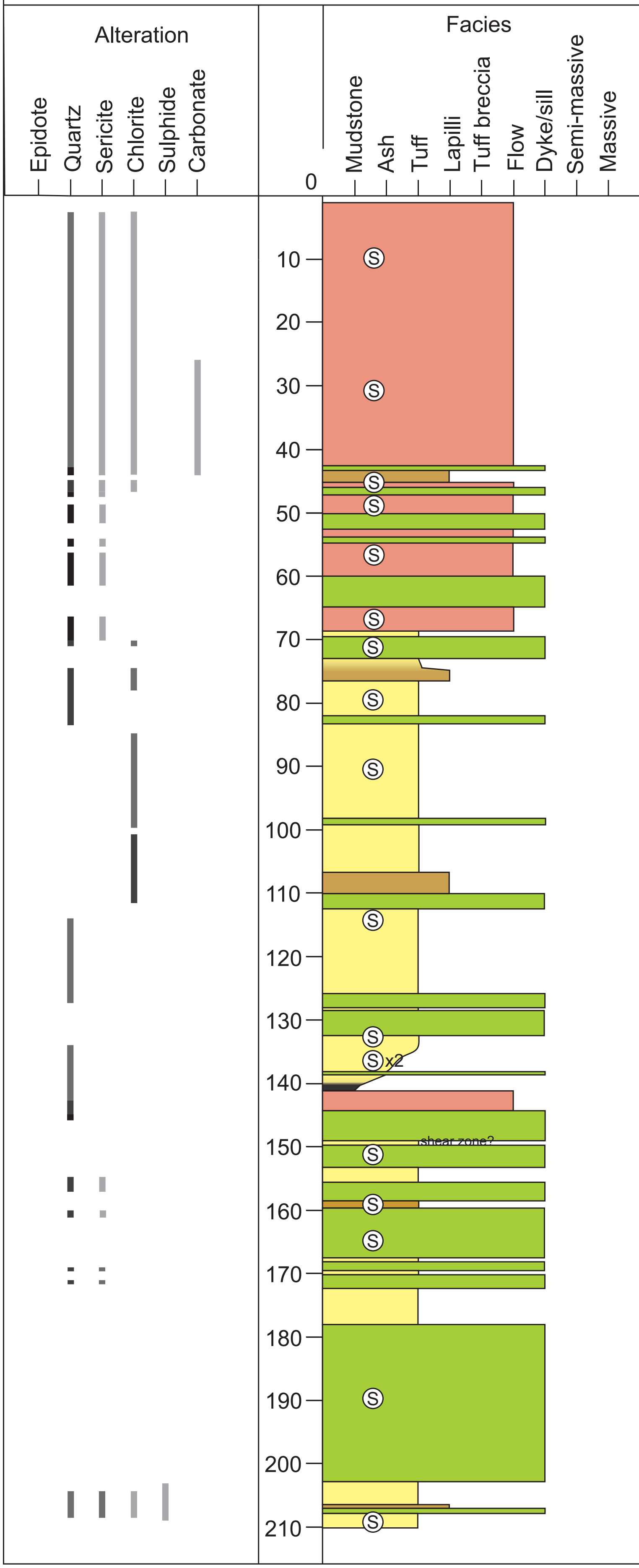

Descriptions

1 to 43.09: interbedded lapilli tuff and qtz-felds porphyritic felsic flow. Lapilli texture could be due to local, weak brecciation in flow, giving pseudo-lapilli look. Matrix of lapilli and/or brecciation is mod ser and locally chl. pale grey to pinkish white in color. Mod to strong sil alt, and mod fol. Local carb overprinting.

43.09 to 43.84: Green-grey mafic dyke
43.84 to 45.72: Strong sil alt lapilli tuff, dominantly felsic fragments with plag xstals.
45.72 to 69.14: Porphyritic felsic flow interleaved with 1 to 5 m mafic dykes. Felsic flows are very strongly sil alt with 5-10% qtz-feldspar xtals. Same as unit above. Mafic dykes are dark green-grey, fine-grained, 1-3% calcite amygdules, locally replaced by ep. 5% ep veinlets. Mafic unit from 60 to 65 could be pillow basalt. Sharp, abrupt contacts between mafic dykes and felsic flow.

69.14 to 70.2: Fine to coarse-grained tuff, heterolithic fragments with dis clustered py.
70.2 to 77: Fine to coarse-grained tuff, grading into heterolithic lapilli tuff.
77 to 108: Crystal tuff, mod to str fol with mod chl alt. qtz xstals are more dom in upper half of unit and become more plag xstal rich down hole. Matrix is fg, dark greyish blue. Local lithic fragments at 107. 7 m with 1-5% dis py.

108 to 110.53: heterolithic lapilli tuff. Lower contact has pepperitic textured.
110.53 to 112.94: Mafic dyke
112.94 to 126.9: Sandy, normally graded tuff. Classic turbidite, lower unit consists of massive, sandy tuff, locally contains lapilli sized fragments. Grades upwards into thinly bedded fine-grained tuff to ash tuff. Approximately 4-6 events.

126.9 to 132.88: Mafic dyke with xenolith of previous unit.
132.88 to 138.5: Very xstal-rich and weakly fol, similar to tuffaceous unit above, displays similar grading. 15% carb veins. Locally unit becomes very chl alt (132.7 to 133 m).

138.5 to 141.59: Normally graded. Interbedded fine to med-grained tuff and ash tuff capped with argillite. Local mudclasts in tuffcaeous units. Potential fault zone?
141.59 to 144.72: Very strongly sil alt felsic flow?
144.72 to 149.45: Dark green-grey mafic dyke, porphyritic with pyroxene laths.
149.45 to 150.15: Shear zone? vfg dark grey with undulating pale grey-pink zones
150.15 to 160: Mafic dykes interleaved with normally graded tuffs. Tuffs locally have thin chert thinly interbedded. QV and shear zone from 157.65 to 157.78 m.
160 to 167.92: Sil alt mafic dyke. 3% sheared amys, <5% carb veins.
167.92 to 168.51: Pale grey, heterolithic LT, strongly fol.
168.51 to 171.5: Interleaving of altered mafic dyke and normally graded tuff.
171.5 to 178.63: Beige to grey, fine to coarse-grained tuff, sandy, locally qtz xstal rich with dise black chl laths, strong fol.
178.63 to 203.45: Dark green-grey mafic sill. Mostly massive with sheared carb-veins, locally xenoliths or thin interbeds of intermediate chl alt tuff, but hard to distinguish difference, one appears more strongly fol.

203.45 to 207.06: Greenish-grey, chl alt tuff with 5-10% qtz xstals, str fol.
207.06 to 207.65: pale grey LT with white round plag xstals, str fol, mod ser-chl
207.65 to 208. 46: dark green grey, str fol, rare sheared carb veins.

Project: Hurricane
Drill Hole: GA-14-277
Date: July 9th-10th, 2015

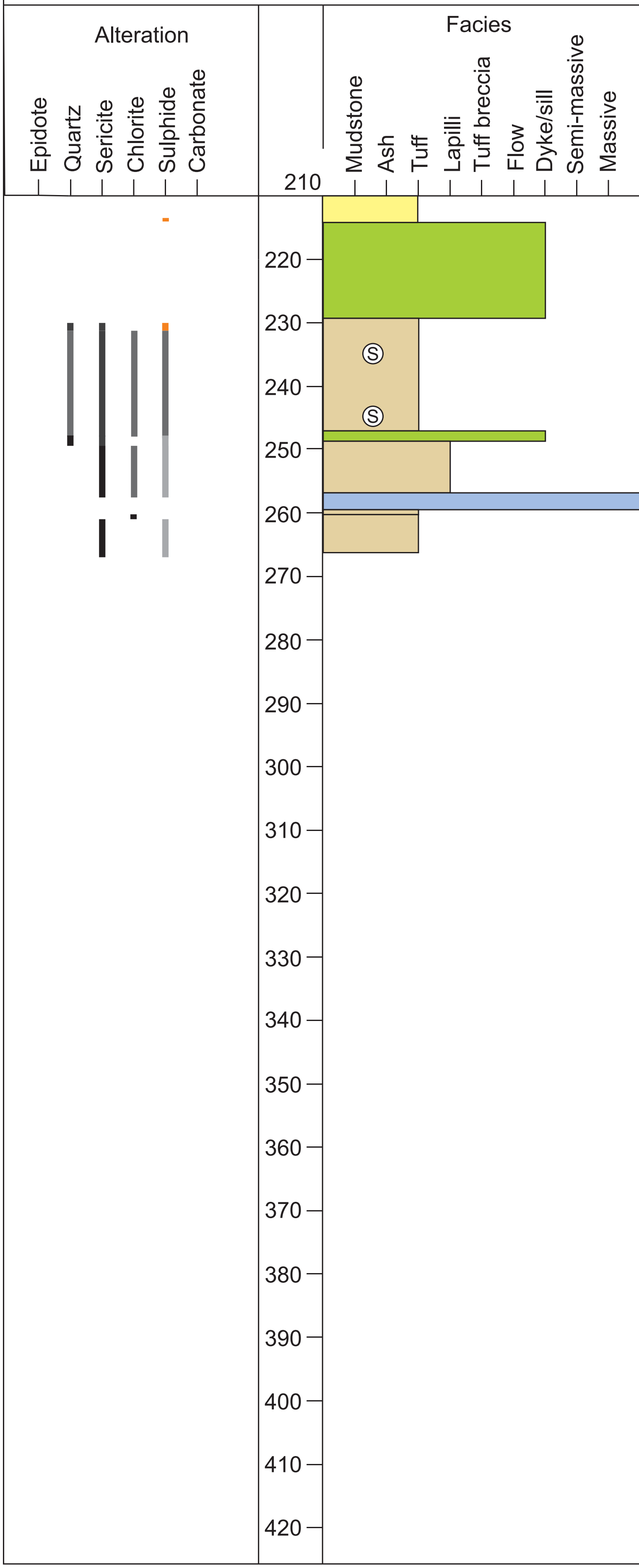

Descriptions

208.46 to 214.4: Pale grey, normally graded, fine- to -coarse-grained tuff with 10% white plag xstals and rare felsic lap fragments. Locally interbedded with ash tuff and chert. Ash and chert intervals are associated with fine-grained banded py. At 212.9 start to get py stringers associated with thin chl bands, these increase in size to 0.5 to 1 cm at 213.5 to 213.65.
214.4 to 229.25 : Mafic sill, fine-grained, dark green-grey. Lots of carb amy and sheared carb veins. Lower contact has 1% coarse-grained py.
229.45 to 246.8: Overall, strongly ser altered with up to 45% mm- cm py stringers. Locally stringers have tr sp. Sulphide stringers are parallel to fol and locally are associated with chl stringers. Local chevron folding is also present.
229.25 to 248.43: Ser-sil alt mafic dyke
248.43 to 256.57: Ser alt tuff to LT, py-chl stwk is common. Faulting near LC
256.57 to 259.27: Quartz vein and fault gouging (85%) with sheared ser alt tuff
259.27 to 260: Very strongly chl alt tuff
260 to 266: Same mod-str ser alt tuff, local fault gouging and folding. Locally ser-py stringers.

Project: Hurricane
Drill Hole: GA-14-278
Date: July 12th, 2015

UTM	Azimuth: 141.0
474166E	Dip: -64.0
5364689N	Depth: 344.0 m

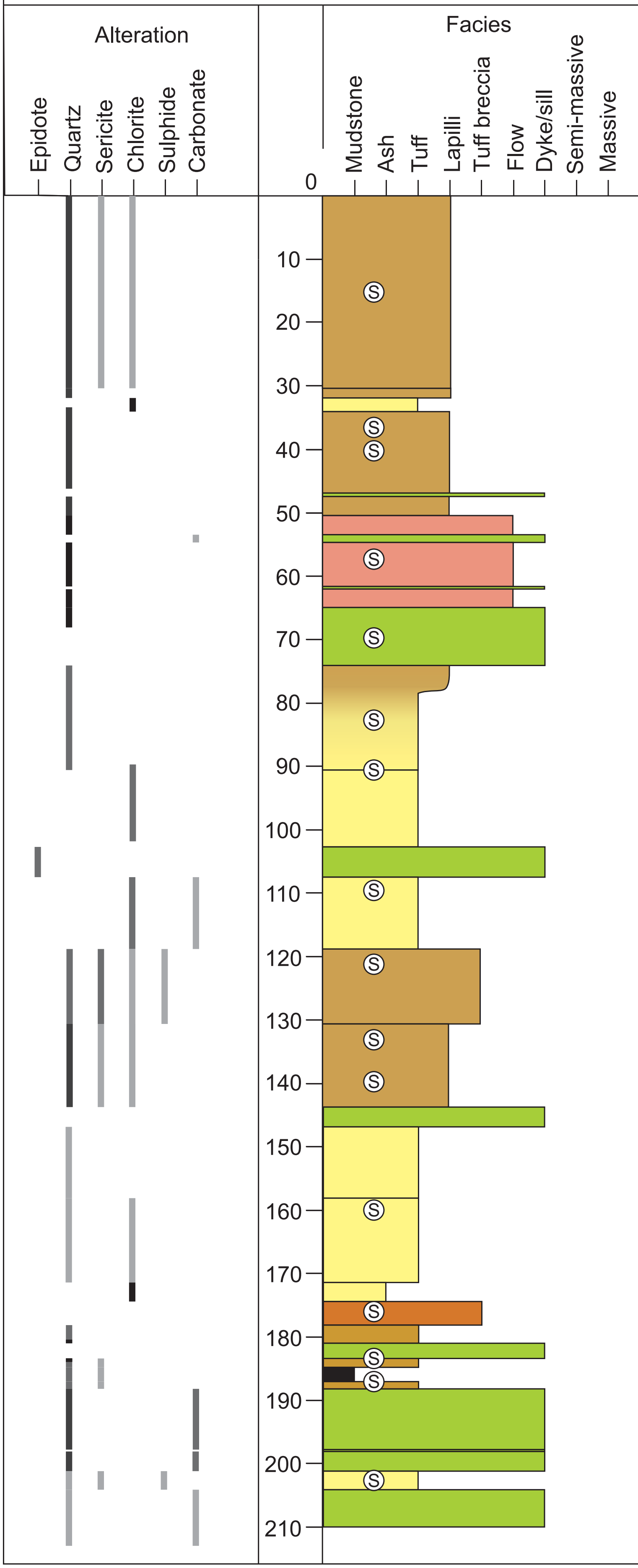

Descriptions

0.4 to 50.41: Overall, this unit consists of interbedded porphyritic felsic flows and lapilli tuffs. They are beige grey to grey to pinkish-white in color with 10-15% white plag xstals/phenocrysts. Mod to str sil alt. Phenocrystas increase in size downhole from 1-2 mm to 2-5 mm. Locally zone are aphyric. . Local dis py (6%) starting at 28.5 m. Mod to str sil, mod fol.

From 30.34 to 31.87 appears to be clast supported tuff breccia or strongly brecciated felsic flow. fine-grained py in matrix.

50.41 to 64.91: Overall, aphyric to plag-porphyritic felsic flow, locally intruded by 0.5-1 m mafic dykes. Felsic units are characterized by being white to pinkish-white, str sil, locally brecciated along margins.

64.91 to 74.05: Mafic sill, dark green-grey, fine-grained along margins and coarsens inwards, three 5-8 cm thick concordant qtz-carb veins. Locally see vfg selvages, could be pillow basalt?
74.05 to 102.66: First 10 m is heterolithic LT with clusters of py in matrix. Downhole, transitions in qtz-plag xstal rich, med-grained tuff. Locally, areas are xstal-poor and fine-grained, likely showing grading.

2 cm fault at 100 m.

102.66 to 107.43: Mafic dyke, massive, dark green to grey, fine-grained,10% concordant carb veins with ep rims. Pyroxene and weakly plag porphyritic.
107.43 to 118.76: Same tuff as above, local lap-sized fragments of felsic flow? 15% dis py.

118.76 to 130.6: Gradational upper contact, increases in gs to matrix supported LT with bomb-sized fragments. Matrix is fine-grained, grey, with 7% fg py, lap are sudrounded, poorly sorted and range in composition from felsic to mafic. weakly graded.
130.6 to 143.86: Very similar to above, but more str sil alt, gs decreases, no bomb sized lap, but still coarse-grained.

143.76 to 146.88. fine-grained, grey 10% x-cutting carb veins, massive, 5% vfg amy.
146.88 to 158.15: fine to med-grained tuff, mod to str fol, 15% dis py. 6% sheared carb veins.

158.15 to 171.45: Gradational upper contact, but unit differs by increase in xstal content. Mostly qtz-rich (30-45%), mod chl alt matrix.

171.45 to 174.5: Similar to above, but appears to be weakly faulted or sheared
174.5 to 177: volcanic breccia?
177 to 181.03: Arg interbedded with tuff. Arg are mod sheared with Qvs. Tuffs are strongly sil alt.
181.03 to 183.43: Fine-grained mafic dyke
183.43 to 188.22: Overall, tuff interbedded with arg. Similar to above.
188.22 to 212.3. Overall, these units dominantly consist of weak to mod alt mafic dykes. They are beige to grey, fine-grained, have sharp upper and lower contacts. Two thin tuffaceous units consist of med to coarse-grained tuff, locally containing very-fine intervals of ash, chert and arg.

Project: Hurricane
Drill Hole: GA-14-278
Date: July 12th, 2015

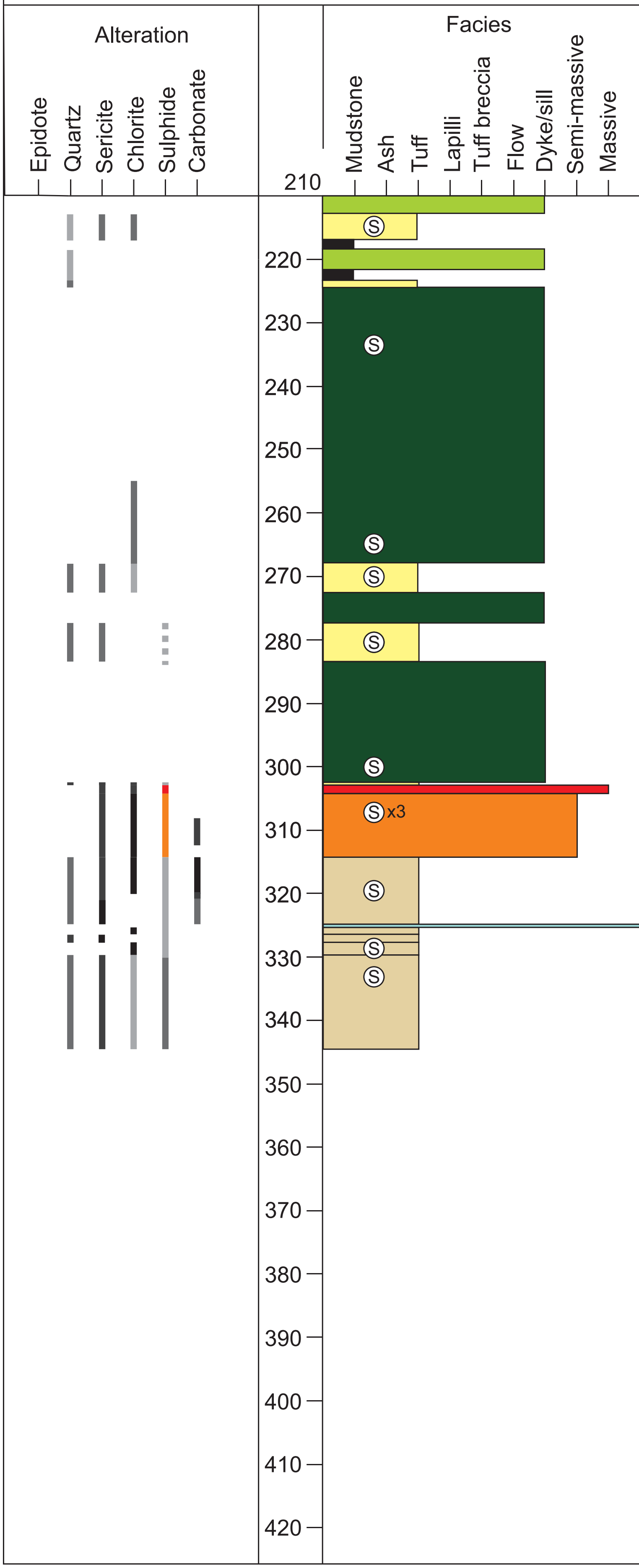

Descriptions

212.3 to 223.95: Similar to arg and interbedded tuffs above, increase chl alt.

223.95 to 267.4: Mafic sill, fine to med-grained, dark green-grey, massive.

267.4 to 302: Overall, unit consists of normally graded plag-rich tuff with thin chert intervals with interleaved mafic sills.

302 to 302.44: Mod to str ser alt tuff with tr vfg py.
302.44 to 303.65: banded sp, gn, py and lesser cp, local tuffaceous fragments in MS
303.65 to 313.68: Semi-massive sulphide (bands of sp, py gn and rare cp) with str chl stwk with mod-str ser alt matrix with disem py throughout. Local CC.
313.68 to 324.25: strong ser alt tuff with local mod to str chl stwk veinlets associated with fg banded py.
324.25 to 325.84: black VMS chl
325.84 to 327.15: Str ser alt tuff
327.15 to 329.15: black VMS chl
329.15 to 344: Str ser alt tuff with py stringers. Local thick quartz veins.

Project: Hurricane Drill Hole: GA-14-279 Date:		UTM 474307E 536660N	Azimuth: 141.0 Dip: -65.0 Depth: 236.0 m

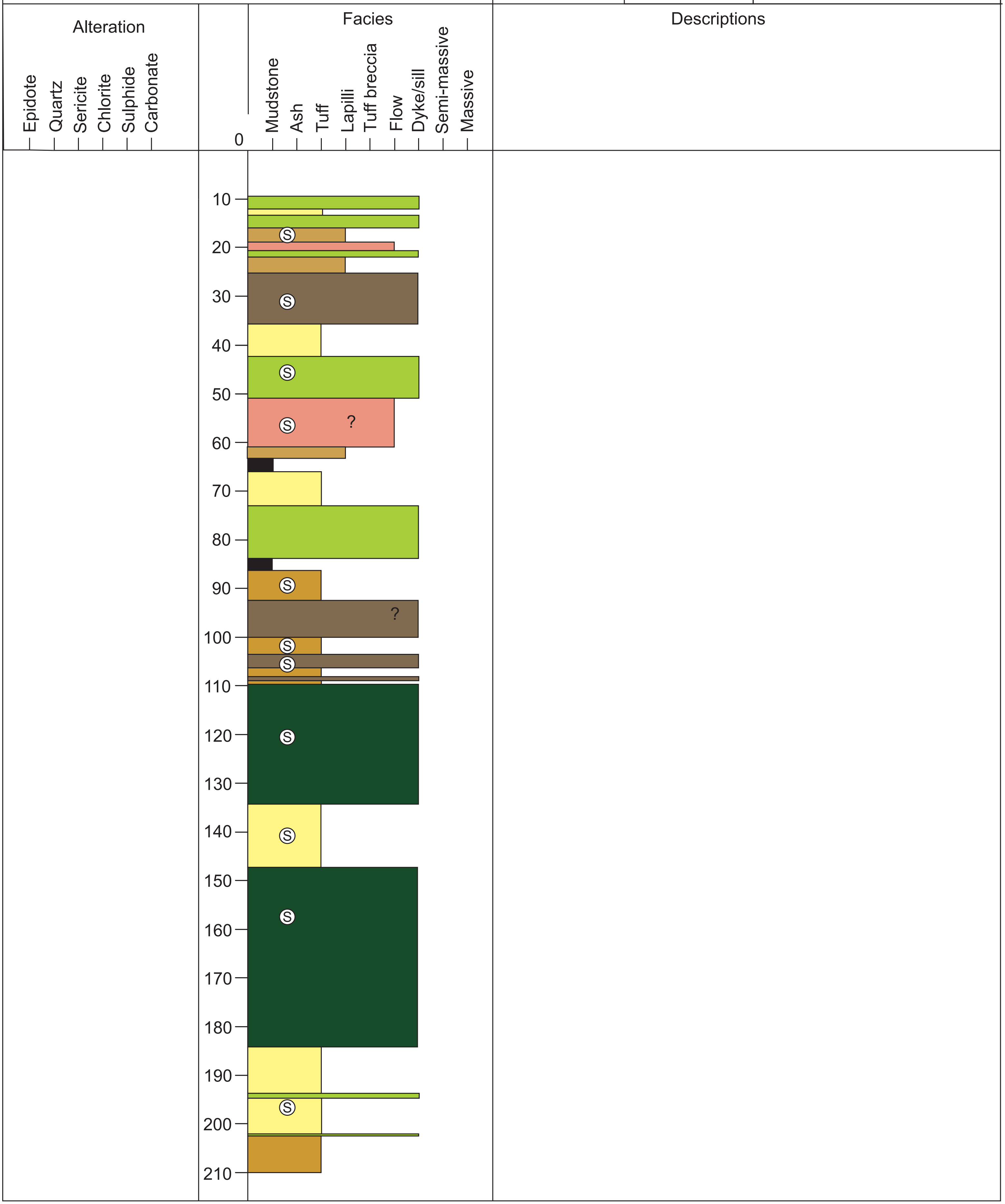

Project: Hurricane
Drill Hole: GA-14-279
Date:

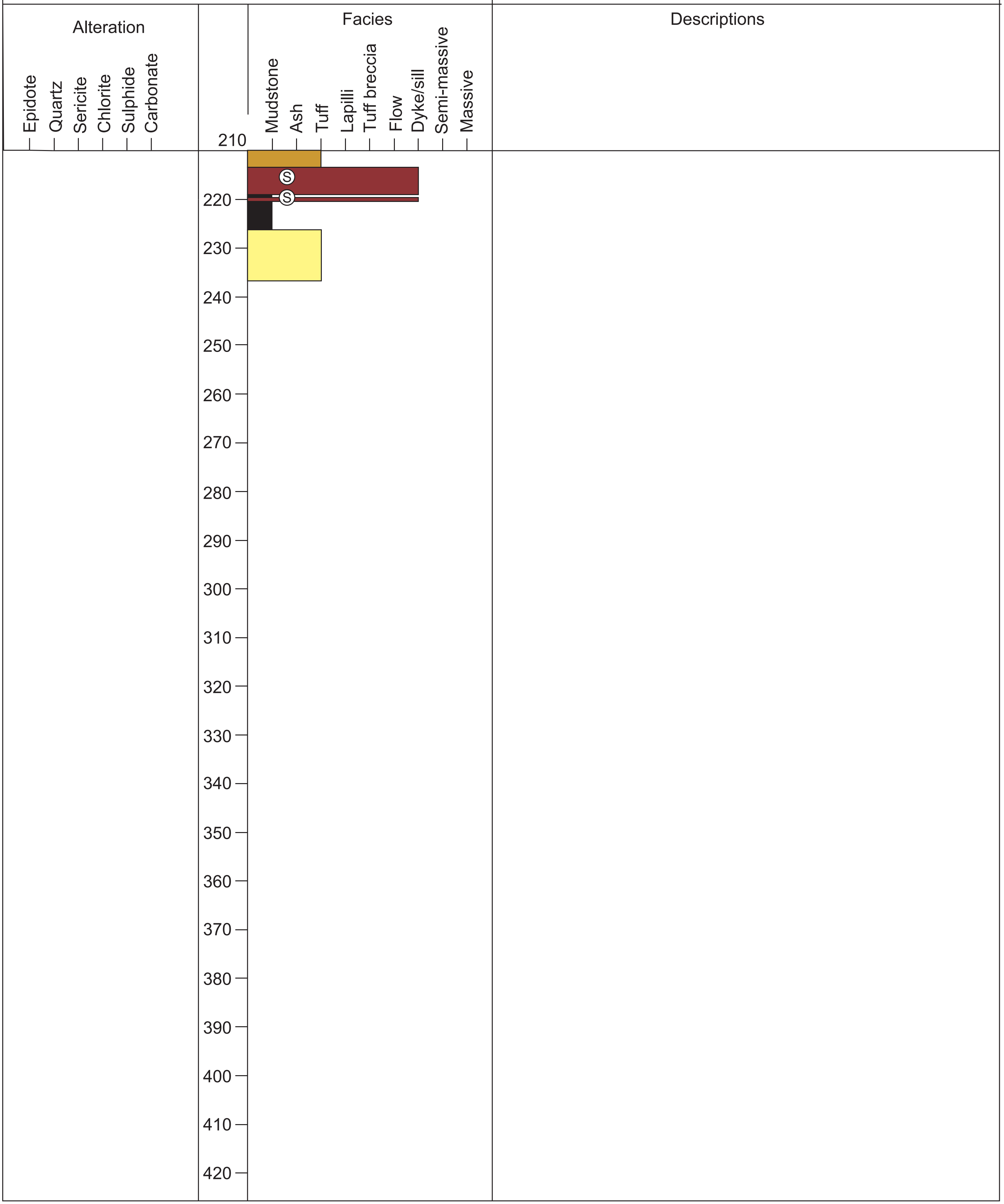

Project: Hurricane Drill Hole: GA-14-283 Date: June 11th to 12th, 2015	UTM 474016E 5364566N	Azimuth: 141.0 Dip: -61 Depth: 272.0 m	

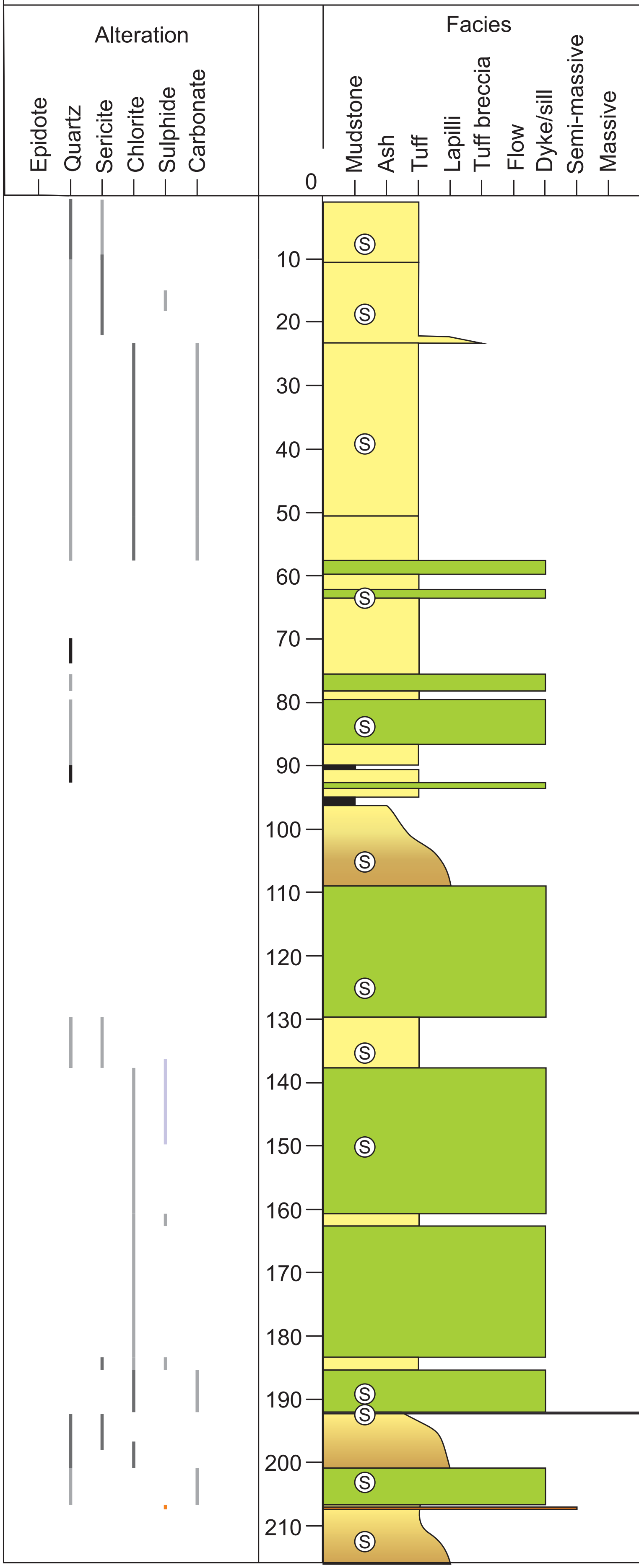

Descriptions

0.5 to 10.53: Light grey porphyritic felsic flow with 5-8% 2-5 mm quartz and plagioclase phenocrysts. Thin wispy pale beige sericite veinlets and dark grey chlorite veinlets. Strong to moderately foliated. Strong quartz alteration, weak chlorite and sericite alteration.
10.53 to 23.3: Brownish-grey rhyolite-dacite crystal bearing tuff with quartz (±plagioclase) crystals. Quartz crystal content and size rapidly increases downhole from 10 to 35% and < mm to 1-4 mm, respectively. Quartz crystals are subrounde, whereas plagioclase crystals are tabular or subangular to subrounded. Crystals are matrix-supported in a fine-grained pale to medium grey ash matrix. Strong to moderately foliated. Weak quartz and sericite alteration.
23.3 to 57.64: Dark bluish-grey plagioclase-bearing crystal tuff. Adundant (20-35%) 3-5 mm milky white plagioclase crystals with lesser (5-10%) quartz crystals in very fine-grained bluish grey matrix. Moderately foliated. Weak quartz alteration, weak to moderate chlorite alteration. Discordant 3mm to 5 cm carbonate veins (approximately 2% of unit) are most abundant between 33.5-34.8 m, 54.81-54.86, and 55.81-55.58 m. Highly veined area is weakly foliated.
57.64 to 59.81: Dark grey-green fine-grained mafic dyke. Dyke has coarser core and sharp chilled upper margins and diffuse lower margins.
59.81 to 61.21: Light grey , fine-grained tuff. Rare (3%) subrounded, white quartz crystals throughout unit. Moderately foliated. Very weakly altered. Sharp lower contact.
61.21 to 62.58: same dyke as above
62.58 to 74.56: Normally graded fine-grained (ash) tuff to matrix-supported medium- to coarse-grained (±lapilli) tuff. Graded beds range from 1mm to 10's of cms. Finer-grained units range from 5-20 cm thick. Locally, fine-grainded units have thin to discontincuous bands of f.g. pyrite. Strongly foliated. Weak to moderate quartz alteration with local weak chlorite alteration.
74.56 to 77.23: Grey, homogenous intermediate (felsic?) dyke with rounded to subrounded 1-5cm pervasive (15%) calcite amygdules. Sharp contacts.
77.23 to 78.56: Same as 62.58-74.56. Dominant by ash tuff (v.f.g tuff) grading to medium tuff. Thin discontinous bands of f.g. py common in v.f.g. tuffaceous layers.
78.56 to 85.65: Same as 74.56-77.23. Pale beige/grey. Diseminated py veins (3%). Strong to moderate quartz alteration. Sharp contacts with chilled upper margin. Lower margin is sharp but undulatory- appears to have load structure with underlying thin graded tuff to mudstone.
85.65 to 88.91: Same as 62.58-74.56. Very thin (few mm thick) argillite cap graded sequence.
88.91 to 89.61: Dark grey to black argillite. First 40 cm have abundant (40-60%) white 2-5 mm feldspars crystals. Abrupt loss in crystals at 89.31 m to v.f.g black argillite with thin (< few mm) discont py veinlets. 1-2 cm thick quartz-carb vein near lower contact.
89.61 to 91.96: same as 62.58-74.56. Soft sediment deformation (flame structures) in fine-grained graded beds on upper contact.
91.96 to 92.62: Pinkish beige f.g. dyke. Upper contact is sharp, lower is erosion/undulatory. Thin black discontinuous veinlets/brecciation infilled with chlorite. Potentially jig-saw fit rhyolite. Strongly quartz alteration.
92.62 to 93.98: fine-grained tuff, str sil alt, str fol, locally cg clusters of py.
93.98 to 95.3: Faulted argillite? discordant Qvs and fragments of felsic flow from above.
95.3 to 108: Normally graded heterolithic tuff with mudstone interbeds. Tuffaceous units range from fine- to coarse-grained, locally xstal-bearing. Mudstones down hole have fine-grained banded py.
108 to 182.4: Overall, thick, massive, fine-grained, dark green-grey mafic sills with thin intervals of pale grey, plag-bearing tuffs. Tuffaceous units increase in alteration downhole with increasing amounts of ser-sil alt, and locally have mod chl laths.
182.4 to 184.4: Normally graded, pale grey tuff with local LT intervals and lap fragments in coarse-grained tuff units. White, round, plagioclase xtals. Alteration consists of ser-chl with lesser sil.
184.4 to 191.0: dark green grey mafic dyke, vfg margins, coarsens inwards, mod fol, sheared amy.
191 to 199.86: Normally graded tuff, same as above, thin 1 m semi-massive sulphide consisting of fine-grained banded py.
199.86 to 205.64: Light brown to beige, fine-grained, ser-sil altered mafic dyke
205.64 to 206: Semi massive sulphide, fine-grained, thinly banded py, sp
206 to 215: Normally graded, pale grey, tuff with white, round plag xstals. Grades into chert.

Project: Hurricane
Drill Hole: GA-07-283
Date: June 11th to 12th, 2015

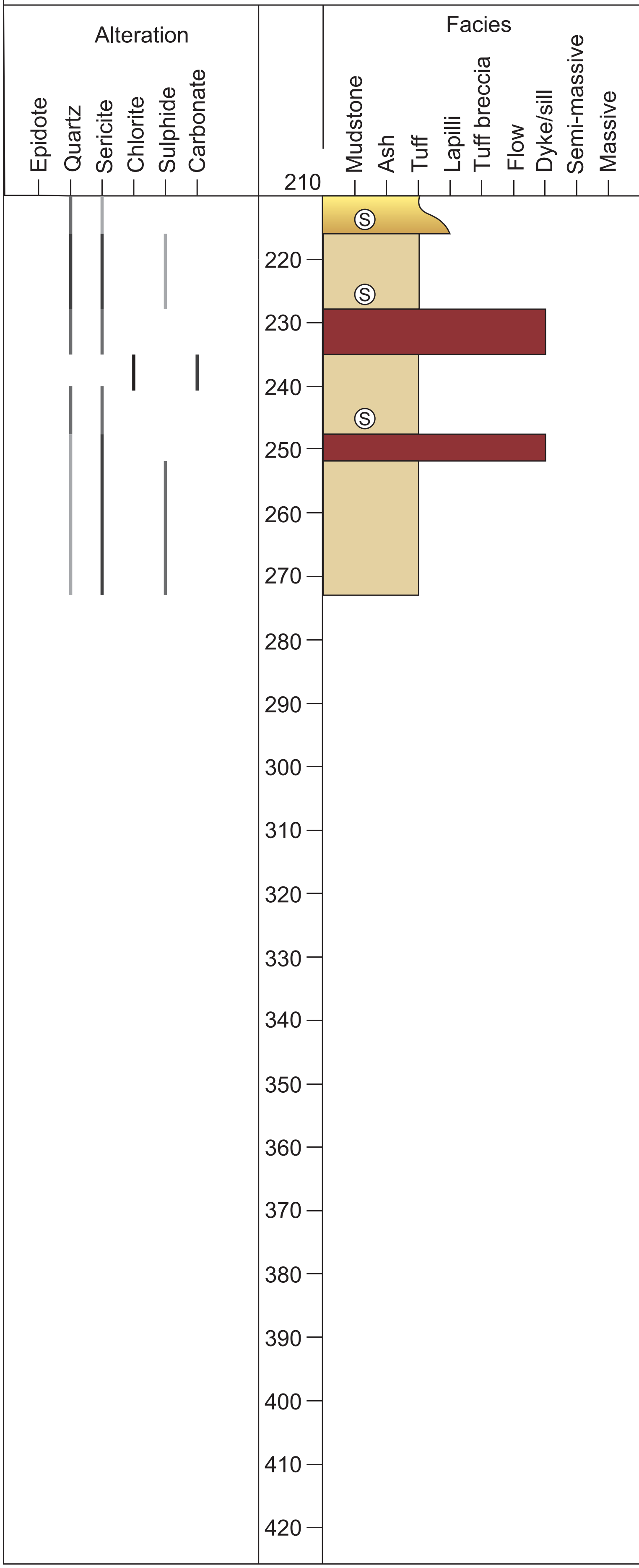

Descriptions

215 to 272: Overall, moderate to strongly altered normally graded tuff interleaved with two ser-sil altered mafic dykes, dykes have rare sulphide mineralization associated with them, locally tr cp and gn.
From 215 to 226.8 broken up quartz and str sil-ser alt with disem/banded py associated with chl stwk. Tr gn and cp in matrix associated with sil alt.

235 to 238: Intense chl-CC alt.

238 to 246.1: Sil-ser alt with increase chl stwk

250.83 to 272: strongly sil-ser alt with weak chl-py

Project: Hurricane
Drill Hole:
Date:

Alteration		Facies	Descriptions
Epidote, Quartz, Sericite, Chlorite, Sulphide, Carbonate	420	Mudstone, Ash, Tuff, Lapilli, Tuff breccia, Flow, Dyke/sill, Semi-massive, Massive	
	430		
	440		
	450		
	460		
	470		
	480		
	490		
	500		

Appendix B: Whole-Rock Geochemistry

Table B1.1. Abbreviation list for whole-rock geochemistry

Alteration	
Bm	Base Metals
Carb	Carbonate
Chl	Chlorite
Pyr	Pyrite
Ser	Sericite
Sil	Silica
Lithology	
CL1a	Coherent lithofacies 1a: plagioclase and/or quartz phyric rhyolite flow
CL1b	Coherent lithofacies 1b: massive aphyric rhyolite flow
VCL1	Volcaniclastic lithofacies 1: intermediate lithic, crystal tuff to lapilli tuff
VCL2	Volcaniclastic lithofacies 2: felsic to intermediate lithic, crystal lapilli tuff to tuff
VCL3	Volcaniclastic lithofacies 3: normally graded, heterolithic lapilli tuff to tuff
VCL4	Volcaniclastic lithofacies 4: crystal-bearing felsic to intermediate tuff
IN1	Intermediate Intrusive
IN2a	Mafic Intrusive (dyke)
IN2b	Mafic Intrusive (sill)
Geochemical Differentiation of VCL1	
A-C	Groups A-C
D	Group D
E	Group E- Outliers

Appendix B: Table B1.1: Whole-rock Lithogeochemistry Data

Sample ID			25415	25417	25418	25419	25420	25422	25424	25425
Hole ID			GA-07-254	GA-07-254	GA-07-254	GA-07-254	GA-07-254	GA-07-254	GA-07-254	GA-07-254
Depth (m)			18.83	45.44	77.75	86.05	101.7	133.45	157.1	184.1
Lithology			CL1a	VCL4	IN2a	VCL4	VCL3	VCL3	VCL2	VCL2
Alteration			sil	chl	unaltered	unaltered	unaltered	chl	ser	ser-sil
SiO_2	%	FUS-ICP	69.63	51.09	47.16	51.82	48.07	43.72	64.17	67.2
Al_2O_3	%	FUS-ICP	13.93	18.17	17.34	20.55	16.87	19.55	15.67	14.3
Fe_2O_3	%	FUS-ICP	1.90	9.15	10.18	9.17	8.38	11.46	5.51	4.38
MnO	%	FUS-ICP	0.04	0.12	0.13	0.09	0.19	0.13	0.05	0.05
MgO	%	FUS-ICP	1.73	3.41	6.20	4.03	3.48	8.09	6.31	3.46
CaO	%	FUS-ICP	1.59	3.31	4.39	1.68	7.28	2.71	0.19	0.41
Na_2O	%	FUS-ICP	1.50	6.90	5.68	4.83	4.96	3.20	0.48	1.75
K_2O	%	FUS-ICP	4.21	0.33	0.17	2.66	1.41	1.94	3.32	3.6
TiO_2	%	FUS-ICP	0.32	0.74	0.96	1.05	1.16	0.99	0.57	0.68
P_2O_5	%	FUS-ICP	0.03	0.07	0.15	0.2	0.16	0.03	0.07	0.11
LOI	%	FUS-ICP	3.70	5.28	6.74	4.63	8.84	8.48	4.60	3.87
Total	%	FUS-ICP	98.58	98.57	99.11	100.70	100.80	100.30	100.90	99.79
Hg	ppb	CV-FIMS	< 5	< 5	< 5	< 5	< 5	< 5	< 5	8
Be	ppm	FUS-ICP	1	< 1	< 1	1	1	< 1	2	2
V	ppm	FUS-ICP	19	243	345	248	233	280	45	34
Cr	ppm	FUS-MS	< 20	30	70	< 20	< 20	110	< 20	< 20
Co	ppm	FUS-MS	2	22	34	17	19	44	6	3
Ni	ppm	FUS-MS	< 20	20	40	< 20	< 20	60	< 20	< 20
Cu	ppm	FUS-MS	< 10	20	50	30	30	30	< 10	< 10
Zn	ppm	FUS-MS	30	110	170	110	90	100	60	110
Ga	ppm	FUS-MS	13	20	16	21	17	19	19	18
Ge	ppm	FUS-MS	1.2	0.8	1.1	0.8	0.6	0.9	1	1
As	ppm	FUS-MS	6	< 5	11	12	7	55	< 5	7
Rb	ppm	FUS-MS	86	6	3	44	20	31	51	56
Sr	ppm	FUS-ICP	22	78	117	51	95	57	10	20
Y	ppm	FUS-MS	29.20	19.00	16.50	23.20	27.30	15.80	54.60	48.90
Zr	ppm	FUS-ICP	168	85	29	79	58	64	212	196
Nb	ppm	FUS-MS	2.60	0.90	< 0.2	1.20	0.50	0.30	1.60	1.80
Mo	ppm	FUS-MS	< 2	< 2	< 2	< 2	< 2	< 2	< 2	< 2
Ag	ppm	FUS-MS	< 0.5	< 0.5	< 0.5	< 0.5	< 0.5	< 0.5	< 0.5	< 0.5
In	ppm	FUS-MS	< 0.1	< 0.1	< 0.1	< 0.1	< 0.1	< 0.1	< 0.1	0.1
Sn	ppm	FUS-MS	< 1	< 1	< 1	< 1	< 1	< 1	1	1
Sb	ppm	FUS-MS	0.5	< 0.2	0.8	< 0.2	0.2	0.5	< 0.2	0.9
Cs	ppm	FUS-MS	0.6	0.1	0.1	0.3	0.2	0.2	0.4	0.5
Ba	ppm	FUS-ICP	512	104	76	571	240	350	1390	1216
La	ppm	FUS-MS	19.3	7.47	4.82	5.35	7.15	4.39	20.3	19.9
Ce	ppm	FUS-MS	37.9	17.6	10.8	14	17.7	10.5	48.6	47
Pr	ppm	FUS-MS	4.32	2.18	1.5	2.04	2.57	1.4	6.47	6.17
Nd	ppm	FUS-MS	16.5	9.44	7.27	10.2	13	7.01	29.9	27.7
Sm	ppm	FUS-MS	4.13	2.52	2.06	3.28	4.27	2.14	8.08	7.22
Eu	ppm	FUS-MS	0.75	0.73	0.81	0.97	1.49	0.662	1.96	2.09
Gd	ppm	FUS-MS	4.65	2.99	2.59	4.05	4.98	2.71	9.05	8.08
Tb	ppm	FUS-MS	0.83	0.54	0.47	0.73	0.9	0.5	1.62	1.46
Dy	ppm	FUS-MS	5.32	3.53	3.07	4.72	5.61	3.24	10.3	9.37
Ho	ppm	FUS-MS	1.09	0.75	0.67	0.96	1.11	0.67	2.15	1.96
Er	ppm	FUS-MS	3.36	2.2	1.88	2.88	3.21	2.01	6.5	5.88
Tm	ppm	FUS-MS	0.53	0.35	0.27	0.44	0.48	0.30	0.99	0.90
Yb	ppm	FUS-MS	3.83	2.5	1.76	2.95	3.13	2.08	6.66	6.12
Lu	ppm	FUS-MS	0.64	0.44	0.28	0.47	0.52	0.33	1.06	0.99
Hf	ppm	FUS-MS	3.40	1.80	0.60	1.70	1.30	1.40	4.10	3.80
Ta	ppm	FUS-MS	0.31	0.16	0.06	0.16	0.12	0.11	0.18	0.2
W	ppm	FUS-MS	1.6	< 0.5	< 0.5	2.4	< 0.5	< 0.5	< 0.5	< 0.5
Tl	ppm	FUS-MS	0.47	< 0.05	< 0.05	0.11	< 0.05	0.08	0.12	0.1
Pb	ppm	FUS-MS	14	< 5	< 5	< 5	< 5	< 5	< 5	8
Bi	ppm	FUS-MS	< 0.1	< 0.1	< 0.1	< 0.1	< 0.1	< 0.1	< 0.1	< 0.1
Th	ppm	FUS-MS	8.69	3.64	0.66	1.12	0.59	1.17	4.6	4.29
U	ppm	FUS-MS	2.37	1.14	0.93	0.8	0.72	0.58	1.59	1.6

Appendix B: Table B1.1: Whole-rock Lithogeochemistry Data

Sample ID			**24526**	**24529**	**24531**	**24532**	**31751**	**31752**	**31753**	**31755**
Hole ID			GA-07-254	GA-07-254	GA-07-254	GA-07-254	GA-07-255	GA-07-255	GA-07-255	GA-07-255
Depth (m)			197.4	267.9	300	320.8	4.12	21.6	47.61	100.5
Lithology			VCL2	VCL2	VCL1	VCL1	CL1b	VCL4	VCL4	VCL3
Alteration			chl	ser-sil	ser-sil-chl	ser-sil-chl	sil	ser-sil	chl	ser
SiO_2	%	FUS-ICP	50.34	66.70	62.43	70.60	83.46	70.90	56.68	49.92
Al_2O_3	%	FUS-ICP	15.88	15.41	9.97	10.07	8.67	13.78	15.4	15.16
Fe_2O_3	%	FUS-ICP	9.77	3.87	5.31	5.28	0.57	2.30	5.94	8.95
MnO	%	FUS-ICP	0.16	0.06	0.45	0.24	0.02	0.03	0.14	0.16
MgO	%	FUS-ICP	6.48	2.57	7.24	5.93	0.36	1.87	3.03	3.94
CaO	%	FUS-ICP	4.04	1.05	3.72	0.4	1.36	1.1	5.59	5.5
Na_2O	%	FUS-ICP	4.67	1.90	0.83	0.81	3.15	2.32	6.24	3.48
K_2O	%	FUS-ICP	0.10	3.51	0.42	0.75	1.25	3.57	0.42	2.15
TiO_2	%	FUS-ICP	0.89	0.41	0.26	0.27	0.19	0.30	0.61	1.00
P_2O_5	%	FUS-ICP	0.07	0.04	0.05	0.05	0.01	0.03	0.09	0.13
LOI	%	FUS-ICP	6.61	4.44	8.87	5.19	1.92	3.48	6.24	9.85
Total	%	FUS-ICP	99.00	99.93	99.54	99.57	100.90	99.67	100.40	100.20
Hg	ppb	CV-FIMS	< 5	9	17	7	< 5	< 5	10	< 5
Sc	ppm	FUS-ICP	33	14	6	5	4	7	24	26
Be	ppm	FUS-ICP	< 1	2	< 1	< 1	< 1	1	< 1	< 1
V	ppm	FUS-ICP	331	19	43	37	9	19	170	205
Cr	ppm	FUS-MS	30	< 20	< 20	< 20	40	30	40	< 20
Co	ppm	FUS-MS	21	< 1	3	3	2	3	21	21
Ni	ppm	FUS-MS	< 20	< 20	< 20	< 20	< 20	< 20	< 20	< 20
Cu	ppm	FUS-MS	30	< 10	180	< 10	< 10	< 10	50	30
Zn	ppm	FUS-MS	90	130	320	160	< 30	40	60	100
Ga	ppm	FUS-MS	15	20	12	9	8	14	14	15
Ge	ppm	FUS-MS	0.7	1.4	1	0.7	1.1	1.5	0.7	0.7
As	ppm	FUS-MS	< 5	12	25	26	< 5	< 5	7	14
Rb	ppm	FUS-MS	1	62	9	14	24	76	8	26
Sr	ppm	FUS-ICP	83	33	32	11	27	21	98	67
Y	ppm	FUS-MS	16.90	50.90	11.20	9.60	19.60	31.80	25.30	20.60
Zr	ppm	FUS-ICP	40	204	74	68	99	149	69	58
Nb	ppm	FUS-MS	0.4	0.8	< 0.2	< 0.2	2.1	2.7	1.2	1.2
Mo	ppm	FUS-MS	< 2	< 2	< 2	2	< 2	3	< 2	< 2
Ag	ppm	FUS-MS	< 0.5	< 0.5	< 0.5	< 0.5	< 0.5	< 0.5	< 0.5	< 0.5
In	ppm	FUS-MS	< 0.1	0.1	0.1	< 0.1	< 0.1	< 0.1	< 0.1	< 0.1
Sn	ppm	FUS-MS	< 1	1	< 1	< 1	3	3	< 1	< 1
Sb	ppm	FUS-MS	0.8	0.5	0.8	0.2	0.6	0.8	0.9	0.3
Cs	ppm	FUS-MS	< 0.1	0.5	< 0.1	0.1	0.2	0.5	0.2	0.2
Ba	ppm	FUS-ICP	42	670	88	289	385	443	129	314
La	ppm	FUS-MS	3.63	20	3.67	4.62	13.8	22.7	10.6	5.99
Ce	ppm	FUS-MS	8.69	48.5	8.43	10.30	27.70	45.70	22.20	13.90
Pr	ppm	FUS-MS	1.25	6.56	1.07	1.19	3.01	5.02	2.62	1.93
Nd	ppm	FUS-MS	6.07	30.6	4.87	4.84	11.1	18.7	11.1	9.7
Sm	ppm	FUS-MS	1.97	8.69	1.35	1.17	2.28	4.27	3.23	2.86
Eu	ppm	FUS-MS	1.04	2.36	0.21	0.15	0.54	0.70	1.10	0.96
Gd	ppm	FUS-MS	2.56	9.35	1.59	1.27	2.27	3.80	3.55	3.50
Tb	ppm	FUS-MS	0.46	1.63	0.28	0.23	0.41	0.72	0.69	0.62
Dy	ppm	FUS-MS	3.15	10.20	1.91	1.54	2.82	4.93	4.48	4.07
Ho	ppm	FUS-MS	0.66	2.09	0.41	0.36	0.63	1.09	0.95	0.84
Er	ppm	FUS-MS	1.95	6.22	1.31	1.21	2.09	3.4	2.81	2.43
Tm	ppm	FUS-MS	0.3	0.94	0.21	0.20	0.34	0.54	0.44	0.34
Yb	ppm	FUS-MS	1.95	6.31	1.54	1.45	2.29	3.82	3.04	2.4
Lu	ppm	FUS-MS	0.316	1.04	0.28	0.26	0.38	0.65	0.5	0.39
Hf	ppm	FUS-MS	0.8	4	1.5	1.4	2.2	3.3	1.4	1.3
Ta	ppm	FUS-MS	0.08	0.17	0.13	0.12	0.19	0.29	0.14	0.13
W	ppm	FUS-MS	1.40	< 0.5	0.90	< 0.5	0.90	2.10	0.70	< 0.5
Tl	ppm	FUS-MS	< 0.05	0.85	0.15	0.27	0.12	0.35	0.05	0.05
Pb	ppm	FUS-MS	< 5	6	35	16	8	10	8	< 5
Bi	ppm	FUS-MS	< 0.1	< 0.1	0.6	0.5	< 0.1	< 0.1	< 0.1	< 0.1
Th	ppm	FUS-MS	0.64	4.02	1.88	1.74	5.32	8.14	3.1	0.88
U	ppm	FUS-MS	0.22	1.04	0.97	1.56	1.34	2.38	1.44	0.52

Appendix B: Table B1.1: Whole-rock Lithogeochemistry Data

Sample ID			**31758**	**31759**	**31760**	**31761**	**31764**	**31768**	**31769**	**14488**
Hole ID			GA-07-255	GA-07-255	GA-07-255	GA-07-255	GA-07-255	GA-07-255	GA-07-255	GA-06-147
Depth (m)			129.8	156.4	187.2	208.7	247.9	274.4	281.2	32.7
Lithology			VCL3	IN2a	VCL3	VCL2	VCL2	VCL1 (A-C)	VCL1 (D)	VCL4
Alteration			chl	unaltered	chl	ser-ep	ser	ser-chl-py	ser-sil-chl	ser-sil
SiO_2	%	FUS-ICP	60.15	47.57	49.33	64.7	64.53	63.60	56.59	70.53
Al_2O_3	%	FUS-ICP	17.4	16.45	15.52	15.49	15.56	14.29	15.3	13.85
Fe_2O_3	%	FUS-ICP	4.75	11.86	10.01	4.39	4.56	6.65	7.81	2.60
MnO	%	FUS-ICP	0.05	0.20	0.18	0.05	0.05	0.15	0.21	0.04
MgO	%	FUS-ICP	4.08	6.39	5.57	3.24	2.98	4.88	8.47	1.70
CaO	%	FUS-ICP	0.66	3.65	3.77	0.19	0.66	0.19	0.17	1.71
Na_2O	%	FUS-ICP	4.10	4.95	5.52	3.83	3.01	0.31	0.26	1.05
K_2O	%	FUS-ICP	2.57	0.18	1.81	2.58	2.8	2.52	1.77	4.75
TiO_2	%	FUS-ICP	0.60	1.01	0.86	0.59	0.56	0.57	0.56	0.33
P_2O_5	%	FUS-ICP	0.14	0.06	0.07	0.09	0.07	0.09	0.11	0.03
LOI	%	FUS-ICP	4.16	7.03	5.82	3.14	4.07	6.37	7.15	3.48
Total	%	FUS-ICP	98.66	99.33	98.45	98.29	98.85	99.63	98.4	100.1
Hg	ppb	CV-FIMS	< 5	< 5	< 5	6	6	6	16	9
Sc	ppm	FUS-ICP	18	38	35	18	18	16	17	7
Be	ppm	FUS-ICP	1	1	< 1	2	2	< 1	< 1	2
V	ppm	FUS-ICP	27	371	329	48	33	141	131	17
Cr	ppm	FUS-MS	< 20	< 20	< 20	< 20	< 20	30	30	20
Co	ppm	FUS-MS	2	31	25	3	3	9	5	2
Ni	ppm	FUS-MS	< 20	< 20	< 20	< 20	< 20	20	< 20	< 20
Cu	ppm	FUS-MS	< 10	40	50	< 10	< 10	< 10	20	20
Zn	ppm	FUS-MS	90	90	90	110	110	110	300	70
Ga	ppm	FUS-MS	18	16	15	20	20	14	16	14
Ge	ppm	FUS-MS	1	1.1	1.1	0.9	1.3	0.9	1	1.5
As	ppm	FUS-MS	12	17	< 5	10	14	32	86	< 5
Rb	ppm	FUS-MS	42	6	55	39	48	49	35	86
Sr	ppm	FUS-ICP	34	153	150	35	35	16	14	34
Y	ppm	FUS-MS	53.80	15.80	16.10	50.20	53.10	14.80	17.70	29.90
Zr	ppm	FUS-ICP	208	41	36	184	200	52	89	166
Nb	ppm	FUS-MS	3.6	0.3	< 0.2	1.1	1.3	< 0.2	1	3.7
Mo	ppm	FUS-MS	< 2	< 2	< 2	< 2	< 2	< 2	3	4
Ag	ppm	FUS-MS	< 0.5	< 0.5	< 0.5	< 0.5	< 0.5	< 0.5	< 0.5	< 0.5
In	ppm	FUS-MS	0.1	< 0.1	< 0.1	0.1	0.1	< 0.1	< 0.1	< 0.1
Sn	ppm	FUS-MS	1	< 1	< 1	1	1	1	4	1
Sb	ppm	FUS-MS	< 0.2	< 0.2	< 0.2	0.8	1.1	0.9	0.7	0.7
Cs	ppm	FUS-MS	0.3	0.4	3.8	0.3	0.4	0.4	0.3	0.8
Ba	ppm	FUS-ICP	402	81	236	869	1577	3998	1165	1411
La	ppm	FUS-MS	19.90	3.81	3.63	18.70	19.90	2.81	11.10	18.40
Ce	ppm	FUS-MS	44.70	9.27	8.83	46.10	48.40	7.90	27.40	36.60
Pr	ppm	FUS-MS	5.88	1.34	1.24	6.27	6.53	1.06	3.39	4.13
Nd	ppm	FUS-MS	26.1	6.6	6.34	28.6	30.3	5.26	14.4	16.2
Sm	ppm	FUS-MS	7.12	1.95	2.02	7.74	8.33	1.53	3.22	3.48
Eu	ppm	FUS-MS	1.41	0.73	0.76	2.22	2.41	0.19	0.42	0.70
Gd	ppm	FUS-MS	8.55	2.68	2.69	8.59	9.27	2.01	3.25	3.87
Tb	ppm	FUS-MS	1.54	0.46	0.48	1.52	1.68	0.40	0.54	0.70
Dy	ppm	FUS-MS	10.2	2.95	3.15	9.84	10.7	2.72	3.35	4.73
Ho	ppm	FUS-MS	2.19	0.63	0.66	2.1	2.19	0.60	0.70	1.05
Er	ppm	FUS-MS	6.67	1.91	1.97	6.12	6.52	1.82	2.17	3.32
Tm	ppm	FUS-MS	1.04	0.28	0.29	0.93	0.99	0.28	0.35	0.55
Yb	ppm	FUS-MS	7.15	1.86	1.94	6.14	6.68	1.96	2.38	3.95
Lu	ppm	FUS-MS	1.18	0.30	0.33	0.97	1.09	0.31	0.40	0.66
Hf	ppm	FUS-MS	4.3	0.9	0.9	3.5	4	1.2	1.8	3.4
Ta	ppm	FUS-MS	0.32	0.08	0.06	0.14	0.16	0.1	0.17	0.33
W	ppm	FUS-MS	< 0.5	< 0.5	< 0.5	< 0.5	< 0.5	2.7	2.7	0.9
Tl	ppm	FUS-MS	0.15	< 0.05	0.36	0.12	1.13	1.65	1.00	0.35
Pb	ppm	FUS-MS	< 5	< 5	< 5	5	7	8	128	27
Bi	ppm	FUS-MS	< 0.1	< 0.1	< 0.1	< 0.1	< 0.1	0.4	0.5	0.2
Th	ppm	FUS-MS	6.34	0.66	0.53	3.5	3.8	1.38	4.5	9.05
U	ppm	FUS-MS	2.22	0.2	0.15	1.2	1.24	1.14	2.59	2.65

Appendix B: Table B1.1: Whole-rock Lithogeochemistry Data

Sample ID			14489	14490	14492	14494	14496	14498	14500	32002
Hole ID			GA-06-147	GA-06-147	GA-06-147	GA-06-147	GA-06-147	GA-06-147	GA-06-147	GA-06-147
Depth (m)			49.2	62.2	94.9	110.6	125.35	189.8	220.45	250.1
Lithology			VCL4	VCL4	VCL3	VCL3	IN1	IN2a	VCL1 (D)	IN2a
Alteration			chl	chl	ser	ser-chl	unaltered	sil-ser	sil-ser	sil-ser
SiO_2	%	FUS-ICP	46.84	57.86	60.72	62.79	50.27	48.84	64.86	61.33
Al_2O_3	%	FUS-ICP	19.05	14.42	12.81	16.79	16.19	14.72	13.58	14.97
Fe_2O_3	%	FUS-ICP	13.56	6.01	5.93	5.36	10.97	10.2	8.27	4.94
MnO	%	FUS-ICP	0.11	0.13	0.11	0.02	0.17	0.26	0.05	0.16
MgO	%	FUS-ICP	7.6	2.58	2.51	4.34	6.3	5.87	1.48	1.54
CaO	%	FUS-ICP	0.94	4.88	4.13	0.61	3.1	4.82	0.43	3.47
Na_2O	%	FUS-ICP	4.94	6.41	4.95	1.88	5.36	3.57	0.39	4.08
K_2O	%	FUS-ICP	0.84	0.54	0.96	3.35	0.03	0.55	3.29	1.68
TiO_2	%	FUS-ICP	0.90	0.58	0.72	0.68	0.99	0.92	0.56	1.05
P_2O_5	%	FUS-ICP	0.10	0.09	0.07	0.08	0.09	0.07	0.06	0.37
LOI	%	FUS-ICP	5.46	5.35	7.26	4.96	7.21	9.38	6.18	6.74
Total	%	FUS-ICP	100.30	98.86	100.20	100.80	100.70	99.20	99.17	100.30
Hg	ppb	CV-FIMS	< 5	< 5	8	< 5	< 5	< 5	81	< 5
Sc	ppm	FUS-ICP	39	24	18	21	37	35	24	14
Be	ppm	FUS-ICP	1	< 1	< 1	1	1	< 1	< 1	2
V	ppm	FUS-ICP	284	188	157	71	380	330	153	82
Cr	ppm	FUS-MS	60	40	30	20	30	< 20	60	< 20
Co	ppm	FUS-MS	32	18	14	6	25	22	19	6
Ni	ppm	FUS-MS	20	< 20	< 20	< 20	< 20	< 20	< 20	< 20
Cu	ppm	FUS-MS	20	40	20	< 10	50	60	40	< 10
Zn	ppm	FUS-MS	140	60	110	60	90	80	600	70
Ga	ppm	FUS-MS	20	13	13	18	15	15	13	17
Ge	ppm	FUS-MS	1.10	0.80	0.60	1.60	1.30	1.20	0.80	1.10
As	ppm	FUS-MS	< 5	< 5	20	27	8	16	160	< 5
Rb	ppm	FUS-MS	17	14	13	60	< 1	10	68	40
Sr	ppm	FUS-ICP	34	114	69	24	188	87	17	166
Y	ppm	FUS-MS	18.20	19.20	17.10	46.50	13.70	18.50	20.30	29.00
Zr	ppm	FUS-ICP	56	68	76	100	42	34	43	183
Nb	ppm	FUS-MS	1.50	1.40	1.30	0.30	0.60	0.50	0.50	4.70
Mo	ppm	FUS-MS	< 2	< 2	4	2	< 2	< 2	3	< 2
Ag	ppm	FUS-MS	< 0.5	< 0.5	< 0.5	< 0.5	< 0.5	< 0.5	< 0.5	< 0.5
In	ppm	FUS-MS	< 0.1	< 0.1	< 0.1	< 0.1	< 0.1	< 0.1	0.1	< 0.1
Sn	ppm	FUS-MS	< 1	< 1	< 1	2	< 1	< 1	1	1
Sb	ppm	FUS-MS	0.60	0.60	1.20	1.50	0.70	0.80	3.40	2.00
Cs	ppm	FUS-MS	0.30	0.60	0.10	0.40	< 0.1	0.10	0.50	0.40
Ba	ppm	FUS-ICP	265	147	126	981	33	126	494	568
La	ppm	FUS-MS	5.93	8.10	5.00	7.60	4.36	4.17	4.00	23.8
Ce	ppm	FUS-MS	12.00	16.50	11.50	19.60	8.87	9.90	8.96	49.00
Pr	ppm	FUS-MS	1.48	1.93	1.57	2.94	1.16	1.42	1.21	5.75
Nd	ppm	FUS-MS	6.15	8.33	7.46	14.6	5.97	6.94	6.00	24.30
Sm	ppm	FUS-MS	1.60	2.16	2.20	5.12	1.70	2.26	1.98	5.56
Eu	ppm	FUS-MS	0.47	0.70	0.67	1.37	0.59	0.93	0.32	1.54
Gd	ppm	FUS-MS	2.33	2.47	2.41	6.52	2.08	2.99	2.61	5.32
Tb	ppm	FUS-MS	0.48	0.47	0.52	1.27	0.4	0.53	0.53	0.89
Dy	ppm	FUS-MS	3.23	3.1	3.11	8.44	2.57	3.45	3.6	5.42
Ho	ppm	FUS-MS	0.67	0.67	0.64	1.69	0.56	0.72	0.79	1.11
Er	ppm	FUS-MS	2	2.08	1.88	4.97	1.66	2.05	2.33	3.28
Tm	ppm	FUS-MS	0.31	0.34	0.32	0.74	0.24	0.31	0.37	0.48
Yb	ppm	FUS-MS	2.09	2.38	2.04	4.8	1.58	2.05	2.45	3.09
Lu	ppm	FUS-MS	0.32	0.39	0.35	0.76	0.25	0.31	0.41	0.49
Hf	ppm	FUS-MS	1.30	1.40	1.50	2.60	1.00	0.80	1.00	3.40
Ta	ppm	FUS-MS	0.12	0.13	0.16	0.07	0.1	0.08	0.09	0.4
W	ppm	FUS-MS	1.1	0.6	1	0.9	1.2	1.6	2	3.6
Tl	ppm	FUS-MS	0.1	0.09	0.07	0.6	< 0.05	0.11	0.98	0.3
Pb	ppm	FUS-MS	< 5	10	6	6	< 5	< 5	297	8
Bi	ppm	FUS-MS	< 0.1	< 0.1	< 0.1	< 0.1	< 0.1	< 0.1	0.3	< 0.1
Th	ppm	FUS-MS	1.87	3.24	1.66	1.81	0.77	0.65	1.17	6.51
U	ppm	FUS-MS	0.81	1.12	1.28	1.32	0.23	0.23	0.9	2.28

Appendix B: Table B1.1: Whole-rock Lithogeochemistry Data

Sample ID			**32004**	**32005**	**32006**	**32007**	**32008**	**14514**	**14516**	**14520**
Hole ID			GA-06-147	GA-06-147	GA-06-147	GA-06-147	GA-06-147	GA-07-208	GA-07-208	GA-07-208
Depth (m)			285.1	316.97	336.2	363.6	380.4	7.3	24.1	44.8
Lithology			VCL1 (A-C)	VCL1 (A-C)	VCL1 (D)	VCL1 (A-C)	VCL1 (A-C)	CL1a	CL1a	VCL4
Alteration			ser-sil-py	ser-sil-py	ser-chl	ser	ser	sil	sil	sil-chl
SiO_2	%	FUS-ICP	62.43	48.79	50.54	60.23	51.21	81.01	81.99	66.56
Al_2O_3	%	FUS-ICP	14.92	14.59	18.50	14.76	17.94	8.40	10.01	14.19
Fe_2O_3	%	FUS-ICP	6.88	7.05	8.68	7.06	8.47	1.69	1.09	4.4
MnO	%	FUS-ICP	0.17	0.49	0.42	0.20	0.47	0.01	0.01	0.07
MgO	%	FUS-ICP	3.31	11.09	8.93	5.93	6.19	0.19	0.59	2.09
CaO	%	FUS-ICP	0.62	4.17	1.91	1.20	3.07	0.75	0.23	2.80
Na_2O	%	FUS-ICP	2.33	0.44	0.49	2.10	1.46	3.05	2.29	4.39
K_2O	%	FUS-ICP	2.18	1.28	2.15	1.28	2.14	1.45	2.07	1.57
TiO_2	%	FUS-ICP	0.73	0.59	0.84	0.61	0.76	0.19	0.19	0.43
P_2O_5	%	FUS-ICP	0.12	0.05	0.10	0.05	0.06	0.01	0.02	0.05
LOI	%	FUS-ICP	5.64	10.85	8.16	6.50	8.55	1.73	1.44	4.27
Total	%	FUS-ICP	99.31	99.39	100.70	99.93	100.30	98.50	99.92	100.80
Hg	ppb	CV-FIMS	23	12	< 5	9	33	169	< 5	6
Sc	ppm	FUS-ICP	18	21	32	20	24	4	5	15
Be	ppm	FUS-ICP	< 1	< 1	< 1	< 1	1	< 1	1	1
V	ppm	FUS-ICP	148	149	235	157	194	14	12	96
Cr	ppm	FUS-MS	< 20	30	50	50	100	30	< 20	20
Co	ppm	FUS-MS	14	16	25	16	17	1	< 1	13
Ni	ppm	FUS-MS	< 20	< 20	20	< 20	30	< 20	< 20	< 20
Cu	ppm	FUS-MS	30	20	40	10	20	< 10	< 10	20
Zn	ppm	FUS-MS	270	400	190	180	140	340	< 30	50
Ga	ppm	FUS-MS	15	13	17	13	17	5	9	13
Ge	ppm	FUS-MS	0.60	0.60	0.80	0.70	0.80	0.90	1.10	0.80
As	ppm	FUS-MS	101	56	55	64	53	15	< 5	17
Rb	ppm	FUS-MS	50	29	49	29	49	14	35	27
Sr	ppm	FUS-ICP	34	54	40	35	37	64	47	69
Y	ppm	FUS-MS	18.70	15.40	22.90	19.60	20.40	14.70	18.40	19.60
Zr	ppm	FUS-ICP	90	52	49	52	58	81	84	96
Nb	ppm	FUS-MS	1.80	0.40	1.00	0.30	0.30	0.40	0.70	0.90
Mo	ppm	FUS-MS	< 2	< 2	4	< 2	< 2	5	< 2	< 2
Ag	ppm	FUS-MS	< 0.5	< 0.5	< 0.5	< 0.5	< 0.5	< 0.5	< 0.5	< 0.5
In	ppm	FUS-MS	0.1	< 0.1	< 0.1	< 0.1	< 0.1	< 0.1	< 0.1	< 0.1
Sn	ppm	FUS-MS	2	2	1	1	< 1	< 1	< 1	< 1
Sb	ppm	FUS-MS	2.30	1.40	1.40	1.60	1.60	0.30	0.30	0.20
Cs	ppm	FUS-MS	0.40	0.30	0.50	0.30	0.80	< 0.1	0.40	0.30
Ba	ppm	FUS-ICP	273	169	291	165	260	4914	1308	981
La	ppm	FUS-MS	6.87	4.13	5.59	3.53	3.08	7.50	10.10	14.40
Ce	ppm	FUS-MS	15.3	10.1	13.7	8.54	8.08	15.7	20.3	29.7
Pr	ppm	FUS-MS	2.01	1.47	1.92	1.23	1.31	1.81	2.23	3.30
Nd	ppm	FUS-MS	9.09	7.42	9.41	6.18	7.00	6.78	8.47	13.40
Sm	ppm	FUS-MS	2.36	2.21	2.95	1.96	2.46	1.54	1.76	2.94
Eu	ppm	FUS-MS	0.46	0.33	0.49	0.37	0.52	0.46	0.34	0.79
Gd	ppm	FUS-MS	2.57	2.39	3.38	2.58	2.78	1.76	2.1	3.12
Tb	ppm	FUS-MS	0.50	0.42	0.63	0.51	0.54	0.34	0.40	0.57
Dy	ppm	FUS-MS	3.29	2.73	4.22	3.53	3.55	2.38	3.07	3.6
Ho	ppm	FUS-MS	0.72	0.59	0.89	0.76	0.75	0.55	0.74	0.77
Er	ppm	FUS-MS	2.17	1.8	2.66	2.22	2.4	1.78	2.37	2.32
Tm	ppm	FUS-MS	0.34	0.29	0.40	0.35	0.37	0.29	0.39	0.38
Yb	ppm	FUS-MS	2.29	1.95	2.62	2.38	2.53	2.01	2.82	2.81
Lu	ppm	FUS-MS	0.37	0.32	0.41	0.38	0.43	0.35	0.48	0.46
Hf	ppm	FUS-MS	1.90	1.20	1.00	1.30	1.30	1.60	2.00	2.00
Ta	ppm	FUS-MS	0.21	0.09	0.12	0.08	0.09	0.16	0.19	0.18
W	ppm	FUS-MS	1.60	1.60	1.50	2.50	1.20	1.10	0.80	1.40
Tl	ppm	FUS-MS	0.43	0.16	0.22	0.16	0.34	< 0.05	< 0.05	< 0.05
Pb	ppm	FUS-MS	36	188	54	146	34	73	< 5	7
Bi	ppm	FUS-MS	< 0.1	< 0.1	< 0.1	< 0.1	< 0.1	< 0.1	< 0.1	< 0.1
Th	ppm	FUS-MS	1.95	0.8	1.21	0.69	0.7	4.36	5.82	4.8
U	ppm	FUS-MS	0.63	0.35	0.40	0.20	0.20	1.28	1.52	1.43

Appendix B: Table B1.1: Whole-rock Lithogeochemistry Data

Sample ID			**14521**	**14523**	**14526**	**14529**	**14532**	**14535**	**14538**	**14540**
Hole ID			GA-07-208	GA-07-208	GA-07-208	GA-07-208	GA-07-208	GA-07-208	GA-07-208	GA-07-208
Depth (m)			44.8	83.5	103.4	124	156.5	169.1	202.8	218.5
Lithology			VCL4	VCL4	VCL4	VCL3	IN1	VCL2	IN2a	VCL2
Alteration			chl	chl	least alt?	chl	unaltered	ser-sil	carb	ser-sil
SiO_2	%	FUS-ICP	49.62	55.47	53.15	48.4	48.86	61.16	51.71	66.27
Al_2O_3	%	FUS-ICP	19.13	15.75	19.67	20.13	16.59	16.67	16.71	14.75
Fe_2O_3	%	FUS-ICP	9.65	6.07	8.73	8.84	11.11	5.67	9.93	5.25
MnO	%	FUS-ICP	0.12	0.12	0.06	0.06	0.19	0.06	0.20	0.04
MgO	%	FUS-ICP	7.17	3.31	5.91	10.8	6.14	5.23	5.64	2.91
CaO	%	FUS-ICP	2.08	5.56	0.48	0.19	4.34	0.61	2.97	0.49
Na_2O	%	FUS-ICP	4.72	6.87	7.19	4.84	5.42	2.33	6.75	4.85
K_2O	%	FUS-ICP	1.41	0.09	0.12	0.37	0.14	3.2	0.1	1.19
TiO_2	%	FUS-ICP	0.74	0.60	1.02	0.84	1.03	0.85	0.90	0.47
P_2O_5	%	FUS-ICP	0.06	0.06	0.12	0.06	0.12	0.11	0.13	0.04
LOI	%	FUS-ICP	5.87	6.73	4.10	6.12	6.92	4.12	5.26	3.37
Total	%	FUS-ICP	100.60	100.60	100.60	100.60	100.90	100.00	100.30	99.63
Hg	ppb	CV-FIMS	< 5	< 5	< 5	5	< 5	< 5	< 5	< 5
Sc	ppm	FUS-ICP	27	23	24	26	37	18	33	15
Be	ppm	FUS-ICP	1	< 1	< 1	< 1	< 1	2	< 1	1
V	ppm	FUS-ICP	223	190	199	206	373	50	299	23
Cr	ppm	FUS-MS	30	30	< 20	< 20	30	< 20	30	< 20
Co	ppm	FUS-MS	21	15	15	19	26	4	21	2
Ni	ppm	FUS-MS	< 20	< 20	< 20	< 20	< 20	< 20	< 20	< 20
Cu	ppm	FUS-MS	20	40	< 10	< 10	20	< 10	30	< 10
Zn	ppm	FUS-MS	90	60	70	80	90	110	90	70
Ga	ppm	FUS-MS	19	13	20	18	16	19	16	16
Ge	ppm	FUS-MS	1	1	1	0.9	1.4	1	0.9	0.8
As	ppm	FUS-MS	< 5	7	11	21	5	5	< 5	12
Rb	ppm	FUS-MS	24	< 1	2	6	4	54	2	21
Sr	ppm	FUS-ICP	46	134	119	32	137	33	151	42
Y	ppm	FUS-MS	24.60	15.20	27.50	15.80	19.90	48.30	18.00	51.50
Zr	ppm	FUS-ICP	104	80	78	81	47	171	50	220
Nb	ppm	FUS-MS	1.20	0.70	0.90	0.20	0.90	1.40	1.00	1.00
Mo	ppm	FUS-MS	< 2	< 2	< 2	< 2	< 2	< 2	< 2	4
Ag	ppm	FUS-MS	< 0.5	< 0.5	< 0.5	< 0.5	< 0.5	< 0.5	< 0.5	< 0.5
In	ppm	FUS-MS	< 0.1	< 0.1	< 0.1	< 0.1	< 0.1	< 0.1	< 0.1	0.1
Sn	ppm	FUS-MS	< 1	< 1	< 1	< 1	< 1	< 1	< 1	< 1
Sb	ppm	FUS-MS	< 0.2	< 0.2	0.2	0.9	0.7	0.4	1.7	1
Cs	ppm	FUS-MS	0.2	< 0.1	< 0.1	< 0.1	0.2	0.4	< 0.1	0.2
Ba	ppm	FUS-ICP	538	45	46	85	59	414	54	484
La	ppm	FUS-MS	8.60	11.50	5.50	3.89	4.48	17.90	4.57	18.50
Ce	ppm	FUS-MS	18.80	22.50	12.40	9.69	10.70	43.40	10.50	46.40
Pr	ppm	FUS-MS	2.32	2.48	1.73	1.38	1.56	5.85	1.54	6.28
Nd	ppm	FUS-MS	9.88	9.64	8.73	6.38	7.26	27.1	6.87	29.4
Sm	ppm	FUS-MS	2.82	2.30	3.02	1.91	2.25	7.16	2.13	7.68
Eu	ppm	FUS-MS	0.91	0.65	1.05	0.66	0.89	2.28	0.78	1.72
Gd	ppm	FUS-MS	3.67	2.52	4.66	2.62	2.91	8.53	2.81	8.04
Tb	ppm	FUS-MS	0.69	0.44	0.88	0.46	0.53	1.5	0.51	1.45
Dy	ppm	FUS-MS	4.50	2.85	5.68	2.88	3.49	9.25	3.29	9.88
Ho	ppm	FUS-MS	0.97	0.62	1.14	0.62	0.74	1.91	0.69	2.13
Er	ppm	FUS-MS	2.85	1.96	3.25	1.95	2.18	5.67	2.14	6.59
Tm	ppm	FUS-MS	0.44	0.31	0.46	0.31	0.32	0.85	0.33	1.02
Yb	ppm	FUS-MS	3.11	2.16	2.88	2.1	2.08	5.59	2.18	6.92
Lu	ppm	FUS-MS	0.52	0.37	0.47	0.36	0.34	0.91	0.35	1.11
Hf	ppm	FUS-MS	2.10	1.70	1.60	1.80	0.90	3.50	1.10	4.30
Ta	ppm	FUS-MS	0.18	0.16	0.16	0.14	0.09	0.18	0.10	0.18
W	ppm	FUS-MS	0.5	0.7	< 0.5	0.8	0.9	< 0.5	2.5	< 0.5
Tl	ppm	FUS-MS	< 0.05	< 0.05	< 0.05	< 0.05	< 0.05	0.09	< 0.05	0.23
Pb	ppm	FUS-MS	< 5	< 5	< 5	19	< 5	9	< 5	6
Bi	ppm	FUS-MS	< 0.1	< 0.1	< 0.1	< 0.1	< 0.1	< 0.1	< 0.1	< 0.1
Th	ppm	FUS-MS	4.63	3.54	1.09	2.3	0.77	3.75	0.88	4.36
U	ppm	FUS-MS	1.25	1.11	0.53	0.81	0.23	1.58	0.31	1.15

Appendix B: Table B1.1: Whole-rock Lithogeochemistry Data

Sample ID			**14544**	**14545**	**14547**	**14450**	**14453**	**14457**	**14459**	**14460**
Hole ID			GA-07-208	GA-07-208	GA-07-208	GA-07-208	GA-07-208	GA-07-218	GA-07-218	GA-07-218
Depth (m)			273.6	295	328.3	242.4	258.3	20.2	50.01	69.5
Lithology			VCL1 (A-C)	IN2a	VCL1 (D)	VCL1 (E)	VCL1 (A-C)	IN2a	CL1a	CL1a
Alteration			ser-sil-py	ser-sil	ser-sil	chl-py	sil-ser-chl-py	unaltered	sil-ser	sil-ser
SiO_2	%	FUS-ICP	69.15	53.40	61.09	46.22	41.78	50.16	77.64	78.42
Al_2O_3	%	FUS-ICP	10.90	14.48	14.87	9.09	12.24	15.20	11.10	11.14
Fe_2O_3	%	FUS-ICP	7.12	10.49	5.64	24.27	15.49	8.75	1.52	1.34
MnO	%	FUS-ICP	0.03	0.36	0.43	0.05	0.32	0.14	0.04	0.03
MgO	%	FUS-ICP	0.31	4.41	3.89	2.49	13.21	6.89	0.56	0.57
CaO	%	FUS-ICP	0.42	3.48	2.41	0.17	1.09	6.51	1.16	0.7
Na_2O	%	FUS-ICP	0.52	0.42	2.56	0.20	0.03	3.68	3.22	3.93
K_2O	%	FUS-ICP	2.52	2.32	1.49	1.69	0.04	0.86	2.86	1.88
TiO_2	%	FUS-ICP	0.40	0.70	0.57	0.24	0.59	1.50	0.26	0.24
P_2O_5	%	FUS-ICP	0.03	0.18	0.13	0.03	0.10	0.36	0.02	0.02
LOI	%	FUS-ICP	6.13	9.69	7.07	13.48	13.49	5.34	2.27	2.07
Total	%	FUS-ICP	97.52	99.93	100.2	97.92	98.38	99.4	100.6	100.3
Hg	ppb	CV-FIMS	479	6	12	62	114	< 5	< 5	15
Sc	ppm	FUS-ICP	15	26	11	9	12	23	6	6
Be	ppm	FUS-ICP	< 1	< 1	< 1	< 1	< 1	2	< 1	< 1
V	ppm	FUS-ICP	108	199	91	10	102	205	13	16
Cr	ppm	FUS-MS	40	50	< 20	< 20	20	260	< 20	40
Co	ppm	FUS-MS	8	30	10	< 1	16	32	1	2
Ni	ppm	FUS-MS	< 20	20	< 20	< 20	< 20	120	< 20	< 20
Cu	ppm	FUS-MS	640	20	30	3610	780	40	< 10	< 10
Zn	ppm	FUS-MS	7680	260	400	280	1810	80	< 30	40
Ga	ppm	FUS-MS	11	14	14	12	17	15	10	10
Ge	ppm	FUS-MS	1.3	0.7	0.7	4.7	1	1.4	1	1.6
As	ppm	FUS-MS	136	57	21	64	38	< 5	< 5	16
Rb	ppm	FUS-MS	55	56	35	30	< 1	17	32	27
Sr	ppm	FUS-ICP	28	70	39	9	5	572	37	38
Y	ppm	FUS-MS	20.00	20.30	19.90	28.80	25.70	20.20	23.00	25.10
Zr	ppm	FUS-ICP	32	52	85	135	86	164	131	110
Nb	ppm	FUS-MS	< 0.2	1.6	2.3	0.9	1.9	5.8	1.2	1.7
Mo	ppm	FUS-MS	< 2	< 2	< 2	6	5	< 2	< 2	3
Ag	ppm	FUS-MS	1.7	0.6	< 0.5	2.7	0.8	< 0.5	< 0.5	< 0.5
In	ppm	FUS-MS	0.2	< 0.1	0.2	0.3	0.9	< 0.1	< 0.1	< 0.1
Sn	ppm	FUS-MS	1	< 1	< 1	24	2	1	< 1	2
Sb	ppm	FUS-MS	10.00	1.20	1.20	13.40	5.20	1.70	0.20	0.70
Cs	ppm	FUS-MS	0.30	0.40	0.30	0.20	< 0.1	0.60	0.20	0.20
Ba	ppm	FUS-ICP	425	360	201	2758	31	246	3032	871
La	ppm	FUS-MS	4.98	4.59	8.46	11.2	6.25	29.6	16.1	15.2
Ce	ppm	FUS-MS	10.50	11.00	18.00	27.00	16.90	60.00	31.80	30.30
Pr	ppm	FUS-MS	1.32	1.56	2.29	3.58	2.36	6.94	3.42	3.33
Nd	ppm	FUS-MS	5.7	7.51	9.51	16.4	11.3	27.4	13.2	12.5
Sm	ppm	FUS-MS	1.71	2.31	2.63	4.54	2.85	5.12	2.83	2.87
Eu	ppm	FUS-MS	0.35	0.58	0.79	1.18	0.40	1.62	0.64	0.57
Gd	ppm	FUS-MS	2.2	2.92	2.81	4.43	3.32	4.4	3.24	2.87
Tb	ppm	FUS-MS	0.45	0.55	0.54	0.83	0.64	0.67	0.59	0.52
Dy	ppm	FUS-MS	3.21	3.66	3.41	5.52	4.29	4.01	3.99	3.85
Ho	ppm	FUS-MS	0.69	0.79	0.74	1.1	0.94	0.77	0.87	0.83
Er	ppm	FUS-MS	2.08	2.38	2.22	3.23	2.82	2.15	2.64	2.62
Tm	ppm	FUS-MS	0.33	0.33	0.36	0.51	0.45	0.29	0.43	0.42
Yb	ppm	FUS-MS	2.14	2.24	2.51	3.49	3.09	2.04	3.06	2.88
Lu	ppm	FUS-MS	0.34	0.36	0.42	0.56	0.51	0.33	0.52	0.51
Hf	ppm	FUS-MS	0.70	1.10	1.80	2.60	1.80	2.80	2.50	2.50
Ta	ppm	FUS-MS	0.06	0.15	0.22	0.15	0.3	0.43	0.24	0.23
W	ppm	FUS-MS	2.30	2.00	1.10	0.80	7.20	2.40	< 0.5	1.80
Tl	ppm	FUS-MS	0.82	0.41	0.24	1.46	0.17	0.09	0.05	0.24
Pb	ppm	FUS-MS	3990	43	19	148	41	8	5	5
Bi	ppm	FUS-MS	< 0.1	< 0.1	< 0.1	0.10	3.20	< 0.1	< 0.1	< 0.1
Th	ppm	FUS-MS	0.40	1.17	2.45	3.07	2.07	3.83	6.69	6.21
U	ppm	FUS-MS	0.97	0.65	0.7	0.85	1.91	1.17	2.02	1.63

Appendix B: Table B1.1: Whole-rock Lithogeochemistry Data

Sample ID			**14461**	**14462**	**14465**	**14466**	**14467**	**14469**	**14472**	**14474**
Hole ID			GA-07-218	GA-07-218	GA-07-218	GA-07-218	GA-07-218	GA-07-218	GA-07-218	GA-07-218
Depth (m)			86.1	104.6	125.8	148.3	162.5	182.2	199.1	239.4
Lithology			CL1a	VCL4	VCL4	VCL4	VCL3	VCL3	VCL3	VCL3
Alteration			sil-chl-ser	sil-ser	chl	unaltered	chl-ser	chl-py	chl-py	ser-chl
SiO_2	%	FUS-ICP	78.09	70.89	54.21	53.29	56.17	39.85	68.21	79.84
Al_2O_3	%	FUS-ICP	11.30	13.95	16.32	20.23	21.72	19.14	7.13	7.48
Fe_2O_3	%	FUS-ICP	1.61	2.28	7.83	8.65	4.20	12.84	10.57	4.35
MnO	%	FUS-ICP	0.03	0.04	0.12	0.08	0.02	0.06	0.02	0.03
MgO	%	FUS-ICP	0.69	1.43	5.49	4.42	3.39	14.77	2.74	1.59
CaO	%	FUS-ICP	0.35	0.71	3.71	1.16	0.23	0.20	0.18	0.37
Na_2O	%	FUS-ICP	3.46	2.73	4.91	6.77	2.69	2.63	0.28	0.51
K_2O	%	FUS-ICP	2.25	3.74	0.48	0.88	5.64	0.13	1.40	2.14
TiO_2	%	FUS-ICP	0.23	0.35	0.66	1.05	0.63	0.84	0.34	0.29
P_2O_5	%	FUS-ICP	0.03	0.03	0.08	0.12	0.07	0.08	0.04	< 0.01
LOI	%	FUS-ICP	1.76	2.79	6.33	4.17	4.32	8.34	7.66	2.47
Total	%	FUS-ICP	99.79	98.93	100.10	100.80	99.09	98.89	98.56	99.08
Hg	ppb	CV-FIMS	11	25	< 5	< 5	23	< 5	14	9
Sc	ppm	FUS-ICP	5	8	26	23	15	24	11	8
Be	ppm	FUS-ICP	< 1	2	1	< 1	2	< 1	< 1	1
V	ppm	FUS-ICP	24	44	200	237	83	315	230	186
Cr	ppm	FUS-MS	< 20	< 20	30	< 20	< 20	30	50	< 20
Co	ppm	FUS-MS	2	3	21	17	8	33	12	4
Ni	ppm	FUS-MS	< 20	< 20	< 20	< 20	< 20	30	30	< 20
Cu	ppm	FUS-MS	< 10	< 10	20	50	< 10	20	20	10
Zn	ppm	FUS-MS	60	50	70	90	40	120	40	100
Ga	ppm	FUS-MS	9	16	16	20	22	19	10	9
Ge	ppm	FUS-MS	0.90	1.10	0.80	1.30	0.80	1.10	1.00	0.70
As	ppm	FUS-MS	16	10	< 5	10	21	40	83	23
Rb	ppm	FUS-MS	29	58	7	14	87	2	21	34
Sr	ppm	FUS-ICP	33	37	96	106	33	16	6	10
Y	ppm	FUS-MS	20.00	26.20	17.80	21.60	33.80	22.00	23.50	21.70
Zr	ppm	FUS-ICP	79	142	77	78	169	92	44	73
Nb	ppm	FUS-MS	0.80	1.80	0.50	1.50	2.20	1.80	1.50	< 0.2
Mo	ppm	FUS-MS	< 2	< 2	< 2	< 2	5	3	12	4
Ag	ppm	FUS-MS	< 0.5	< 0.5	< 0.5	< 0.5	< 0.5	< 0.5	< 0.5	< 0.5
In	ppm	FUS-MS	< 0.1	< 0.1	< 0.1	< 0.1	< 0.1	< 0.1	< 0.1	< 0.1
Sn	ppm	FUS-MS	< 1	< 1	< 1	< 1	1	< 1	1	< 1
Sb	ppm	FUS-MS	0.30	0.60	0.50	0.30	1.10	0.60	4.60	1.30
Cs	ppm	FUS-MS	0.40	0.70	0.10	0.10	0.80	< 0.1	0.20	0.30
Ba	ppm	FUS-ICP	2438	1418	427	497	1184	38	425	332
La	ppm	FUS-MS	14.30	16.90	7.20	3.92	13.70	4.79	13.50	13.10
Ce	ppm	FUS-MS	28.20	33.40	15.00	9.90	31.50	10.80	29.50	29.20
Pr	ppm	FUS-MS	3.21	3.80	1.84	1.44	4.00	1.45	3.52	3.76
Nd	ppm	FUS-MS	12.1	14.5	7.74	7.28	17.5	6.84	14.8	16.9
Sm	ppm	FUS-MS	2.71	3.27	2.10	2.40	4.51	2.10	3.36	4.19
Eu	ppm	FUS-MS	0.63	0.81	0.64	0.73	1.10	0.75	1.04	1.39
Gd	ppm	FUS-MS	2.78	3.39	2.65	3.26	5.19	3.15	3.28	4.31
Tb	ppm	FUS-MS	0.51	0.64	0.46	0.6	0.99	0.61	0.57	0.71
Dy	ppm	FUS-MS	3.41	4.49	3.12	4.06	6.56	4.03	3.68	4.33
Ho	ppm	FUS-MS	0.76	1.01	0.69	0.86	1.37	0.89	0.77	0.88
Er	ppm	FUS-MS	2.37	3.05	2.12	2.58	4.03	2.82	2.36	2.69
Tm	ppm	FUS-MS	0.38	0.49	0.33	0.39	0.61	0.44	0.35	0.42
Yb	ppm	FUS-MS	2.65	3.52	2.25	2.49	3.98	2.93	2.36	2.99
Lu	ppm	FUS-MS	0.47	0.59	0.38	0.40	0.66	0.50	0.39	0.48
Hf	ppm	FUS-MS	2.00	3.00	1.60	1.60	3.60	2.00	0.90	1.40
Ta	ppm	FUS-MS	0.19	0.27	0.13	0.14	0.29	0.16	0.18	0.15
W	ppm	FUS-MS	< 0.5	< 0.5	3.3	< 0.5	< 0.5	1.6	0.5	< 0.5
Tl	ppm	FUS-MS	0.06	0.15	< 0.05	< 0.05	0.33	< 0.05	0.24	< 0.05
Pb	ppm	FUS-MS	< 5	8	< 5	< 5	7	< 5	16	32
Bi	ppm	FUS-MS	< 0.1	< 0.1	< 0.1	< 0.1	< 0.1	< 0.1	< 0.1	< 0.1
Th	ppm	FUS-MS	5.37	7.12	3.28	1.11	4.74	2.4	2.47	2.44
U	ppm	FUS-MS	1.89	2.63	1.18	0.45	3.96	1.37	5.04	1.85

Appendix B: Table B1.1: Whole-rock Lithogeochemistry Data

Sample ID			**14477**	**14478**	**14480**	**14482**	**14483**	**14485**	**32128**	**32131**
Hole ID			GA-07-218	GA-07-218	GA-07-218	GA-07-218	GA-07-218	GA-07-218	GA-10-272	GA-10-272
Depth (m)			294.8	318.1	323.3	344.5	363.9	394.8	43.1	89.8
Lithology			VCL2	VCL2	VCL2	VCL1 (D)	VCL1 (D)	VCL1 (A-C)	VCL3	VCL4
Alteration			ser-chl	ser-sil	ser-chl-py	ser-chl-py	ser-chl-py	ser-chl-py	sil-chl	chl
SiO_2	%	FUS-ICP	66.44	76.3	59.34	53.31	62.42	49.27	68.24	58.15
Al_2O_3	%	FUS-ICP	15.54	9.70	14.42	12.49	12.89	17.92	12.60	16.08
Fe_2O_3	%	FUS-ICP	4.31	4.22	7.63	10.43	6.35	7.53	3.80	7.21
MnO	%	FUS-ICP	0.047	0.02	0.10	0.42	0.33	0.23	0.10	0.12
MgO	%	FUS-ICP	3.21	2.00	5.72	13.03	9.60	3.74	1.31	4.30
CaO	%	FUS-ICP	0.49	0.38	0.30	0.20	0.23	5.45	3.38	2.77
Na_2O	%	FUS-ICP	3.12	3.51	0.23	0.13	1.83	0.85	1.86	4.73
K_2O	%	FUS-ICP	3.09	0.65	2.74	0.15	0.14	2.96	3.67	1.52
TiO_2	%	FUS-ICP	0.54	0.29	0.59	0.27	0.34	0.85	0.36	0.64
P_2O_5	%	FUS-ICP	0.07	0.04	0.13	0.06	0.08	0.05	0.06	0.08
LOI	%	FUS-ICP	3.51	2.92	7.50	9.73	6.33	10.94	4.41	4.30
Total	%	FUS-ICP	100.40	100.00	98.72	100.20	100.50	99.78	99.79	99.9
Hg	ppb	CV-FIMS	7	11	135	14	< 5	6	363	5
Sc	ppm	FUS-ICP	18	8	12	5	7	33	10	26
Be	ppm	FUS-ICP	2	< 1	< 1	< 1	< 1	< 1	1	< 1
V	ppm	FUS-ICP	40	25	95	83	61	233	58	192
Cr	ppm	FUS-MS	30	20	< 20	< 20	< 20	80	< 20	30
Co	ppm	FUS-MS	4	3	10	10	6	23	6	20
Ni	ppm	FUS-MS	< 20	< 20	< 20	< 20	< 20	30	< 20	< 20
Cu	ppm	FUS-MS	< 10	< 10	190	30	< 10	30	< 10	20
Zn	ppm	FUS-MS	130	50	1520	390	130	120	90	110
Ga	ppm	FUS-MS	21	10	14	18	14	17	11	15
Ge	ppm	FUS-MS	1.70	1.60	0.50	0.60	0.80	1.20	0.50	< 0.5
As	ppm	FUS-MS	12	17	16	92	26	47	23	< 5
Rb	ppm	FUS-MS	58	12	48	3	3	65	59	22
Sr	ppm	FUS-ICP	38	24	15	5	11	46	59	65
Y	ppm	FUS-MS	64.90	17.50	20.70	20.70	13.20	13.60	21.70	21.80
Zr	ppm	FUS-ICP	183	76	94	95	90	51	100	76
Nb	ppm	FUS-MS	1.7	< 0.2	0.9	0.4	0.4	< 0.2	1.8	1.8
Mo	ppm	FUS-MS	< 2	5	< 2	10	< 2	< 2	< 2	< 2
Ag	ppm	FUS-MS	< 0.5	< 0.5	< 0.5	< 0.5	< 0.5	< 0.5	< 0.5	< 0.5
In	ppm	FUS-MS	0.1	< 0.1	< 0.1	< 0.1	< 0.1	< 0.1	< 0.1	< 0.1
Sn	ppm	FUS-MS	2	< 1	1	< 1	< 1	< 1	< 1	< 1
Sb	ppm	FUS-MS	0.90	1.10	2.60	0.60	0.50	0.90	1.70	< 0.2
Cs	ppm	FUS-MS	0.40	0.10	0.40	< 0.1	< 0.1	0.40	0.60	0.50
Ba	ppm	FUS-ICP	598	309	2188	74	38	159	1599	1161
La	ppm	FUS-MS	21.20	6.19	9.11	2.24	3.28	3.04	10.5	7.28
Ce	ppm	FUS-MS	51.20	15.4	22.6	5.87	8.84	8.38	22.5	15.7
Pr	ppm	FUS-MS	6.69	2.14	2.75	0.81	1.21	1.27	2.66	1.90
Nd	ppm	FUS-MS	30.60	10.10	12.20	3.94	5.74	6.48	10.9	8.63
Sm	ppm	FUS-MS	8.03	2.49	3.02	1.32	1.44	2.20	2.58	2.43
Eu	ppm	FUS-MS	2.63	0.81	0.70	0.14	0.13	0.60	0.74	0.69
Gd	ppm	FUS-MS	8.61	2.30	3.32	2.31	1.78	2.52	3.04	2.93
Tb	ppm	FUS-MS	1.62	0.37	0.59	0.47	0.32	0.44	0.53	0.53
Dy	ppm	FUS-MS	10.80	2.58	3.71	3.29	2.20	2.97	3.38	3.38
Ho	ppm	FUS-MS	2.26	0.59	0.78	0.74	0.49	0.61	0.74	0.72
Er	ppm	FUS-MS	6.76	2.06	2.42	2.34	1.54	1.80	2.28	2.35
Tm	ppm	FUS-MS	1.02	0.36	0.37	0.40	0.26	0.27	0.35	0.38
Yb	ppm	FUS-MS	6.89	2.64	2.58	2.61	1.91	1.84	2.6	2.64
Lu	ppm	FUS-MS	1.10	0.47	0.44	0.46	0.33	0.30	0.45	0.44
Hf	ppm	FUS-MS	4.10	1.60	2.00	2.00	1.90	1.20	2.60	2.10
Ta	ppm	FUS-MS	0.12	0.06	0.18	0.16	0.18	0.09	0.13	0.11
W	ppm	FUS-MS	0.60	1.10	< 0.5	< 0.5	< 0.5	< 0.5	1.00	< 0.5
Tl	ppm	FUS-MS	0.41	0.29	1.42	0.18	< 0.05	0.42	1.02	0.13
Pb	ppm	FUS-MS	7	7	724	160	8	26	42	17
Bi	ppm	FUS-MS	< 0.1	< 0.1	0.10	0.70	< 0.1	< 0.1	< 0.1	< 0.1
Th	ppm	FUS-MS	3.55	0.92	1.99	2.53	2.32	0.5	4.39	3.6
U	ppm	FUS-MS	1.20	0.96	2.03	1.17	1.42	0.21	1.27	1.00

Appendix B: Table B1.1: Whole-rock Lithogeochemistry Data

Sample ID			**32134**	**32136**	**32137**	**32145**	**32146**	**32147**	**32148**	**32152**
Hole ID			GA-10-272	GA-10-272	GA-10-272	GA-10-272	GA-10-272	GA-10-272	GA-10-272	GA-10-272
Depth (m)			119.6	134.7	142.3	255	262.2	280.4	292.5	237
Lithology			IN1	IN1	VCL4	VCL1 (D)	VCL1 (A-C)	VCL1 (A-C)	VCL1 (A-C)	VCL1 (D)
Alteration			unaltered	sil-carb	sil	ser-py	ser-chl-carb	ser-chl-carb	ser-py	carb-chl
SiO_2	%	FUS-ICP	51.78	49.44	63.17	70.51	53.81	39.71	62.58	22.69
Al_2O_3	%	FUS-ICP	16.5	16.31	16.14	11.96	14.34	12.51	14.84	13.45
Fe_2O_3	%	FUS-ICP	9.96	12.44	4.79	5.72	7.78	9.81	6.74	9.9
MnO	%	FUS-ICP	0.17	0.07	0.06	0.04	0.30	0.68	0.20	0.81
MgO	%	FUS-ICP	3.83	8.21	2.17	0.83	3.93	5.33	2.11	20.75
CaO	%	FUS-ICP	4.73	0.96	0.55	0.42	5.08	9.18	2.01	10.24
Na_2O	%	FUS-ICP	5.97	3.70	4.40	0.33	0.61	0.42	0.47	0.09
K_2O	%	FUS-ICP	0.12	0.41	2.60	3.04	2.41	2.73	3.32	0.62
TiO_2	%	FUS-ICP	0.91	1.63	0.75	0.50	0.61	0.56	0.65	0.50
P_2O_5	%	FUS-ICP	0.08	0.26	0.14	0.05	0.07	0.05	0.05	0.09
LOI	%	FUS-ICP	6.04	7.11	5.24	5.95	9.65	17.51	6.55	19.05
Total	%	FUS-ICP	100.10	100.50	100.00	99.35	98.59	98.49	99.52	98.21
Hg	ppb	CV-FIMS	< 5	< 5	< 5	2070	15	13	38	148
Sc	ppm	FUS-ICP	34	35	21	12	30	22	26	15
Be	ppm	FUS-ICP	< 1	< 1	< 1	< 1	< 1	< 1	< 1	< 1
V	ppm	FUS-ICP	299	204	83	93	191	157	189	99
Cr	ppm	FUS-MS	< 20	< 20	< 20	< 20	110	60	70	< 20
Co	ppm	FUS-MS	24	15	10	8	24	25	18	3
Ni	ppm	FUS-MS	< 20	< 20	< 20	< 20	30	20	< 20	< 20
Cu	ppm	FUS-MS	40	20	10	20	30	30	50	1070
Zn	ppm	FUS-MS	110	110	50	< 30	130	80	200	1440
Ga	ppm	FUS-MS	16	23	17	13	14	12	14	22
Ge	ppm	FUS-MS	0.7	0.8	< 0.5	< 0.5	0.7	< 0.5	< 0.5	0.7
As	ppm	FUS-MS	16	30	17	97	38	83	373	147
Rb	ppm	FUS-MS	1	6	40	66	54	60	74	11
Sr	ppm	FUS-ICP	161	46	46	21	45	44	28	77
Y	ppm	FUS-MS	21.40	54.80	28.50	15.60	20.20	12.30	15.20	12.30
Zr	ppm	FUS-ICP	52	125	104	70	40	33	40	77
Nb	ppm	FUS-MS	1.30	6.40	2.20	1.10	0.50	< 0.2	< 0.2	1.50
Mo	ppm	FUS-MS	< 2	< 2	< 2	9	< 2	6	< 2	< 2
Ag	ppm	FUS-MS	< 0.5	< 0.5	< 0.5	0.60	< 0.5	< 0.5	< 0.5	1.10
In	ppm	FUS-MS	< 0.1	< 0.1	< 0.1	< 0.1	< 0.1	< 0.1	< 0.1	0.2
Sn	ppm	FUS-MS	< 1	< 1	< 1	< 1	< 1	< 1	< 1	5
Sb	ppm	FUS-MS	< 0.2	< 0.2	< 0.2	18.40	0.40	2.00	2.60	68.00
Cs	ppm	FUS-MS	< 0.1	< 0.1	0.40	0.40	0.40	0.30	0.40	0.10
Ba	ppm	FUS-ICP	85	63	3176	640	244	187	249	588
La	ppm	FUS-MS	4.92	10.6	6.02	5.36	3.79	2.02	2.06	4.08
Ce	ppm	FUS-MS	11.70	26.40	15.30	12.00	8.83	5.29	5.60	8.44
Pr	ppm	FUS-MS	1.63	3.78	2.21	1.50	1.20	0.78	0.85	1.00
Nd	ppm	FUS-MS	7.26	18.70	10.70	6.17	5.89	4.13	4.46	4.82
Sm	ppm	FUS-MS	2.39	6.01	3.28	1.58	1.88	1.39	1.56	1.34
Eu	ppm	FUS-MS	0.75	1.9	0.779	0.229	0.665	0.469	0.421	0.442
Gd	ppm	FUS-MS	3.32	8.56	4.43	2.11	2.64	1.79	2.21	2.02
Tb	ppm	FUS-MS	0.57	1.51	0.79	0.39	0.48	0.32	0.41	0.35
Dy	ppm	FUS-MS	3.75	9.35	4.96	2.56	3.30	2.11	2.75	2.19
Ho	ppm	FUS-MS	0.78	1.95	1.01	0.54	0.71	0.47	0.58	0.44
Er	ppm	FUS-MS	2.37	5.78	3.08	1.81	2.15	1.47	1.73	1.33
Tm	ppm	FUS-MS	0.36	0.84	0.46	0.30	0.34	0.23	0.26	0.22
Yb	ppm	FUS-MS	2.39	5.34	2.99	2.06	2.24	1.62	1.73	1.49
Lu	ppm	FUS-MS	0.37	0.83	0.48	0.32	0.34	0.27	0.27	0.24
Hf	ppm	FUS-MS	1.50	3.50	2.60	1.70	1.10	1.10	1.10	2.20
Ta	ppm	FUS-MS	0.02	0.38	0.12	0.07	< 0.01	< 0.01	< 0.01	0.07
W	ppm	FUS-MS	< 0.5	2.30	0.90	3.10	< 0.5	0.70	1.20	4.70
Tl	ppm	FUS-MS	< 0.05	< 0.05	0.28	6.90	1.08	0.86	1.01	0.89
Pb	ppm	FUS-MS	9	< 5	5	106	23	94	201	2180
Bi	ppm	FUS-MS	< 0.1	< 0.1	< 0.1	1.1	< 0.1	< 0.1	< 0.1	0.8
Th	ppm	FUS-MS	1.04	1.41	2.31	1.88	1.04	0.37	0.43	1.67
U	ppm	FUS-MS	0.31	0.70	0.74	3.44	1.52	0.46	0.16	2.20

Appendix B: Table B1.1: Whole-rock Lithogeochemistry Data

Sample ID			**32154**	**14769**	**14770**	**14772**	**14774**	**14775**	**14776**	**14778**
Hole ID			GA-10-272	GA-14-275	GA-14-275	GA-14-275	GA-14-275	GA-14-275	GA-14-275	GA-14-275
Depth (m)			240.4	148.8	163.8	196.5	213.6	239.6	248.1	253.1
Lithology			VCL1 (D)	VCL2	IN2a	VCL2	VCL1 (A-C)	VCL1 (D)	IN1	VCL1 (A-C)
Alteration			chl-ser-pyr	ser-chl	unaltered	sil-ser	ser-sil-py	ser-sil-py	sil	ser-chl-py
SiO_2	%	FUS-ICP	44.83	66.06	51.85	77.8	72.83	64.34	59.92	51.98
Al_2O_3	%	FUS-ICP	14.6	14.93	16.56	10.58	11.92	12.28	14.95	15.78
Fe_2O_3	%	FUS-ICP	10.30	4.60	10.11	2.77	5.56	5.86	5.51	11.69
MnO	%	FUS-ICP	0.34	0.06	0.18	0.03	0.05	0.39	0.13	0.53
MgO	%	FUS-ICP	13.38	3.33	5.93	2.96	0.53	3.24	1.49	6.32
CaO	%	FUS-ICP	0.38	1.00	2.72	0.22	0.30	2.02	4.05	0.40
Na_2O	%	FUS-ICP	0.1	2.96	6.26	0.33	0.34	0.94	3.49	0.74
K_2O	%	FUS-ICP	1.16	2.71	0.58	2.28	3.16	2.03	1.39	1.78
TiO_2	%	FUS-ICP	0.61	0.68	0.86	0.25	0.54	0.41	1.00	0.64
P_2O_5	%	FUS-ICP	0.07	0.14	0.08	0.05	0.05	0.09	0.33	0.08
LOI	%	FUS-ICP	11.46	3.68	5.20	2.77	4.57	8.05	7.64	8.78
Total	%	FUS-ICP	97.24	100.20	100.30	100.00	99.86	99.63	99.9	98.71
Hg	ppb	CV-FIMS	1790	< 5	< 5	< 5	55	98	< 5	239
Sc	ppm	FUS-ICP	14	16	34	11	22	11	13	22
Be	ppm	FUS-ICP	< 1	1	< 1	1	< 1	< 1	1	< 1
V	ppm	FUS-ICP	105	28	301	11	162	70	61	183
Cr	ppm	FUS-MS	< 20	< 20	< 20	< 20	80	< 20	< 20	50
Co	ppm	FUS-MS	10	5	26	< 1	20	8	7	19
Ni	ppm	FUS-MS	< 20	< 20	< 20	< 20	20	< 20	< 20	< 20
Cu	ppm	FUS-MS	110	< 10	50	< 10	50	50	< 10	150
Zn	ppm	FUS-MS	6990	80	90	50	340	2200	70	5520
Ga	ppm	FUS-MS	19	17	16	14	12	11	17	16
Ge	ppm	FUS-MS	1	< 0.5	0.8	0.9	< 0.5	< 0.5	0.8	< 0.5
As	ppm	FUS-MS	187	< 5	< 5	< 5	114	59	7	67
Rb	ppm	FUS-MS	22	48	14	44	73	48	31	41
Sr	ppm	FUS-ICP	11	49	143	9	16	57	178	39
Y	ppm	FUS-MS	24.00	53.60	19.50	58.50	14.20	19.90	30.60	21.90
Zr	ppm	FUS-ICP	96	184	49	179	34	77	178	57
Nb	ppm	FUS-MS	2	2.6	0.9	1.3	< 0.2	1.2	3.8	0.5
Mo	ppm	FUS-MS	11	< 2	< 2	< 2	< 2	< 2	< 2	< 2
Ag	ppm	FUS-MS	1	< 0.5	< 0.5	< 0.5	< 0.5	< 0.5	< 0.5	< 0.5
In	ppm	FUS-MS	< 0.1	< 0.1	< 0.1	< 0.1	< 0.1	0.5	< 0.1	2.1
Sn	ppm	FUS-MS	10	< 1	< 1	1	< 1	< 1	< 1	1
Sb	ppm	FUS-MS	26.1	< 2	0.8	< 0.2	1.7	0.4	< 0.2	2.4
Cs	ppm	FUS-MS	0.20	< 3	1.00	0.30	0.40	0.40	0.30	0.30
Ba	ppm	FUS-ICP	997	< 4	237	214	469	259	381	217
La	ppm	FUS-MS	6.79	< 5	4.17	19	2.35	6.95	25.2	4.09
Ce	ppm	FUS-MS	16.50	< 6	10.20	45.50	5.96	15.50	51.80	11.00
Pr	ppm	FUS-MS	2.08	< 7	1.49	6.13	0.80	1.91	6.12	1.68
Nd	ppm	FUS-MS	8.97	< 8	7.25	28.1	4.11	8.38	24.6	7.81
Sm	ppm	FUS-MS	2.39	< 9	2.09	7.79	1.35	2.33	5.62	2.44
Eu	ppm	FUS-MS	0.27	< 10	0.76	2.02	0.21	0.33	1.57	0.32
Gd	ppm	FUS-MS	3.2	< 11	2.98	8.01	1.86	2.99	5.78	3.08
Tb	ppm	FUS-MS	0.60	< 12	0.52	1.48	0.35	0.52	0.96	0.58
Dy	ppm	FUS-MS	4.04	< 13	3.3	9.97	2.45	3.37	5.83	3.79
Ho	ppm	FUS-MS	0.88	< 14	0.72	2.13	0.53	0.72	1.12	0.80
Er	ppm	FUS-MS	2.62	< 15	2.19	6.56	1.56	2.13	3.25	2.42
Tm	ppm	FUS-MS	0.41	< 16	0.33	1.02	0.24	0.34	0.50	0.35
Yb	ppm	FUS-MS	2.89	< 17	2.19	6.93	1.70	2.31	3.36	2.36
Lu	ppm	FUS-MS	0.47	< 18	0.335	1.12	0.283	0.379	0.512	0.388
Hf	ppm	FUS-MS	2.50	< 19	1.30	4.50	0.90	1.90	4.50	1.70
Ta	ppm	FUS-MS	0.1	< 20	0.04	0.03	< 0.01	0.04	0.28	< 0.01
W	ppm	FUS-MS	5.10	< 21	< 0.5	< 0.5	1.90	1.20	7.10	1.20
Tl	ppm	FUS-MS	2.83	< 22	0.15	0.62	0.70	0.39	0.26	0.54
Pb	ppm	FUS-MS	4660	< 23	7	< 5	234	71	9	19
Bi	ppm	FUS-MS	< 0.1	< 24	< 0.1	< 0.1	< 0.1	< 0.1	< 0.1	0.10
Th	ppm	FUS-MS	2.13	< 25	0.74	4.07	0.43	1.87	6.57	0.92
U	ppm	FUS-MS	1.77	< 26	0.27	1.32	0.85	0.56	2.13	0.27

Appendix B: Table B1.1: Whole-rock Lithogeochemistry Data

Sample ID			**14781**	**14787**	**14797**	**14799**	**14800**	**32051**	**32053**	**32208**
Hole ID			GA-10-276	GA-10-276	GA-10-276	GA-10-276	GA-10-276	GA-10-276	GA-10-276	GA-07-257
Depth (m)			46.8	131.2	259.3	307.5	311.63	333	368.1	424.8
Lithology			CL1a	VCL4	VCL2	VCL2	VCL1 (D)	VCL1 (D)	VCL1 (A-C)	VCL2
Alteration			sil-chl	unaltered	ser-chl	chl-carb	sil-carb	ser-chl-pyr	sil-ser-pyr	ser-chl
SiO_2	%	FUS-ICP	75.12	69.80	64.94	27.32	25.42	40.5	43.96	64.61
Al_2O_3	%	FUS-ICP	12.87	13.81	16.3	17.41	11.87	16.03	14.09	15.51
Fe_2O_3	%	FUS-ICP	1.80	3.49	4.78	6.96	4.39	12.7	7.64	5.59
MnO	%	FUS-ICP	0.03	0.05	0.06	0.68	0.75	0.41	0.35	0.07
MgO	%	FUS-ICP	0.59	1.42	3.00	24.95	12.86	18.06	2.18	3.49
CaO	%	FUS-ICP	0.74	1.25	0.38	3.76	15.29	0.25	11.56	0.78
Na_2O	%	FUS-ICP	4.12	5.69	5.1	0.05	0.25	0.08	0.79	2.85
K_2O	%	FUS-ICP	2.7	1.16	1.91	0.03	2.43	0.07	2.61	2.29
TiO_2	%	FUS-ICP	0.29	0.39	0.60	0.80	0.46	0.32	0.55	0.66
P_2O_5	%	FUS-ICP	0.03	0.05	0.09	0.17	0.19	0.1	0.16	0.1
LOI	%	FUS-ICP	1.95	2.04	3.16	16.34	24.25	11.73	15.56	3.81
Total	%	FUS-ICP	100.3	99.15	100.30	98.48	98.16	100.30	99.44	99.76
Hg	ppb	CV-FIMS	< 5	< 5	9	12	23	54	47	7
Sc	ppm	FUS-ICP	7	12	19	21	11	9	22	21
Be	ppm	FUS-ICP	1	< 1	1	< 1	< 1	< 1	< 1	2
V	ppm	FUS-ICP	19	85	41	148	79	85	139	60
Cr	ppm	FUS-MS	< 20	30	< 20	< 20	< 20	< 20	40	< 20
Co	ppm	FUS-MS	2	6	3	7	5	14	26	5
Ni	ppm	FUS-MS	< 20	< 20	< 20	< 20	< 20	< 20	< 20	< 20
Cu	ppm	FUS-MS	< 10	20	< 10	< 10	< 10	630	80	< 10
Zn	ppm	FUS-MS	< 30	40	120	200	200	470	770	130
Ga	ppm	FUS-MS	11	12	19	19	13	24	13	20
Ge	ppm	FUS-MS	0.60	< 0.5	< 0.5	< 0.5	< 0.5	< 0.5	< 0.5	0.80
As	ppm	FUS-MS	6	< 5	8	20	19	105	438	10
Rb	ppm	FUS-MS	32	12	32	< 1	45	1	56	46
Sr	ppm	FUS-ICP	35	61	51	49	138	4	58	32
Y	ppm	FUS-MS	24.00	19.70	55.60	13.80	24.00	15.90	21.70	68.80
Zr	ppm	FUS-ICP	122	84	184	107	76	91	41	193
Nb	ppm	FUS-MS	2.30	1.50	1.90	2.50	1.80	1.30	0.50	1.70
Mo	ppm	FUS-MS	< 2	< 2	< 2	3.00	6.00	< 2	< 2	< 2
Ag	ppm	FUS-MS	< 0.5	< 0.5	< 0.5	< 0.5	< 0.5	2.60	< 0.5	< 0.5
In	ppm	FUS-MS	< 0.1	< 0.1	0.10	< 0.1	< 0.1	0.40	0.10	< 0.1
Sn	ppm	FUS-MS	1	< 1	1	1	5	2	< 1	< 1
Sb	ppm	FUS-MS	< 0.2	< 0.2	< 0.2	< 0.2	< 0.2	0.40	1.90	< 0.2
Cs	ppm	FUS-MS	0.20	0.40	0.20	< 0.1	0.30	< 0.1	0.40	0.30
Ba	ppm	FUS-ICP	1315	1130	488	66	4466	76	163	185
La	ppm	FUS-MS	15.10	13.50	18.30	4.98	4.80	1.26	4.26	18.70
Ce	ppm	FUS-MS	30.20	26.60	44.60	14.50	13.30	3.28	10.30	46.30
Pr	ppm	FUS-MS	3.32	2.79	6.07	1.94	1.98	0.46	1.37	6.21
Nd	ppm	FUS-MS	11.80	11.10	28.40	8.46	9.74	2.67	6.59	28.30
Sm	ppm	FUS-MS	2.68	2.45	7.36	2.21	3.33	0.95	2.03	7.79
Eu	ppm	FUS-MS	0.54	0.68	2.67	0.42	0.74	0.13	0.65	2.45
Gd	ppm	FUS-MS	2.65	2.75	8.79	2.58	4.19	1.73	2.91	9.58
Tb	ppm	FUS-MS	0.52	0.49	1.46	0.40	0.70	0.34	0.51	1.79
Dy	ppm	FUS-MS	3.73	3.25	9.50	2.43	4.22	2.29	3.50	11.50
Ho	ppm	FUS-MS	0.82	0.73	2.00	0.53	0.85	0.50	0.77	2.42
Er	ppm	FUS-MS	2.61	2.24	5.99	1.64	2.51	1.66	2.36	7.18
Tm	ppm	FUS-MS	0.46	0.34	0.90	0.27	0.39	0.27	0.38	1.12
Yb	ppm	FUS-MS	3.26	2.48	6.18	2.06	2.54	2.05	2.45	7.27
Lu	ppm	FUS-MS	0.51	0.37	0.97	0.35	0.39	0.35	0.38	1.11
Hf	ppm	FUS-MS	3.00	2.20	4.70	2.80	2.00	2.40	1.20	4.90
Ta	ppm	FUS-MS	0.17	0.08	0.06	0.14	0.10	0.09	< 0.01	0.03
W	ppm	FUS-MS	0.60	< 0.5	< 0.5	1.60	1.10	0.70	< 0.5	< 0.5
Tl	ppm	FUS-MS	0.18	< 0.05	0.15	0.11	1.94	0.14	0.52	0.52
Pb	ppm	FUS-MS	5	< 5	< 5	19	17	87	111	< 5
Bi	ppm	FUS-MS	< 0.1	< 0.1	< 0.1	0.30	0.40	1.00	< 0.1	< 0.1
Th	ppm	FUS-MS	7.37	5.17	4.01	2.17	1.93	2.52	0.95	4.30
U	ppm	FUS-MS	1.97	1.46	1.34	0.57	0.72	1.73	1.20	1.33

Appendix B: Table B1.1: Whole-rock Lithogeochemistry Data

Sample ID			**32212**	**32214**	**32216**	**32217**	**32218**	**32219**	**32220**	**32076**
Hole ID			GA-07-257	GA-10-273	GA-10-273	GA-10-273	GA-10-273	GA-10-273	GA-10-273	GA-10-274
Depth (m)			482.9	248.2	281.7	297.6	304.8	267.8	273	270.9
Lithology			VCL1	IN2a	VCL1	IN2a	VCL1 (A-C)	VCL1 (A-C)	VCL1 (A-C)	VCL2
Alteration			ser-chl-pyr	carb	ser-carb-pyr	ser	ser-sil-pyr	ser-chl-pyr	ser-chl-pyr	chl-ser
SiO_2	%	FUS-ICP	46.35	49.13	51.3	63.03	55.58	49.67	24.88	35.9
Al_2O_3	%	FUS-ICP	6.45	16.36	9.82	13.42	14.82	11.71	15.40	17.98
Fe_2O_3	%	FUS-ICP	9.91	12.94	6.40	5.95	5.42	14.42	21.74	10.72
MnO	%	FUS-ICP	0.32	0.15	0.32	0.12	0.45	0.18	0.52	0.38
MgO	%	FUS-ICP	5.93	7.36	4.88	3.56	3.36	7.31	18.7	19.53
CaO	%	FUS-ICP	1.68	1.86	7.60	3.38	5.41	0.35	1.63	1.62
Na_2O	%	FUS-ICP	0.41	5.54	0.40	1.15	0.57	0.13	0.01	0.06
K_2O	%	FUS-ICP	0.38	0.05	2.26	1.50	3.23	1.61	0.03	0.48
TiO_2	%	FUS-ICP	0.13	1.017	0.429	0.755	0.613	0.488	0.493	0.821
P_2O_5	%	FUS-ICP	< 0.01	0.08	0.12	0.17	0.14	0.05	0.10	0.20
LOI	%	FUS-ICP	10.57	5.25	15.21	7.02	10.76	10.47	16.65	11.54
Total	%	FUS-ICP	82.11	99.74	98.74	100.10	100.40	96.37	100.20	99.24
Hg	ppb	CV-FIMS	7250	< 5	313	< 5	10	5010	133	16
Sc	ppm	FUS-ICP	3	43	10	21	25	11	11	19
Be	ppm	FUS-ICP	< 1	< 1	< 1	< 1	< 1	< 1	< 1	< 1
V	ppm	FUS-ICP	33	444	79	52	169	133	118	148
Cr	ppm	FUS-MS	80	< 20	< 20	< 20	30	< 20	< 20	< 20
Co	ppm	FUS-MS	29	35	7	6	13	13	25	11
Ni	ppm	FUS-MS	30	< 20	< 20	< 20	< 20	< 20	< 20	< 20
Cu	ppm	FUS-MS	> 10000	50	10	< 10	30	930	60	10
Zn	ppm	FUS-MS	> 10000	90	90	110	70	> 10000	450	420
Ga	ppm	FUS-MS	10	16	11	14	13	16	23	24
Ge	ppm	FUS-MS	0.50	1.00	< 0.5	0.80	< 0.5	0.60	0.90	1.00
As	ppm	FUS-MS	92	< 5	43	< 5	144	335	193	58
Rb	ppm	FUS-MS	9	< 1	48	32	69	29	1	10
Sr	ppm	FUS-ICP	19	76	49	64	40	9	10	17
Y	ppm	FUS-MS	5.40	17.50	12.90	29.80	17.70	24.70	23.60	19.70
Zr	ppm	FUS-ICP	18	37	65	90	41	25	35	125
Nb	ppm	FUS-MS	< 0.2	0.70	0.90	2.10	0.40	< 0.2	< 0.2	3.50
Mo	ppm	FUS-MS	7	< 2	2	< 2	< 2	24	15	2
Ag	ppm	FUS-MS	42.9	< 0.5	< 0.5	< 0.5	< 0.5	7.50	2.20	< 0.5
In	ppm	FUS-MS	11.9	< 0.1	< 0.1	< 0.1	< 0.1	0.40	< 0.1	< 0.1
Sn	ppm	FUS-MS	25	< 1	< 1	< 1	< 1	10	1	3
Sb	ppm	FUS-MS	26	1.30	2.40	< 0.2	0.90	12.20	3.70	0.70
Cs	ppm	FUS-MS	0.10	< 0.1	0.30	0.20	0.40	0.20	< 0.1	< 0.1
Ba	ppm	FUS-ICP	75	39	392	477	268	833	10	293
La	ppm	FUS-MS	0.95	3.14	2.37	8.76	3.50	4.34	3.32	5.08
Ce	ppm	FUS-MS	2.40	7.82	6.89	20.4	7.74	10.80	11.20	12.5
Pr	ppm	FUS-MS	0.32	1.13	0.94	2.68	1.06	1.56	1.67	1.73
Nd	ppm	FUS-MS	1.60	6.07	4.68	12.7	5.14	7.44	7.77	8.15
Sm	ppm	FUS-MS	0.58	1.91	1.49	3.69	1.77	2.42	2.46	2.29
Eu	ppm	FUS-MS	0.09	0.74	0.26	1.28	0.61	0.29	0.31	0.23
Gd	ppm	FUS-MS	0.49	2.74	1.82	4.68	2.38	3.25	2.83	2.76
Tb	ppm	FUS-MS	0.10	0.48	0.33	0.81	0.44	0.66	0.54	0.49
Dy	ppm	FUS-MS	0.78	3.02	2.24	5.20	3.02	4.33	3.85	3.24
Ho	ppm	FUS-MS	0.19	0.64	0.47	1.07	0.64	0.92	0.82	0.73
Er	ppm	FUS-MS	0.65	1.96	1.48	3.21	1.91	2.55	2.54	2.35
Tm	ppm	FUS-MS	0.11	0.30	0.25	0.52	0.30	0.38	0.43	0.40
Yb	ppm	FUS-MS	0.80	2.04	1.83	3.53	2.08	2.42	2.84	2.75
Lu	ppm	FUS-MS	0.14	0.31	0.29	0.56	0.32	0.36	0.44	0.44
Hf	ppm	FUS-MS	< 0.1	1.00	1.60	2.20	1.10	< 0.1	0.60	3.30
Ta	ppm	FUS-MS	< 0.01	< 0.01	< 0.01	0.08	< 0.01	< 0.01	0.01	0.36
W	ppm	FUS-MS	10.9	< 0.5	1.80	0.80	< 0.5	15.00	5.50	3.00
Tl	ppm	FUS-MS	0.47	< 0.05	1.54	0.43	0.83	1.62	0.14	0.67
Pb	ppm	FUS-MS	> 10000	< 5	37	7	52	9300	248	225
Bi	ppm	FUS-MS	94.80	< 0.1	1.20	< 0.1	< 0.1	9.60	6.10	1.30
Th	ppm	FUS-MS	1.13	0.59	1.51	2.11	1.08	1.48	1.74	2.79
U	ppm	FUS-MS	0.66	0.16	1.98	0.62	0.52	6.76	2.5	1.22

Appendix B: Table B1.1: Whole-rock Lithogeochemistry Data

Sample ID			**32079**	**32080**	**32157**	**32162**	**32174**	**32175**	**32177**	**32178**
Hole ID			GA-10-274	GA-10-274	GA-10-277	GA-10-277	GA-10-277	GA-10-278	GA-10-278	GA-10-278
Depth (m)			307.2	319.4	45.8	81.5	243.2	18.5	42.9	60.9
Lithology			VCL1 (D)	VCL1 (A-C)	VCL4	CL1a	VCL1 (D)	CL1a	CL1a	CL1b
Alteration			ser-carb-pyr	ser-carb-pyr	sil-ser	sil-chl	ser-sil-pyr	sil-ser-pyr	sil-pyr	sil
SiO_2	%	FUS-ICP	44.87	45.07	77.81	67.00	67.30	61.89	67.16	83.72
Al_2O_3	%	FUS-ICP	12.85	11.62	10.38	12.78	14.73	13.70	13.27	9.62
Fe_2O_3	%	FUS-ICP	5.71	8.83	1.62	2.47	4.07	4.14	5.99	0.71
MnO	%	FUS-ICP	0.25	0.64	0.05	0.07	0.05	0.12	0.04	0.01
MgO	%	FUS-ICP	6.41	3.89	0.68	0.94	0.90	2.13	4.50	0.07
CaO	%	FUS-ICP	9.19	10.08	0.92	4.53	1.26	3.69	0.30	0.13
Na_2O	%	FUS-ICP	0.60	0.69	3.49	5.21	0.62	4.59	3.39	5.03
K_2O	%	FUS-ICP	3.11	2.67	1.73	2.06	4.22	1.93	1.2	0.27
TiO_2	%	FUS-ICP	0.58	0.52	0.24	0.36	0.62	0.53	0.53	0.23
P_2O_5	%	FUS-ICP	0.11	0.06	0.04	0.05	0.15	0.07	0.06	0.04
LOI	%	FUS-ICP	15.26	15.54	2.30	4.40	5.07	7.05	3.54	0.22
Total	%	FUS-ICP	98.95	99.6	99.26	99.87	98.99	99.86	99.98	100.00
Hg	ppb	CV-FIMS	24	48	< 5	< 5	15	6	6	2.5
Sc	ppm	FUS-ICP	15	21	6	12	15	22	22	3
Be	ppm	FUS-ICP	< 1	< 1	< 1	< 1	1	0.50	0.50	0.50
V	ppm	FUS-ICP	116	149	19	75	106	159	164	15
Cr	ppm	FUS-MS	< 20	50	< 20	20	< 20	30	40	50
Co	ppm	FUS-MS	11	16	2	6	10	10	18	2
Ni	ppm	FUS-MS	< 20	< 20	< 20	< 20	< 20	10	10	10
Cu	ppm	FUS-MS	10	10	< 10	20	< 10	30	5	5
Zn	ppm	FUS-MS	50	70	< 30	< 30	70	30	90	15
Ga	ppm	FUS-MS	14	12	9	11	15	12	13	5
Ge	ppm	FUS-MS	< 0.5	< 0.5	< 0.5	< 0.5	0.5	0.25	0.25	0.25
As	ppm	FUS-MS	23	59	7	< 5	88	8	29	2.5
Rb	ppm	FUS-MS	67	56	21	26	86	20	15	3
Sr	ppm	FUS-ICP	70	49	37	80	31	69	28	27
Y	ppm	FUS-MS	21.90	16.00	22.00	22.70	27.50	17.00	10.70	15.30
Zr	ppm	FUS-ICP	86	37	123	100	104	63	59	88
Nb	ppm	FUS-MS	2.30	0.50	2.40	1.80	2.20	0.80	0.60	1.30
Mo	ppm	FUS-MS	< 2	< 2	7	< 2	< 2	1	1	3
Ag	ppm	FUS-MS	< 0.5	< 0.5	< 0.5	< 0.5	< 0.5	0.25	0.25	0.25
In	ppm	FUS-MS	< 0.1	< 0.1	< 0.1	< 0.1	< 0.1	0.05	0.05	0.05
Sn	ppm	FUS-MS	< 1	< 1	< 1	< 1	< 1	0.5	0.5	0.5
Sb	ppm	FUS-MS	1.10	0.60	< 0.2	< 0.2	1.10	0.10	0.10	0.10
Cs	ppm	FUS-MS	0.50	0.40	0.20	0.50	0.60	0.20	0.10	0.05
Ba	ppm	FUS-ICP	392	155	441	880	631	299	227	173
La	ppm	FUS-MS	7.01	2.71	16.00	12.40	9.85	7.22	4.70	7.44
Ce	ppm	FUS-MS	16.00	6.65	31.60	25.50	21.00	15.80	9.12	15.80
Pr	ppm	FUS-MS	2.08	1.02	3.50	2.80	2.70	1.89	1.00	1.75
Nd	ppm	FUS-MS	9.59	5.45	13.40	11.20	12.20	7.78	4.32	6.66
Sm	ppm	FUS-MS	2.81	1.91	2.98	2.66	3.19	2.10	1.10	1.69
Eu	ppm	FUS-MS	0.56	0.66	0.51	0.67	0.40	0.70	0.32	0.35
Gd	ppm	FUS-MS	3.46	2.52	2.99	3.01	3.82	2.52	1.33	1.84
Tb	ppm	FUS-MS	0.58	0.44	0.52	0.55	0.68	0.43	0.27	0.34
Dy	ppm	FUS-MS	3.67	2.80	3.32	3.65	4.40	2.72	1.89	2.41
Ho	ppm	FUS-MS	0.79	0.59	0.76	0.80	0.92	0.58	0.39	0.56
Er	ppm	FUS-MS	2.37	1.79	2.54	2.41	2.88	1.85	1.19	1.73
Tm	ppm	FUS-MS	0.37	0.27	0.42	0.39	0.47	0.29	0.20	0.29
Yb	ppm	FUS-MS	2.66	1.80	3.08	2.74	3.07	1.98	1.53	2.04
Lu	ppm	FUS-MS	0.42	0.28	0.52	0.43	0.48	0.31	0.26	0.34
Hf	ppm	FUS-MS	2.20	1.00	2.90	2.50	2.60	1.50	1.40	2.40
Ta	ppm	FUS-MS	0.21	0.06	0.27	0.19	0.17	0.02	0.005	0.03
W	ppm	FUS-MS	2	2.8	4.5	< 0.5	2	0.25	0.25	0.9
Tl	ppm	FUS-MS	0.97	0.67	0.14	0.14	1.45	0.10	0.06	0.03
Pb	ppm	FUS-MS	18	21	15	< 5	15	9	12	2.50
Bi	ppm	FUS-MS	< 0.1	< 0.1	< 0.1	< 0.1	< 0.1	0.05	0.05	0.05
Th	ppm	FUS-MS	1.88	0.38	6.56	4.90	2.41	3.14	3.07	5.20
U	ppm	FUS-MS	0.95	0.27	2.11	1.34	2.90	1.01	0.79	1.30

Appendix B: Table B1.1: Whole-rock Lithogeochemistry Data

Sample ID			32180	32182	32185	32187	32189	32192	32193	32196
Hole ID			GA-10-278	GA-10-278	GA-10-278	GA-10-278	GA-10-278	GA-10-278	GA-10-278	GA-10-278
Depth (m)			84	111.4	138.3	163.5	183.7	215.3	234.4	280.1
Lithology			VCL4	VCL4	VCL3	VCL3	VCL2	VCL2	VCL2	VCL2
Alteration			ser-chl	chl	sil	sil-chl	ser	ser-chl	chl	chl-ser
SiO_2	%	FUS-ICP	67.03	54.53	71.76	53.48	65.96	63.93	51.01	68.41
Al_2O_3	%	FUS-ICP	13.33	14.80	11.62	19.50	15.08	14.82	17.32	13.38
Fe_2O_3	%	FUS-ICP	4.03	8.45	2.14	7.73	4.17	5.47	11.35	5.32
MnO	%	FUS-ICP	0.05	0.14	0.09	0.09	0.05	0.04	0.12	0.07
MgO	%	FUS-ICP	1.98	6.07	0.85	3.69	3.38	5.99	7.14	3.22
CaO	%	FUS-ICP	2.45	3.8	3.48	2.01	1.71	0.34	1.76	0.63
Na_2O	%	FUS-ICP	4.8	3.65	5.56	5.58	1.49	2.05	5.91	4.19
K_2O	%	FUS-ICP	1.40	0.90	0.37	2.02	3.36	2.23	0.42	1.30
TiO_2	%	FUS-ICP	0.36	0.64	0.24	0.97	0.51	0.70	0.91	0.58
P_2O_5	%	FUS-ICP	0.05	0.07	0.04	0.13	0.08	0.13	0.09	0.09
LOI	%	FUS-ICP	3.99	5.96	3.84	4.45	4.87	3.89	4.68	3.14
Total	%	FUS-ICP	99.47	99.01	100.00	99.65	100.70	99.6	100.70	100.30
Hg	ppb	CV-FIMS	< 5	< 5	< 5	< 5	< 5	< 5	< 5	6
Sc	ppm	FUS-ICP	12	29	10	24	15	17	36	18
Be	ppm	FUS-ICP	< 1	< 1	< 1	< 1	2	2	< 1	1
V	ppm	FUS-ICP	91	238	13	244	27	40	336	68
Cr	ppm	FUS-MS	20	40	20	20	< 20	< 20	< 20	< 20
Co	ppm	FUS-MS	13	25	2	17	2	7	27	7
Ni	ppm	FUS-MS	< 20	< 20	< 20	< 20	< 20	< 20	< 20	< 20
Cu	ppm	FUS-MS	20	40	10	40	40	< 10	50	20
Zn	ppm	FUS-MS	50	70	40	80	60	70	100	150
Ga	ppm	FUS-MS	13	15	9	21	17	17	17	16
Ge	ppm	FUS-MS	< 0.5	< 0.5	< 0.5	1	0.7	0.5	0.6	0.7
As	ppm	FUS-MS	15	< 5	< 5	13	9	< 5	< 5	237
Rb	ppm	FUS-MS	18	10	5	28	51	42	11	26
Sr	ppm	FUS-ICP	41	75	82	67	35	25	105	41
Y	ppm	FUS-MS	19.30	15.40	41.80	26.80	55.80	61.10	18.20	48.90
Zr	ppm	FUS-ICP	97	57	129	83	188	188	45	142
Nb	ppm	FUS-MS	3.40	2.30	3.50	3.00	4.30	3.80	1.30	2.00
Mo	ppm	FUS-MS	< 2	< 2	< 2	< 2	< 2	< 2	< 2	< 2
Ag	ppm	FUS-MS	< 0.5	< 0.5	< 0.5	< 0.5	< 0.5	< 0.5	< 0.5	< 0.5
In	ppm	FUS-MS	< 0.1	< 0.1	< 0.1	< 0.1	< 0.1	< 0.1	< 0.1	< 0.1
Sn	ppm	FUS-MS	< 1	< 1	< 1	< 1	1	< 1	< 1	< 1
Sb	ppm	FUS-MS	0.60	< 0.2	< 0.2	< 0.2	< 0.2	< 0.2	0.50	0.50
Cs	ppm	FUS-MS	0.20	0.20	< 0.1	0.30	0.40	0.30	0.60	0.30
Ba	ppm	FUS-ICP	241	287	65	354	2200	546	102	293
La	ppm	FUS-MS	10.90	5.31	13.50	3.67	17.10	19.40	4.12	13.20
Ce	ppm	FUS-MS	22.80	12.00	29.80	9.30	40.20	46.00	9.96	34.80
Pr	ppm	FUS-MS	2.55	1.51	3.54	1.33	5.05	5.99	1.40	4.79
Nd	ppm	FUS-MS	9.68	6.47	14.80	6.66	23.00	27.20	7.20	22.00
Sm	ppm	FUS-MS	2.52	1.92	4.24	2.49	6.37	7.53	2.21	6.71
Eu	ppm	FUS-MS	0.68	0.71	1.02	0.77	1.26	2.10	0.79	2.45
Gd	ppm	FUS-MS	2.77	2.38	5.28	3.78	7.63	9.23	2.76	8.32
Tb	ppm	FUS-MS	0.48	0.41	0.99	0.71	1.38	1.66	0.48	1.37
Dy	ppm	FUS-MS	3.14	2.54	6.82	4.61	9.24	10.6	3.05	8.24
Ho	ppm	FUS-MS	0.69	0.55	1.48	1.02	1.92	2.27	0.64	1.72
Er	ppm	FUS-MS	2.15	1.73	4.51	2.89	5.81	6.59	1.95	5.04
Tm	ppm	FUS-MS	0.34	0.26	0.71	0.43	0.94	0.99	0.30	0.75
Yb	ppm	FUS-MS	2.37	1.79	5.05	2.81	6.29	6.52	1.94	5.08
Lu	ppm	FUS-MS	0.39	0.31	0.78	0.46	1.01	0.98	0.29	0.81
Hf	ppm	FUS-MS	2.60	1.60	3.60	2.30	5.20	4.90	1.20	3.60
Ta	ppm	FUS-MS	0.32	0.24	0.37	0.23	0.34	0.30	0.12	0.15
W	ppm	FUS-MS	0.5	0.8	< 0.5	< 0.5	< 0.5	< 0.5	0.5	< 0.5
Tl	ppm	FUS-MS	0.11	< 0.05	< 0.05	0.18	0.39	0.23	0.1	0.37
Pb	ppm	FUS-MS	15	< 5	< 5	< 5	< 5	< 5	< 5	17
Bi	ppm	FUS-MS	< 0.1	< 0.1	< 0.1	< 0.1	< 0.1	< 0.1	< 0.1	0.2
Th	ppm	FUS-MS	4.94	2.32	7.28	1.50	5.97	4.62	0.7	2.95
U	ppm	FUS-MS	2.35	0.70	2.10	0.79	1.95	1.70	0.22	1.03

Appendix B: Table B1.1: Whole-rock Lithogeochemistry Data

Sample ID			**32199**	**32200**	**32202**	**32203**	**32087**	**32088**	**32091**	**32098**
Hole ID			GA-10-278	GA-10-278	GA-10-278	GA-10-278	GA-06-180	GA-06-180	GA-06-180	GA-06-180
Depth (m)			306.7	309.3	328.2	332.6	111.2	123.7	187.4	261.1
Lithology			VCL1 (D)	VCL1 (D)	VCL1 (D)	VCL1 (D)	VCL4	CL1b	VCL4	VCL3
Alteration			ser-chl-pyr	chl-carb-bm	chl-carb	ser-sil-pyr	sil-chl	sil	sil	unaltered
SiO_2	%	FUS-ICP	40.33	31.90	25.14	65.01	56.49	74.52	46.07	66.34
Al_2O_3	%	FUS-ICP	14.48	16.15	17.37	11.56	13.33	10.85	15.54	14.85
Fe_2O_3	%	FUS-ICP	12.56	12.31	11.87	6.48	4.89	2.06	8.52	4.67
MnO	%	FUS-ICP	0.37	0.41	0.54	0.15	0.15	0.07	0.19	0.06
MgO	%	FUS-ICP	13.27	18.60	19.75	6.26	2.81	0.93	5.03	4.06
CaO	%	FUS-ICP	2.66	3.05	5.72	1.03	5.43	1.96	6.65	0.54
Na_2O	%	FUS-ICP	0.48	0.63	0.71	0.32	4.47	4.33	3.21	4.46
K_2O	%	FUS-ICP	1.16	0.53	0.45	1.52	2.41	1.49	2.92	1.55
TiO_2	%	FUS-ICP	0.58	0.75	0.75	0.33	0.52	0.27	0.66	0.50
P_2O_5	%	FUS-ICP	0.11	0.12	0.12	0.05	0.06	0.03	0.07	0.07
LOI	%	FUS-ICP	12.53	14.14	16.18	6.63	9.13	3.46	10.68	3.20
Total	%	FUS-ICP	98.52	98.6	98.58	99.34	99.69	99.98	99.56	100.30
Hg	ppb	CV-FIMS	69	454	108	< 5	< 5	< 5	< 5	5
Sc	ppm	FUS-ICP	14	17	17	8	22	8	31	19
Be	ppm	FUS-ICP	< 1	< 1	< 1	< 1	< 1	< 1	< 1	2
V	ppm	FUS-ICP	118	142	166	68	163	29	234	43
Cr	ppm	FUS-MS	< 20	< 20	< 20	< 20	30	< 20	40	< 20
Co	ppm	FUS-MS	14	20	15	6	15	3	22	4
Ni	ppm	FUS-MS	< 20	< 20	< 20	< 20	< 20	< 20	< 20	< 20
Cu	ppm	FUS-MS	20	30	10	< 10	40	< 10	40	< 10
Zn	ppm	FUS-MS	150	3580	380	130	80	< 30	100	110
Ga	ppm	FUS-MS	18	21	20	13	13	11	15	19
Ge	ppm	FUS-MS	0.7	< 0.5	0.5	< 0.5	< 0.5	< 0.5	< 0.5	< 0.5
As	ppm	FUS-MS	76	55	34	25	8	< 5	9	< 5
Rb	ppm	FUS-MS	24	11	10	32	25	18	32	25
Sr	ppm	FUS-ICP	34	35	59	19	97	38	100	44
Y	ppm	FUS-MS	18.80	16.90	29.70	14.90	20.30	25.10	20.60	60.10
Zr	ppm	FUS-ICP	104	106	109	77	76	117	67	230
Nb	ppm	FUS-MS	2.60	3.10	3.10	1.30	1.40	2.20	1.30	2.50
Mo	ppm	FUS-MS	14	12	2	< 2	< 2	4	< 2	< 2
Ag	ppm	FUS-MS	< 0.5	0.6	< 0.5	< 0.5	< 0.5	< 0.5	< 0.5	< 0.5
In	ppm	FUS-MS	< 0.1	0.3	< 0.1	< 0.1	< 0.1	< 0.1	< 0.1	< 0.1
Sn	ppm	FUS-MS	2	2	2	1	< 1	< 1	< 1	1
Sb	ppm	FUS-MS	1.50	4.20	0.90	< 0.2	< 0.2	< 0.2	< 0.2	< 0.2
Cs	ppm	FUS-MS	0.20	0.10	< 0.1	0.20	0.30	0.20	0.30	0.20
Ba	ppm	FUS-ICP	1214	383	94	278	1040	253	504	946
La	ppm	FUS-MS	4.77	3.9	8.05	4.85	7.29	15.5	7.19	19.90
Ce	ppm	FUS-MS	12.70	11.50	23.30	11.00	15.80	31.30	15.90	48.20
Pr	ppm	FUS-MS	1.64	1.65	3.49	1.42	1.91	3.51	2.00	6.36
Nd	ppm	FUS-MS	7.62	8.12	15.20	6.26	8.25	13.6	9.32	28.2
Sm	ppm	FUS-MS	2.25	2.01	4.06	1.72	2.42	3.26	2.73	7.99
Eu	ppm	FUS-MS	0.27	0.25	0.67	0.22	0.83	0.85	0.83	1.74
Gd	ppm	FUS-MS	2.68	2.5	4.55	2.05	2.99	3.75	3.43	9.32
Tb	ppm	FUS-MS	0.49	0.45	0.77	0.36	0.52	0.65	0.57	1.57
Dy	ppm	FUS-MS	3.3	2.85	4.76	2.32	3.34	4.06	3.56	10.3
Ho	ppm	FUS-MS	0.72	0.62	1.00	0.51	0.69	0.87	0.76	2.13
Er	ppm	FUS-MS	2.25	1.96	3.07	1.61	2.08	2.86	2.23	6.36
Tm	ppm	FUS-MS	0.35	0.32	0.48	0.25	0.32	0.47	0.34	1.00
Yb	ppm	FUS-MS	2.53	2.38	3.36	1.73	2.22	3.25	2.32	6.95
Lu	ppm	FUS-MS	0.42	0.40	0.54	0.28	0.36	0.51	0.38	1.06
Hf	ppm	FUS-MS	2.70	2.90	2.80	1.90	2.00	3.00	1.70	5.40
Ta	ppm	FUS-MS	0.27	0.32	0.29	0.21	0.14	0.22	0.09	0.15
W	ppm	FUS-MS	4.70	3.50	2.50	2.00	< 0.5	< 0.5	< 0.5	< 0.5
Tl	ppm	FUS-MS	1.58	1.08	0.65	0.65	0.20	0.06	0.11	0.15
Pb	ppm	FUS-MS	70	2340	128	29	< 5	< 5	22	13
Bi	ppm	FUS-MS	1.80	0.30	1.00	0.30	< 0.1	< 0.1	< 0.1	< 0.1
Th	ppm	FUS-MS	2.11	2.36	2.35	1.95	3.34	6.46	2.57	5.06
U	ppm	FUS-MS	5.17	6.34	1.49	0.77	0.96	2.27	0.75	1.65

Appendix B: Table B1.1: Whole-rock Lithogeochemistry Data

Sample ID			**32101**	**32102**	**32103**	**32108**
Hole ID			GA-06-180	GA-06-180	GA-06-180	GA-06-180
Depth (m)			321.68	327.2	338.4	397.9
Lithology			VCL3	VCL1 (D)	VCL1 (D)	VCL1 (D)
Alteration			ser-chl	ser-sil-pyr	ser-sil-pyr	sil-ser-pyr
SiO_2	%	FUS-ICP	66.07	49.92	49.13	35.56
Al_2O_3	%	FUS-ICP	14.77	11.25	12.01	4.28
Fe_2O_3	%	FUS-ICP	4.81	15.52	13.48	7.49
MnO	%	FUS-ICP	0.09	0.13	0.13	0.97
MgO	%	FUS-ICP	2.84	6.87	7.11	9.46
CaO	%	FUS-ICP	1.31	0.31	0.22	16.70
Na_2O	%	FUS-ICP	3.72	3.09	0.20	0.20
K_2O	%	FUS-ICP	2.24	0.16	2.12	1.01
TiO_2	%	FUS-ICP	0.58	0.57	0.53	0.18
P_2O_5	%	FUS-ICP	0.10	0.11	0.10	0.08
LOI	%	FUS-ICP	3.94	10.36	10.79	22.34
Total	%	FUS-ICP	100.50	98.28	95.82	98.27
Hg	ppb	CV-FIMS	10	443	1850	160
Sc	ppm	FUS-ICP	19	14	11	5
Be	ppm	FUS-ICP	2	< 1	< 1	< 1
V	ppm	FUS-ICP	59	108	99	41
Cr	ppm	FUS-MS	< 20	< 20	< 20	< 20
Co	ppm	FUS-MS	4	13	9	8
Ni	ppm	FUS-MS	< 20	< 20	< 20	< 20
Cu	ppm	FUS-MS	< 10	30	700	30
Zn	ppm	FUS-MS	160	1840	> 10000	740
Ga	ppm	FUS-MS	17	13	13	6
Ge	ppm	FUS-MS	< 0.5	< 0.5	0.90	< 0.5
As	ppm	FUS-MS	306	57	132	45
Rb	ppm	FUS-MS	41	3	39	19
Sr	ppm	FUS-ICP	58	25	6	81
Y	ppm	FUS-MS	55	16.50	17	15.20
Zr	ppm	FUS-ICP	164	84	72	30
Nb	ppm	FUS-MS	1.6	1.5	2.4	0.5
Mo	ppm	FUS-MS	< 2	3	2	2
Ag	ppm	FUS-MS	< 0.5	< 0.5	1.3	< 0.5
In	ppm	FUS-MS	< 0.1	0.2	0.4	< 0.1
Sn	ppm	FUS-MS	< 1	3	1	< 1
Sb	ppm	FUS-MS	< 0.2	1.30	23.30	3.80
Cs	ppm	FUS-MS	0.4	< 0.1	0.4	0.2
Ba	ppm	FUS-ICP	507	46	948	184
La	ppm	FUS-MS	18	3.65	4.08	4.37
Ce	ppm	FUS-MS	44.1	9.21	9.78	9.91
Pr	ppm	FUS-MS	5.81	1.18	1.28	1.33
Nd	ppm	FUS-MS	27.2	5.58	6.16	6.87
Sm	ppm	FUS-MS	7.55	1.62	1.86	2.21
Eu	ppm	FUS-MS	2.37	0.32	0.36	0.35
Gd	ppm	FUS-MS	8.59	2.2	2.16	2.63
Tb	ppm	FUS-MS	1.52	0.4	0.42	0.45
Dy	ppm	FUS-MS	9.87	2.7	2.93	3.13
Ho	ppm	FUS-MS	2.06	0.6	0.64	0.6
Er	ppm	FUS-MS	6.04	1.85	2.06	1.72
Tm	ppm	FUS-MS	0.94	0.30	0.34	0.27
Yb	ppm	FUS-MS	6.31	2.19	2.41	1.73
Lu	ppm	FUS-MS	0.97	0.37	0.41	0.27
Hf	ppm	FUS-MS	4.00	2.50	1.70	0.70
Ta	ppm	FUS-MS	0.11	0.12	0.13	< 0.01
W	ppm	FUS-MS	< 0.5	1.00	3.70	1.00
Tl	ppm	FUS-MS	0.82	0.27	2.03	1.62
Pb	ppm	FUS-MS	10	682	4250	247
Bi	ppm	FUS-MS	< 0.1	1.10	0.30	1.20
Th	ppm	FUS-MS	3.84	1.69	1.64	0.72
U	ppm	FUS-MS	1.22	1.49	1.5	2.30

Appendix C: Mass Change Calculations

Mass balance calculations were performed using the single precursor method after MacLean (1990). This method utilizes elements with high degrees of immobility (i.e., Al_2O_3, Zr, TiO_2) during hydrothermal alteration to determine the composition of the parent rock and the associated quantitative changes in elements as the result of hydrothermal alteration. In order to discern chemically different volcaniclastic rock units in the Hurricane zone several immobile compatible vs. immobile incompatible binary plots were created (e.g., Al_2O_3,vs. Zr, TiO_2 vs. La). Rocks with similar magmatic affinities and alteration precursors will lie along linear "alteration lines" that pass through the origin in immobile-immobile element plots (MacLean, 1990).On these linear plots a least altered precursor sample is often denoted and variations from this precursor location are due to mass gains and losses during the alteration processes. Three chemically distinct groups were identified from VCL1 and VCL2; these include Groups A-C (VCL1; Fig. 2-9e and 2-9f) Group D (VCL1; Fig. 2-9e and 2-9f) and VCL2. In these plots, least altered samples from each of the distinct groups were selected based on having minimal losses of Na_2O (2-5 wt %), low loss of ignition (LOI) and low base metal values (i.e., <100 ppm). Plots of Al_2O_3, TiO_2, and Zr illustrate linear relationships (not shown), as would be expected for immobile elements and for single precursors that had various mass changes during the alteration process.

The mass change of any mobile element can be calculated based on the dilution or concentration of an immobile component (MacLean and Kranidiotis, 1987). The steps in calculating the mass changes, using Al_2O_3 as the immobile element, are the following:

1. Calculate the enrichment factor (EF) for a given immobile element for each sample: EF= Al_2O_3precursor/ Al_2O_3altered.
2. Calculate the reconstructed composition (RC) of the rock by multiplying the enrichment factor by wt% or ppm of the component in the altered sample: RC=EF x %$component_{altered}$. The RC is the actual corrected mass of the sample after alteration.
3. Calculate the mass change for the various elements: MC=RC- precursor composition.

Calculations explained above were completed using excel. Only samples that contained detectable levels were used in the calculations. LOD in the tables below indicate samples that were below detection limit.

Table C.1 Calculated Mass Changes

Appendix C: Table C1.1: Mass Change for samples at the Hurricane Deposit

Sample ID	**25424**	**24529**	**24531**	**24532**	**31761**	**31764**	**31768**	**14494**	**32004**
Hole ID	GA-07-254	GA-07-254	GA-07-254	GA-07-254	GA-07-255	GA-07-255	GA-07-255	GA-06-147	GA-06-147
Depth (m)	157.1	267.9	300	320.8	208.7	247.9	274.4	110.6	285.1
Lithology	VCL2	VCL2	VCL1	VCL1	VCL2	VCL2	VCL1	VCL3	VCL1
Alteration	ser	ser-sil	ser-sil-chl	ser-sil-chl	least altered	ser	ser-chl-py	ser-chl	ser-sil-py
SiO2	8.09	2.35	32.02	43.16	0.00	-0.46	5.46	-6.77	1.13
Al2O3	0.00	0.00	0.00	0.00	0.00	0.00	0.00	0.00	0.00
Fe2O3	0.35	-0.50	2.28	2.16	0.00	0.15	-0.19	0.55	1.22
MnO	0.01	0.01	0.23	-0.09	0.00	0.00	-0.04	-0.02	-0.27
MgO	0.51	-0.66	6.91	4.87	0.00	-0.27	-0.89	0.76	-0.59
CaO	0.25	0.87	3.14	-1.82	0.00	0.47	-1.00	0.37	-1.79
Na2O	-1.93	-1.92	-1.32	-1.36	0.00	-0.83	-1.78	-2.10	-0.24
K2O	1.32	0.95	-0.86	-0.38	0.00	0.21	1.32	0.51	0.68
TiO2	0.14	-0.18	-0.18	-0.17	0.00	-0.03	-0.02	0.04	0.16
P2O5	0.03	-0.05	-0.06	-0.06	0.00	-0.02	0.04	-0.02	-0.01
LOI	1.05	1.32	6.16	0.59	0.00	0.91	0.08	1.44	-1.45
Total	9.80	2.16	48.26	46.83	0.00	0.12	2.98	-5.29	-1.22
Hg	2.67	3.05	13.36	-1.66	0.00	-0.03	-2.80	-3.69	10.92
Sc	-1.75	-3.93	-2.05	-3.62	0.00	-0.08	-3.47	1.37	6.94
Be	0.17	0.01	0.25	0.24	0.00	-0.01	0.02	-1.08	0.00
V	-11.17	-28.90	-26.87	-36.36	0.00	-15.15	-11.36	17.50	56.50
Cr	0.83	0.05	4.91	4.77	0.00	-0.04	-19.01	8.45	-0.03
Co	0.25	-2.50	-5.53	-5.57	0.00	-0.01	-6.70	2.54	3.95
Ni	0.83	0.05	4.91	4.77	0.00	-0.04	10.66	-0.77	-0.03
Cu	0.42	0.03	238.47	-22.62	0.00	-0.02	-4.84	-0.39	-0.10
Zn	9.15	20.67	77.27	-163.73	0.00	-0.49	-66.38	-54.65	-130.90
Ga	-0.50	0.10	3.90	-0.71	0.00	-0.09	1.46	-3.39	0.95
Ge	0.18	0.51	0.79	0.33	0.00	0.39	0.23	0.58	-0.10
As	-2.42	2.06	16.29	17.39	0.00	3.94	-30.95	14.91	79.66
Rb	21.66	23.32	-21.58	-14.33	0.00	8.78	21.61	16.35	14.83
Sr	-13.34	-1.83	8.73	-22.76	0.00	-0.16	-18.47	-12.86	-5.11
Y	2.77	0.96	-3.20	-5.72	0.00	2.66	-4.31	-7.30	-1.26
Zr	28.31	21.06	25.37	15.41	0.00	15.10	1.71	-91.74	4.70
Nb	0.85	-0.30	-2.15	-2.15	0.00	0.19	-0.20	-0.82	-0.51
Mo	0.08	0.01	LOD	LOD	0.00	0.00	LOD	0.85	LOD
Ag	0.02	0.00	LOD	LOD	0.00	0.00	LOD	-0.02	LOD
In	0.01	0.00	-0.05	LOD	0.00	0.00	LOD	-0.05	-0.10
Sn	0.08	0.01	LOD	LOD	0.00	0.00	0.03	0.85	LOD
Sb	0.17	-0.30	-0.01	-0.90	0.00	0.30	-0.67	0.58	1.09
Cs	0.24	0.20	LOD	-0.15	0.00	0.10	0.11	0.07	0.10
Ba	448.19	-195.52	-69.75	225.76	0.00	700.91	3964.49	36.04	71.09
La	2.86	1.40	-2.99	-1.64	0.00	1.11	-0.63	-11.69	-1.61
Ce	4.81	2.65	-5.43	-2.79	0.00	2.08	-0.38	-28.02	-2.75
Pr	0.41	0.32	-0.69	-0.53	0.00	0.23	-0.14	-3.56	-0.29
Nd	1.41	2.16	-2.25	-2.36	0.00	1.56	-0.75	-15.13	-0.45
Sm	0.08	1.00	-0.62	-0.90	0.00	0.55	-0.38	-3.02	-0.28
Eu	0.04	0.15	-0.48	-0.57	0.00	0.18	-0.17	-0.96	-0.34
Gd	0.16	0.81	-0.44	-0.93	0.00	0.64	-0.50	-2.57	-0.25
Tb	0.06	0.12	-0.12	-0.20	0.00	0.15	-0.10	-0.35	-0.04
Dy	0.31	0.41	-0.56	-1.14	0.00	0.81	-0.72	-2.05	-0.13
Ho	0.02	0.00	-0.13	-0.21	0.00	0.08	-0.14	-0.54	-0.02
Er	0.25	0.13	-0.27	-0.43	0.00	0.37	-0.34	-1.53	-0.06
Tm	0.04	0.01	-0.04	-0.07	0.00	0.05	-0.06	-0.25	-0.02
Yb	0.49	0.20	-0.21	-0.37	0.00	0.51	-0.36	-1.71	-0.23
Lu	0.10	0.07	0.00	-0.03	0.00	0.11	-0.06	-0.27	-0.05
Hf	0.62	0.52	0.44	0.27	0.00	0.48	-0.06	-1.10	0.09
Ta	0.08	0.03	-0.03	-0.04	0.00	0.02	0.02	-0.08	-0.01
W	0.02	0.00	0.24	LOD	0.00	0.00	0.29	0.58	0.49
Tl	-0.01	0.73	-0.02	0.16	0.00	1.00	1.54	0.43	0.19
Pb	3.67	1.03	33.20	4.63	0.00	1.97	-137.74	0.54	16.88
Bi	0.00	0.00	LOD	LOD	0.00	0.00	LOD	0.00	LOD
Th	1.15	0.54	0.35	0.12	0.00	0.28	0.74	-1.83	-0.51
U	0.53	-0.15	0.75	1.60	0.00	0.03	0.98	0.02	-0.07

Appendix C: Table C1.1: Mass Change for samples at the Hurricane Deposit

Sample ID	**14453**	**14469**	**14477**	**14478**	**14480**	**14482**	**14483**	**14485**	**32145**
Hole ID	GA-07-208	GA-07-218	GA-07-218	GA-07-218	GA-07-218	GA-07-218	GA-07-218	GA-07-218	GA-10-272
Depth (m)	258.3	182.2	294.8	318.1	323.3	344.5	363.9	394.8	255
Lithology	VCL1	VCL3	VCL2	VCL2	VCL2	VCL1	VCL1	VCL1	VCL1
Alteration	sil-ser-chl-py	chl-py	ser-chl	ser-sil	ser-chl-py	ser-chl-py	ser-chl-py	ser-chl-py	ser-py
SiO2	10.27	-32.45	1.53	57.14	0.10	2.38	10.92	-19.65	26.58
Al2O3	0.00	0.00	0.00	0.00	0.00	0.00	0.00	0.00	0.00
Fe2O3	1.93	6.00	-0.09	2.35	2.23	6.78	1.69	-0.86	1.47
MnO	-0.14	0.00	0.00	-0.01	-0.33	0.07	-0.05	-0.02	-0.39
MgO	-4.32	8.71	-0.04	-0.05	2.01	11.62	7.18	-2.85	-2.86
CaO	-0.73	-0.03	0.30	0.42	-2.10	-2.17	-2.14	3.29	-1.89
Na2O	-1.68	-1.70	-0.72	1.78	-2.32	-2.41	-0.45	-1.40	-2.15
K2O	2.30	-2.47	0.50	-1.54	1.34	-1.31	-1.33	1.16	2.29
TiO2	0.00	0.09	-0.06	-0.12	0.04	-0.25	-0.17	0.09	0.05
P2O5	0.02	-0.03	-0.02	-0.03	0.00	-0.06	-0.04	-0.01	-0.07
LOI	0.22	3.61	0.36	1.52	0.66	4.51	0.23	2.51	0.33
Total	7.86	-18.26	1.79	61.40	1.60	19.09	15.74	-17.75	23.32
Hg	79.04	-3.98	0.98	11.57	127.21	4.67	-9.12	-4.06	2561.65
Sc	6.09	1.42	-0.06	-5.22	1.37	-5.05	-2.92	7.18	3.92
Be	0.04	-1.60	-0.01	-1.20	0.02	0.10	0.08	-0.09	0.12
V	9.29	206.93	-8.13	-8.08	6.96	7.82	-20.63	34.91	24.63
Cr	15.21	14.28	19.90	21.94	0.31	1.91	1.54	15.89	2.43
Co	4.65	23.71	0.99	1.79	0.31	1.91	-3.08	2.94	-0.05
Ni	0.87	14.28	-0.03	5.97	0.31	1.91	1.54	14.71	2.43
Cu	33.48	11.19	-0.02	2.98	165.93	5.72	-24.23	14.71	-5.13
Zn	472.14	-12.88	19.58	-30.15	1167.43	64.32	-250.03	-81.16	-381.35
Ga	1.13	-4.62	0.93	-4.03	0.44	7.43	2.15	1.00	2.16
Ge	0.17	-0.01	0.79	1.66	-0.18	0.01	0.22	0.29	-0.39
As	109.90	22.37	1.96	17.15	-4.50	88.53	8.99	-25.29	99.60
Rb	44.91	-37.38	18.81	-19.84	14.50	-31.43	-31.54	24.54	47.06
Sr	-16.52	-22.05	2.88	3.33	-23.53	-33.05	-26.31	2.89	-12.89
Y	2.46	-32.40	14.49	-22.25	1.45	4.74	-4.67	-8.40	-0.50
Zr	-5.26	-109.54	-1.59	-62.64	11.93	28.10	18.82	-9.99	2.03
Nb	0.24	0.36	0.59	-0.94	-1.37	-1.82	-1.84	-0.22	-0.93
Mo	LOD	1.43	0.00	6.98	LOD	LOD	LOD	LOD	LOD
Ag	LOD	-0.05	0.00	0.15	LOD	LOD	LOD	LOD	LOD
In	LOD	-0.06	0.00	-0.02	4.96	LOD	LOD	LOD	-0.14
Sn	0.09	-0.60	0.99	-0.20	LOD	LOD	LOD	LOD	LOD
Sb	2.10	-0.31	0.10	0.96	1.48	-0.49	-0.62	-0.86	21.68
Cs	0.24	-0.26	0.10	-0.14	0.11	LOD	LOD	0.03	0.20
Ba	371.92	-838.25	-272.92	-375.56	2055.28	-112.90	-157.16	-34.04	594.72
La	0.82	-14.82	2.43	-8.82	0.93	-5.79	-4.68	-1.03	-1.80
Ce	1.20	-37.36	4.94	-21.51	5.31	-11.01	-7.80	-1.64	-3.08
Pr	0.09	-5.10	0.40	-2.85	0.55	-1.33	-0.89	-0.18	-0.43
Nd	0.34	-23.06	1.90	-12.47	3.07	-4.82	-2.89	-0.84	-1.84
Sm	0.19	-6.04	0.26	-3.76	0.48	-1.06	-0.97	-0.15	-0.67
Eu	-0.02	-1.61	0.40	-0.93	-0.07	-0.63	-0.64	0.12	-0.51
Gd	0.26	-6.04	-0.01	-4.92	0.61	-0.06	-0.76	-0.50	-0.19
Tb	0.07	-1.03	0.09	-0.93	0.07	0.02	-0.17	-0.15	-0.06
Dy	0.38	-6.58	0.93	-5.72	0.42	0.51	-0.87	-1.08	-0.23
Ho	0.10	-1.38	0.15	-1.16	0.06	0.14	-0.17	-0.26	-0.07
Er	0.31	-3.84	0.62	-2.83	0.28	0.57	-0.44	-0.74	0.03
Tm	0.05	-0.57	0.08	-0.36	0.02	0.11	-0.05	-0.12	0.01
Yb	0.28	-3.77	0.73	-1.92	0.15	0.60	-0.31	-0.86	0.05
Lu	0.06	-0.57	0.12	-0.23	0.03	0.12	-0.04	-0.14	-0.02
Hf	-0.21	-1.88	0.59	-0.94	0.26	0.58	0.39	-0.31	0.31
Ta	0.02	-0.01	-0.02	-0.04	-0.03	-0.03	-0.01	-0.01	-0.13
W	-0.33	1.04	0.35	1.51	-0.84	LOD	LOD	LOD	2.75
Tl	0.91	-0.10	0.29	0.34	1.22	-0.03	LOD	0.19	8.34
Pb	176.81	-2.98	1.98	6.18	727.59	171.49	-9.77	-124.58	112.79
Bi	LOD	-0.01	0.00	0.03	LOD	LOD	LOD	LOD	LOD
Th	0.58	-1.56	0.04	-2.03	-0.40	0.56	0.23	-0.28	-0.11
U	0.78	-0.09	0.00	0.33	1.39	0.69	0.94	-0.03	3.58

Appendix C: Table C1.1: Mass Change for samples at the Hurricane Deposit

Sample ID	32005	32006	32007	32008	14535	14540	14544	14545	14547
Hole ID	GA-06-147	GA-06-147	GA-06-147	GA-06-147	GA-07-208	GA-07-208	GA-07-208	GA-07-208	GA-07-208
Depth (m)	316.97	336.2	363.6	380.4	169.1	218.5	273.6	295	328.3
Lithology	VCL1	VCL1	VCL1	VCL1	VCL2	VCL2	VCL1	IN2a	VCL1
Alteration	ser-sil-py	ser-chl	least altered	ser	ser-sil	ser-sil	ser-sil-py	ser-sil	least altered
SiO2	-10.87	-19.91	0.00	-18.10	-7.87	4.89	33.41	-5.80	0.00
Al2O3	0.00	0.00	0.00	0.00	0.00	0.00	0.00	0.00	0.00
Fe2O3	0.07	-0.13	0.00	-0.09	0.88	1.12	2.58	3.63	0.00
MnO	0.29	0.13	0.00	0.18	0.01	0.00	-0.16	0.16	0.00
MgO	5.29	1.19	0.00	-0.84	1.62	-0.18	-5.51	-1.43	0.00
CaO	3.02	0.32	0.00	1.33	0.38	0.32	-0.63	2.35	0.00
Na2O	-1.65	-1.71	0.00	-0.90	-1.66	1.26	-1.40	-1.67	0.00
K2O	0.01	0.44	0.00	0.48	0.39	-1.33	2.13	1.08	0.00
TiO2	-0.02	0.06	0.00	0.01	0.20	-0.10	-0.07	0.10	0.00
P2O5	0.00	0.03	0.00	0.00	0.01	-0.05	-0.01	0.13	0.00
LOI	4.48	0.01	0.00	0.53	0.69	0.40	1.80	3.38	0.00
Total	0.62	-19.59	0.00	-17.41	-5.37	6.34	32.12	1.93	0.00
Hg	3.14	-7.01	0.00	18.15	-3.68	-3.37	639.63	-2.88	0.00
Sc	1.24	5.53	0.00	-0.25	-1.27	-2.25	0.31	6.50	0.00
Be	0.01	-0.10	0.00	0.32	-0.14	-0.95	0.18	0.01	0.00
V	-6.26	30.49	0.00	2.61	-1.54	-23.85	-10.75	45.85	0.00
Cr	-19.65	-10.11	0.00	32.27	-0.71	0.50	4.17	0.97	0.00
Co	0.19	3.95	0.00	-2.01	0.72	-0.90	-5.17	14.58	0.00
Ni	0.12	5.96	0.00	14.68	-0.71	0.50	3.54	10.39	0.00
Cu	10.23	21.91	0.00	6.45	-0.35	0.25	856.64	10.39	0.00
Zn	224.66	-28.41	0.00	-64.82	-7.79	-36.49	10219.71	85.03	0.00
Ga	0.15	0.56	0.00	0.99	-2.34	-3.20	1.90	1.27	0.00
Ge	-0.09	-0.06	0.00	-0.04	0.03	-0.06	1.06	0.01	0.00
As	-7.35	-20.12	0.00	-20.39	-5.35	2.60	120.16	-5.90	0.00
Rb	0.34	10.09	0.00	11.31	11.18	-16.95	45.48	28.08	0.00
Sr	19.63	-3.09	0.00	-4.56	-4.34	9.11	2.92	36.35	0.00
Y	-4.02	-1.33	0.00	-2.82	-5.32	3.88	7.48	1.09	0.00
Zr	0.61	-12.91	0.00	-4.28	-25.10	47.04	-8.67	1.01	0.00
Nb	0.10	0.50	0.00	-0.05	0.20	-0.05	-0.16	1.33	0.00
Mo	LOD	LOD	LOD	LOD	-0.07	3.20	LOD	LOD	LOD
Ag	LOD	LOD	LOD	LOD	-0.02	0.01	LOD	LOD	LOD
In	LOD	LOD	LOD	LOD	-0.05	0.01	LOD	LOD	0.00
Sn	1.02	-0.20	0.00	LOD	-0.54	-0.47	0.35	LOD	LOD
Sb	-0.18	-0.48	0.00	-0.28	-0.43	0.25	11.94	-0.38	0.00
Cs	0.00	0.10	0.00	0.36	0.07	-0.09	0.11	0.11	0.00
Ba	5.97	67.17	0.00	48.91	-484.31	-360.72	410.50	201.96	0.00
La	0.65	0.93	0.00	-1.00	-2.07	0.73	3.21	1.15	0.00
Ce	1.68	2.39	0.00	-1.89	-5.77	2.63	5.68	2.67	0.00
Pr	0.26	0.30	0.00	-0.15	-0.83	0.33	0.56	0.36	0.00
Nd	1.33	1.33	0.00	-0.42	-3.42	2.27	1.54	1.48	0.00
Sm	0.28	0.39	0.00	0.06	-1.09	0.33	0.36	0.39	0.00
Eu	-0.04	0.03	0.00	0.06	-0.10	-0.41	0.10	0.22	0.00
Gd	-0.16	0.12	0.00	-0.29	-0.66	-0.15	0.40	0.40	0.00
Tb	-0.09	-0.01	0.00	-0.07	-0.13	0.00	0.10	0.05	0.00
Dy	-0.77	-0.16	0.00	-0.61	-1.24	0.54	0.82	0.20	0.00
Ho	-0.16	-0.05	0.00	-0.14	-0.33	0.14	0.17	0.05	0.00
Er	-0.40	-0.10	0.00	-0.25	-0.85	0.80	0.60	0.21	0.00
Tm	-0.06	-0.03	0.00	-0.04	-0.15	0.14	0.11	-0.01	0.00
Yb	-0.41	-0.29	0.00	-0.30	-0.95	1.13	0.52	-0.10	0.00
Lu	-0.06	-0.05	0.00	-0.03	-0.13	0.19	0.08	-0.01	0.00
Hf	-0.09	-0.50	0.00	-0.23	-0.25	1.02	-0.35	-0.18	0.00
Ta	0.01	0.02	0.00	-0.01	0.03	0.05	0.00	0.07	0.00
W	-0.88	-1.30	0.00	-1.51	-0.02	0.01	0.61	-0.46	0.00
Tl	0.00	0.02	0.00	0.12	-0.04	0.12	0.95	0.26	0.00
Pb	44.19	-102.92	0.00	-118.03	3.36	1.30	5256.97	-102.17	0.00
Bi	LOD	LOD	LOD	LOD	0.00	0.00	LOD	LOD	LOD
Th	0.12	0.28	0.00	-0.11	-0.02	1.08	-0.15	0.50	0.00
U	0.15	0.12	0.00	-0.04	0.27	0.01	1.11	0.46	0.00

Appendix C: Table C1.1: Mass Change for samples at the Hurricane Deposit

Sample ID	**32146**	**32147**	**32148**	**32152**	**32154**	**14769**	**14772**	**14774**	**14775**
Hole ID	GA-10-272	GA-10-272	GA-10-272	GA-10-272	GA-10-272	GA-14-275	GA-14-275	GA-14-275	GA-14-275
Depth (m)	262.2	280.4	292.5	237	240.4	148.8	196.5	213.6	239.6
Lithology	VCL1	VCL1	VCL1	VCL1	VCL1	VCL2	VCL2	VCL1	VCL1
Alteration	ser-chl-carb	ser-chl-carb	ser-py	carb-chl	chl-ser-pyr	ser-chl	sil-ser	ser-sil-py	ser-sil-py
SiO2	-4.84	-13.38	2.01	-36.00	-15.43	3.84	49.21	29.95	16.82
Al2O3	0.00	0.00	0.00	0.00	0.00	0.00	0.00	0.00	0.00
Fe2O3	0.95	4.51	-0.36	5.31	4.85	0.38	-0.33	-0.18	1.46
MnO	0.11	0.60	0.00	0.46	-0.08	0.01	-0.01	-0.14	0.03
MgO	-1.88	0.36	-3.83	19.05	9.74	0.21	1.09	-5.27	0.03
CaO	4.03	9.63	0.80	8.91	-2.02	0.85	0.13	-0.83	0.04
Na2O	-1.47	-1.60	-1.63	-2.46	-2.46	-0.76	-3.35	-1.68	-1.42
K2O	1.20	1.94	2.02	-0.80	-0.31	0.23	0.76	2.63	0.97
TiO2	0.02	0.05	0.03	-0.01	0.05	0.11	-0.23	0.06	-0.07
P2O5	0.02	0.01	0.00	-0.03	-0.06	0.06	-0.02	0.01	-0.02
LOI	3.43	14.16	0.01	13.99	4.60	0.68	0.92	-0.84	2.68
Total	1.55	16.27	-0.95	8.38	-1.16	5.67	48.12	23.72	20.44
Hg	6.44	6.34	28.80	151.63	1811.10	-3.41	-2.34	59.10	106.67
Sc	10.88	5.96	5.86	5.58	3.26	-1.40	-1.90	7.24	2.32
Be	LOD	LOD	LOD	0.05	0.01	-0.96	-0.54	LOD	LOD
V	39.59	28.24	30.98	18.45	15.94	-18.95	-31.90	43.60	-6.24
Cr	63.22	20.79	19.62	1.06	0.18	0.38	4.64	49.06	2.11
Co	8.70	13.50	1.90	-6.68	0.18	2.19	-2.27	8.77	-0.31
Ni	20.88	13.60	LOD	1.06	0.18	0.38	4.64	14.77	2.11
Cu	20.88	25.40	39.73	1152.97	82.03	0.19	2.32	51.91	30.55
Zn	-46.19	-85.61	18.92	1192.03	6719.27	-27.00	-36.80	241.01	2264.01
Ga	1.41	1.16	0.92	10.32	5.35	-2.36	0.50	1.86	-0.68
Ge	0.02	LOD	LOD	0.07	0.32	-0.64	0.42	LOD	LOD
As	-24.89	33.93	306.99	141.52	169.46	-7.41	-6.34	77.16	50.44
Rb	26.58	41.79	44.60	-22.84	-12.59	10.80	25.42	61.39	23.12
Sr	11.32	16.91	-7.15	46.13	-27.80	15.84	-21.82	-15.19	30.02
Y	1.19	-5.09	-4.48	-6.30	4.54	5.41	35.45	-2.02	4.20
Zr	-10.83	-13.06	-12.22	0.13	12.78	6.90	78.07	-9.90	8.24
Nb	0.21	-0.18	-0.20	-0.64	-0.26	1.60	0.80	-0.18	-0.85
Mo	LOD	LOD	LOD	LOD	LOD	0.04	0.46	LOD	LOD
Ag	LOD	LOD	LOD	LOD	LOD	0.01	0.12	LOD	LOD
In	LOD	LOD	LOD	0.02	LOD	-0.05	-0.03	LOD	0.41
Sn	LOD	LOD	LOD	LOD	LOD	-0.48	0.46	LOD	LOD
Sb	-1.19	0.76	0.99	73.98	25.38	-0.70	-0.65	0.51	-0.72
Cs	0.11	0.05	0.10	-0.19	-0.10	0.01	0.14	0.20	0.18
Ba	86.15	55.63	82.66	449.08	814.44	-396.93	-555.69	415.74	112.63
La	0.37	-1.15	-1.48	-3.95	-1.54	-0.44	9.12	-0.62	-0.04
Ce	0.55	-2.30	-2.97	-8.67	-1.19	-2.32	20.52	-1.16	0.77
Pr	0.01	-0.31	-0.38	-1.18	-0.17	-0.44	2.70	-0.24	0.02
Nd	-0.12	-1.31	-1.74	-4.18	-0.37	-1.94	12.54	-1.09	0.64
Sm	-0.02	-0.32	-0.41	-1.15	-0.20	-0.47	3.67	-0.29	0.19
Eu	0.32	0.19	0.05	-0.31	-0.52	-0.14	0.74	-0.10	-0.39
Gd	0.14	-0.47	-0.38	-0.58	0.45	-0.61	3.14	-0.28	0.81
Tb	-0.02	-0.13	-0.10	-0.15	0.07	-0.08	0.65	-0.08	0.09
Dy	-0.13	-1.04	-0.79	-0.99	0.70	-0.36	4.76	-0.50	0.67
Ho	-0.03	-0.21	-0.18	-0.25	0.16	-0.11	1.02	-0.10	0.13
Er	-0.01	-0.49	-0.50	-0.75	0.45	-0.12	3.48	-0.29	0.36
Tm	0.00	-0.07	-0.08	-0.12	0.05	-0.01	0.56	-0.05	0.06
Yb	-0.07	-0.47	-0.66	-0.86	0.43	0.07	4.01	-0.27	0.29
Lu	-0.03	-0.07	-0.11	-0.15	0.06	0.01	0.67	-0.03	0.04
Hf	-0.17	0.00	-0.21	0.63	0.75	1.07	3.09	-0.19	0.50
Ta	LOD	LOD	LOD	-0.14	-0.12	-0.06	-0.10	LOD	-0.17
W	LOD	-1.67	-1.31	4.10	4.09	0.01	0.12	-0.15	0.35
Tl	0.95	0.85	0.84	0.74	2.64	0.23	0.79	0.71	0.23
Pb	-122.33	-35.09	53.92	2391.16	4727.18	7.45	-1.34	143.75	66.97
Bi	LOD	LOD	LOD	LOD	LOD	0.00	0.02	LOD	LOD
Th	0.38	-0.25	-0.26	-0.60	-0.28	1.37	2.46	-0.16	-0.19
U	1.36	0.34	-0.04	1.73	1.10	0.45	0.73	0.85	-0.02

Appendix C: Table C1.1: Mass Change for samples at the Hurricane Deposit

Sample ID	14778	14797	14799	14800	32051	32053	32208	32216	32218
Hole ID	GA-14-275	GA-10-276	GA-10-276	GA-10-276	GA-10-276	GA-10-276	GA-07-257	GA-10-273	GA-10-273
Depth (m)	253.1	259.3	307.5	311.63	333	368.1	424.8	281.7	304.8
Lithology	VCL1	VCL2	VCL2	VCL1	VCL1	VCL1	VCL2	VCL1	VCL1
Alteration	ser-chl-py	ser-chl	chl-carb	sil-carb	ser-chl-pyr	sil-ser-pyr	ser-chl	ser-carb-pyr	ser-sil-pyr
SiO2	-11.61	-2.99	-37.76	-29.25	-23.52	-14.18	-0.17	16.59	-4.88
Al2O3	0.00	0.00	0.00	0.00	0.00	0.00	0.00	0.00	0.00
Fe2O3	3.87	0.15	0.30	-0.14	6.14	0.94	1.19	4.05	-1.66
MnO	0.29	0.01	0.14	0.51	-0.05	0.16	0.02	0.05	0.25
MgO	-0.02	-0.39	17.42	12.22	12.86	-3.65	0.25	3.50	-2.58
CaO	-0.83	0.17	0.80	16.74	-2.18	10.91	0.59	9.10	4.19
Na2O	-1.41	1.02	-2.52	-2.25	-2.49	-1.27	-0.98	-1.95	-1.53
K2O	0.38	-0.76	-1.46	1.55	-1.43	1.45	-0.29	1.93	1.94
TiO2	-0.02	-0.03	0.12	0.01	-0.27	-0.04	0.07	0.08	0.00
P2O5	0.02	0.00	0.02	0.11	-0.04	0.12	0.01	0.05	0.09
LOI	1.71	-0.14	6.89	23.31	3.81	9.80	0.67	15.96	4.22
Total	-7.60	-2.97	-16.09	22.77	-7.16	4.24	1.34	49.32	0.06
Hg	214.55	2.55	-1.75	16.81	38.09	40.23	0.99	461.96	0.96
Sc	0.58	0.06	6.94	2.78	-2.65	3.05	2.97	4.14	4.90
Be	LOD	-1.05	-0.07	0.13	-0.04	LOD	0.00	0.26	LOD
V	14.17	-9.04	35.41	7.97	-12.15	-11.39	11.92	28.63	11.32
Cr	-3.23	-0.50	-1.46	2.53	-0.72	-8.10	-0.01	5.14	-20.12
Co	1.77	-0.15	-4.02	-3.74	2.99	11.24	1.99	0.60	-3.05
Ni	LOD	-0.50	-1.46	2.53	-0.72	LOD	-0.01	5.14	LOD
Cu	130.30	-0.25	-25.73	-23.74	554.41	73.80	-0.01	-14.86	19.88
Zn	4983.19	4.04	-229.18	-149.45	35.99	626.61	19.83	-263.72	-110.28
Ga	1.97	-1.94	2.23	2.29	8.26	0.62	-0.03	2.66	-0.05
Ge	LOD	-0.66	-0.49	-0.39	-0.47	LOD	-0.10	-0.40	LOD
As	-1.33	-2.40	-3.92	2.80	76.40	394.83	-0.01	44.11	79.42
Rb	9.35	-8.59	-34.57	21.37	-34.07	29.66	6.94	37.68	39.72
Sr	1.48	13.47	2.85	133.88	-35.29	25.76	-3.04	35.20	4.84
Y	0.88	2.64	-8.11	10.17	-5.15	3.13	18.51	-0.37	-1.97
Zr	1.32	-9.14	6.39	10.21	-0.59	-9.05	8.75	13.43	-11.17
Nb	0.17	0.71	-0.16	-0.05	-1.09	0.22	0.60	-0.94	0.10
Mo	LOD	-0.05	LOD	LOD	LOD	LOD	0.00	LOD	LOD
Ag	LOD	-0.01	LOD	LOD	LOD	LOD	0.00	LOD	LOD
In	LOD	-0.05	-0.16	LOD	0.17	LOD	-0.05	-0.12	LOD
Sn	-0.06	-0.05	LOD	LOD	LOD	LOD	-0.50	LOD	LOD
Sb	0.64	-0.70	-1.11	LOD	-0.83	0.39	LOD	2.43	-0.70
Cs	-0.02	-0.11	-0.26	0.08	LOD	0.12	0.00	0.15	0.10
Ba	37.97	-405.25	-144.63	5393.73	-130.50	5.75	-684.24	392.59	101.91
La	0.30	-1.31	-4.21	-2.45	-7.29	0.93	-0.02	-4.87	-0.04
Ce	1.75	-3.72	-5.62	-1.34	-14.96	2.25	0.14	-7.57	-0.83
Pr	0.34	-0.50	-0.63	0.19	-1.86	0.21	-0.07	-0.87	-0.17
Nd	1.13	-1.61	-2.28	2.69	-7.03	0.72	-0.34	-2.42	-1.06
Sm	0.32	-0.75	-0.74	1.54	-1.75	0.17	0.04	-0.37	-0.20
Eu	-0.07	0.32	-0.44	0.14	-0.68	0.32	0.23	-0.40	0.24
Gd	0.30	-0.24	-0.61	2.44	-1.21	0.47	0.98	-0.05	-0.21
Tb	0.03	-0.13	-0.20	0.34	-0.22	0.02	0.27	-0.04	-0.07
Dy	0.02	-0.81	-1.33	1.88	-1.29	0.14	1.65	-0.02	-0.52
Ho	-0.01	-0.20	-0.29	0.32	-0.28	0.05	0.32	-0.03	-0.12
Er	0.04	-0.43	-0.82	0.92	-0.68	0.25	1.05	0.02	-0.32
Tm	-0.02	-0.07	-0.13	0.13	-0.10	0.05	0.19	0.02	-0.05
Yb	-0.17	-0.27	-0.75	0.67	-0.61	0.19	1.12	0.26	-0.31
Lu	-0.02	-0.05	-0.12	0.07	-0.09	0.01	0.14	0.02	-0.07
Hf	0.29	0.97	0.59	0.71	0.43	-0.04	1.39	0.62	-0.20
Ta	LOD	-0.08	-0.10	-0.09	-0.14	LOD	-0.11	LOD	LOD
W	-1.38	-0.01	0.27	0.28	-0.45	LOD	0.00	1.63	LOD
Tl	0.35	0.02	-0.15	2.19	-0.11	0.38	0.40	2.09	0.67
Pb	-128.23	-2.62	-2.77	2.30	61.70	-29.72	-2.50	37.03	-94.21
Bi	LOD	0.00	LOD	LOD	LOD	LOD	0.00	LOD	LOD
Th	0.17	0.31	-0.60	-0.03	-0.11	0.31	0.79	-0.16	0.39
U	0.05	0.07	-0.21	0.20	0.90	1.06	0.13	2.30	0.32

Appendix C: Table C1.1: Mass Change for samples at the Hurricane Deposit

Sample ID	32219	32220	32076	32079	32080	32174	32196	32199	32200
Hole ID	GA-10-273	GA-10-273	GA-10-274	GA-10-274	GA-10-274	GA-10-277	GA-10-278	GA-10-278	GA-10-278
Depth (m)	267.8	273	270.9	307.2	319.4	243.2	280.1	306.7	309.3
Lithology	VCL1	VCL1	VCL2	VCL1	VCL1	VCL1	VCL2	VCL1	VCL1
Alteration	ser-chl-pyr	ser-chl-pyr	chl-ser	ser-carb-pyr	ser-carb-pyr	ser-sil-pyr	chl-ser	ser-chl-pyr	chl-carb-bm
SiO2	2.38	-36.38	-31.40	-9.17	4.82	6.85	14.50	-19.67	-31.72
Al2O3	0.00	0.00	0.00	0.00	0.00	0.00	0.00	0.00	0.00
Fe2O3	11.12	13.78	3.23	0.97	3.70	-1.53	1.77	7.26	5.69
MnO	0.02	0.29	-0.12	-0.14	0.39	-0.39	0.04	-0.06	-0.05
MgO	3.28	11.99	12.26	3.53	1.93	-2.98	0.49	9.74	13.24
CaO	-0.76	0.36	-1.07	8.22	2.70	-1.14	0.54	0.32	0.40
Na2O	-1.94	-2.09	-2.51	-1.87	-0.25	-1.93	1.02	-2.07	-1.98
K2O	0.75	-1.25	-1.09	2.11	1.44	2.77	-1.07	-0.30	-1.00
TiO2	0.00	-0.14	0.11	0.10	0.35	0.05	0.08	0.03	0.12
P2O5	0.01	0.05	0.04	0.00	0.03	0.02	0.01	-0.02	-0.02
LOI	6.70	9.46	2.47	10.59	4.36	-1.95	0.50	5.80	5.95
Total	21.54	-3.89	-18.13	14.30	27.47	-0.27	17.83	0.97	-9.41
Hg	6305.91	118.47	1.23	15.77	51.97	3.14	0.95	58.86	406.02
Sc	-6.13	-9.46	4.71	6.36	10.49	4.14	2.84	3.38	4.65
Be	LOD	LOD	-0.09	0.08	0.77	0.00	-0.84	0.01	-0.04
V	10.64	-43.90	31.40	43.24	89.42	16.01	30.72	30.18	39.75
Cr	LOD	LOD	-1.73	1.57	77.02	0.10	1.58	0.27	-0.79
Co	0.39	7.96	-0.90	2.73	5.59	0.10	5.10	4.38	8.41
Ni	LOD	LOD	-1.73	1.57	28.11	0.10	1.58	0.27	-0.79
Cu	1162.23	47.51	-21.73	-18.43	15.40	-24.95	18.15	-9.46	-2.38
Zn	LOD	251.30	-52.65	-342.14	-2.17	-329.33	63.65	-245.96	2896.26
Ga	7.17	9.04	5.85	2.20	8.59	1.14	-1.48	4.48	5.34
Ge	0.06	0.16	0.13	-0.41	0.32	-0.20	-0.09	0.02	-0.47
As	358.25	120.98	26.97	5.62	3.32	67.84	264.37	57.05	29.64
Rb	7.55	-28.04	-26.73	42.53	33.24	51.82	-8.90	-10.35	-24.87
Sr	-23.66	-25.42	-24.94	42.00	12.00	-7.71	12.47	-4.08	-6.77
Y	11.53	3.02	-3.61	5.44	6.31	7.86	6.41	-0.59	-4.34
Zr	-20.49	-18.45	18.38	14.52	21.67	19.99	-19.61	21.80	12.60
Nb	-0.17	-0.20	0.59	0.36	0.08	-0.08	1.22	0.37	0.55
Mo	LOD	LOD	LOD	LOD	LOD	LOD	0.16	LOD	LOD
Ag	LOD	LOD	LOD	LOD	LOD	LOD	0.04	LOD	LOD
In	LOD	LOD	-0.16	-0.14	LOD	LOD	-0.04	-0.15	0.08
Sn	11.60	-0.04	LOD	LOD	LOD	LOD	-0.42	LOD	LOD
Sb	13.78	1.95	-0.62	0.07	0.43	-0.09	-0.22	0.34	2.67
Cs	-0.05	LOD	-0.26	0.28	0.72	0.31	0.05	-0.09	-0.21
Ba	884.96	-155.42	41.32	252.62	165.26	436.00	-529.79	1045.70	151.64
La	1.94	-0.35	-4.26	-0.35	0.38	1.48	-3.42	-3.56	-4.87
Ce	5.07	2.19	-7.66	0.52	1.72	3.20	-5.81	-4.96	-7.41
Pr	0.74	0.37	-0.86	0.12	0.43	0.44	-0.72	-0.61	-0.77
Nd	3.20	1.27	-2.77	1.59	2.71	2.81	-3.13	-1.68	-2.03
Sm	1.09	0.40	-0.74	0.62	1.16	0.59	0.03	-0.32	-0.78
Eu	0.00	-0.07	-0.60	-0.14	0.29	-0.39	0.62	-0.51	-0.56
Gd	1.52	0.13	-0.53	1.19	0.95	1.05	1.04	-0.06	-0.51
Tb	0.32	0.01	-0.13	0.13	0.18	0.15	0.07	-0.04	-0.13
Dy	1.93	0.16	-0.73	0.84	0.98	1.03	-0.30	-0.02	-0.79
Ho	0.40	0.03	-0.14	0.17	0.19	0.19	-0.11	0.00	-0.17
Er	0.99	0.21	-0.28	0.52	0.83	0.69	-0.29	0.09	-0.42
Tm	0.13	0.06	-0.03	0.07	0.13	0.11	-0.06	0.01	-0.06
Yb	0.67	0.34	-0.24	0.57	0.83	0.59	-0.26	0.09	-0.32
Lu	0.08	0.04	-0.05	0.07	0.17	0.07	-0.04	0.01	-0.05
Hf	LOD	-0.72	0.93	0.75	0.35	0.82	0.67	0.97	0.87
Ta	LOD	-0.07	0.08	0.02	0.03	-0.05	0.03	0.06	0.07
W	16.41	2.77	1.38	1.21	-0.98	0.92	0.04	3.73	2.12
Tl	1.88	-0.03	0.31	0.88	0.27	1.22	0.31	1.38	0.75
Pb	11576.29	91.69	167.08	1.83	-102.81	-3.86	14.68	52.89	2135.54
Bi	LOD	LOD	LOD	LOD	LOD	LOD	0.18	LOD	LOD
Th	1.18	0.98	-0.14	-0.27	0.20	-0.02	-0.08	-0.28	-0.28
U	8.32	2.20	0.31	0.40	0.05	2.23	-0.01	4.61	5.14

Appendix C: Table C1.1: Mass Change for samples at the Hurricane Deposit

Sample ID	**32202**	**32203**	**32101**	**32102**	**32103**	**32108**
Hole ID	GA-10-278	GA-10-278	GA-06-180	GA-06-180	GA-06-180	GA-06-180
Depth (m)	328.2	332.6	321.68	327.2	338.4	397.9
Lithology	VCL1	VCL1	VCL3	VCL1	VCL1	VCL1
Alteration	chl-carb	ser-sil-pyr	ser-chl	ser-sil-pyr	ser-sil-pyr	sil-ser-pyr
SiO2	-39.57	22.53	4.59	4.89	-0.26	62.46
Al2O3	0.00	0.00	0.00	0.00	0.00	0.00
Fe2O3	4.52	2.70	0.65	14.87	11.05	20.38
MnO	0.03	-0.25	0.05	-0.27	-0.27	2.93
MgO	13.02	4.16	-0.26	5.19	4.91	28.98
CaO	2.49	-1.09	1.18	-2.00	-2.14	55.61
Na2O	-1.95	-2.15	0.07	1.52	-2.31	-1.87
K2O	-1.10	0.47	-0.23	-1.28	1.13	2.02
TiO2	0.08	-0.14	0.02	0.18	0.09	0.07
P2O5	-0.03	-0.07	0.01	0.02	-0.01	0.15
LOI	6.78	1.46	0.99	6.62	6.29	70.55
Total	-15.81	27.58	7.11	29.70	18.44	241.22
Hg	80.46	-8.78	4.49	573.55	2278.55	543.89
Sc	3.55	-0.71	1.93	7.50	2.62	6.37
Be	-0.07	0.14	0.10	0.16	0.12	1.24
V	51.11	-3.53	13.88	51.75	31.58	51.45
Cr	-1.44	2.86	0.49	3.22	2.38	24.74
Co	2.84	-2.28	1.19	7.18	1.14	17.79
Ni	-1.44	2.86	0.49	3.22	2.38	24.74
Cu	-21.44	-23.57	0.24	9.65	836.69	LOD
Zn	-74.69	-232.78	57.80	2032.07	LOD	2170.98
Ga	3.12	2.72	-2.17	3.18	2.10	6.85
Ge	-0.27	-0.38	-0.64	LOD	0.41	0.17
As	8.11	11.16	310.92	54.34	142.43	135.34
Rb	-26.44	6.16	4.00	-31.03	13.29	31.01
Sr	11.51	-14.56	25.83	-5.96	-31.57	242.42
Y	5.53	-0.73	7.48	1.91	1.15	32.91
Zr	8.31	14.05	-12.01	26.03	4.15	19.23
Nb	0.35	-0.63	0.58	-0.32	0.67	-0.56
Mo	LOD	LOD	0.05	LOD	LOD	LOD
Ag	LOD	LOD	0.01	LOD	LOD	LOD
In	-0.16	LOD	-0.05	0.06	0.30	LOD
Sn	LOD	LOD	-0.48	LOD	LOD	LOD
Sb	-0.43	LOD	-0.70	0.52	27.65	12.00
Cs	-0.26	-0.04	0.12	-0.23	0.20	0.39
Ba	-120.53	156.60	-337.29	-140.20	972.75	438.27
La	-1.57	-2.22	0.18	-3.64	-3.41	6.72
Ce	1.95	-3.85	0.15	-5.83	-5.89	16.43
Pr	0.70	-0.46	-0.18	-0.73	-0.71	2.33
Nd	3.50	-1.46	-0.07	-2.13	-1.88	14.36
Sm	0.85	-0.42	0.18	-0.49	-0.33	5.05
Eu	-0.22	-0.51	0.27	-0.37	-0.35	0.44
Gd	1.09	-0.17	0.42	0.10	-0.14	6.33
Tb	0.12	-0.08	0.07	-0.01	-0.02	1.02
Dy	0.66	-0.43	0.51	0.16	0.22	7.46
Ho	0.12	-0.08	0.06	0.05	0.05	1.34
Er	0.41	-0.15	0.21	0.23	0.33	3.76
Tm	0.06	-0.03	0.05	0.04	0.06	0.57
Yb	0.37	-0.28	0.48	0.38	0.47	3.50
Lu	0.04	-0.06	0.05	0.07	0.09	0.53
Hf	0.60	0.64	0.69	1.50	0.30	0.63
Ta	0.03	0.05	-0.02	-0.06	-0.06	LOD
W	1.04	1.47	0.01	0.22	3.48	2.37
Tl	0.32	0.60	0.74	0.12	2.27	5.39
Pb	90.58	18.30	5.49	882.45	5243.07	839.15
Bi	LOD	LOD	0.00	LOD	LOD	LOD
Th	-0.44	0.06	0.53	-0.22	-0.42	0.05
U	0.58	0.29	0.08	1.27	1.16	7.29

Appendix D: Quality Control and Quality Assurance

Quality control and quality assurance were monitored using internal certified references materials (Appendix D.1) and duplicates performed by Actlabs (Appendix D.2). Internal reference materials include a matrix matched basalt (BAMAP-01) and granodiorite (GSP-2) standard from the USGS. The reference materials were sent as pulps and inserted as unknowns after every 25th sample. Precision and accuracy calculations were completed using relative standard deviation (RSD_i (%); Jenner, 1996) and percent relative difference (RD_i (%) and used to monitor the laboratories performance.

$$(1)\quad RSDi\ (\%) = 100 * \frac{Si}{\mu i}$$

$$(2)\quad RDi\ (\%) = 100 * \left(\frac{\mu i - ci}{ci}\right)$$

Table D.1: Internal Certified Reference Material

Appendix D.1 Internal Certified Reference Material (BAMAP-01)

Analyte Symbol	Unit Symbol	Detection Limit	Analysis Method	BAMAP-01	BAMAP-01	BAMAP-01	BAMAP-01	BAMAP-01	Accepted Values	Accuracy
SiO_2	%	0.01	FUS-ICP	48.42	48.17	48.27	48.16	49.4	–	–
Al_2O_3	%	0.01	FUS-ICP	14.84	15.31	15.16	15.74	15.18	15.24	0.00
Fe_2O_3	%	0.01	FUS-ICP	12.02	12.5	12.15	12.63	11.98	12.34	-0.03
MnO	%	0.001	FUS-ICP	0.153	0.157	0.151	0.155	0.156	0.16	-0.18
MgO	%	0.01	FUS-ICP	8.08	8.16	7.8	7.8	8.08	8.18	-0.12
CaO	%	0.01	FUS-ICP	8.24	8.3	8.25	8.32	8.5	8.33	0.00
Na_2O	%	0.01	FUS-ICP	3.8	3.79	3.79	3.76	3.77	4	-0.27
K_2O	%	0.01	FUS-ICP	1.57	1.51	1.47	1.47	1.5	1.57	-0.21
TiO_2	%	0.001	FUS-ICP	2.236	2.306	2.329	2.44	2.339	2.31	0.04
P_2O_5	%	0.01	FUS-ICP	0.44	0.47	0.52	0.5	0.51	0.45	0.42
LOI	%		FUS-ICP	-0.33	-0.4	-0.11	-0.35	-0.49	–	–
Total	%	0.01	FUS-ICP	99.48	100.3	99.78	100.6	100.9	–	–
Hg	ppb	5	CV-FIMS	< 5	< 5	< 5	< 5	< 5	–	–
Sc	ppm	1	FUS-ICP	19	18	18	18	18	20.1	-0.47
Be	ppm	1	FUS-ICP	2	2	2	2	2	–	–
V	ppm	5	FUS-ICP	217	221	223	230	234	216	0.21
Cr	ppm	20	FUS-MS	270	270	250	250	250	–	–
Co	ppm	1	FUS-MS	48	48	46	43	44	49	-0.33
Ni	ppm	20	FUS-MS	190	180	190	170	180	187	-0.13
Cu	ppm	10	FUS-MS	50	50	50	50	50	57	-0.61
Zn	ppm	30	FUS-MS	110	110	110	120	110	178	-1.85
Ga	ppm	1	FUS-MS	22	22	22	21	21	22	-0.09
Ge	ppm	0.5	FUS-MS	1	0.9	1.4	1.2	1.4	–	–
As	ppm	5	FUS-MS	< 5	< 5	< 5	< 5	< 5	–	–
Rb	ppm	1	FUS-MS	21	21	20	20	19	26.1	-1.13
Sr	ppm	2	FUS-ICP	621	620	627	622	617	<450	–
Y	ppm	0.5	FUS-MS	18.9	19.1	16.5	16.8	16.9	21.3	-0.86
Zr	ppm	1	FUS-ICP	165	168	170	169	170	178	-0.27
Nb	ppm	0.2	FUS-MS	24.2	26	23.4	23.5	24.4	31.13	-1.10
Mo	ppm	2	FUS-MS	< 2	2	< 2	2	2	3	–
Ag	ppm	0.5	FUS-MS	< 0.5	< 0.5	< 0.5	< 0.5	< 0.5	–	–
In	ppm	0.1	FUS-MS	< 0.1	< 0.1	< 0.1	< 0.1	< 0.1	–	–
Sn	ppm	1	FUS-MS	1	1	1	2	2	1.8	-1.11
Sb	ppm	0.2	FUS-MS	< 0.2	< 0.2	< 0.2	0.4	0.5	–	–
Cs	ppm	0.1	FUS-MS	0.3	0.3	0.3	0.3	0.3	0.37	-0.95
Ba	ppm	3	FUS-ICP	301	296	294	292	297	399	-1.29
La	ppm	0.05	FUS-MS	24	24.5	23.5	22.9	22.8	25.2	-0.33
Ce	ppm	0.05	FUS-MS	48.8	50	47.4	45.9	45.9	47.7	-0.01
Pr	ppm	0.01	FUS-MS	5.85	5.88	5.68	5.51	5.57	6.78	-0.80
Nd	ppm	0.05	FUS-MS	24.7	25.4	23.9	23.3	23.2	26	-0.37
Sm	ppm	0.01	FUS-MS	5.66	5.71	5.27	5.31	5.24	5.77	-0.29
Eu	ppm	0.005	FUS-MS	1.95	2.01	1.8	1.77	1.81	1.95	-0.21
Gd	ppm	0.01	FUS-MS	5.16	5.77	4.95	4.55	4.73	5.25	-0.21
Tb	ppm	0.01	FUS-MS	0.73	0.8	0.71	0.71	0.75	0.81	-0.43
Dy	ppm	0.01	FUS-MS	3.95	4.26	3.8	3.85	3.86	4.37	-0.49
Ho	ppm	0.01	FUS-MS	0.71	0.74	0.66	0.66	0.67	0.85	-0.95
Er	ppm	0.01	FUS-MS	1.72	1.84	1.73	1.72	1.65	2.09	-0.86
Tm	ppm	0.005	FUS-MS	0.219	0.258	0.225	0.23	0.212	0.27	-0.76
Yb	ppm	0.01	FUS-MS	1.3	1.55	1.33	1.34	1.24	1.41	-0.21
Lu	ppm	0.002	FUS-MS	0.197	0.215	0.19	0.185	0.189	0.23	-0.76
Hf	ppm	0.1	FUS-MS	3.7	3.9	2.9	3	3	4.5	-1.33
Ta	ppm	0.01	FUS-MS	1.64	1.77	1.68	1.62	1.66	2	-0.82
W	ppm	0.5	FUS-MS	< 0.5	< 0.5	< 0.5	< 0.5	< 0.5	0.39	–
Tl	ppm	0.05	FUS-MS	< 0.05	0.06	< 0.05	0.12	0.08	<0.3	–
Pb	ppm	5	FUS-MS	< 5	< 5	< 5	< 5	< 5	3.1	–
Bi	ppm	0.1	FUS-MS	< 0.1	< 0.1	< 0.1	< 0.1	< 0.1	–	–
Th	ppm	0.05	FUS-MS	2.48	2.47	2.32	2.57	2.57	2.91	-0.74
U	ppm	0.01	FUS-MS	0.6	0.67	0.61	0.71	0.7	0.77	-0.73

Appendix D.1: Internal Certified Reference Material (GSP-2)

Analyte Symbol	Unit Symbol	Detection Limit	Analysis Method	GSP-2	GSP-2	GSP-2	GSP-2	GSP-2	Accepted Values	Accuracy
SiO_2	%	0.01	FUS-ICP	66.51	66.76	64.83	65.91	66.2	–	–
Al_2O_3	%	0.01	FUS-ICP	15.02	14.96	15.39	15.72	14.92	14.9	0.10
Fe_2O_3	%	0.01	FUS-ICP	4.86	4.97	5.01	5.17	4.89	4.9	0.08
MnO	%	0.001	FUS-ICP	0.042	0.042	0.042	0.041	0.043	–	–
MgO	%	0.01	FUS-ICP	0.94	0.93	0.91	0.92	0.93	0.96	-0.18
CaO	%	0.01	FUS-ICP	2.09	2.09	2.11	2.08	2.13	2.1	0.00
Na_2O	%	0.01	FUS-ICP	2.75	2.67	2.72	2.7	2.72	2.78	-0.12
K_2O	%	0.01	FUS-ICP	5.64	5.35	5.36	5.24	5.31	5.38	0.00
TiO_2	%	0.001	FUS-ICP	0.678	0.663	0.708	0.736	0.69	0.66	0.27
P_2O_5	%	0.01	FUS-ICP	0.27	0.28	0.29	0.28	0.29	0.29	-0.14
LOI	%		FUS-ICP	1.11	0.96	1.24	1.13	0.94	–	–
Total	%	0.01	FUS-ICP	99.91	99.67	98.62	99.92	99.06	–	–
Hg	ppb	5	CV-FIMS	17	15	16	15	16	–	–
Sc	ppm	1	FUS-ICP	7	6	7	7	6	6.3	0.24
Be	ppm	1	FUS-ICP	2	2	2	2	2	–	–
V	ppm	5	FUS-ICP	57	56	60	61	62	52	0.69
Cr	ppm	20	FUS-MS	30	30	20	30	30	20	2.00
Co	ppm	1	FUS-MS	7	7	7	7	6	7.3	-0.34
Ni	ppm	20	FUS-MS	< 20	< 20	< 20	< 20	20	17	–
Cu	ppm	10	FUS-MS	40	40	40	40	40	43	-0.35
Zn	ppm	30	FUS-MS	100	110	110	120	110	120	-0.42
Ga	ppm	1	FUS-MS	22	23	24	23	23	22	0.23
Ge	ppm	0.5	FUS-MS	1	1.1	1.8	1.6	1.7	–	–
As	ppm	5	FUS-MS	< 5	< 5	< 5	< 5	< 5	–	–
Rb	ppm	1	FUS-MS	237	239	234	231	228	245	-0.23
Sr	ppm	2	FUS-ICP	251	240	248	249	241	240	0.12
Y	ppm	0.5	FUS-MS	25.1	26.2	23.2	23.6	23.2	28	-0.67
Zr	ppm	1	FUS-ICP	552	544	566	569	567	550	0.09
Nb	ppm	0.2	FUS-MS	17.6	19.3	19.3	20.6	19.8	27	-1.42
Mo	ppm	2	FUS-MS	2	2	2	3	3	–	–
Ag	ppm	0.5	FUS-MS	1.5	1.6	0.9	1.4	1.1	–	–
In	ppm	0.1	FUS-MS	< 0.1	< 0.1	< 0.1	< 0.1	< 0.1	–	–
Sn	ppm	1	FUS-MS	6	6	6	7	9	–	–
Sb	ppm	0.2	FUS-MS	< 0.2	< 0.2	0.2	0.7	0.6	–	–
Cs	ppm	0.1	FUS-MS	1.1	1	1.1	1.1	1	6.3	-4.16
Ba	ppm	3	FUS-ICP	1425	1372	1354	1324	1340	1340	0.09
La	ppm	0.05	FUS-MS	190	193	185	181	182	180	0.17
Ce	ppm	0.05	FUS-MS	451	457	432	424	428	410	0.35
Pr	ppm	0.01	FUS-MS	55.4	55.1	53.1	51.9	52.3	–	–
Nd	ppm	0.05	FUS-MS	203	202	199	195	195	200	-0.03
Sm	ppm	0.01	FUS-MS	26.1	26.6	25.3	24.7	24.5	27	-0.29
Eu	ppm	0.005	FUS-MS	2.32	2.38	2.15	2.2	2.21	2.3	-0.10
Gd	ppm	0.01	FUS-MS	12.1	13.2	11.7	10.4	10.4	–	–
Tb	ppm	0.01	FUS-MS	1.21	1.28	1.27	1.13	1.16	–	–
Dy	ppm	0.01	FUS-MS	5.49	5.63	5.45	5.34	5.22	–	–
Ho	ppm	0.01	FUS-MS	0.88	0.95	0.86	0.87	0.88	–	–
Er	ppm	0.01	FUS-MS	2.3	2.45	2.23	2.3	2.25	–	–
Tm	ppm	0.005	FUS-MS	0.296	0.303	0.283	0.277	0.274	–	–
Yb	ppm	0.01	FUS-MS	1.61	1.65	1.58	1.57	1.56	1.6	-0.02
Lu	ppm	0.002	FUS-MS	0.218	0.228	0.233	0.24	0.234	–	–
Hf	ppm	0.1	FUS-MS	13	14.1	10.6	10.8	10.7	–	–
Ta	ppm	0.01	FUS-MS	0.74	0.85	0.78	0.84	0.84	–	–
W	ppm	0.5	FUS-MS	< 0.5	< 0.5	< 0.5	1.8	< 0.5	–	–
Tl	ppm	0.05	FUS-MS	1.06	1.28	0.91	1.06	0.99	–	–
Pb	ppm	5	FUS-MS	31	33	28	30	31	42	-1.36
Bi	ppm	0.1	FUS-MS	< 0.1	< 0.1	< 0.1	< 0.1	< 0.1		–
Th	ppm	0.05	FUS-MS	103	102	95.8	105	105	105	-0.14
U	ppm	0.01	FUS-MS	2.32	2.42	2.24	2.54	2.56	2.4	0.03

Table D.2: Duplicates

Appendix D.2 Duplicates

Analyte Symbol	Unit Symbol	LOD	LOI	Analysis Method
SiO2	%	0.01	0.03	FUS-ICP
Al2O3	%	0.01	0.03	FUS-ICP
Fe2O3(T)	%	0.01	0.03	FUS-ICP
MnO	%	0.00	0.00	FUS-ICP
MgO	%	0.01	0.03	FUS-ICP
CaO	%	0.01	0.03	FUS-ICP
Na2O	%	0.01	0.03	FUS-ICP
K2O	%	0.01	0.03	FUS-ICP
TiO2	%	0.00	0.00	FUS-ICP
P2O5	%	0.01	0.03	FUS-ICP
LOI	%		0.00	FUS-ICP
Total	%	0.01	0.03	FUS-ICP
Hg	ppb	5.00	16.50	CV-FIMS
Sc	ppm	1.00	3.30	FUS-ICP
Be	ppm	1.00	3.30	FUS-ICP
V	ppm	5.00	16.50	FUS-ICP
Cr	ppm	20.00	66.00	FUS-MS
Co	ppm	1.00	3.30	FUS-MS
Ni	ppm	20.00	66.00	FUS-MS
Cu	ppm	10.00	33.00	FUS-MS
Zn	ppm	30.00	99.00	FUS-MS
Ga	ppm	1.00	3.30	FUS-MS
Ge	ppm	0.50	1.65	FUS-MS
As	ppm	5.00	16.50	FUS-MS
Rb	ppm	1.00	3.30	FUS-MS
Sr	ppm	2.00	6.60	FUS-ICP
Y	ppm	0.50	1.65	FUS-MS
Zr	ppm	1.00	3.30	FUS-ICP
Nb	ppm	0.20	0.66	FUS-MS
Mo	ppm	2.00	6.60	FUS-MS
Ag	ppm	0.50	1.65	FUS-MS
In	ppm	0.10	0.33	FUS-MS
Sn	ppm	1.00	3.30	FUS-MS
Sb	ppm	0.20	0.66	FUS-MS
Cs	ppm	0.10	0.33	FUS-MS
Ba	ppm	3.00	9.90	FUS-ICP
La	ppm	0.05	0.17	FUS-MS
Ce	ppm	0.05	0.17	FUS-MS
Pr	ppm	0.01	0.03	FUS-MS
Nd	ppm	0.05	0.17	FUS-MS
Sm	ppm	0.01	0.03	FUS-MS
Eu	ppm	0.01	0.02	FUS-MS
Gd	ppm	0.01	0.03	FUS-MS
Tb	ppm	0.01	0.03	FUS-MS
Dy	ppm	0.01	0.03	FUS-MS
Ho	ppm	0.01	0.03	FUS-MS
Er	ppm	0.01	0.03	FUS-MS
Tm	ppm	0.01	0.02	FUS-MS
Yb	ppm	0.01	0.03	FUS-MS
Lu	ppm	0.00	0.01	FUS-MS
Hf	ppm	0.10	0.33	FUS-MS
Ta	ppm	0.01	0.03	FUS-MS
W	ppm	0.50	1.65	FUS-MS
Tl	ppm	0.05	0.17	FUS-MS
Pb	ppm	5.00	16.50	FUS-MS
Bi	ppm	0.10	0.33	FUS-MS
Th	ppm	0.05	0.17	FUS-MS
U	ppm	0.01	0.03	FUS-MS

Appendix D.2		25419			25422			STAN-2		
Analyte Symbol	**Unit Symbol**	**Original**	**Duplicate**	**Prec (CV-av %)**	**Original**	**Duplicate**	**Prec (CV-av %)**	**Original**	**Duplicate**	**Prec (CV-av %)**
SiO_2	%	–	–	–	43.45	43.98	-1.21	–	–	–
Al_2O_3	%	–	–	–	19.73	19.37	1.86	–	–	–
Fe_2O_3	%	–	–	–	11.61	11.32	2.56	–	–	–
MnO	%	–	–	–	0.129	0.123	4.88	–	–	–
MgO	%	–	–	–	8.1	8.08	0.25	–	–	–
CaO	%	–	–	–	2.72	2.7	0.74	–	–	–
Na_2O	%	–	–	–	3.22	3.17	1.58	–	–	–
K_2O	%	–	–	–	1.93	1.95	-1.03	–	–	–
TiO_2	%	–	–	–	0.986	0.984	0.20	–	–	–
P_2O_5	%	–	–	–	0.02	0.04	-50.00	–	–	–
LOI	%	–	–	–	8.48	8.48	0.00	–	–	–
Total	%	–	–	–	100.4	100.2	0.20	–	–	–
Hg	ppb	< 5	9	–	–	–	–	< 5	< 5	–
Sc	ppm	–	–	–	35	36	-2.78	–	–	–
Be	ppm	–	–	–	< 1	1	–	–	–	–
V	ppm	–	–	–	278	282	-1.42	–	–	–
Cr	ppm	–	–	–	110	110	0.00	–	–	–
Co	ppm	–	–	–	44	43	2.33	–	–	–
Ni	ppm	–	–	–	60	60	0.00	–	–	–
Cu	ppm	–	–	–	30	30	0.00	–	–	–
Zn	ppm	–	–	–	100	100	0.00	–	–	–
Ga	ppm	–	–	–	18	19	-5.26	–	–	–
Ge	ppm	–	–	–	0.9	1	-10.00	–	–	–
As	ppm	–	–	–	55	55	0.00	–	–	–
Rb	ppm	–	–	–	31	31	0.00	–	–	–
Sr	ppm	–	–	–	58	56	3.57	–	–	–
Y	ppm	–	–	–	16.8	14.8	13.51	–	–	–
Zr	ppm	–	–	–	64	64	0.00	–	–	–
Nb	ppm	–	–	–	0.3	0.3	0.00	–	–	–
Mo	ppm	–	–	–	< 2	< 2	–	–	–	–
Ag	ppm	–	–	–	< 0.5	< 0.5	–	–	–	–
In	ppm	–	–	–	< 0.1	< 0.1	–	–	–	–
Sn	ppm	–	–	–	< 1	< 1	–	–	–	–
Sb	ppm	–	–	–	0.5	0.5	0.00	–	–	–
Cs	ppm	–	–	–	0.2	0.2	0.00	–	–	–
Ba	ppm	–	–	–	347	353	-1.70	–	–	–
La	ppm	–	–	–	4.53	4.25	6.59	–	–	–
Ce	ppm	–	–	–	10.7	10.3	3.88	–	–	–
Pr	ppm	–	–	–	1.42	1.39	2.16	–	–	–
Nd	ppm	–	–	–	7.16	6.85	4.53	–	–	–
Sm	ppm	–	–	–	2.21	2.07	6.76	–	–	–
Eu	ppm	–	–	–	0.682	0.642	6.23	–	–	–
Gd	ppm	–	–	–	2.8	2.61	7.28	–	–	–
Tb	ppm	–	–	–	0.52	0.48	8.33	–	–	–
Dy	ppm	–	–	–	3.44	3.05	12.79	–	–	–
Ho	ppm	–	–	–	0.72	0.63	14.29	–	–	–
Er	ppm	–	–	–	2.13	1.88	13.30	–	–	–
Tm	ppm	–	–	–	0.317	0.291	8.93	–	–	–
Yb	ppm	–	–	–	2.16	1.99	8.54	–	–	–
Lu	ppm	–	–	–	0.342	0.321	6.54	–	–	–
Hf	ppm	–	–	–	1.4	1.4	0.00	–	–	–
Ta	ppm	–	–	–	0.11	0.1	10.00	–	–	–
W	ppm	–	–	–	< 0.5	< 0.5	–	–	–	–
Tl	ppm	–	–	–	0.09	0.06	50.00	–	–	–
Pb	ppm	–	–	–	< 5	< 5	–	–	–	–
Bi	ppm	–	–	–	< 0.1	< 0.1	–	–	–	–
Th	ppm	–	–	–	1.19	1.16	2.59	–	–	–
U	ppm	–	–	–	0.59	0.57	3.51	–	–	–

Appendix D.2		14469			14474			14516		
Analyte Symbol	**Unit Symbol**	**Original**	**Duplicate**	**Prec (CV-av %)**	**Original**	**Duplicate**	**Prec (CV-av %)**	**Original**	**Duplicate**	**Prec (CV-av %)**
SiO_2	%	39.85	41.47	-3.91	80.18	79.5	0.86	–	–	–
Al_2O_3	%	19.14	18.87	1.43	7.35	7.62	-3.54	–	–	–
Fe_2O_3	%	12.84	12.79	0.39	4.27	4.42	-3.39	–	–	–
MnO	%	0.058	0.059	-1.69	0.031	0.032	-3.13	–	–	–
MgO	%	14.77	14.64	0.89	1.58	1.6	-1.25	–	–	–
CaO	%	0.2	0.21	-4.76	0.37	0.37	0.00	–	–	–
Na_2O	%	2.63	2.74	-4.01	0.51	0.51	0.00	–	–	–
K_2O	%	0.13	0.12	8.33	2.13	2.15	-0.93	–	–	–
TiO_2	%	0.837	0.857	-2.33	0.282	0.29	-2.76	–	–	–
P_2O_5	%	0.08	0.1	-20.00	0.03	< 0.01	–	–	–	–
LOI	%	8.34	8.25	1.09	2.47	2.47	0.00	–	–	–
Total	%	98.89	100.1	-1.21	99.19	98.97	0.22	–	–	–
Hg	ppb	< 5	< 5	–	–	–	–	< 5	< 5	–
Sc	ppm	24	25	-4.00	8	8	0.00	–	–	–
Be	ppm	< 1	< 1	–	1	1	0.00	–	–	–
V	ppm	315	316	-0.32	185	186	-0.54	–	–	–
Cr	ppm	30	40	-25.00	< 20	< 20	–	–	–	–
Co	ppm	33	33	0.00	4	4	0.00	–	–	–
Ni	ppm	30	30	0.00	< 20	< 20	–	–	–	–
Cu	ppm	20	20	0.00	10	10	0.00	–	–	–
Zn	ppm	120	120	0.00	100	100	0.00	–	–	–
Ga	ppm	19	18	5.56	9	9	0.00	–	–	–
Ge	ppm	1.1	0.9	22.22	0.6	0.7	-14.29	–	–	–
As	ppm	40	36	11.11	24	22	9.09	–	–	–
Rb	ppm	2	2	0.00	34	34	0.00	–	–	–
Sr	ppm	16	16	0.00	11	10	10.00	–	–	–
Y	ppm	22	21.7	1.38	21.7	21.6	0.46	–	–	–
Zr	ppm	92	95	-3.16	76	70	8.57	–	–	–
Nb	ppm	1.8	1.8	0.00	0.3	< 0.2	–	–	–	–
Mo	ppm	3	3	0.00	4	4	0.00	–	–	–
Ag	ppm	< 0.5	< 0.5	–	< 0.5	< 0.5	–	–	–	–
In	ppm	< 0.1	< 0.1	–	< 0.1	< 0.1	–	–	–	–
Sn	ppm	< 1	< 1	–	< 1	< 1	–	–	–	–
Sb	ppm	0.6	1.1	-45.45	1.3	1.2	8.33	–	–	–
Cs	ppm	< 0.1	< 0.1	–	0.3	0.3	0.00	–	–	–
Ba	ppm	38	41	-7.32	331	332	-0.30	–	–	–
La	ppm	4.79	4.77	0.42	12.8	13.4	-4.48	–	–	–
Ce	ppm	10.8	10.6	1.89	28.8	29.7	-3.03	–	–	–
Pr	ppm	1.45	1.39	4.32	3.73	3.8	-1.84	–	–	–
Nd	ppm	6.84	6.46	5.88	17	16.8	1.19	–	–	–
Sm	ppm	2.1	1.88	11.70	4.21	4.17	0.96	–	–	–
Eu	ppm	0.754	0.694	8.65	1.39	1.39	0.00	–	–	–
Gd	ppm	3.15	2.87	9.76	4.32	4.3	0.47	–	–	–
Tb	ppm	0.61	0.57	7.02	0.72	0.71	1.41	–	–	–
Dy	ppm	4.03	3.79	6.33	4.33	4.32	0.23	–	–	–
Ho	ppm	0.89	0.84	5.95	0.88	0.88	0.00	–	–	–
Er	ppm	2.82	2.61	8.05	2.72	2.67	1.87	–	–	–
Tm	ppm	0.443	0.415	6.75	0.435	0.411	5.84	–	–	–
Yb	ppm	2.93	2.8	4.64	3.02	2.95	2.37	–	–	–
Lu	ppm	0.495	0.48	3.13	0.488	0.478	2.09	–	–	–
Hf	ppm	2	2	0.00	1.4	1.3	7.69	–	–	–
Ta	ppm	0.16	0.19	-15.79	0.16	0.14	14.29	–	–	–
W	ppm	1.6	4.3	-62.79	< 0.5	< 0.5	–	–	–	–
Tl	ppm	< 0.05	< 0.05	–	< 0.05	< 0.05	–	–	–	–
Pb	ppm	< 5	< 5	–	30	33	-9.09	–	–	–
Bi	ppm	< 0.1	< 0.1	–	< 0.1	< 0.1	–	–	–	–
Th	ppm	2.4	2.77	-13.36	2.43	2.44	-0.41	–	–	–
U	ppm	1.37	1.62	-15.43	1.87	1.84	1.63	–	–	–

Appendix D.2		14540			14547			STANDARD-2		
Analyte Symbol	**Unit Symbol**	**Original**	**Duplicate**	**Prec (CV-av %)**	**Original**	**Duplicate**	**Prec (CV-av %)**	**Original**	**Duplicate**	**Prec (CV-av %)**
SiO_2	%	66.83	65.71	1.70	61.09	61.51	-0.68	–	–	–
Al_2O_3	%	14.73	14.76	-0.20	14.87	14.59	1.92	–	–	–
Fe_2O_3	%	5.24	5.26	-0.38	5.64	5.55	1.62	–	–	–
MnO	%	0.041	0.042	-2.38	0.434	0.436	-0.46	–	–	–
MgO	%	2.89	2.93	-1.37	3.89	4.03	-3.47	–	–	–
CaO	%	0.48	0.49	-2.04	2.41	2.44	-1.23	–	–	–
Na_2O	%	4.86	4.84	0.41	2.56	2.64	-3.03	–	–	–
K_2O	%	1.19	1.2	-0.83	1.49	1.59	-6.29	–	–	–
TiO_2	%	0.474	0.466	1.72	0.566	0.539	5.01	–	–	–
P_2O_5	%	0.05	0.04	25.00	0.13	0.11	18.18	–	–	–
LOI	%	3.37	3.37	0.00	7.07	7.1	-0.42	–	–	–
Total	%	100.1	99.11	1.00	100.2	100.5	-0.30	–	–	–
Hg	ppb	–	–	–	12	12	0.00	< 5	< 5	–
Sc	ppm	15	15	0.00	11	13	-15.38	–	–	–
Be	ppm	1	1	0.00	< 1	< 1	–	–	–	–
V	ppm	24	23	4.35	91	94	-3.19	–	–	–
Cr	ppm	< 20	< 20	–	< 20	< 20	–	–	–	–
Co	ppm	2	2	0.00	10	11	-9.09	–	–	–
Ni	ppm	< 20	< 20	–	< 20	< 20	–	–	–	–
Cu	ppm	< 10	< 10	–	30	30	0.00	–	–	–
Zn	ppm	70	70	0.00	400	390	2.56	–	–	–
Ga	ppm	16	16	0.00	14	14	0.00	–	–	–
Ge	ppm	0.8	0.8	0.00	0.7	0.7	0.00	–	–	–
As	ppm	12	12	0.00	21	23	-8.70	–	–	–
Rb	ppm	21	21	0.00	35	35	0.00	–	–	–
Sr	ppm	42	42	0.00	39	40	-2.50	–	–	–
Y	ppm	51.6	51.4	0.39	19.9	20	-0.50	–	–	–
Zr	ppm	232	209	11.00	85	95	-10.53	–	–	–
Nb	ppm	1.1	0.9	22.22	2.3	2	15.00	–	–	–
Mo	ppm	4	4	0.00	< 2	< 2	–	–	–	–
Ag	ppm	< 0.5	< 0.5	–	< 0.5	< 0.5	–	–	–	–
In	ppm	0.1	0.1	0.00	0.2	0.1	100.00	–	–	–
Sn	ppm	1	< 1	–	< 1	< 1	–	–	–	–
Sb	ppm	1.1	0.9	22.22	1.2	1.3	-7.69	–	–	–
Cs	ppm	0.2	0.2	0.00	0.3	0.3	0.00	–	–	–
Ba	ppm	482	487	-1.03	201	212	-5.19	–	–	–
La	ppm	18.6	18.4	1.09	8.46	8.15	3.80	–	–	–
Ce	ppm	46.4	46.5	-0.22	18	17.5	2.86	–	–	–
Pr	ppm	6.27	6.29	-0.32	2.29	2.13	7.51	–	–	–
Nd	ppm	29.2	29.7	-1.68	9.51	9.25	2.81	–	–	–
Sm	ppm	7.59	7.78	-2.44	2.63	2.46	6.91	–	–	–
Eu	ppm	1.71	1.73	-1.16	0.794	0.784	1.28	–	–	–
Gd	ppm	8.01	8.07	-0.74	2.81	2.85	-1.40	–	–	–
Tb	ppm	1.49	1.42	4.93	0.54	0.52	3.85	–	–	–
Dy	ppm	9.93	9.84	0.91	3.41	3.39	0.59	–	–	–
Ho	ppm	2.11	2.15	-1.86	0.74	0.75	-1.33	–	–	–
Er	ppm	6.5	6.67	-2.55	2.22	2.28	-2.63	–	–	–
Tm	ppm	1.02	1.03	-0.97	0.358	0.365	-1.92	–	–	–
Yb	ppm	7	6.83	2.49	2.51	2.61	-3.83	–	–	–
Lu	ppm	1.1	1.11	-0.90	0.418	0.428	-2.34	–	–	–
Hf	ppm	4.5	4.1	9.76	1.8	1.9	-5.26	–	–	–
Ta	ppm	0.2	0.17	17.65	0.22	0.2	10.00	–	–	–
W	ppm	< 0.5	< 0.5	–	1.1	3.8	-71.05	–	–	–
Tl	ppm	0.22	0.24	-8.33	0.24	0.19	26.32	–	–	–
Pb	ppm	6	6	0.00	19	12	58.33	–	–	–
Bi	ppm	< 0.1	< 0.1	–	< 0.1	< 0.1	–	–	–	–
Th	ppm	4.32	4.41	-2.04	2.45	2.43	0.82	–	–	–
U	ppm	1.12	1.18	-5.08	0.7	0.77	-9.09	–	–	–

Appendix D.2		14500			32005			14498		
Analyte Symbol	Unit Symbol	Original	Duplicate	Prec (CV-av %)	Original	Duplicate	Prec (CV-av %)	Original	Duplicate	Prec (CV-av %)
SiO_2	%	64.86	64.68	0.28	49.19	48.39	1.65	–	–	–
Al_2O_3	%	13.58	13.44	1.04	14.41	14.77	-2.44	–	–	–
Fe_2O_3	%	8.27	8.21	0.73	7.01	7.08	-0.99	–	–	–
MnO	%	0.053	0.054	-1.85	0.486	0.492	-1.22	–	–	–
MgO	%	1.48	1.47	0.68	11.02	11.17	-1.34	–	–	–
CaO	%	0.43	0.43	0.00	4.15	4.2	-1.19	–	–	–
Na_2O	%	0.39	0.39	0.00	0.44	0.44	0.00	–	–	–
K_2O	%	3.29	3.25	1.23	1.28	1.28	0.00	–	–	–
TiO_2	%	0.562	0.557	0.90	0.593	0.587	1.02	–	–	–
P_2O_5	%	0.06	0.08	-25.00	0.04	0.06	-33.33	–	–	–
LOI	%	6.18	6.19	-0.16	10.85	10.85	0.00	–	–	–
Total	%	99.17	98.76	0.42	99.46	99.31	0.15	–	–	–
Hg	ppb	81	83	-2.41	–	–	–	< 5	< 5	–
Sc	ppm	24	23	4.35	21	21	0.00	–	–	–
Be	ppm	< 1	< 1	–	< 1	< 1	–	–	–	–
V	ppm	153	159	-3.77	148	151	-1.99	–	–	–
Cr	ppm	60	50	20.00	30	30	0.00	–	–	–
Co	ppm	19	19	0.00	16	16	0.00	–	–	–
Ni	ppm	< 20	20	–	< 20	< 20	–	–	–	–
Cu	ppm	40	40	0.00	20	20	0.00	–	–	–
Zn	ppm	600	620	-3.23	400	410	-2.44	–	–	–
Ga	ppm	13	13	0.00	13	13	0.00	–	–	–
Ge	ppm	0.8	0.9	-11.11	0.6	0.6	0.00	–	–	–
As	ppm	160	228	-29.82	53	58	-8.62	–	–	–
Rb	ppm	68	68	0.00	28	29	-3.45	–	–	–
Sr	ppm	17	17	0.00	54	54	0.00	–	–	–
Y	ppm	20.3	19.9	2.01	15.3	15.5	-1.29	–	–	–
Zr	ppm	43	40	7.50	54	51	5.88	–	–	–
Nb	ppm	0.5	0.4	25.00	0.4	0.4	0.00	–	–	–
Mo	ppm	3	3	0.00	< 2	< 2	–	–	–	–
Ag	ppm	< 0.5	< 0.5	–	< 0.5	< 0.5	–	–	–	–
In	ppm	0.1	< 0.1	–	< 0.1	< 0.1	–	–	–	–
Sn	ppm	1	2	-50.00	2	2	0.00	–	–	–
Sb	ppm	3.4	3.9	-12.82	1.5	1.4	7.14	–	–	–
Cs	ppm	0.5	0.5	0.00	0.3	0.3	0.00	–	–	–
Ba	ppm	494	496	-0.40	168	170	-1.18	–	–	–
La	ppm	4	4.06	-1.48	4.06	4.21	-3.56	–	–	–
Ce	ppm	8.96	9.17	-2.29	10.2	9.97	2.31	–	–	–
Pr	ppm	1.21	1.19	1.68	1.47	1.46	0.68	–	–	–
Nd	ppm	6	5.65	6.19	7.27	7.57	-3.96	–	–	–
Sm	ppm	1.98	1.98	0.00	2.14	2.28	-6.14	–	–	–
Eu	ppm	0.323	0.339	-4.72	0.329	0.322	2.17	–	–	–
Gd	ppm	2.61	2.75	-5.09	2.34	2.43	-3.70	–	–	–
Tb	ppm	0.53	0.52	1.92	0.42	0.43	-2.33	–	–	–
Dy	ppm	3.6	3.47	3.75	2.73	2.72	0.37	–	–	–
Ho	ppm	0.79	0.79	0.00	0.59	0.6	-1.67	–	–	–
Er	ppm	2.33	2.42	-3.72	1.77	1.82	-2.75	–	–	–
Tm	ppm	0.366	0.369	-0.81	0.287	0.283	1.41	–	–	–
Yb	ppm	2.45	2.39	2.51	1.99	1.9	4.74	–	–	–
Lu	ppm	0.405	0.373	8.58	0.328	0.311	5.47	–	–	–
Hf	ppm	1	0.9	11.11	1.2	1.1	9.09	–	–	–
Ta	ppm	0.09	0.08	12.50	0.1	0.09	11.11	–	–	–
W	ppm	2	2.1	-4.76	1.6	1.6	0.00	–	–	–
Tl	ppm	0.98	1.13	-13.27	0.18	0.13	38.46	–	–	–
Pb	ppm	297	380	-21.84	181	196	-7.65	–	–	–
Bi	ppm	0.3	0.4	-25.00	< 0.1	< 0.1	–	–	–	–
Th	ppm	1.17	1.18	-0.85	0.8	0.79	1.27	–	–	–
U	ppm	0.9	0.91	-1.10	0.34	0.35	-2.86	–	–	–

Appendix D.2		32002			32152			14769		
Analyte Symbol	Unit Symbol	Original	Duplicate	Prec (CV-av %)	Original	Duplicate	Prec (CV-av %)	Original	Duplicate	Prec (CV-av %)
SiO_2	%	61.49	61.18	0.51	–	–	–	66.39	65.74	0.70
Al_2O_3	%	15.24	14.71	3.60	–	–	–	15.12	14.74	1.80
Fe_2O_3	%	5.03	4.86	3.50	–	–	–	4.64	4.57	1.07
MnO	%	0.162	0.156	3.85	–	–	–	0.06	0.06	1.21
MgO	%	1.57	1.52	3.29	–	–	–	3.36	3.31	1.06
CaO	%	3.5	3.44	1.74	–	–	–	1.01	1.00	0.70
Na_2O	%	4.11	4.04	1.73	–	–	–	2.98	2.93	1.20
K_2O	%	1.69	1.66	1.81	–	–	–	2.74	2.68	1.57
TiO_2	%	1.077	1.031	4.46	–	–	–	0.69	0.67	1.56
P_2O_5	%	0.36	0.37	-2.70	–	–	–	0.14	0.14	0.00
LOI	%	6.74	6.74	0.00	–	–	–	3.68	3.68	0.00
Total	%	101	99.72	1.28	–	–	–	100.80	99.50	0.92
Hg	ppb	–	–	–	146.00	150.00	1.91	–	–	–
Sc	ppm	14	14	0.00	–	–	–	16.00	16.00	0.00
Be	ppm	2	2	0.00	–	–	–	2.00	1.00	47.14
V	ppm	83	82	1.22	–	–	–	28.00	27.00	2.57
Cr	ppm	< 20	< 20	–	–	–	–	< 20	< 20	–
Co	ppm	6	6	0.00	–	–	–	5.00	5.00	0.00
Ni	ppm	< 20	< 20	–	–	–	–	< 20	< 20	–
Cu	ppm	20	< 10	–	–	–	–	< 10	< 10	–
Zn	ppm	70	70	0.00	–	–	–	80.00	80.00	0.00
Ga	ppm	17	17	0.00	–	–	–	17.00	17.00	0.00
Ge	ppm	1.1	1.2	-8.33	–	–	–	< 0.5	< 0.5	–
As	ppm	< 5	< 5	–	–	–	–	< 5	< 5	–
Rb	ppm	40	40	0.00	–	–	–	48.00	48.00	0.00
Sr	ppm	169	162	4.32	–	–	–	50.00	49.00	1.43
Y	ppm	29	28.9	0.35	–	–	–	52.80	54.40	2.11
Zr	ppm	184	182	1.10	–	–	–	183.00	186.00	1.15
Nb	ppm	4.5	4.8	-6.25	–	–	–	2.50	2.70	5.44
Mo	ppm	< 2	< 2	–	–	–	–	2.00	< 2	–
Ag	ppm	< 0.5	< 0.5	–	–	–	–	< 0.5	< 0.5	–
In	ppm	< 0.1	< 0.1	–	–	–	–	< 0.1	< 0.1	–
Sn	ppm	1	1	0.00	–	–	–	1.00	< 1	–
Sb	ppm	2	1.9	5.26	–	–	–	0.50	< 0.2	–
Cs	ppm	0.4	0.4	0.00	–	–	–	0.30	0.30	0.00
Ba	ppm	572	563	1.60	–	–	–	458.00	451.00	1.09
La	ppm	23.9	23.7	0.84	–	–	–	17.80	17.40	1.61
Ce	ppm	49.5	48.5	2.06	–	–	–	42.90	41.50	2.35
Pr	ppm	5.79	5.72	1.22	–	–	–	5.69	5.55	1.76
Nd	ppm	24.7	23.8	3.78	–	–	–	25.80	25.70	0.27
Sm	ppm	5.67	5.46	3.85	–	–	–	6.93	7.09	1.61
Eu	ppm	1.55	1.53	1.31	–	–	–	1.99	2.02	1.06
Gd	ppm	5.26	5.38	-2.23	–	–	–	7.73	7.66	0.64
Tb	ppm	0.88	0.9	-2.22	–	–	–	1.37	1.42	2.53
Dy	ppm	5.46	5.38	1.49	–	–	–	8.97	9.31	2.63
Ho	ppm	1.11	1.11	0.00	–	–	–	1.88	1.97	3.31
Er	ppm	3.32	3.23	2.79	–	–	–	5.65	5.91	3.18
Tm	ppm	0.484	0.469	3.20	–	–	–	0.87	0.91	3.11
Yb	ppm	3.05	3.12	-2.24	–	–	–	5.90	6.09	2.24
Lu	ppm	0.492	0.481	2.29	–	–	–	0.93	0.96	2.39
Hf	ppm	3.4	3.4	0.00	–	–	–	4.20	4.60	6.43
Ta	ppm	0.4	0.39	2.56	–	–	–	0.06	0.10	35.36
W	ppm	3.2	3.9	-17.95	–	–	–	< 0.5	< 0.5	–
Tl	ppm	0.32	0.29	10.34	–	–	–	0.37	0.30	14.78
Pb	ppm	8	8	0.00	–	–	–	11.00	13.00	11.79
Bi	ppm	< 0.1	< 0.1	–	–	–	–	< 0.1	< 0.1	–
Th	ppm	6.58	6.43	2.33	–	–	–	4.59	4.79	3.02
U	ppm	2.23	2.34	-4.70	–	–	–	1.56	1.62	2.67

Appendix D.2		STAN-2			31935			32178		
Analyte Symbol	**Unit Symbol**	**Original**	**Duplicate**	**Prec (CV-av %)**	**Original**	**Duplicate**	**Prec (CV-av %)**	**Original**	**Duplicate**	**Prec (CV-av %)**
SiO_2	%	–	–	–	62.06	62.84	0.88			
Al_2O_3	%	–	–	–	13.52	13.78	1.35			
Fe_2O_3	%	–	–	–	8.31	8.52	1.76			
MnO	%	–	–	–	0.30	0.31	2.53			
MgO	%	–	–	–	4.94	5.06	1.70			
CaO	%	–	–	–	0.90	0.93	2.32			
Na_2O	%	–	–	–	0.77	0.79	1.81			
K_2O	%	–	–	–	1.66	1.70	1.68			
TiO_2	%	–	–	–	0.60	0.61	1.40			
P_2O_5	%	–	–	–	0.05	0.04	15.71			
LOI	%	–	–	–	5.90	5.90	0.00			
Total	%	–	–	–	99.01	100.50	1.06			
Hg	ppb	< 5	< 5	–	–	–	–	< 5	< 5	
Sc	ppm	–	–	–	21.00	21.00	0.00			
Be	ppm	–	–	–	< 1	< 1	–			
V	ppm	–	–	–	176.00	183.00	2.76			
Cr	ppm	–	–	–	50.00	60.00	12.86			
Co	ppm	–	–	–	17.00	17.00	0.00			
Ni	ppm	–	–	–	< 20	< 20	–			
Cu	ppm	–	–	–	40.00	40.00	0.00			
Zn	ppm	–	–	–	360.00	370.00	1.94			
Ga	ppm	–	–	–	13.00	13.00	0.00			
Ge	ppm	–	–	–	< 0.5	< 0.5	–			
As	ppm	–	–	–	74.00	76.00	1.89			
Rb	ppm	–	–	–	39.00	40.00	1.79			
Sr	ppm	–	–	–	18.00	19.00	3.82			
Y	ppm	–	–	–	19.10	19.60	1.83			
Zr	ppm	–	–	–	34.00	36.00	4.04			
Nb	ppm	–	–	–	< 0.2	< 0.2	–			
Mo	ppm	–	–	–	< 2	< 2	–			
Ag	ppm	–	–	–	< 0.5	< 0.5	–			
In	ppm	–	–	–	< 0.1	< 0.1	–			
Sn	ppm	–	–	–	< 1	< 1	–			
Sb	ppm	–	–	–	0.80	1.00	15.71			
Cs	ppm	–	–	–	0.30	0.30	0.00			
Ba	ppm	–	–	–	270.00	276.00	1.55			
La	ppm	–	–	–	2.92	2.92	0.00			
Ce	ppm	–	–	–	7.46	7.64	1.69			
Pr	ppm	–	–	–	1.09	1.14	3.17			
Nd	ppm	–	–	–	5.35	5.59	3.10			
Sm	ppm	–	–	–	1.81	1.98	6.34			
Eu	ppm	–	–	–	0.28	0.24	11.22			
Gd	ppm	–	–	–	2.42	2.82	10.80			
Tb	ppm	–	–	–	0.46	0.52	8.66			
Dy	ppm	–	–	–	3.26	3.46	4.21			
Ho	ppm	–	–	–	0.67	0.71	4.10			
Er	ppm	–	–	–	1.93	2.08	5.29			
Tm	ppm	–	–	–	0.31	0.32	4.04			
Yb	ppm	–	–	–	2.09	2.23	4.58			
Lu	ppm	–	–	–	0.30	0.34	7.54			
Hf	ppm	–	–	–	0.90	1.00	7.44			
Ta	ppm	–	–	–	< 0.01	< 0.01	–			
W	ppm	–	–	–	0.70	0.70	0.00			
Tl	ppm	–	–	–	0.33	0.30	6.73			
Pb	ppm	–	–	–	108.00	111.00	1.94			
Bi	ppm	–	–	–	< 0.1	< 0.1	–			
Th	ppm	–	–	–	0.41	0.42	1.70			
U	ppm	–	–	–	0.12	0.13	5.66			

Appendix D.2		32152			14769			STAN-2		
Analyte Symbol	**Unit Symbol**	**Original**	**Duplicate**	**Prec (CV-av %)**	**Original**	**Duplicate**	**Prec (CV-av %)**	**Original**	**Duplicate**	**Prec (CV-av %)**
SiO_2	%	–	–	–	66.39	65.74	0.70	–	–	–
Al_2O_3	%	–	–	–	15.12	14.74	1.80	–	–	–
Fe_2O_3	%	–	–	–	4.64	4.57	1.07	–	–	–
MnO	%	–	–	–	0.06	0.06	1.21	–	–	–
MgO	%	–	–	–	3.36	3.31	1.06	–	–	–
CaO	%	–	–	–	1.01	1.00	0.70	–	–	–
Na_2O	%	–	–	–	2.98	2.93	1.20	–	–	–
K_2O	%	–	–	–	2.74	2.68	1.57	–	–	–
TiO_2	%	–	–	–	0.69	0.67	1.56	–	–	–
P_2O_5	%	–	–	–	0.14	0.14	0.00	–	–	–
LOI	%	–	–	–	3.68	3.68	0.00	–	–	–
Total	%	–	–	–	100.80	99.50	0.92	–	–	–
Hg	ppb	146.00	150.00	1.91	–	–	–	< 5	< 5	–
Sc	ppm	–	–	–	16.00	16.00	0.00	–	–	–
Be	ppm	–	–	–	2.00	1.00	47.14	–	–	–
V	ppm	–	–	–	28.00	27.00	2.57	–	–	–
Cr	ppm	–	–	–	< 20	< 20	–	–	–	–
Co	ppm	–	–	–	5.00	5.00	0.00	–	–	–
Ni	ppm	–	–	–	< 20	< 20	–	–	–	–
Cu	ppm	–	–	–	< 10	< 10	–	–	–	–
Zn	ppm	–	–	–	80.00	80.00	0.00	–	–	–
Ga	ppm	–	–	–	17.00	17.00	0.00	–	–	–
Ge	ppm	–	–	–	< 0.5	< 0.5	–	–	–	–
As	ppm	–	–	–	< 5	< 5	–	–	–	–
Rb	ppm	–	–	–	48.00	48.00	0.00	–	–	–
Sr	ppm	–	–	–	50.00	49.00	1.43	–	–	–
Y	ppm	–	–	–	52.80	54.40	2.11	–	–	–
Zr	ppm	–	–	–	183.00	186.00	1.15	–	–	–
Nb	ppm	–	–	–	2.50	2.70	5.44	–	–	–
Mo	ppm	–	–	–	2.00	< 2	–	–	–	–
Ag	ppm	–	–	–	< 0.5	< 0.5	–	–	–	–
In	ppm	–	–	–	< 0.1	< 0.1	–	–	–	–
Sn	ppm	–	–	–	1.00	< 1	–	–	–	–
Sb	ppm	–	–	–	0.50	< 0.2	–	–	–	–
Cs	ppm	–	–	–	0.30	0.30	0.00	–	–	–
Ba	ppm	–	–	–	458.00	451.00	1.09	–	–	–
La	ppm	–	–	–	17.80	17.40	1.61	–	–	–
Ce	ppm	–	–	–	42.90	41.50	2.35	–	–	–
Pr	ppm	–	–	–	5.69	5.55	1.76	–	–	–
Nd	ppm	–	–	–	25.80	25.70	0.27	–	–	–
Sm	ppm	–	–	–	6.93	7.09	1.61	–	–	–
Eu	ppm	–	–	–	1.99	2.02	1.06	–	–	–
Gd	ppm	–	–	–	7.73	7.66	0.64	–	–	–
Tb	ppm	–	–	–	1.37	1.42	2.53	–	–	–
Dy	ppm	–	–	–	8.97	9.31	2.63	–	–	–
Ho	ppm	–	–	–	1.88	1.97	3.31	–	–	–
Er	ppm	–	–	–	5.65	5.91	3.18	–	–	–
Tm	ppm	–	–	–	0.87	0.91	3.11	–	–	–
Yb	ppm	–	–	–	5.90	6.09	2.24	–	–	–
Lu	ppm	–	–	–	0.93	0.96	2.39	–	–	–
Hf	ppm	–	–	–	4.20	4.60	6.43	–	–	–
Ta	ppm	–	–	–	0.06	0.10	35.36	–	–	–
W	ppm	–	–	–	< 0.5	< 0.5	–	–	–	–
Tl	ppm	–	–	–	0.37	0.30	14.78	–	–	–
Pb	ppm	–	–	–	11.00	13.00	11.79	–	–	–
Bi	ppm	–	–	–	< 0.1	< 0.1	–	–	–	–
Th	ppm	–	–	–	4.59	4.79	3.02	–	–	–
U	ppm	–	–	–	1.56	1.62	2.67	–	–	–

Appendix D.2		31935			32178		
Analyte Symbol	**Unit Symbol**	**Original**	**Duplicate**	**Prec (CV-av %)**	**Original**	**Duplicate**	**Prec (CV-av %)**
SiO_2	ppb	–	–	–	< 5	< 5	–
Al_2O_3	%	62.06	62.84	0.88	–	–	–
Fe_2O_3	%	13.52	13.78	1.35	–	–	–
MnO	%	8.31	8.52	1.76	–	–	–
MgO	%	0.30	0.31	2.53	–	–	–
CaO	%	4.94	5.06	1.70	–	–	–
Na_2O	%	0.90	0.93	2.32	–	–	–
K_2O	%	0.77	0.79	1.81	–	–	–
TiO_2	%	1.66	1.70	1.68	–	–	–
P_2O_5	%	0.60	0.61	1.40	–	–	–
LOI	%	0.05	0.04	15.71	–	–	–
Total	%	5.90	5.90	0.00	–	–	–
Hg	%	99.01	100.50	1.06	–	–	–
Sc	ppm	21.00	21.00	0.00	–	–	–
Be	ppm	< 1	< 1	–	–	–	–
V	ppm	176.00	183.00	2.76	–	–	–
Cr	ppm	50.00	60.00	12.86	–	–	–
Co	ppm	17.00	17.00	0.00	–	–	–
Ni	ppm	< 20	< 20	–	–	–	–
Cu	ppm	40.00	40.00	0.00	–	–	–
Zn	ppm	360.00	370.00	1.94	–	–	–
Ga	ppm	13.00	13.00	0.00	–	–	–
Ge	ppm	< 0.5	< 0.5	–	–	–	–
As	ppm	74.00	76.00	1.89	–	–	–
Rb	ppm	39.00	40.00	1.79	–	–	–
Sr	ppm	18.00	19.00	3.82	–	–	–
Y	ppm	19.10	19.60	1.83	–	–	–
Zr	ppm	34.00	36.00	4.04	–	–	–
Nb	ppm	< 0.2	< 0.2	–	–	–	–
Mo	ppm	< 2	< 2	–	–	–	–
Ag	ppm	< 0.5	< 0.5	–	–	–	–
In	ppm	< 0.1	< 0.1	–	–	–	–
Sn	ppm	< 1	< 1	–	–	–	–
Sb	ppm	0.80	1.00	15.71	–	–	–
Cs	ppm	0.30	0.30	0.00	–	–	–
Ba	ppm	270.00	276.00	1.55	–	–	–
La	ppm	2.92	2.92	0.00	–	–	–
Ce	ppm	7.46	7.64	1.69	–	–	–
Pr	ppm	1.09	1.14	3.17	–	–	–
Nd	ppm	5.35	5.59	3.10	–	–	–
Sm	ppm	1.81	1.98	6.34	–	–	–
Eu	ppm	0.28	0.24	11.22	–	–	–
Gd	ppm	2.42	2.82	10.80	–	–	–
Tb	ppm	0.46	0.52	8.66	–	–	–
Dy	ppm	3.26	3.46	4.21	–	–	–
Ho	ppm	0.67	0.71	4.10	–	–	–
Er	ppm	1.93	2.08	5.29	–	–	–
Tm	ppm	0.31	0.32	4.04	–	–	–
Yb	ppm	2.09	2.23	4.58	–	–	–
Lu	ppm	0.30	0.34	7.54	–	–	–
Hf	ppm	0.90	1.00	7.44	–	–	–
Ta	ppm	< 0.01	< 0.01	–	–	–	–
W	ppm	0.70	0.70	0.00	–	–	–
Tl	ppm	0.33	0.30	6.73	–	–	–
Pb	ppm	108.00	111.00	1.94	–	–	–
Bi	ppm	< 0.1	< 0.1	–	–	–	–
Th	ppm	0.41	0.42	1.70	–	–	–
U	ppm	0.12	0.13	5.66	–	–	–

Appendix E: TerraSpec™ Data

Appendix E: Table E.1: TerraSpec^{TM} Data for Hurricane Zone

Drill Hole: GA-07-254			**Drill Hole: GA-07-255**			**Drill Hole: GA-14-283**		
Depth	2200W	2255W	Depth	2200W	2255W	Depth	2200W	2255W
7.7	2218.72	*NULL*		2217.87	*NULL*	4.8	2217.2	*NULL*
11.7	2217.43	*NULL*		2219.41	*NULL*	8.9	2216.81	*NULL*
15.8	2217.87	*NULL*	6.3	2219.51	*NULL*	13	2218.01	*NULL*
19.7	2219.43	*NULL*	10.3	2216.99	*NULL*	17.1	2220.34	*NULL*
23.9	2219.94	*NULL*	14.5	2217.68	*NULL*	21.4	2221.56	2253.18
27.9	2219.42	*NULL*	18.7	2218.59	*NULL*	25.3	2219.85	2252.41
32.2	2224.9	2254.1	22.7	2219.8	*NULL*	29.2	2221.92	2255.05
36.5	2220.51	2253.08	26.5	2219.1	*NULL*	33.3	2223.11	2253.42
40.6	2223.46	2255.26	30.7	2224.15	2254.39	37.7	2223.2	2251.68
44.8	2223.92	2255.57	34.9	2220.53	2254.46	41.9	*NULL*	2255.57
49.2	2224.02	2255.62	39.1	2224.63	2255.37	44.2	*NULL*	2255.29
53.3	2223.29	2252.45	43.5	2222.89	2255.21	50.3	*NULL*	2254.78
57.6	*NULL*	2254.13	47.8	2222.71	2253.56	54.7	2226.35	2256.71
61.4	*NULL*	2254.19	51.8	*NULL*	2254.12	59	*NULL*	2252.44
66.2	*NULL*	2254.4	56.2	2223.26	2252.53	63.2	2222.45	2253
70.4	*NULL*	2254.2	60.3	*NULL*	2256.15	67.5	2221.1	*NULL*
74.2	*NULL*	2254.05	64	*NULL*	2254.73	71.6	2222.54	2254.15
78.5	2225.26	2252.9	68	*NULL*	2253.68	75.2	*NULL*	2256.89
82.8	*NULL*	2254.12	72	*NULL*	2254.62	79.5	*NULL*	2256.71
87	2222.56	2253.2	76.2	*NULL*	2254.03	83.5	2215.79	2256.2
91.1	2221.98	2253.8	80	*NULL*	2254.78	87.3	2201.97	*NULL*
95.1	2220.6	*NULL*	83	2222.87	2252.58	91.3	2201.74	2255.47
99.5	2220.78	*NULL*	87.4	2219.64	2254.87	95.3	2200.95	2249.46
103.7	*NULL*	2252.44	91.4	2221.17	*NULL*	99.5	*NULL*	2252.4
108.1	2213.4	2255.26	95.7	2220.97	2250.41	103.6	2214.65	2249.59
112.3	2208.58	2253.96	99.8	2219.77	2254.59	107.8	*NULL*	2256.28
116.2	*NULL*	2255.26	103.9	2212.64	2254.18	111.8	*NULL*	2256.26
120.1	2203.71	2250.34	108	2211.26	2254.57	115.9	*NULL*	2260.38
128.6	*NULL*	2253.43	112	*NULL*	2252.72	120.1	*NULL*	2255.63
132.9	2217.48	2252.75	115.8	*NULL*	2253	124.2	*NULL*	2254.45
141.2	2213.93	2250.26	120	2220.55	2252.45	128.4	2221.44	2249.02
145.4	2216.29	2251.64	124.2	2215.13	2249.14	132.5	*NULL*	2255.83
149.7	2211.29	*NULL*	136	2214.36	2248.88	140.7	*NULL*	2252.56
161.5	2216.15	*NULL*	139.6	2215.37	*NULL*	145.1	*NULL*	2253.54
165.1	*NULL*	2254.81	143.1	2214.75	2251.43	149.3	*NULL*	2253.44
169.4	2222.47	*NULL*	146.5	2213.58	2250.83	153.6	*NULL*	2253.69
173.5	2222.43	*NULL*	150.6	*NULL*	2255.61	157.9	*NULL*	2255.24
178	2220.84	*NULL*	154.7	*NULL*	2255.83	162.1	*NULL*	2254.75
182.1	2221.56	*NULL*	158.5	*NULL*	2255.41	166.3	*NULL*	2254.92
186.2	2221.46	*NULL*	162.3	*NULL*	2254.76	17.4	*NULL*	2254.99
190.1	2222.78	2248.82	166.2	*NULL*	2253.59	174.6	*NULL*	2255.56
193.7	*NULL*	2252.59	170.2	*NULL*	2255.49	178.9	2219.88	2248.53
197.8	*NULL*	2254.39	174.1	*NULL*	2254.85	185	*NULL*	2255.68
202.3	*NULL*	2254.48	178.2	2222.17	2249.23	186.9	*NULL*	2256.57
206.2	*NULL*	2253.3	181.9	*NULL*	2254.86	190.9	2208.34	2253.59
210	*NULL*	2255.01	186.6	*NULL*	2255.05	194.9	2208.63	*NULL*
214.3	*NULL*	2253.56	190.5	*NULL*	2255.5	199	2194.38	2257.31
218.3	*NULL*	2254.65	194.6	*NULL*	2253.63	203	2202.7	2252.75
222.6	*NULL*	2254.27	198.8	*NULL*	2254.17	207.2	2201.74	2254.97
226.8	*NULL*	2253.99	203.1	*NULL*	2253.14	211.3	2198.25	*NULL*
231.1	*NULL*	2253.96	206.4	*NULL*	2255.23	215.6	2195.83	*NULL*
235.3	*NULL*	2252.71	210.1	*NULL*	2254.29	219.9	2196.71	*NULL*
239.2	*NULL*	2253.72	214.3	2221.6	*NULL*	224.3	2192.16	2257.3
243.2	*NULL*	2254.12	218.1	2222.41	2251.04	228.5	2195.6	2257.62
247.3	*NULL*	2251.86	222.3	*NULL*	2255.38	232.1	2196.68	2254.96
251.5	*NULL*	2254.18	226.4	*NULL*	2255.25	236.9	2197.65	2253.71
255.7	*NULL*	2254.62	230.4	*NULL*	2254.08	241.2	2197.16	2253.94
260.1	*NULL*	2255.2	234	*NULL*	2255.19	245.8	2197.54	*NULL*
263.7	*NULL*	2252.77	238.1	*NULL*	2254.03	254.1	2197.03	2253.79
271.5	2215.56	*NULL*	242.2	*NULL*	2254.5	258.5	2197.08	2250.86
275.5	2207.04	2249.43	246.3	*NULL*	2254.78	262.8	2196.57	2253.53
279.8	2205.18	2249.82	250.3	2212.43	2253.02	267	2196.89	2253.27
283.8	*NULL*	2250.74	257.1	2203.49	2254.3	271.1	2198.1	2253.29
287.9	*NULL*	2250.7	260.1	2209.93	2249.41	272	2196.87	2252.5
292.1	*NULL*	2250.37	276.2	*NULL*	2251.51			
296.4	2200.09	2251.13	280.5	2199.75	2252.02			
300	2199.46	2251.43	284.7	2199.26	2250.98			
304.3	2200.52	2251.94	287.1	*NULL*	2252.95			
308.3	*NULL*	2252.69						
312.6	*NULL*	2252.86						
316.8	*NULL*	2253.41						
320.9	2194.97	2252.66						
322.2	2192.22	2252.39						

Appendix E: Table E.1: TerraSpec^{TM} Data for Hurricane Zone

GA-06-147			GA-07-208			GA-07-209		
Depth	2200W	2255W	Depth	2200W	2255W	Depth	2200W	2255W
6.1	2205.74	*NULL*	5.9	2208.37	*NULL*	5.2	2207.08	*NULL*
10.2	2214.92	*NULL*	10.1	2202.92	*NULL*	9.3	2218.98	*NULL*
14.3	2220.28	*NULL*	14.1	2219.51	*NULL*	13.7	2218.82	*NULL*
18.4	2220.84	*NULL*	18.3	2221.23	*NULL*	17	2221.13	*NULL*
22.55	2221.16	2252.12	22.4	2220.99	*NULL*	21.3	2222.07	*NULL*
26.5	*NULL*	2253.68	26.6	2220.49	*NULL*	25.4	2221.11	*NULL*
30.8	2218.56	*NULL*	31	2217.24	2252.58	29.5	2220.02	2252.24
34.95	2219.54	*NULL*	35.1	*NULL*	2253.28	33.8	*NULL*	2253.74
39.15	2221.65	*NULL*	39.5	2218.88	*NULL*	38	2219.51	*NULL*
42.7	2220.31	2251.16	43.5	2220.11	*NULL*	42.3	2219.98	*NULL*
47.5	2223.26	2252.46	47.8	2222.3	2251.53	46.6	2220.78	2249.45
51.3	*NULL*	2252.44	52.1	2221.2	2249.57	50.7	2223.18	2252.79
55.1	2226.88	2253.6	56	2223.38	2254.01	54.8	2223.7	2253.5
63.9	2223.71	2247.92	60.2	2226.13	2253.03	58.8	*NULL*	2253.87
68.1	*NULL*	2256.25	64.3	*NULL*	2253.31	63	*NULL*	2252.8
76.4	*NULL*	2255.91	68.3	2224.02	2252.09	66.5	2222.39	2249.62
80.8	2222.33	2253.18	72.3	*NULL*	2255.32	69.5	2224.9	2251.24
84.9	*NULL*	2254.59	76.6	*NULL*	2254.37	74.2	2224.86	2252.46
89.1	2216.7	2256	80.8	*NULL*	2255.59	78.2	*NULL*	2253.74
97.5	2217.1	*NULL*	85.1	*NULL*	2255.25	82.4	2217.77	2250.45
101.5	2202.5	2253.82	89.4	*NULL*	2256.5	86.7	2215.02	2253.09
121.6	2206	2256.93	93.6	*NULL*	2256.22	90.85	2215.65	2254.15
125.8	*NULL*	2255.58	98	*NULL*	2256.85	95.1	*NULL*	2255.15
129.3	*NULL*	2255.31	102.1	2221.66	2256	99.4	2222.77	2254.36
133.3	*NULL*	2255.13	106	2215.54	2255.41	103.4	2224.21	2255.09
137.7	2219.76	2251.84	109.6	2209.58	2257.64	107.8	2218.99	2253.2
141.1	2219.88	2248.85	113.9	2214.81	2250.82	112	2214.88	2256.25
145.1	*NULL*	2254.28	118.1	2199.71	2248.64	115.55	2203.12	2255.71
148.4	*NULL*	2253.57	123	2198.89	*NULL*	119.7	*NULL*	2254.38
152.4	*NULL*	2253.66	126.6	*NULL*	2253.44	124	*NULL*	2253.67
156.2	*NULL*	2254.76	130.3	2210.9	2252.3	128.2	2200.91	*NULL*
161	*NULL*	2256.05	134.2	2210.34	2252.74	132.25	2204.16	2253.74
165.2	*NULL*	2255.48	142	*NULL*	2256.16	136.5	2207.3	*NULL*
169.4	*NULL*	2254.22	146.3	*NULL*	2255.35	140.4	2210.96	*NULL*
173.3	*NULL*	2254.07	150.6	*NULL*	2256	144.3	2211.99	2251.05
177.2	*NULL*	2255.41	154.6	*NULL*	2257.08	148.4	2212.46	*NULL*
181	2218.66	*NULL*	159	*NULL*	2255.04	151.95	*NULL*	2255.81
184.9	*NULL*	2256.03	163	*NULL*	2254.51	156	*NULL*	2255.14
188.1	*NULL*	2257.34	167.1	*NULL*	2255.17	164	*NULL*	2255.04
191.9	2200.08	2256.96	170.8	2220.29	*NULL*	168.4	*NULL*	2255.82
196	2206.13	2250.82	175.1	2220.07	*NULL*	172.45	*NULL*	2256.53
200	2200.33	2255.09	179	2220.54	2250.85	176.8	*NULL*	2255.47
204.4	2200.51	*NULL*	183.2	*NULL*	2253.44	181.2	2222.55	2251.19
212.3	2197.81	2253.23	187.3	*NULL*	2256.04	185.15	2220.94	*NULL*
216.2	2197.66	*NULL*	191.5	*NULL*	2255.43	189.1	2221.51	*NULL*
220.5	2197.55	2252.12	196	*NULL*	2253.44	193	*NULL*	2253.44
224.2	2197.64	2252.76	200.1	*NULL*	2252.34	196.8	*NULL*	2254.4
228.3	2197.22	2251.81	204.1	*NULL*	2251.95	200.1	*NULL*	2255.09
232.7	2197.45	*NULL*	208.4	*NULL*	2253.69	204.1	*NULL*	2254.61
236.85	2197.06	2250.59	212.5	*NULL*	2255.99	208.25	*NULL*	2255.27
241.2	2196.54	2253.54	216.2	2218.98	*NULL*	212.2	*NULL*	2254.73
245.4	2196.23	2251.62	219.2	2217.89	*NULL*	216.1	*NULL*	2255.43
249.6	2195.95	2254.43	222.4	*NULL*	2255.05	219.9	*NULL*	2255.61
253.3	2194.69	*NULL*	226	2200.74	2255.71	223.2	*NULL*	2255.44
257.45	2195.85	2254.13	230.1	*NULL*	2256.48	226.2	*NULL*	2254.02
265.75	2196.62	2252.38	233.6	*NULL*	2256.39	230.6	2219.61	2250.64
269.9	2195.91	2253.39	271.3	2192.42	2253.78	234.1	2219.54	2251.74
274	2197.2	2253.6	275.1	2195.66	2252.1	237.55	*NULL*	2256.67
278.2	*NULL*	2252.55	279.1	2196.52	*NULL*	241.85	*NULL*	2254.99
282.25	2197.21	2252.96	283.3	2196.14	2254.52	245.7	*NULL*	2254.47
286.3	2197.64	2252.29	287.6	2196.1	2254.61	250	*NULL*	2257.33
290.5	2197.59	2252.54	291.7	2195.67	2258.53	254.35	2204.6	2250.55
294.4	2195.64	2251.83	296	2195.79	2256.74	258.5	2203.62	*NULL*
298.8	2195.55	2252.57	300.1	2196.06	*NULL*	262.3	2203.92	*NULL*
302.7	*NULL*	2251.7	304.3	2195.86	2255.45	266.5	2203.48	*NULL*
306.4	*NULL*	2251.77	308.4	2195.8	2253.86	270.75	*NULL*	2250.22
310.1	2197.03	2251.9	312.6	2195.42	2254.99	274.8	2198.47	2251.15
314.1	2195.79	2251.95	316.8	2195.34	2252.64	279.1	2197.22	2251.54
318.2	*NULL*	2253.02	321	2197.41	2252.43	283.4	2191.62	2252.64
321.9	2197.73	2251.68	324.9	2195.69	2253.44	287.8	2193.31	2252.33
325.8	*NULL*	2252.54	329.1	2195.81	2253.77	292	2192.96	2252.06
330.1	*NULL*	2252.11	332.2	2196.44	2253.62	296.2	2194.26	2251.77
334.3	2197.06	2251.9				297.2	2193.72	2258.11
331	*NULL*	2252.21						
343.3	2197.4	2252.84						
347.5	2197.83	2252.61						
351.2	*NULL*	2252.22						
355.4	2196.9	2252.21						
359.5	2197.24	2252.18						
363.6	2196.77	2251.5						
367.8	2193.93	*NULL*						
372	2196.99	2252.39						
376.1	2199.23	2252.36						
380.4	2196.74	2252.35						
384.5	2197.84	2253.88						
388.7	2198.36	2252.96						
343.1	2202.46	2252.94						
397.3	2198.1	2253.36						

Appendix E: Table E.1: TerraSpec^{TM} Data for Hurricane Zone

GA-07-214			GA-07-218			GA-07-256		
Depth	2200W	2255W	Depth	2200W	2255W	Depth	2200W	2255W
6.8	2210.65	*NULL*	7.8	2220.6	*NULL*	6.8	2220.08	2249.06
10.9	2206.98	*NULL*	11.8	2220.17	*NULL*	11.1	2220.77	*NULL*
15	2217.24	*NULL*	15.4	2219.36	2249.4	15.2	2221.9	*NULL*
19.1	2222.17	*NULL*	19.4	*NULL*	2253.58	19.2	2221.79	*NULL*
23.2	2222.58	*NULL*	23.6	*NULL*	2253.09	23.7	2220.63	*NULL*
27.3	2222.36	*NULL*	27.3	*NULL*	2253.57	27.3	2221.61	*NULL*
31.4	2223.07	*NULL*	31.2	2220.93	*NULL*	31.4	2220.66	*NULL*
35.5	2219.17	*NULL*	35.5	2222.38	*NULL*	35.7	2219.71	*NULL*
39.6	2218.65	*NULL*	39.6	2221.79	*NULL*	39.8	2219.38	*NULL*
43.7	2218.67	*NULL*	43.6	2219.88	*NULL*	43.8	2219.33	*NULL*
47.8	2218.68	*NULL*	48	2220.35	*NULL*	48.1	2220.73	*NULL*
51.9	2221.57	2252.91	52.3	2219.77	*NULL*	52.3	2221.12	2253.49
56	2221.51	2251.35	56.6	2220.91	*NULL*	56.4	2221.5	*NULL*
60.1	2219.15	2251.08	60.5	2220.69	*NULL*	60.6	2221.8	*NULL*
64.2	*NULL*	2254.4	64.3	2219.32	*NULL*	64.6	2221.46	*NULL*
68.3	2224.35	2254.98	68.7	2218.04	*NULL*	68.7	2221.33	*NULL*
72.4	*NULL*	2254.18	72.8	2216.7	*NULL*	72.7	2221.02	*NULL*
76.5	*NULL*	2253.99	76.7	2220.34	*NULL*	76.7	2221.15	*NULL*
80.6	2223.16	2252.55	80.8	2219.76	*NULL*	80.9	2217.86	2252.87
84.7	2221.55	2253.58	84.9	2220.22	*NULL*	84.9	2222.84	2251.59
88.8	2221.95	2253.75	89.2	2222.01	*NULL*	88.7	2222	*NULL*
92.9	2218.62	2254.27	93.2	2220.37	*NULL*	92.8	2219.93	*NULL*
97	2219.66	2252.11	97.2	2220.68	*NULL*	96.6	2222.4	2252.94
101.1	2220.58	2253.24	101.6	2223.91	2253.69	100.3	2218.8	*NULL*
105.2	*NULL*	2255.43	105.8	2219.87	*NULL*	104.5	2223.08	2252.66
109.3	*NULL*	2254.54	110	2222.34	*NULL*	108.8	2222.97	2252.61
113.4	2222.48	2254.49	113.9	*NULL*	2253.22	113	*NULL*	2253.22
117.5	2217.19	*NULL*	118.2	2221.95	*NULL*	117.3	2214.45	2249.64
121.6	2217.44	*NULL*	122.3	2220.53	*NULL*	121.3	2202.53	2254.97
125.7	2208.56	2252.07	126.6	2221.95	2253.27	125.6	2219.24	2252.29
129.8	2207.54	2255.1	130.8	2225.83	2253.57	129.2	*NULL*	2254.29
133.9	2201.28	2258.53	135.1	*NULL*	2254.07	133.4	2217.73	2256.13
138	2199.26	2253.9	139.3	2218.83	2254.06	137.3	2216.53	2251.13
142.1	2199.07	2250.45	143.6	*NULL*	2255.45	141.4	2215.92	2253.67
146.2	*NULL*	2252.81	147.6	*NULL*	2254.12	145.1	*NULL*	2254.83
150.3	2206.37	*NULL*	152	2223.97	2253.95	148.7	*NULL*	2252
154.4	2214.46	*NULL*	156.1	2221.05	2254.83	153	*NULL*	2254.59
158.5	2212.14	2255.41	160.3	*NULL*	2255.78	157.1	2200.38	2245.62
162.6	2215.05	*NULL*	164.3	2220	*NULL*	161.2	2210.01	*NULL*
166.7	2203.72	2255.58	167.9	2218.62	*NULL*	165.6	2215.42	*NULL*
170.8	*NULL*	2255.27	171.3	*NULL*	2255.2	168.7	2217	2250.04
174.9	2211.38	*NULL*	175.6	*NULL*	2253.98	172.4	2201.73	2256.75
179	2209.39	*NULL*	179.7	*NULL*	2253.65	176.8	2213.27	2252.64
183.1	*NULL*	2256.13	186.4	*NULL*	2256.43	180.6	2213.75	2251.13
187.2	*NULL*	2255.49	194.4	2212.29	2256.09	184.9	*NULL*	2254.98
191.3	*NULL*	2255.9	198.6	2213.07	2249.94	188.2	*NULL*	2254.63
195.4	*NULL*	2255.62	202.4	2210.51	2253.08	191.7	*NULL*	2255.78
199.5	*NULL*	2254.12	206.6	*NULL*	2257.16	195.6	*NULL*	2255.07
203.6	*NULL*	2254.58	211.1	*NULL*	2254.1	199.7	*NULL*	2256.15
207.7	*NULL*	2254.76	215.2	*NULL*	2254.15	202.3	2199.38	2254.92
211.8	*NULL*	2254.13	219.6	*NULL*	2255.36	205.4	2201.88	2255.51
215.9	*NULL*	2254.59	223.7	*NULL*	2254.79	209.3	2216.64	2253.35
220	*NULL*	2255.35	228.1	*NULL*	2257.55	212.8	2219.23	*NULL*
224.1	*NULL*	2254.24	232.4	*NULL*	2255.55	216.9	2218.9	*NULL*
228.2	2222.6	2250.82	236.3	*NULL*	2259.85	220.7	2206.53	2252.46
232.3	*NULL*	2254.9	240.4	2221.69	*NULL*	224.5	*NULL*	2253.89
236.4	*NULL*	2255.19	244.3	2220.35	*NULL*	228.6	*NULL*	2253.46
240.5	*NULL*	2254.68	248	2221.16	*NULL*	232.5	*NULL*	2253.91
244.6	2219.78	*NULL*	252.2	*NULL*	2254.24	236.3	*NULL*	2254.29
248.7	2219.22	*NULL*	256.3	*NULL*	2255.4	2540.2	*NULL*	2254.98
252.8	2218.99	2248.75	260.5	*NULL*	2256.9	243.8	*NULL*	2255.72
256.9	2218.13	*NULL*	264.5	2222.56	*NULL*	246.9	*NULL*	2255.56
261	*NULL*	2254.58	268.5	2222.62	*NULL*	250.9	*NULL*	2255.27
265.1	2213.99	2251.5	272.6	2222.08	*NULL*	262.5	2200.25	2256.5
269.2	*NULL*	2254.2	276.7	2219.21	*NULL*	266.6	*NULL*	2256.78
273.3	*NULL*	2256.08	281	*NULL*	2255.38	274.9	*NULL*	2255.01
277.4	*NULL*	2256.47	285.3	*NULL*	2255.93	279.1	2205.41	*NULL*
281.5	*NULL*	2254.25	289.6	*NULL*	2255.88	283.3	2211.33	*NULL*
285.6	2201.25	*NULL*	293.7	*NULL*	2254.87	287.5	2208.99	2247.5
289.7	2202.84	*NULL*	298.1	2222.22	*NULL*	291.8	*NULL*	2249.94
293.8	*NULL*	2251.32	301.9	2220.9	2248.14	296.1	*NULL*	2249.29
297.9	*NULL*	2251.55	305.8	*NULL*	2256.01	300.4	*NULL*	2249.64
302	2199.54	2251.8	310	*NULL*	2255.56	304.6	*NULL*	2250.19
306.1	2198.79	2251.55	313.5	*NULL*	2254.23	308.5	*NULL*	2250.73
310.3	2199.16	2251.67	316.8	*NULL*	2255.67			
314.5	*NULL*	2254.47	320.3	2208.81	2253.64			
318.8	2195.85	2253.49	324.5	2202.75	*NULL*			
322.8	2190.71	2254	328.6	2204.16	2249.91			
327	2191.11	2254.21	332.6	*NULL*	2250.22			
331.1	2191.15	*NULL*	336.8	*NULL*	2250.5			
335.2	2193.68	2259.57	341.1	2199.29	2251.17			
339.5	2194.64	2257.89	345.4	*NULL*	2251.42			
340.8	2195.26	*NULL*	349.5	*NULL*	2251.51			
			353.6	2189.39	2250.52			
			357.8	2198.32	2251.09			
			361.9	2196.78	2251.49			
			366.1	*NULL*	2251.52			
			370.1	2198.07	2251.37			
			374.6	2193.81	2251.82			
			378.8	2193.65	2252.12			
			382.9	2193.37	2258.8			
			387.2	2195.1	2258.27			
			391.5	2195.12	2258.71			
			395.8	2195.16	*NULL*			
			400	2195.08	2258.96			
			400.5	2195.09	2262.39			

Appendix E: Table E.1: TerraSpec™ Data for Hurricane Zone

GA-10-272			GA-14-275			GA-14-276		
Depth	2200W	2255W	Depth	2200W	2255W	Depth	2200W	2255W
3.98	2220.43	*NULL*	4.8	2220.48	2248.55	4	2220.27	2250.83
8.2	2220.98	*NULL*	9	2218.71	*NULL*	8	2219.63	*NULL*
12.2	2218.51	*NULL*	13.3	2219.35	*NULL*	12.3	2221.51	*NULL*
16.2	2219.58	*NULL*	17.7	2220.41	*NULL*	16.3	2221.69	*NULL*
20.3	2220.74	*NULL*	21.9	2220.52	*NULL*	20.4	2220.5	*NULL*
24.3	2218.61	*NULL*	26	2218.85	*NULL*	24.5	2220.83	*NULL*
28.3	2220.97	*NULL*	30.2	2215.61	*NULL*	28.7	2221.12	*NULL*
32.7	2220.39	*NULL*	34.1	2219.07	*NULL*	32.9	2220.64	*NULL*
36.9	2219.04	*NULL*	38.3	2221.75	*NULL*	37.2	2220.47	*NULL*
40.9	2220.08	*NULL*	42.6	2220.97	*NULL*	41.3	2220.1	*NULL*
45.2	2221.28	*NULL*	46.8	2220.74	*NULL*	45.75	2219.63	*NULL*
49.5	2224.78	2254.96	51.1	2220.19	*NULL*	50	2219.64	*NULL*
53.5	2220.07	*NULL*	55.3	2220.28	2249.74	54.2	2219.56	*NULL*
57.8	2220.17	*NULL*	59.5	*NULL*	2253.96	58.6	2219.93	*NULL*
62	2221.78	2252.67	64	*NULL*	2253.61	62.9	2220.33	*NULL*
66.3	2220.57	2251.66	68.1	*NULL*	2253.65	67.2	2221.97	*NULL*
70.6	2226.4	2252.12	72.6	*NULL*	2253.51	71.5	2221.09	*NULL*
74.7	2224.22	2252.11	76.5	2224.92	2252.25	75.7	2221.79	*NULL*
78.9	*NULL*	2254.1	80.7	*NULL*	2253.9	80	2220.16	*NULL*
83.1	*NULL*	2254.75	85	*NULL*	2255	84.5	2221.67	*NULL*
87.3	2223.46	2250.58	89.3	*NULL*	2254.85	88	2221.4	*NULL*
91.5	2224.29	2251.88	93.4	*NULL*	2255.57	92.2	2222.71	2251.2
95.7	*NULL*	2254.25	97.7	*NULL*	2254.85	97.5	*NULL*	2254.28
100	*NULL*	2255.03	102.1	2223.15	2254.85	101.6	2221.71	2247.52
104.1	*NULL*	2255.43	106.4	2219.59	*NULL*	105.9	2221.69	*NULL*
108.9	*NULL*	2254.59	110.6	*NULL*	2255.54	110	2221.3	*NULL*
112.5	2223.68	2254.19	115.1	2203.13	2255.59	114.5	2221.66	2248.44
116.7	*NULL*	2256.08	119.4	*NULL*	2256.33	118.7	2220.69	*NULL*
121	*NULL*	2257.56	123.8	2199.68	*NULL*	122	2221.75	2248.39
125.3	2215.74	*NULL*	132.2	*NULL*	2255.04	127.2	2221.41	2249.6
129	*NULL*	2253.26	136.6	*NULL*	2255.96	131.4	2219.94	2252.05
133.4	*NULL*	2255.23	140.4	*NULL*	2255.69	135.6	*NULL*	2254.16
137.1	2202.39	2251.7	145.1	2218.08	2247.77	139.9	2216.7	*NULL*
141.1	2207.25	*NULL*	149.2	2217.62	2249.18	144	2200.37	2256.06
145.4	2206.02	*NULL*	153.4	2218.47	2250.95	148.4	2199.17	*NULL*
149.4	2204.89	2252.73	157.5	*NULL*	2255.25	152.6	*NULL*	2253.47
153.5	2211.98	2250.41	161.8	*NULL*	2254.22	156.8	2212.89	*NULL*
157.9	*NULL*	2255.98	166	*NULL*	2253.26	161	2208.51	2256.32
162	*NULL*	2255.65	170.3	*NULL*	2251.73	165	*NULL*	2255.3
166	*NULL*	2256.31	174.7	*NULL*	2253.07	169.1	2200.8	*NULL*
169.3	*NULL*	2254.09	179	*NULL*	2254.15	173	2200.93	2251.74
173.4	2207.72	2253.81	183.2	*NULL*	2252.99	180.9	*NULL*	2252.46
177	2213.99	*NULL*	187.5	2219.14	*NULL*	185	2210.83	2253.14
181	2217.58	2247.5	191.8	*NULL*	2255.74	189.4	2214.96	*NULL*
185.2	2217.99	2247.3	196.1	2203.89	*NULL*	193.2	2213.38	2253.18
189.7	*NULL*	2255.35	200.2	2199.33	2252.85	197.3	2217.09	2252.5
193.6	*NULL*	2254.33	204.5	2196.33	2254.25	201.7	2209.61	2256.01
197.9	*NULL*	2253.49	208.6	2197.24	*NULL*	209.3	*NULL*	2255.1
202.2	*NULL*	2253.92	212.8	2197.64	2251.21	213.7	*NULL*	2254.51
206.3	*NULL*	2252.87	217.2	2196.98	2255.04	218	2220.44	*NULL*
210.3	*NULL*	2255.01	221.5	2196.94	2253.79	222.3	*NULL*	2253.72
214.6	*NULL*	2254.87	226.8	2197.45	2254.85	226.1	*NULL*	2253.29
218.7	2218.23	*NULL*	230	2196.81	2254.48	230.2	*NULL*	2254.28
222.6	2217.08	*NULL*	234.4	2195.86	2254.55	234.6	*NULL*	2253.89
226.7	*NULL*	2256.04	238.7	2194.67	2252.58	238.8	*NULL*	2256.05
231.2	2215.95	2246.76	242.9	2194.08	*NULL*	243	*NULL*	2254.41
235.4	2206.49	2248.61	247.2	2194.14	*NULL*	247.1	*NULL*	2255.87
239.6	2203.68	*NULL*	251.5	2192.87	2254.23	250.5	2220.93	2248.84
243.7	2201.71	2250.41	254	2194.61	2254.14	254.4	2220.96	2246.86
247.9	2197.79	2250.42				258.5	2219.98	2248.29
252	2198.82	*NULL*				262.6	*NULL*	2254.48
256.1	2198.45	2250.03				266.3	2217.07	*NULL*
260.2	2192.51	2258.03				270.2	2215.78	2251.92
264.4	2196.33	*NULL*				274.5	2211.97	2255.96
268.5	2195.94	2257.8				278	*NULL*	2255.79
277.7	2196.49	2257.47				281.4	*NULL*	2255.21
281.2	2196.07	2256.71				285.6	*NULL*	2255.46
285.3	2195.92	2257.03				287.7	2203.21	2255.48
289.2	2196.86	2259.19				293.8	2208.81	*NULL*
293.4	2195.93	2256.42				298.8	2205.74	2250.85
297.6	2196.5	2257.89				302.2	2207.55	2248.11
301.8	2192.87	*NULL*				306.6	*NULL*	2249.45
305.9	2196.39	2254.54				311	2203.9	2248.33
309.9	2196.41	2255.83				315	2202.24	2249.07
314.2	2196.18	2254.21				319.3	*NULL*	2250.29
						323.5	2200.04	2251.14
						327.7	2198.45	2250.6
						332	2191.27	2251.65
						336.2	2196.05	2251.56
						340.4	2190.21	2251.45
						344.7	2190.74	2251.36
						348.8	2190.3	2255.2
						353	2189.38	2253.29
						357.3	2194.23	*NULL*
						361.5	2195.31	*NULL*
						365.6	2194.32	*NULL*

Appendix E: Table E.1: TerraSpec^{TM} Data for Hurricane Zone

GA-07-257			GA-06-153			GA-10-274		
Depth	2200W	2255W	Depth	2200W	2255W	Depth	2200W	2255W
423.3	*NULL*	2254.23	7	2214.5	*NULL*	5	2212.94	*NULL*
427	2212.52	2255.19	11.3	*NULL*	2256.79	8.7	2215.96	*NULL*
431.4	2202.93	2257.67	15	2217.39	*NULL*	12.8	2208.61	2254.93
435.6	2200.9	*NULL*	19.1	2215.61	*NULL*	16.9	2214.02	*NULL*
439.7	2199.31	2249.25	23.2	2217.45	2249.84	20.7	2199.05	*NULL*
443.8	2199.5	*NULL*	27	*NULL*	2252.24	24.5	2211.7	*NULL*
448	2199.34	*NULL*	30.4	*NULL*	2255.5	28.5	2210.89	*NULL*
451.9	2199.99	*NULL*	33.3	2204.96	2251.81	32.6	2212.15	*NULL*
456.2	2199.06	2251.74	37.1	*NULL*	2252.65	36.8	2219.78	*NULL*
460.1	2198.85	2251.73	41.7	2202.51	2252.13	40.7	2219.06	2251.27
464	2199.49	2251.89	44.9	2200.11	2251.33	44.7	*NULL*	2252.39
468.2	*NULL*	2251.61	49.1	2199.68	2251.67	48.8	2218.67	2253.64
471.5	2194.52	2251.17	53.3	2200.7	2251.33	52.9	2218.05	*NULL*
474.8	2197.89	2250.67	57.1	2202.3	2250.94	57	2219	*NULL*
478.5	2196.37	2251.13	60.5	2202.73	2251.57	61.3	2219.64	*NULL*
482.3	*NULL*	2251.44	64.8	2200.23	*NULL*	65.4	2219.76	*NULL*
485.5	2193.24	2251.47	68.8	2205.12	*NULL*	69.7	2219.24	2255.2
489.2	2197.9	2250.84	72.9	2216.62	2256.47	73.6	2220.39	*NULL*
493	2193.52	2251.5	76.8	*NULL*	2255.32	78	*NULL*	2254.64
495.9	2197.9	2251.06	80.9	*NULL*	2254.2	82.3	2222.54	*NULL*
			85.1	*NULL*	2255.36	86.4	2221.85	*NULL*
			89.4	*NULL*	2256.15	90.6	2225.71	2251.84
			93.3	*NULL*	2255.07	94.8	2220.94	2250.28
			96.8	*NULL*	2254.7	99	2222.36	2251.43
			100.8	*NULL*	2254.54	103.1	2223.18	2251.89
			105.2	2220.23	2254.7	107.3	*NULL*	2254.09
			109.1	2218.49	*NULL*	111.3	*NULL*	2253.74
			113.35	2215.43	*NULL*	115.4	*NULL*	2253.79
			117.4	*NULL*	2253.47	119.7	2220.54	*NULL*
			121.4	2215.05	2252.78	123.7	2220.95	*NULL*
			125.7	2217.53	*NULL*	127.9	*NULL*	2255.34
			129.8	2216.69	*NULL*	131.7	2221.98	2250.99
			138.3	2220.24	2251.26	135.6	2220.75	*NULL*
			142.3	2223.29	2251.49	139.6	2220.31	2250.6
			146.5	2220.04	*NULL*	143.9	2220.16	2249.09
			150.7	2220.02	*NULL*	147.3	2222.01	2254.88
			155	2219.56	*NULL*	152.8	2218.84	2252.11
			158.9	2220.53	*NULL*	156	2206.04	2256.98
			162.9	2219.12	*NULL*	160.1	2200.15	2256.35
			166.7	2219.35	*NULL*	163.9	2202.55	2256
			171	2220.86	*NULL*	168.1	2200.22	2256.21
			175.3	2222.34	2251.46	171.8	2211.01	2251.89
			179.5	2226.05	2253.09	176	2215.26	2252.89
			183.7	2216.99	2248.9	180.3	2216.81	2254.71
			187.7	2220.52	*NULL*	184.6	2203.17	2255.69
			191.1	2216.04	*NULL*	188	2210.42	2249.3
			195.9	2217.69	*NULL*	192.4	*NULL*	2254.65
			201	2214.47	2251.52	196.9	*NULL*	2255.03
			205	2216.18	2256.9	201.4	*NULL*	2254.02
			208.8	2215.24	2255.37	205.5	2217.16	2250.9
			212.7	2219.46	2254.63	209.7	*NULL*	2255.01
			216.8	2215.02	*NULL*	214	*NULL*	2254.18
			221.2	2218.61	*NULL*	218.2	*NULL*	2254.3
			225.4	2218.13	2252.47	221.9	*NULL*	2254.13
			229.5	*NULL*	2254.51	226	*NULL*	2254.36
			233.7	2216.8	2254.08	230	*NULL*	2253.99
			237.9	2204.13	2253.97	234.3	*NULL*	2254.4
			242.4	2208.33	2249.08	238.2	*NULL*	2256.14
			246	2213.59	2252.22	242.4	*NULL*	2255.93
			249.7	2216.36	2251.82	246.7	2220.32	*NULL*
			253.6	2218.09	2254.96	250.6	*NULL*	2255.85
			257.8	*NULL*	2252.08	254.4	*NULL*	2253.15
			261.9	2219.58	2250.62	258.6	*NULL*	2257.29
			265.5	*NULL*	2255.42	262.8	*NULL*	2254.79
			269.6	*NULL*	2255.55	266.7	2214.3	*NULL*
			273.9	*NULL*	2253.24	270.6	2211.81	*NULL*
			278.1	*NULL*	2254.41	275	2199.91	2248.77
			282.2	2215.02	2254.33	279.3	2199.71	2250.94
			286.6	2213.18	2255.52	287.7	2198.29	*NULL*
			291.1	*NULL*	2253.35	292	2198.25	*NULL*
			294.4	2201.47	2255.55	296.1	2198.16	*NULL*
			298.4	*NULL*	2251.41	300.1	2197.49	*NULL*
			302.5	*NULL*	2254.64	304.4	2197.32	*NULL*
			306.7	*NULL*	2253.67	308.7	2197.33	*NULL*
			311	*NULL*	2254.56	312.8	2194.67	2255.99
			315	*NULL*	2255.42	317.1	2196.53	*NULL*
			319.2	2220.32	2247.52	320.6	2194.47	*NULL*
			323.4	*NULL*	2255.12			
			327.7	2219.72	2250.9			
			331.7	*NULL*	2253.74			
			336.1	*NULL*	2253.89			
			340.3	*NULL*	2255.76			
			344.5	*NULL*	2258.2			
			349.1	2195.49	*NULL*			
			353.2	2196.69	2251.56			
			357.4	2195.64	2251.56			
			361.2	2196.7	2252.14			
			365.5	2195.77	2253.08			
			368.9	2193.15	2253.17			
			374.1	2193.99	2256.83			
			378.3	2195.72	*NULL*			
			382.2	2195.73	*NULL*			
			386.4	2195.15	2261.76			
			390.7	2195.53	2255.27			
			394.8	2195.69	2256.8			
			398.9	2196.06	2256.1			
			403.1	2196.14	2259.5			
			407.5	2195.71	2256.2			
			411.6	2194.4	*NULL*			
			415.5	2196.36	2255.75			
			420.9	2196.35	2255.43			
			424.2	2195.96	2254.35			
			428.1	2196.03	2254.11			
			432.1	2196.72	2254.31			
			436.5	2196.9	2254.45			
			440.6	2196.89	2254.09			
			444.6	2196.88	2253.59			
			448.7	2197.17	2254.5			
			453.1	2196.47	2255.31			
			461	2196.98	2254.21			
			465.2	2196.94	2253.8			
			469.5	2196.82	2254.26			
			473.8	2196.12	2255.45			
			477.6	2196.12	2254.89			

Appendix E: Table E.1: TerraSpec™ Data for Hurricane Zone

GA-14-277			GA-14-278			GA-06-176		
Depth	2200W	2255W	Depth	2200W	2255W	Depth	2200W	2255W
5.5	2215.95	*NULL*	20.1	2203.34	*NULL*	251.5	*NULL*	2256.37
9.5	2219.27	2250.25	23.4	*NULL*	2253.25	255.5	*NULL*	2256.54
13.3	2219.89	2248.17	27.5	2204.89	*NULL*	259.1	*NULL*	2256.63
17.6	2218.93	*NULL*	31.8	*NULL*	2250.02	263	*NULL*	2253.82
21.2	2219.61	2253.4	35.6	*NULL*	2253.22	266.95	*NULL*	2253.52
24.9	2211.55	*NULL*	39.7	2216.63	2248.82	271.1	*NULL*	2255.16
29.1	2212.04	2252.25	43.3	*NULL*	2251.85	275.3	*NULL*	2254.42
33.1	2218.64	2252.89	47	*NULL*	2254.28	279.5	*NULL*	2257.49
36.7	2217.21	2251.48	51.1	2217.43	*NULL*	283.1	*NULL*	2255.72
41	2219.3	2252.8	54.9	2216.09	*NULL*	287.4	*NULL*	2256.95
45.2	2219.77	*NULL*	59.1	2218.47	*NULL*	291.5	*NULL*	2254.96
49	2211.51	*NULL*	63	2214.48	*NULL*	295.4	*NULL*	2253.89
53	2217.09	2256.16	66.9	*NULL*	2255.85	299.8	2219.54	2249.21
57.1	2220.26	*NULL*	71.2	*NULL*	2255.3	303.9	*NULL*	2255.45
61.3	2219.63	*NULL*	75.6	2220.93	*NULL*	308.1	*NULL*	2255.74
65.6	2220.44	*NULL*	79.6	2222.12	2250.99	312.3	*NULL*	2253.51
69.6	2221.5	2250.2	83.4	2222.43	2250.55	336.2	*NULL*	2254.14
73.9	2221.94	2251.84	88.1	2221.71	*NULL*	339.5	*NULL*	2257.07
77.4	2222.22	*NULL*	92.3	2223.35	2252.45	342.9	*NULL*	2254.86
84.4	2221.04	*NULL*	96.5	*NULL*	2253.08	347.1	2219.82	2251.12
86	2221.77	2250.95	100	*NULL*	2252.2	399.8	*NULL*	2255.26
90.2	2222.65	2252.25	100.1	2224.05	2250.81			
94.5	2221.51	2250.65	108.4	*NULL*	2253.74			
98.7	*NULL*	2254.19	112.6	2224.71	2252.83			
103.1	*NULL*	2253.24	121	2221.31	*NULL*			
107.4	*NULL*	2254.6	124.2	2222.27	*NULL*			
111.6	2222.25	*NULL*	128.3	2220.89	*NULL*			
115.8	2221.29	2254.46	132	2218.78	2253.71			
120.8	2221.13	2254.79	136.3	2220.26	2253.52			
124.4	2220.39	2252.08	140.5	2220.28	2253.66			
128.6	*NULL*	2256.52	144.7	*NULL*	2255.29			
133	2216.47	2254.79	149	2219.48	2252.07			
137.3	2208.04	*NULL*	152.4	2220.18	2249.21			
141.4	*NULL*	2251.41	156.6	2220.26	2250.23			
145.1	*NULL*	2256.87	160.9	2220.39	2253.87			
153.5	*NULL*	2256.14	165	2218.88	2255.4			
157.1	2217.85	2255.08	169.2	2208.75	2254.62			
161.9	*NULL*	2254.94	173.4	*NULL*	2254.52			
165.4	*NULL*	2256.22	177.5	*NULL*	2255.86			
169	*NULL*	2255.47	189.8	2213.45	*NULL*			
173.6	*NULL*	2256.5	194	2217.66	2251.18			
177.7	*NULL*	2253.42	198.1	2216.83	*NULL*			
185.9	*NULL*	2254.22	202.3	2217.62	*NULL*			
185.9	*NULL*	2253.82	206.3	*NULL*	2254.84			
190	*NULL*	2253.2	210.4	*NULL*	2255.94			
194.4	*NULL*	2253.47	214.4	2219.8	2250.01			
198.6	*NULL*	2253.27	218.5	*NULL*	2254.76			
202.9	*NULL*	2253.68	222.1	*NULL*	2253.54			
207.2	*NULL*	2257	225.8	*NULL*	2256.32			
211.4	2220.23	*NULL*	229.6	*NULL*	2256.31			
215.5	*NULL*	2254.45	233.7	*NULL*	2253.2			
228.1	*NULL*	2256.85	237.9	*NULL*	2253.82			
232.1	2201.45	*NULL*	242.2	*NULL*	2253.77			
236.3	2200.54	2249.45	246.5	*NULL*	2253.34			
240.5	2199.24	*NULL*	250.9	*NULL*	2253.61			
244.7	2197.28	*NULL*	255.2	*NULL*	2251.87			
248.7	2194.93	2256.49	263.8	*NULL*	2256.65			
252.8	2196.45	2253.57	268	2220.57	*NULL*			
255.6	2196.28	*NULL*	272.2	2220.11	2247.55			
259.8	2196.97	2253.09	280.5	2220.38	2251.35			
263.4	2197.04	*NULL*	284.3	*NULL*	2253.73			
266	2197.26	*NULL*	300.7	2199.75	2255.87			
			305	*NULL*	2250.24			
			309.1	2203.27	2251.15			
			313.4	2204.04	2249.65			
			317.5	2191.65	2250.98			
			321.6	2196.29	*NULL*			
			325.6	2200.59	2250.84			
			329.7	*NULL*	2250.42			
			333.9	2196.94	2250.73			
			338	2197.4	2251.48			
			342.2	2197.75	2253.44			
			344	2197.5	2252.99			

Appendix E: Table E.1: TerraSpec™ Data for Hurricane Zone

GA-06-180			GA-14-279			GA-07-196		
Depth	2200W	2255W	Depth	2200W	2255W	Depth	2200W	2255W
9	2215.13	*NULL*	12.3	2216.4	*NULL*	334.1	*NULL*	2255.76
12.8	2214.69	2252.46	16.3	2218.45	2249.74	338.1	2214.82	*NULL*
16.4	*NULL*	2251.04	19.2	2219.85	*NULL*	342.2	*NULL*	2256.87
19.8	2214.85	2248.58	23.1	2220.06	*NULL*	346.3	*NULL*	2254.93
23.1	2215.63	2251.39	27.3	2218.29	2253.22	350.5	*NULL*	2255.07
26.6	*NULL*	2252.34	31.6	2221.37	2251.42	354.5	*NULL*	2255.09
30.6	2217.56	*NULL*	35.8	2221.51	2253.73	358.6	*NULL*	2255.75
35.2	2220.56	2254.21	39.6	2220.45	2253.83	362.8	*NULL*	2254.9
39.1	2220.98	2250.33	43.3	*NULL*	2255.12	367.1	*NULL*	2255.35
43	2219.63	*NULL*	47.4	2214.89	2254	371.2	2220.1	2253.22
47.2	2217	*NULL*	51.1	*NULL*	2255.32	375.3	*NULL*	2253.83
51.3	2212.1	*NULL*	54.4	2211.12	2253.65	379.2	*NULL*	2255.23
55.6	2209.16	*NULL*	58.7	2204.36	2252.12			
59.5	2204.92	2251.7	62.7	2200.56	2249.35			
63.75	2199.67	*NULL*	66.2	2199.95	2257.43			
67.9	2204.17	*NULL*	70.2	*NULL*	2258.18			
72.2	2206	2252.99	74.1	*NULL*	2255.01			
76.5	2217.04	*NULL*	77.4	2203.98	2254.63			
80.5	2218.08	*NULL*	80.9	2204.54	2254.38			
84.6	2218.75	*NULL*	84.4	2205.46	2250.86			
88.6	2220.23	*NULL*	88	2208.38	2248.43			
92.5	2220.07	*NULL*	95.5	*NULL*	2254.62			
96.6	2218.4	*NULL*	99.3	*NULL*	2252.05			
100.9	2219.41	*NULL*	103	2209.1	2254.32			
105.45	2217.41	*NULL*	107	2217.12	2252.7			
109.05	2216.76	2250.15	110.4	*NULL*	2254.8			
113.3	2216.81	*NULL*	114.6	*NULL*	2253.94			
117.9	2215.95	*NULL*	118.1	*NULL*	2254.72			
121.9	2217.99	*NULL*	121.8	*NULL*	2254.7			
126.2	2207.87	*NULL*	125.2	*NULL*	2255.13			
130.2	2215.54	*NULL*	128.6	*NULL*	2254.52			
134.3	2217.87	*NULL*	131.1	2210.53	2254.59			
138.6	2216.83	*NULL*	135.3	2205.42	2247.15			
142.6	2218.27	2251.24	138	2201.1	2254.33			
147.1	2218.87	2252.4	141.9	2201.15	*NULL*			
151.4	2214.19	2252.06	145.5	2201.31	*NULL*			
154.9	*NULL*	2253.52	149	*NULL*	2256.17			
159	*NULL*	2255.43	150.8	*NULL*	2256.33			
162.8	2215.53	2255.01	153.7	2203.07	2253.93			
166.5	2216.21	2255.44	157.9	*NULL*	2254.68			
169.6	*NULL*	2255.22	160.9	*NULL*	2254.31			
173.2	*NULL*	2254.63	164	*NULL*	2254.84			
176.9	2215.3	2256.24	166.8	*NULL*	2255.07			
181.3	2220.12	2250.29	170	2205.85	2253.33			
185.15	2219.5	*NULL*	173	*NULL*	2254.23			
189.25	2221.13	*NULL*	176.9	*NULL*	2253.49			
193.5	2219.85	*NULL*	181.9	2223.54	2252.72			
197.7	2220.91	2250.37	185	2220.14	*NULL*			
201.65	2219.29	2253.7	189.1	2219.95	*NULL*			
205.7	2208.2	*NULL*	193.7	*NULL*	2254.06			
210	2200.9	2254.79	197.8	2219.58	2251.91			
214.1	2202.54	*NULL*	202	2220.35	2251.01			
218.5	2202.72	2255.94	206.1	2216.96	2255.21			
222.7	2204.92	*NULL*	214.5	2198.13	2258.45			
226.55	2210.02	2254.89	218	2197.48	*NULL*			
2306	*NULL*	2256.8	222	2198.41	2252.94			
235.1	2204.4	2247.61	226	2197.29	2258.97			
239.1	2209.66	2252.58	230.2	2195.8	2259.74			
243	2208.11	*NULL*						
246.9	*NULL*	2254.85						
250.4	*NULL*	2253.5						
253.6	*NULL*	2253.73						
257.35	*NULL*	2255.26						
261.5	2218.48	2251.85						
265.5	*NULL*	2256.75						
269.7	*NULL*	2255.59						
273.9	2217.71	2248.33						
277	2218.59	*NULL*						
282.6	2213.68	2255.33						
286.15	*NULL*	2254.45						
319.4	2217.7	2251.16						
322.6	2218.73	2247.64						
327.2	*NULL*	2250.17						
331.3	*NULL*	2255.15						
335.33	2215.9	2255.98						
339.2	2213.17	*NULL*						
343.5	*NULL*	2251.11						
347.75	2213.83	2251.28						

Appendix F: Drill Hole Intervals and Samples

Section 3850

GA-07-255

Tag	Depth (m)	Rock Type (initial)	Purpose	Photo	Thin Section
31751	4.12-4.34	felsic tuff or dyke; v.sil alt; few qtz pheno; some ser veins	Geochem	4898-4900	5525-5526
31752	21.6-21.88	well foliated lapilli tuff; mu/cl; qtz eyes; mod ser>sil	Geochem	4901-4903	
31753	47.61-47.8	amygdule diabase or xstal tuff, dark grey w/ white qtz pheno (10-15%). Some fe-carb staining, minor wk chl alt (v.black)	Geochem	4904-4906	
31754	64.82-65.04	mineralized diabase mod chl alt	geochem	4907-4909	
31755	100.45-100.76	lapilli tuff; wk ser alt	geochem	4910-4912	
31756	106.29-106.49	K-alt tuff/lapilli tuff		4913-4914	
31757	111.83-112.00	chlorotoid tuff, black speckled	TS?	4915-4916	
31758	129.82-130.02	foliated lapilli tuff; graded fl--> fu/ml; 3% py; weak chl alt	geochem	4917-4920	
31759	156.41-156.66	massive ash tuff and/or mafic; 1% po, py; least alt?	geochem	4921-4924	
31760	187.2-187.48	massive black/chlorite tuff; v.f mod fol; mod chl alt	geochem	4925-4926	
31761	208.7-208.9	ser+ep lapilli tuff; wk alt, yellow staining	geochem	4927-4930	
31762	232.1-232.29	massive dark tuff (chloritic); could be mafic volcanics? V.dark; v.f.g well fol, v.black; wk-mod chl alt	geochem	4931-4932	
31764	247.98-248.28	foliated lapilli tuff; fu w/ ml-->cl; wk-mod ser	geochem	4933-4935	
31765	251.12-251.35	foliated lapilli; v.f.g ser/sil alt; partially graded; only a little part.	geochem	4940-4942	
31766	264.54-264.8	massive sulphide		4936-4939	
31767	266.52-266.8	vein and sulphide		4943	
31768	274.39-274.69	minor chl + sulphides alt; elongated lapilli; strong ser; med-coarse-gr L.T.; lap mu (0.5cm)--~2cm; ~7% disem py.	geochem	4944-4947	
31769	281.15-281.33	ser+py elongated lap; chl in interstial space; ~5-7% py	geochem	4948-4950	
31770	285.19-285.49	chl alt lapilli tuff with sulphides; contact b/t ser and chl alt. w/ chl stringers in ser; sulphides dom in chl alt zone	geochem	4951-4952	
GA-07-254					

Tag	Depth (m)	Rock Type (initial)	Purpose	Photo number	Thin Section
31800	6.04-6.32	felsic ash tuff or felsic dyke; biege/grey smalllglassy 1-2mm glassy qtz phenos (3%), small black flecks (py; 1-2%).		4953-4955	
25415	18.83-19.23	felsic tuff; light grey, 20-25% qtz<plg xstals, ml/fu + mu--> VCL (incl qtz) mod ser alt		4956-4958	
25416	31.23-31.55	sil alt) xstal tuff approx 25-30% qtz (could be some plag) some ri[up qtz/carb cveins		4959-4962	
25417	45.44-45.7	x-stal tuff; chl alt; dark grey w/white qtz/plag xstals 25-30% wk chl alt rip up of carbonate veins and qtz irreguarly shaped (3-4%)		4963-4966	5531-5532
25418	77.75-78.05	mafic dyke; very dark grey/black carb belbs (1-3mm) carb discont veinlets. , disem py (1%), clustered py and po (1%)		4967-4969	
25419	86.05-86.25	x-stal tuff w/ pale phenocrysts; dark grey 25-30% subrounded		4970-4972	
25420	101.7-101.8	graded lapilli tuff --> ash (v.f.u) tuff; least alt, minor carb veins in mu, mod fol, , no carb clasts in v.f.g, sharp contact		4973-4975	
25421	119.9-120.1	pyritic mudstone w/ brecciation; graded v.f.u--> mud clasts; interbeds mud increases down hole. Py in both. Clasts are light grey, vf.g, mod sil, sub angular, near tpo some irregular qtz veining		4976-4979	
25422	133.45-133.69	med lapilli tuff ± bombs;; ML matrix w/ 1mm-6mm (rare 1 cm), plag and qtz grains, elongate chl alt clasts/ MC		4980-4983	
25423	140.4-140.64	deformed mudstone;w/ v.f.l tuff, clsuters of disem py (~10%) mostly in v.f.g but some along margins of mud.		4984-4988	
25424	157.1-157.33	mod sericitic lapilli tuff; well fol, fl w/ fu/ml white qtz+plag (20%)		4989-4991	
25425	184.1-184.36	f.gr. Felsic tuff + sericite; elongated black clasts (10%) disem py (5%)		4992-4994	
25426	197.38-197.62	mafic unit; f.g. dark v. chl alt		4995-4996	
25427	231.9-232.2	compositional layering; mod-st black and green chl alt, larger sample but big gap		4997-4998	
25428	238.76-238.97	felsic tuff; similar to 184 ser and chl		4999-5001	
25429	267.89-268.09	tuff fl+/- fu w/ fu +/- cl white plag and qtz (20%). V. simiar to above +184 strong-mod ser alt		5002-5004	

25430	286.07-286.29	mineralized, sericite felsic tuff? Well fol, ml, sul in chl bands, disem in ser/sil or cert elong clasts		5005-5006	
25431	300.05-300.25	felsic lapilli tuff with mudclasts?1% in py in right corner		5007-5008	
25432	3208-321.0	elongated felsic tuff ; some elongated chert clasts, other could be ser alt plag chl>ser strong		5009-5010	
25433	155.58-155.80	chlorotized A.T	geochem		
25434	160.6-160.83	felsic dyke? Massive tuff?	geochem/ TS		

Section 3900
GA-06-147

Tag	Depth (m)	Rock Type (initial)	Purpose	photo	Thin Section
14486	5.17-5.3	ash tuff; v.sil alt, beige, py; white x-cutting+ concordant qtz veinlets	geochem	5028-5030	
14487	16.28-16.55	kind of xstal tuff >20% xtals but xtasl are lap. M-coarse-gr tuff w/ some lap sized frags. Some fe-carb over print "infilling" between lap, almost L.T w/ some lap clasts, more sandy than sil; mod-wk sil ± ser.	geochem	5024-5027	
14488	32.7-32.90	sil	geochem	5037-5039	
14489	49.2-49.35	Chlorotized xstal tuff	rep litho, geochem, **TS**	5043-5044	
14490	62.2-62.45	ash xstal tuff, carb blebs, chl alt; med-dark grey	geochem	5033-5034	
14491	77.05-77.32	felsic mineralized "breccia"	neat	5031-5032	
14492	94.9-95.1	med-grained tuff; mod-wk ser alt; "sandy" tuff, med-light grey; fe-carb overprint w/ 2-5% subangular white (milky; plag?) grains; 1-3% black grains, mod fol; wk sil > ser?;some concordant carb veining.	geochem/**TS**	5046-5048	
14493	102.59-102.69	mudstone w/ thin abnds of f.g py (~7%) host in thin interbeds of f.g tuff	mud stuff/TS	5050-5051	
14494	110.6-110.8	med-grained tuff with interbedded mudstone; f-med-gr tuff w/ v.thin undulating interbeds of chl alt mud. Tuff is med-dark grey; mod-wk chl alt; dis py in thin bands <5%	mud stuff	5055-5056	
14495	114.1-114.2	layered mudstone+py + chert? Or v.f.g tuff; mod chl alt	mud stuff/**TS**	5035-5036	
14496	125.35-125.55	intrusive unit (alt mafic?) +carb blebs; dark grey, f.g; fe-carb overprint	geochem	5062-5063	

14497	134.80-135.0	+ thin bands chloritzied clasts, lap are light grey ranging from mu-1cm; there are white round-subround xstals w/ finer grains + some are in grey 1-1.5 cm lap. Chll is in interstitial space. Mod ser>chl alt.	geochem	5068-5069	
14498	189.8-189.9	silified mafic dyke; light-med grey beigde grey f.g 1% boudinage qt\ "veins" or pieces of veins. 20% fe-carb overprint	geochem		
14499	200.55-200.7	sericite altered tuff stwk	geochem		
14500	220.45-220.65	sericite altered tuff stwk; half cor, fissile	geochem		
32001	232.2-232.2	altered tuff stwk; sil>ser w/ bands of chl; clustered bands of py + thin bands fine po, some carb veins.	geochem		
32002	250.1-250.2	altered dyke	geochem		
32003	263.60-263.70	altered tuff stwk; chl>ser; ser is bluish green; cherty clasts or boudinage veins	geochem		
32004	285.10-285.23	f-c tuff; disem m-gr py± bands/clasts of chl	geochem	5582-5584	
32005	316.97-317.09	altered tuff stwk mix of ser and sil ± chl (broken pieces)	geochem		
32006	336.19-336.35	altered tuff strong sericite weak chl (broken pieces)	geochem		
32007	363.6-363.96	sericite altered tuff stwk--> could be TS 4 broken pieces	geochem		
32008	380.4-380.6	intensely altered tuff, v.f.g stwk	geochem		

GA-07-208

Tag	Depth (m)	Rock Type (initial)	Purpose	Photo #	Thin Section
14514*	7.33-7.55	felsic flow; v.sil alt; light bright grey, v.f.g with 1-4 cm thick discont and discordant qtz veins (can appear almost brecciated-looking); thin med-gr py veins, some 1-4% dis py (f-med-grained), trace gn; 1-3% round white qtz xtstals.	geochem	5179-5182	
14515	16.42-16.65	f.g tuff; med grey; fl with fu clear, glassy qtz xtals (20%); mu (could have been plag, now carb overprinted) white-beige (5%), subangular; vuggy, has dark brown weathering	geochem	5183-5185	
14516	24.08-24.28	sil alt xstal tuff;light grey, v.f.g sil alt tuff (or flow?) with thin (1mm) discordant and irregular chl (black) veins; 7-10% qtz xstals (fu-cl)± plag (rare).; wk ser alt in thin spider-like veins; minor carb overprint (1%).	geochem	5186-5189	

14517	30.21-30.40	mafic dyke; v.f.g dark grey green dyke with v.f golden beige flakes of ? Prob fe-carb (fizzes a bit when scratched)	geochem	5190-519	5510
14518	35.38-35.58	sil alt+ wispy chl (tuff?); light grey f.g tuff w/ ml-vcu qtz xtsals (10%); thin black concordant chl veins, but discont, wispy as well; discondorant 1 cm qtz vein xcutting core; mod-strong sil; wk chl, mod fol. Cut in half, f-gr xstal tuff. 15-20% qtz xtals (clear and glassy or pale and white-round to subround).	geochem/ co	5192-5195	
14519	38.63-38.86	increase chl alt in xstal tuff ± sil; could be fine-med-gr L.T with qtz xstals in it. Could be graded unit. Because downhole is finer (even just in sample) but it could be weather that makes it look like lap. Med-grey. Orange, yellow staining	geochem	5196-5201	
14520	44.83-44.98	xstal tuff with pheno least alt?; clear glassy and creamy white qtz pheno (30%; mu; subrounded) in light-med-grey fine-gr matrix; wk sil, v.wk chl	geochem	5202-520	5661-5663
14521	59.95-60.2	xstal tuff with pheno chl increase; dark grey green f.g tuff w/ 25-30% pale subrounded qtz xstals, mu-cl; irregular qtz bleb; mod chl alt	geochem	5203-5208	
14522	69.3-69.54	weird black pheno; med grey with dark black subangular xstals, thought were qtz but can scratch. 3-4% qtz veins (boundinaged), some pulled apart; mod-wk chl alt, wk sil.	TS?	5209-5212	
14523	83.47-83.6	xtal tuff with pheno increase chl; dark grey f.g tuff with qtz plag pheno 20% subrounded-rounded; some pale grey elongate "lap"; some sulphide staining; mod chl alt	geochem	5213-5214	
14524	88.25-88.4	mafic unit? Massive; few carb veins; vuggy thin veins and blebs, dark brown in color.	geochem/ re	5215-5216	
14525	95.84-96.0	pyhotite in sample; v.f.g dark grey/blackish dyke with thin veinlets/ cluster of veinlets of py and pyro (3%) and some disem py; irregular carb veining, discordant 0.5-1.2 cm; mod chl alt	geochem/ re	5217-5219	
14526	103.41-10.61	xstal tuff; med grey with fine matrix and pale white subrounded fu-cu qtz xstals (35%); massive; least alt?	least alt?	5220-522	5537

14527	108.15-108.41	light grey tuff; fine-grained with fl qtz xstals, subangular.	geochem	5223-5227	
14528	117.76-117.94	v.chl alt, effed up; almost everything is replaced by chl, euhedral fe-carb xstals disseminated throughout (<30%), weathered on outer surface	geochem	5228-523	5666-5668
14529	124.0-124.23	graded f.g tuff with chl laminae/ discont thin v.f.g beds.	geochem	5233-5236	
14530	132.45-132.64	thin interbedded mud/ v.f.u tuff with med-coarse-grained cubic disseminated py in tuff layers (5%). Mud layers are approx 0.2-1cm	TS/~~geochem~~	5237-524	5515
14531	139.91-140.1	intrusive unit (intermediate?); fu/ml with mu black pellets, some subrounded qtz grains (fl-cu; rare; 5%); thin fe-carb veins (1%); beige grey in color	geochem	5241-5243	
14532	156.48-156.67	intrusive unit (intermediate?) increase chl alt	geochem	5244-5246	
14533	161.93-162.18	L.T with minor chl and fe-carb; fine-med-grained L.T w/ fu-ml plag and qtz xtals. Lap are light grey and elongated; thin bands of black chl in interstial space. Reddish-yellow staining	geochem	5247-525	5579
14534	164.11-164.29	intermediate intrusive?; fu/ml with mu black pellets, some subrounded qtz grains (fl-cu; rare; 5%); thin fe-carb veins (1%); beige grey in color	geochem	5251-5253	
14535	169.1-169.24	fine-med L.T ser < chl alt, similar to 14533, but finer, same mineralogy. Could be considered coarse-grain tuff, kind of sandy, med-light grey in color. Lap aren't elongated or as obvious as last sample; wk ser, wk chl.	geochem	5254-525	5544
14536	176.1-176.3	v.chl alt A.T?	geochem		
14537	182.82-183.04	mafic dyke; fine-grained dark grey green; thin carb veins (2%) and carb blebs (1%); rare euhedral py	geochem	5257-5259	
14538	202.88-203.06	mafic dyke	geochem	5260-5262	
14540	218.45-218.6	tuff; same as 14535; med-coarse-grained tuff; plag and qtz xstals, rare chl bands, minor fe-carb overprint; mod-wk ser	geochem	5263-5264	
14541	220.34-220.47	A.T with pinkish white flecks--> carb	geochem/ co	5265-5266	
14542	231.15-231.29	A.T with increase ?similar to above	geochem	5267-5268	
14543	225.66-225.8	qtz vein with mus/ep ± kspar?	cool	5269-5270	

14544	273.6-273.78	ser alt tuff + mineralizatized. Strong to intensely ser alt L.T (f-coarse?); diseminated bands of med-gr py with rare ccp; possible ep? Some green rounded-tabular mineral.	geochem	5271-527	5673-5676
14545	295.0-295.20	ser alt tuff + mineralizatized close to dyke; a.t with strong ser ≥ or = to chl	geochem	5274	
14546	306.75-306.92	chl, carb, ser tuff; fine-gr disem py	rep litho	5275-5276	
14547	328.33-328.49	chl < ser ± py; fine-grain light grey tuff with strong-mod ser alt.	geochem	5277-5278	
14548	236.98-237.21	muddy looking py banded tuff; v.f.g py in matrix with v.f.g tuff (brownish gold)? Discont bands of f.g py (10% is bands of py) approx 2-3 cm long and 0.5-1.5 cm thick, parallel with fol; 7% elongated chert/qtz fragments (3mm) in f.g matrix.	geochem, TS	5282-5283	
14549	241.73-241.88	banded py, sp, gn; folded	TS, geochem	5279-5281	
14450	242.41-242.58	py undulatory band in tuff (muddy?); same v.f.g matrix of golden brown py with tuff? But this has very thin bands of cont undulating py bands (brighter golden color); possible sp, rare coarser grains of ccp in boundinage band (3cm long). Some qtz blebs in matrix.	geochem, TS	5284-5285	
14451	248.14-248.3	thin to medium banding (1-[illegible]cm) of light grey v.f.l (appears more si-rich, thin bands, appears on tops? Of beds, some loading structures (flames) with lower dark grey fl unit). Med-grey beds (thickest) that are v.f.l-fl with disem py(f.g; 2%), in between med-grey beds are dark-grey fl-fu more sandy looking thin-med bedded, could be base and grade into lighter grey, but not always; mod to strong ser alt.	geochem, TS	5286-5289	
14452	253.34-253.56	v.chl alt (VMS?); v.black, v.f.g (no grains in black can be seen, chl replacing original tuff) w/ small bleds (1-2mm) of qtz (white, or carb??); 2-3% carb veins with py, trace ccp and possible sp. (<5%)	geochem	5290-5292	
14453	258.3-258.45	py ± qtz veins are irregular; clast of chl alt a.t with clusters of med-gr py (~90 of "clast"); mod-strong ser alt in light grey a.t.	geochem, TS	5293-529	5677

14454	264.96-265.14	ser/sil tuff ± py ± thin chl bed; light grey a.t with thin dark (chl alt?) blebs; thin layers of darker of (chl alt?) with fine-med-gr py; v.f.g py is diseminated throughout the sample; 4% of randomly distrubuted qtz fragments, typically subrounded.	geochem	5296-5299
14455	254.23-254.37	mud + py? +qtz lap	TS	5300-5302

GA-07-209

Tag	Depth (m)	Rock Type (initial)	Purpose	Photo	TS
25437	4.3-4.48	Felsic flow or A.T; v.f.g; light grey/ beige with irregular white qtz veins (5%); v.sil alt; 3% dis py; few minor sericite veins	geochem, TS, rep litho	5303-5304	
25438	22.38-22.54	f-m.gr L.T w/ strong sil ± ser/chl; light to med grey in color. Lapilli are light to dark grey in color with finer matrix. Qtz and plag xtals in interstial space, some chl infilling interstial space, appear as dark grey elongated fragments (rare). Lapilli are subangular and slight elongated looking. mod fol.	geochem	5305-5306	
25439	34.81-34.98	1st mafic dyke; med-gr dark grey green mafic dyke. Appears granular looking, green, black and white "grains". Rare v.thin carb vein; massive; wk chl alt	geochem	5307-530	5682-5686
25440	40.08-40.23	A.T increase alt (hydrothermal breccia?); mix of white and light grey; worm like texture; both have mu-sized qtz xtals; white is sil alt, whereas grey is more ser alt; white:grey 60:40; strong sil, wk ser.	geochem, rep litho	5310-531	5687-5693
25441	50.7-50.9	xstal tuff; med-grey fl with m-cu white qtz xtals (40%); rare carb clast/amygdule; rare disem py; strong sil	geochem, rep litho	5313-5315	
25442	58.72-58.8	matrix is dark grey; there is more red/brown staining (fe-carb) which is kind of replacing xtals (maybe some plag then) still mod-strongly sil alt w/ wk-med chl alt.	geochem	5316-5320	
25443	73.78-73.9	(xstal) tuff; dark grey- almost black fl-v.f.u matrix with fl-mu qtz and plag xstals (15%). Not an obvious xstal tuff. More sandy in apperance. 5% carb over print; mod chl alt.	geochem	5320-5323	
25444	83.12-18.36	xstal tuff: dark grey to blackish green fu wi	geochem	5324-5328	

25445	98.47-98.65	sil tuff breccia; clasts are subangular. Some large rhyolite clasts are fractures with carb infilling interstitial space. Most clasts are sil alt light grey fine-gr rhyolite piece (I think?), some chert/qtz fragments and some thicker carb veins, few darker grey blebs. strong sil alt.	geochem, rep litho	5329-5332	
25446	104.09-104.33	amygdaloidal dyke; med-grey green; oval 0.5-1 cm carb amygdule; possibly elongated, seems to wk-mod fol; cluster of amygdules, few thin discordant carb veinlets.	geochem	5333-533	5503-5507
25447	113.32-113.49	fu-ml tuff, well fol,; fe-carb overprint pervasive, rare carb concordant veinlet; least alt? Or wk chl alt	geochem, rep litho	5337-5339	
25448	124.57-124.73	sil ash tuff with chaotic carb and chl alt in a 3 cm discont band	rep litho	5340-5341	
25449	125.2-125.4	sil with wispy chl/mud beds; med-light fl grey tuff with v.thin wispy layers of v.f.g dark grey (pos chl alt; 5%) and thin layers of lighter grey v.f.g; wk alt (part of fining sequence of 25447	geochem	5342-534	5528-5530
25450	127.56-127.74	chl mud with crazy veining	mud stuff (T	5345-5346	
14501	146.52-146.67	sil+ chl alt L.T or tuff breccia; some areas appear hydrothermally brecciated; med-gr L.T with some rare coarse lapilli; lapilli are darker grey whereas interstial space is light grey; mod chl and sil alt.	geochem	5347-5349	
14502	153.69-153.9	part; also diseminated py in v.black, f.g chl.	mud stuff/ geochem?	5350-5353	
14503	174.44-174.68	dark grey green mafic dyke; ml; wk fol to massive; rare carb amydgules, thin pin like black minerals (20-30%), rare thin carb veinlets.	geochem	5354-5356	
14504	188.79-189	mod ser, wk chl alt fine-gr L.T w/ some coarser grains, med grey with elongated lapilli, coarse lap are med (darker) grey and massive, fu-mu qtz and plag xtals, thin elongated dark grey fragments, some sulphide staining. Matrix is mu light-med grey; sulphide staining	geochem	5357-5358	
14505	200.8-201.02	dark green/black mafic dyke; f.g wk fol, rare py.	geochem	5359-5361	
14506	225.66-225.84	dark green/black mafic dyke; f.g wk fol, rare carb vein; v.f carb over print	geochem	5362-5364	
14507	233.05-233.25	ser alt fu tuff with few fl qtz xstals (white)	geochem	5365-5367	
14508	242.03-242.21	other dyke (grey/brown); f.g; few fe-carb fi	geochem	5368-5371	

14509	257.46-257.6	tuff (ser); light-med grey, med-gr tuff with few white xtals, finer version of above, sandy-ish. Not really fol	geochem	5372-5375	
14510	291.3-291.6	chl alt and chaotic carb- can see py replaci	geochem	5376-538	5521
14511	261.55-261.81	super mineralized, banded red sp, py, ccp, few qtz blebs	geochem? TS?	5382-5387	
14512	269.36-269.59	chl matrix with sulphides, py, patches of gn, bands of qtz (or carb?)	representativ	5388-5392	
14513	273.45-273.7	chl matrix with sulphides	representativ	5393-5395	
GA-07-214					
Tag	Depth (m)	Rock Type (initial)	Purpose	Photo	
31775	5.71-6.12	Felsic flow/ ash tuff; v.sil alt. Light grey/beige in color; <5% dis anhedral py; discordant qtz veins (white); thin disem sericite veining; few qtz white xtals.	geochem	5397-5399	
31776	17.55-17.82	f.g med-grey tuff with white round to subround white qtz xtals; appears to be discont banded or web-like with light grey (v.sil alt) and med-dark grey (w/ vein-like more chl rich zones, v.thin, ropey looking); strong sil alt, wk chl.	geochem	5400-540	5633-5636
31777	30.58-30.85	light-med grey mod sil, wk ser alt ash- fu tuff with few qtz phenos; irregular qtz veining (less then above); few 1-2 cm chert-looking fragments.	geochem	5405-5409	
31778	40.55-40.87	mafic dyke; fu/ml-gr dark grey-green dyke; somewhat granular looking; black specs, some carb-over print, v.g.f golden yellow flecks; few carb amygdules (round to rod-like), thick qtz-carb vein, rare qtz discordant qtz veins; rare disem py	geochem, TS	5410-5413	
31779	47.53-4.9	felsic xtal tuff; light-med grey fu-mu-gr; fu-cu pale white and clear glassy qtz xtals (20-25%); 2-4% elongate (oval-like) and irregular shaped carb lap; carb may be infilling some of interstitial space (in photos light grey/white area in middle); mod fol, mod sil alt, wk chl	geochem, TS	5414-541	5640-5644
31780	65.48-65.83	felsic tuff; med-dark grey fl tuff with fu-m white qtz xtals (rounded-subrounded); 1-2% subangular carb lap; patches of v.f.g py, wk carb overprint (5%); few lap sized qtz fragments; wk-mod chl alt; mod fol.	geochem	5420-5424	

31781	81.7-82.0	lapilli/ash tuff; dark-grey, fl/fu w/ fu-mu pale white subrounded qtz xstals (20%), mod-strong fol, mod-str chl alt, mod fe-carb overprint; 2-3% lap sized qtz fragments (or chert).	geochem	5425-5428	
31782	108.2-108.5	felsic flow? Or fl tuff? Dark-grey f-gr with few (5%) qtz xtals, rare rod-like carb amygdules, 3% carb veinlets, mod chl alt.	geochem	5429-5433	
31783	118.67-118.97	Light grey, fl-gr, well fol, 15% reddish-dark brown flecks (prob py), orange sulphide staining, few quartz frags; mod-strong ser	geochem	5434-543	5648-5651
31784	130.27-130.52	felsic flow? Or sil alt ash tuff. Light pale grey with discont bands of beige; v.f.g w/ <10% qtz xtals, 3-4% lap sized carb fragments, mod fol, strong sil alt, wk chl? Orange staining.	geochem	5437-5439	
31785	150.83-151.07	mafic dyke; pale grey with black flecks, f-m-grained, with 10% carb amygdules. Rare carb veinelts. Sil alt?	geochem	5440-5441	
31786	157.07-157.27	mudstone/siltstone; black v.f.g w/ thin concondrant veinlets of carb; thin interbeds of sil-grey light grey ash tuff (1-3cm) down hole. Mod chl, small patches (<5mm) of v.f.g py.	geochem	5442-5444	
31787	176.98-177.3	mafic dyke (look for chilled margins); ml-gr with black shards (5%), 0.5-1.5 cm carb filled amygdules; rare qtz and plag xtals; 3% carb veining (discordant and irregular); wk chl alt.	geochem	5445-5447	
31788	207.09-204.31	fine-grained mafic; dark grey green in color. Rare cubic py; massive- wk fol, wk-mod chl alt.	geochem	5448-5449	
31789	242.68-243.03	fine-grained alt dyke; light grey-green; disem py (5%), x-cutting qtz vein with py in and around veinlet (3mm thick); wk-mod chl, mod ep, massive.	geochem	5450-5453	
31790	243.74-244.05	felsic med-gr tuff + sericite alt; 10% white pheno, wk fol, wk-mod ser alt	geochem	5454-5455	
31791	257.99-258.22	mafic unit; fu/ml, dark grey green with strong fe-carb overprint (speckled), few fragments of broken-up carb veins and some carb veins.	geochem	5456-5459	
31792	267.73-268.11	felsic lapilli tuff; fine-med-gr L.T; light-med grey, mod fol, mod ser and chl.	geochem	5460-5462	

31771	270.13-270.4	med-light grey f-gr tuff with fine-gr py disem (70%); thin bands < 1cm of chl alt (black) tuff?; fine-coarse-grained py clusters in these bands; discont qtz veins 1-1.5 cm thick also contain abundant f-c-gr py.	geochem	5472-5475
31772	280.33-281.05	contact b/t chl alt fine-gr tuff w/ disem y and bedded sulphides (py, red sp, cp, gn); fine-gr tuff fragments are in interstitial space between py and rare ccp until hit massive sulphide.; well foliated. 2nd sample is similar except thick bladed barite fragment 7 cm long 4-2 cm thick with 0.5 cm ccp vein through centre.	geochem, cool sample	5476-5478
31773	292.68-292.94	thin (<1cm-2cm) thick pinch and swell and discont chl (black) alt f.g tuff with disem fine-med-gr py. Sulphides are dominately py (50%) with 15% gn, 7% sp and 2% ccp. All bedded sulphides are f.g. Few blebs of barite (1 v. large one 6x3 cm), and few qtz lap. bedded sulphides wrap barite fragment.	rep geo of mineralization	5479-5483
31774	293.6-293.9	massive to semi-massive sulphide, almost bedded, parallel with fol; coarse-fine-gr py with stringers of ccp, rare small clusters of sp; with black chl alt matrix (v.f.g) some white specks of qtz?? Sulphides are in cluser bands or diseminated throughout the black matrix. few coarse qtz veins, thin rare barite vein?	geochem?	5484-5487
31794	295.2-295.42	py-chl alt f-gr tuff ± cp outside massive sulphide zone; fine-coarse gr-py in clusters and disem bands in chl alt tuff. Fragments of light grey mu-gr sil alt tuff ranging in size from 1-7cm x 0.5-2cm. Rare ccp with py. Py is rarely euhedral.	geochem	5467-5471
31793	297.2-297.48	coarse-gr L.T; lapilli are elongated and light grey f.g; chl is in interstitial space; some black elongated lapilli (1-2%; 1.5 cm x1cm); rare bands of fine-coarse-gr clustered py. + disem py (1-2%), speckled mod carb overprint; strong ser; wk-mod chl.	geochem	5463-5466

31795	309.71-309.90	felsic graded med tuff ± lapilli --> v.fine-grained tuff; fu/ml light grey felsic tuff with thin (1-2cm) discont bands of med-gr black chl alt tuff with white subrounded qtz grains; rare dis py. Elongate black clasts in light grey tuff. Grey could be elongated lapilli; strong ser alt.	geochem	5488-5490	
31796	316.96-317.24	med-gr py parallel to fol (80%); bands of light grey f.g sil alt tuff with thin elongated dark grey fragments (15%) blebs of qtz (or chert) subrounded (0.3-1cm).	geochem	5491-5495	
31797	321.59-321.85	sil alt tuff (or qtz veins) with thin discont bands of chl alt tuff? Or infilling interstitial space. Sil alt tuff has ml qtx xtals in lap fragmets with rare dis py. Clusters of med-gr py are associated with bands/blebs of chl alt. Euhedral py is disem throughout, whereas, fine-gr py is clusterd in thicker bands. milky white veins pinch and swell 5mm thick, discont.		5496-5499	
31798	322.2-322.41	chaotic carbonate+vein contact+v.f.g chl alt tuff; with disem f.g p; rare red sp near veins, blebs of qtz/ chaotic carb fragments in matrix, larger clusters of coarse qtz fragments milky white to clear white in color; wk to mod fol; strong chl alt.		5500-5502	
25435	160.96-161.2	alt dyke?	geochem		
25436	171.1-171.26	alt f.g mafic?	geochem		

GA-07-218

Tag	Depth (m)	Rock Type (initial)	Purpose	Photo	Thin Section
14456	5.79-5.93	felsic tuff? ± py, sil alt, carb overprint	geochem/ TS	5078-5080	
14457	20.23-20.42	med-grained mafic dyke; chl alt green in color	geochem		
14458	30.4-30.67	f.g tuff with grey pheno (qtz?) or chl alt clast; thin py veinlets, wk sil alt	geochem/rep litho	5081-5085	
14459	50.01-50.17	mod sil alt f.g tuff with qtz xstals ± qtz/carb veins	geochem/rep litho/**TS**	5086-5089	
14460	69.5-69.68	mod sil alt f.g tuff with qtz xstals + ser veinlets	geochem	5090-5095	
14461	86.17-86.38	lapilli tuff with qtz xstals (0.5-1cm) chl veinlets + mod sil alt	geochem/rep litho	5096-5102	
14462	104.65-104.9	f.g tuff with pale white qtz and glassy xstals, minor chl veinlets, sil alt		5103-5109	
14463	112.2-112.46	patchy tuff, chl + sil alt ± ccp? Some white + glassy xstals.	geochem/ TS?		

14464	111.31-111.46	fine/med-grained (fl/ml), graded grey tuff, mod sil alt	geochem/rep litho/**TS**		
14465	125.8-126.10	f.g xstal tuff pale white qtz, some plag, some pulled qtz veins, shear zone? +wk-mod chl alt	rep litho/ geochem	5110-5116	
14466	148.34-148.52	xstal tuff, massive? Pale white qtz xstals (<1mm-7mm)	rep litho/ geochem	5117-5120	
14467	162.51-162.76	graded tuff with chl alt interbeds	rep litho/ geochem	5121-5126	
14468	174.55-174.77	v. Sil alt xstal ash tuff or felsic dyke	geochem		
14469	182.21-182.41	mm interbeds of chl alt silt? + ash tuff	geochem/TS?	5127-5132	
14470	192.22-192.39	mm interbeds of chl alt silt? + ash tuff + py, med-grained tuff	geochem/**TS**	5133-5137	
14471	195.65-195.85	med-grained tuff (sandyish) with chl clasts, mod sil alt	geochem	5138-5143	
14472	199.15-199.37	mudstone v.alt	geochem/ **mud stuff**		5545-5550
14473	200.90-201.16	mafic tuff?	geochem/TS?		
14474	239.44-237.72	graded tuff (mu/cl-->f.g);py in thin bands; mod ser alt, chl bands	geochem	5144-515	5527
14475	252.05-252.2	med-grey f.g tuff, vuggy? Could be **dyke**, thin carb veins	geochem-->	5151-5154	
14476	266.4-266.55	sil alt tuff f.g ± few qtz xstals	geochem		
14477	294.81-295.01	sil alt/ **ser** alt tuff f.g ± few qtz xstals; well fol	geochem/**TS**	5155-5158	
14478	318.05-318.20	ash tuff with sil and ser alt	geochem		
14479	327.61-327.86	tuff with chl alt >sil+ser	geochem		
14480	332.3-32.48	mod-strong ser< chl; thin bands of py (10-15%) in chl + disem py, trace sp?	geochem	5175-5178	
14481	335.6-335.85	semi-massive sulphide with alt chl and "un-alt" patches; ser alt too, chl > ser, 2% py, tr sp	geochem	5159-5162	
14482	344.55-344.79	bands of chl matrix with sil?ser? Lap?	geochem/**TS**	5163-516	5515
14483	363.9-364.14	stwk alt; f.g tuff w/ chl and ser alt; patches of more chl alt w/ py.	geochem	5167-5170	
14484	376.54-376.74	alt mafic dyke?	geochem		
14485	394.87-395.1	v.ser alt tuff; f-m-gr w/ some thin black clasts	TS? Geochem	5170-5174	
Section 3950					
GA-07-256					
Tag	Depth (m)	Rock Type (initial)	Purpose	Photo	

31937	10.76-11.04	grey veinlets (few mm). White round to subrounded qtz xstals or blotches with clear qtz xstals in them. Approx 10-15% clear qtz xstals. Med grey in color with few light grey botches. White blotches/ xstals are <10%. approx 5% disem py. **f-**m-gr tuff.	GC	4188-4195
31938	32.25-35.45	mod sil alt L.T. or tuff ser alt; if it is a lap then lap would be light grey color, elongated few cm each. With darker grey making up fine0-gr matrix, however some of the matrix is lighter grey/white which is probably siliceous alt or replacement. <1% disem py. approx 8% pale white xtsls and 3% clear qtz xstals.	GC	4196-4202
31939	53.12-53.32	L.T (new?) hetero wk chl?; looks more like a xstal bearing tuff with round to subrounded qtz xstals with 0.5-1.5 cm med grey laps that are elongated with a fine dark grey matrix, look lath-like. Cut side looks like described above but none-cut side does look like LT/tuff. dark grey matrix is discont and appears lath like, could be chl alt. weaky ser alt. similar to two above samples with less sil alt and more defined crystals and lap. rare clusters of fine py +1-2% disem py.	GC	4203-4209
31940	77.61-77.84	f-m grey tuff (graded seq), mostly f-g. 5-7% v.f.g disem py. 5% black round qtz xstals in v.f.g matrix, wk ser? Mod fol	GC (TS?)	4210-4215
31941	83.82-84.02	f.g dark grey green mafic dyke; 4% disem p	GC	4216-4220
31942	103.91-104.15	xstal tuff wk-mod chl, dark grey in color with 20-25% white dominantly plagioclase xstals. Xstals are typically subround to tabular however some are lath-life and others are round. Rare qtz blobs and 5% qtz clear xstals. Matrix is v.f.g. 2 qtz veins, one which has chl alt? blotchy green patch. could be **porphyrtici felsic?** flow. wkly chl alt.	GC	4221-4230
31943	126.62-126.90	Mafic dyke (carb overprint?) f-m-gr MD. Rare py grain (not in geochem side)	GC	4231-4237

31944	146.2-146.46	f-m tuff mod sil/ser + tr ccp/py; py stringers of f-m-gr py xstals, some boudinage some are just straight with fol, all are concordant. <1mm clear qtz xstals >40% v.f.g. could be sheared carb veins (creamy white bleds that pretty much follow fol) can be associated with py stringers. they range in size from 1 cm to > mm elongated blebs.	GC	4238-4245
31945	169.65-169.87	felsic dyke sil alt, with 7% qtz xstals mostly round few mm.	GC	4246-4250
31946	175.09-175.32	L.T hetero; mostly composted of MC? With some grey felsic lap clasts, strongly fol, mod ser, f-gr speckled and disem py. Clasts are 1x0.5 - 1.5-4 cm. could be considered a greywacke	rep litho/TS	4251-4254
31947	176.16-176.61	nice graded seq	rep litho/TS	
31948	186.02-186.24	f. tuff with wk-mod ser alt, 2 thin beds of arg, rare m-c-gr py in matrix. 8% f.g. py in thin laths, look like could be replacing tuffaceous grains. Incorporated in matrix and with fol.	GC	4255-4259
31949	189.62-189.84	mud interbeds; f.g tuff with thin arg interbeds, mostly continuous. Some are faulted? Or scoured. Obvious load structures with f.g arg and slightly coarser tuffs (m.g). 3% m-c-gr py mostly in tuffaceous beds but can cut through arg. <10% v.f.g py in fol in tuffaceous layers, similar to above. get some clustering of py in elongated pods.	GC	4260-4265
31950	206.57-206.72	felsic dyke? F.gr light grey, 4 0.5 cm white	GC	4266-4270
14751	214.41-214.58	hetero tuff/L.T. <5% euhedral py xstals.	GC/TS?	4271-4274
14752	242.25-242.49	mafic sill + chl	GC	4275-4276
14753	272.48-272.69	L.T ser + chl; heterolithic tuff with mostly grey lap, light grey, dark grey (v. thin). And 5% white round xstals (plag).	GC (TS?)	4277-4280
14754	213.58-213.76	weird qtz veins/stwk; par tof MS? 25% sp, 15-20% gn, 15% py, 3% cp. White veins are irregular, 10% veins, rest is gangue.	rep litho/TS	4281-4285
14755	289.37-289.59	chl/ser stwk py; sericite alt tuff with chl+py stringers few mm thick.	GC	4286-4289
14756	305.15-305.45	chl/ser stwk py; chl=ser alt tuff with 45% py. Semi massive sulphide. F-c gr py. Can see some relic qtz xstals in matrix.	GC	4290-4296

GA-10-272

Tag	Depth (m)	Rock Type (initial)	Purpose	Photo #

32125	1.84-2.12	xstal tuff; xstal bearing tuff/l.t could be due to alt; mod sil +ser/chl veinlets with 1-2% disem py. If lap is fine, would be elgonated light grey laps. Xstals (15%) are tabular (rare) to round, white qtz with lesser plagioclase, lesser clear qtz	GC	3535-3541
32126	20.64-20.87	ash tuff or L.T (homo) sil; homo L.T, lap are pale grey and sil alt with darker (chl?) alt in matrix f.g. with few mm qtz (clear) xstals in it. <5% white 5-6 mm white qtz xtals (round) in pale grey lap. Some lap appear "fractured" or broken up within the lap fragments., could be autoclastic?	GC/REP	3542-3549
32127	34.4-34.66	are pale grey with chl+ disem py (rare sp + silverly colored vein) veinlets with lesser ser veinlets (5-7% veinlets). Few mm clear round qtz xtstals throughout ~10% in pale grey laps. Mod-strong sil alt, wk chl>ser	GC	3350-3556
32128	43.1-43.44	chl alt hetero tuff/LT; disem med-gr py, <10% clear/dark qtz crystals, lap are grey with some darker grey, but dark grey mostly makes up matrix which is very f.g. lap are elongated. Some subrounded qtz crystals ~1cm pale white (<3%). Wk-mod sil/ wk-mod chl.	GC/REP	3557-3568
32129	55.57-55.8	sil/chl alt L.T w/ f.g in matrix; 0.5-1cm white qtz xtals (5%). Could also be a flow?? Ale grey and black elongated/boudinaged lap?? Pale grey is thicker + dark grey appears to be making up matrix. Similar to above, no sulphides	GC	3569-3576
32130	64.8-65.03	mafic dyke (1); f.g. dark green grey	GC	3577-3580
32131	89.8-90.04	either mafic or chl alt xstal tuff; pretty sure chl alt xstal tuff. ~20% qtz xstals both white and clear, >1% thin (mm-scale) carb veinlets and some carb replacement along xstal faces?	GC/**TS (PIC**	3581-3588
32132	104.32-104.5	xstal tuff w/ ch alt (could be the same - above), same as above but this has plagioclase xstals, where I don't think the one above does. Plag > qtz; white and clear qtz and white tabular to subrounded plagioclase. F.g, approx 20-25% xstals, strong chl alt.	GC/**TS**	3589-3594
32133	111.6-111.1	chl alt TB/LT w/ py	TS?-cool sar	3595-3599
32134	119.59-119.8	mafic dyke (2); f.g, dark grey	GC	3600-3605

32135	124.34-124.58	v. chl alt tuff w/ disem py (change in alt) possible sheared qtz veins? Pieces of white qtz, 2 contacts, one with disem sulphide and one with mud? Or alt a.t	GC	3606-3612
32136	134.70-134.95	intermediate dyke (prob mafic); pale grey in color with plag xstals in f.g matrix. X-cutting carb? Veins + euhedral med gr py (<5%) + 3% pyrhotite in black (chl?) veinlets.	GC	3613-3619
32137	142.3-142.55	Lots of qtz crystals all different sizes. From fu-cl. With rare granule size particles. Strongly ser/sil alt? 1-2% clusters of py.	GC	3620-3627
32138	152.06-152.3	m.gr tuff + MC + py (6%), wk-mod ser	GC	3628-3634
32139	167.8-168.0	intermediate dyke? Or MD (3) f.g. 1% carb mm-scale amy	GC	3635-3639
32140	172.08-172.3	mod ser + wk chl f.g L.T/ m-c- tuff (2% py) w/ mud clasts, heterolithic, rare (1%) pyrhotite.	GC	3640-3645
32141	177.34-177.76	sil alt +ser/chl tuff (change in alt)	GC- good ex TS?	
32142	181.8-181.98	ser + chl tuff (coarse) sim to above, coarser then previous, but similar composition of pale grey with black mud clasts and white plag xstals + murky white coarse qtz xstals. Rare py	GC	3646-3652
32143	201.75-202.02	mafic sill, f.g massive, f.g black xstals elongated/tabular	GC	3653-3659
32144	220.7-221.0	mod ser/chl f/m tuff + white round crystals	GC	3660-3364
32145	255-255.19	strong ser alt +py tuff FW	GC	3665-3672
32146	262.25-262.47	ser/chl/carb tuff FW	GC	3673-3681
32147	280.37-280.57	ser alt +chl/py bands FW + chaotic carb	GC	3682-3686
32148	292.47-292.66	ser w/ discont py bands	GC/TS	
32149	298.3-298.58	fold ser tuff +py	NEATO	
32151	224.46-224.8	chl + MS	TS	
32152	237.01-237.15	chaotic carb	TS	
32153	240.22-240.26	bands of py, gn, sp in ser	TS	
32154	240.43-240.65	chl/ser alt tuff + py	GC	
GA-14-275				
Tag	Depth (m)	Rock Type (initial)	Purpose	Photo
14757	5.87-6.06	sil alt tuff w/ xstals, looks like a tuff because look like lap fragments, but could potentially be a flow fragments look coherent	GC	5322-5327
14758	23.4-23.64	probably a flow, felsic, with wormy looking qtz veins and silverly thick veins. Very coherent looking, few xstals, some sericite veins.	GC	5328-5332

14759	39.61-39.82	heterolithic tuff/L.T mod sil/chl	GC	5333-5336
14760	58.83-59	qtz-felds tuff wk chl	GC	5337-5339
14761	63.79-63.9	mafic dyke	GC	5340-5344
14762	77.23-77.43	qtz-felds tuff mod chl	GC	5345-5347
14763	98.83-99.14	mafic dyke	GC	5348-5349
14764	105.63-105.89	graded tuff--> chert/A.T	TS/REP/GC	5350-5355
14765	109.62-109.94	fine tuff/A.T? (1% py)	GC	5356-5358
14766	118.44-118.7	felsic dyke? Wk chl	GC	5359-5362
14767	126.5-126.83	mudstone, few pieces ; arg with f-m gr grey tuffs with disem m-g py disem and f-m-gr in veins in arg	GC	5363-5364
14768	140.28-140.49	felsic dyke/ alt mafic or int?	GC	5365-5367
14769	148.8-149	hetero tuff w/ MC (or thin black elongated clasts) 2% f.g disem po	GC/REP	5368-5376
14770	163.81-164	mafic sill	GC	5377-5382
14771	180.71-180.89	mafic sill	GC	5383-5385
14772	196.54-196.74	finely lam sil/ser A.T	GC	5386-5387
14773	198.3-198.5	ser alt hetero tuff	GC	5388-5390
14774	213.58-213.76	ser/sil (v) alt tuff w/ py	GC	5391-5401
14775	239.6-239.88	ser/sil (v) w/qtz xstals tuff +py chl stringers (py is more concentrated in), can see relict qtz xstals!!	GC/TS	5402-5411
14776	248.17-24.37	alt dyke	GC?	5412-5414
14777	250.71-250.89	ser/sil alt tuff + py+ 4% sp, 2% gn - seem to be assocaited with more sil alt lap, can see relict qtz xstals!	GC/REP	5415-5426
14778	253.15-253.35	ser/ sil atl w/ sheared chl stringers + py	GC/REP	5427-5438

GA-14-276

Tag	Depth (m)	Rock Type (initial)	Purpose	Photo
14779	6.9-7.13	qtz-felds (15%) mod sil alt tuff; light-med grey in color. Qtz-feldspar xstals are 1-3mm. Matrix is fu/ml, ser veinlets are parallel to fol, f.g py is disem (5%) and (1%) f-m gr py is in thin ser veinlets. Qtz>felds	GC	4644-4648
14780	23.4-23.64	tuff?);white to pale grey in color, with reddish-orange staining (fe-carb or sulphide staining?) 0.5- 3mm round clear qtz xstals, looks coherent, thin sericite veinlets (2%).	GC/rep	4649-4655
14781	46.88-46.98	sil xstal bearing L.T + ser; light grey with med/dark grey matrix. Lap are ghostly looking and pale grey	GC	4456-4463
14782	58.56-58.92	sil xstal bearing L.T + ser w/ chl veins?	GC	4664-4669
14783	75.10-75.37	heterolithic L.T (chl) f-m gr.	GC/rep	4670-4674
14784	95.22-95.44	Qtz- (>)felds bearing f-gr tuff mod chl, med grey greenish	GC	4675-4679

14785	97.77-98	mafic dyke, f.g dark green grey.	GC	4680-4683
14786	115.85-116	xstal tuff (qtz>felds); disem clusters of f-m gr py in matrix, some of matrix is chl alt, some sheared qtz veins?	GC	4684-4690
14787	131.25-134.47	felds+qtz xstal tuff	GC	4691-4698
14788	147.47-148	with carb? Get bleached zone. Overall m-gr, few white qtz phenocrysts. Wek-mod sil	GC	4699-4703
14789	154.55-154.75	f-m pale grey/white tuff with f-m disem py throughout. Rare po vein	unsure?	4704-4713
14790	171.14-171.36	arg interbeds +p.y. v.f-f-gr tuffs/greywackes? Boudinage qtz veins	GC?	4714-4719
14791	177.29-177.42	arg w/ py- deformed, fault zone? Py is prob remobilized.	GC	4720-4725
14792	183.45-183.65	strong sil L.T hetero?some clasts? Look aphantic whereas others look crstallize/granular and there is black in between some fragments which is v.f.g but not continous. 1% disem clusters of f.g. py. F.g flecks of white/silver v.f.g, in one lap(?) there are round black xstals surround inside. looks somewhat deformed, could potentially be flow??	GC	4726-4731
14793	194-194.23	felsic dyke? w/carb alt; carb amygdules, 5% qtz xstals. Looks like dyke. But light grey. Thin x-cutting vein with po (5%) and py (2%).	GC	4732-4737
14794	217.47-217.74	Fine elongated anhedral py in matrix >1mm (5%), rare po, 2nd gen is euhderal (1%) m-gr disem throughout (even in clasts) OP?	GC	4738-4743
14795	224-224.2	arg w/ qtz veins, qtz veins are erratic, probably fault zone, v.v.f-gr py in fol (35)? Or is aligned, there are also f.g clusters of py (1%).	GC?	4744-4746
14796	238.6-238.8	mafic sill, v.v.f (common) and ml carb amygdules	GC	4747-4753
14797	259.29-259.57	med tuff w/ round white felds xstals; 2% disem v.f.g py, mod ser alt, wk chl.	GC	4754-4759
14798	295.70-295.93	ser alt tuff; white round qtz xstals, pretty xstal rich, fu/ml, few darker grey thin discont bands, v.v.f.g pale yellow flecks disem everywhere (10%).	GC	4760-4765
14799	307.54-307.71	chl alt tuff? With erratic qtz veins wormy looking and carb OP and f.g disem throughout (7%) but closer more close to the QTZ veins.	GC	4766-4772

14800	311.63-311.84	alt tuff with blobs of chaotic carb and qtz?? Thin py veins in chl alt (5%) OR they could be clasts of rhyolite?? Can see similar fragments/ lithologies in the upper part of the footwall (try and find what section)	GC?	4773-4778	
32051	333-333.48	stwk chl/ser py; grey laps of felsic material (mod ser alt?) with chl replacing matrix. F-m/c-gr disem in chl stwk veins.	GC	4779-4782	
32052	352.09-352.3	strongly ser alt tuff with v. siliceous globs and possible carb overprint?? (orange). Py veinlets and m-gr clusters	GC	4783-4789	
32053	368.14-368.34	ser+py (clusters of m-gr, 10%). Lap fragme	GC	4790-4798	

Section 4000

GA-07-257

Tag	Depth (m)	Rock Type (initial)	Purpose	Photo #	Thin Section
32207	421.11-421.31	mafic dyke or could be int or ser alt MD. 3% finely disem py, and fe-carb OP (upwards of 15%).	GC	6158-6163	
32208	424.79-424.99	heterolithic felsic dom tuff w/ white plag + py wk ser, wk py mineralization (f.g disem <1%)	GC	6164-6171	
32209	435.01-435.18	stringers, rare sp in veinlets not associated with chl	GC	6172-6179	
32210	451.0-451.25	strong sil/ser w/ py (15%) tuff rare golden sp.	GC	6179-6190	
32211	472.97-473.14	maybe ff? str sil, wk py	GC	6191-6194	
32212	482.97-483.25	mod ser/sil +cp +py+ gn (sp and gn are f.g. in thin bands whereas py and cp are coarse grained and more disemminated)	GC	6195-620	6209-6213
32213	489.5-489.7	mod-str ser+ sil + sp +py wk chl - thin veins of sp and py together and py alone	GC	6205-6208	

GA-10-273

Tag	Depth (m)	Rock Type (initial)	Purpose	Photo #	Thin Section
32214	248.24-248.46	dark green grey md with carb OP	GC	6214-6217	
32215	277.58-277.83	ser alt tuff	GC	6218-6223	
32216	281.72-281.92	ser + cc (?) tuff	GC	6224-6228	
32217	297.68-298.88	alt MD	GC	6229-6232	
32218	304.79-305.03	ser alt with intense ser alt stringers?? + py + wk chl tuff and partial flow??	GC	6233-6239	
32219	267.8-268.09	ser alt w/ py + sp stringers + gn +chl stringers	GC	6240-624	6244-6248
32220	273.00-273.2	mostly chl alt + py and chl	GC	6249-6251	

GA-06-153

Tag	Depth (m)	Rock Type (initial)	Purpose	Photo #	Thin Section
31916	17.60-17.6	felsic x stal sil alt; felsic xstal-bearing f-m .g light grey tuff. Mod sil alt, 5% plag xstals. Lap are grey and very light grey, elongated few mm. 3% f.g disem py stringers. Some areas are more strongly sil alt ie. white blotches.	geochem	4297-4300	
31917	26.64-26.84	sil alt tuff with plag xstals; could be felsic flow.. Strongly sil alt with light grey. Or could be homogenous/autoclastic L.T. chl/ser veinlets are outlining lap fragments. Py in chl veinlets (only just 10%). 2 mm white plagoclase xstals (7%).	geochem	4301-4303	
31918	44.25-44.5	mafic dyke; f.g with v.f.g disem py (<5%).	geochem	4304-4308	
31919	97.95-98.17	mod sil xstal tuff; med grey f.g with some darker grey wavy blotches. 10% white plagioclase xstals 2-3 mm. and lesser finer clear qtz xstals. Rare m.g anhedral py, <10% v.f.g disem py.	geochem	4309-4314	
31920	135.82-136.04	xstal tuff? Feldspar xstals; mod sil alt ; could be porphyritic felsic flow with 15% plagioclase xstals, light/med grey matrix, <10% qtz xstals clear/grey, light creamy beige blotches that look like they could be replacing plagioclase xstals, some places it looks like sp (3%). blotches are elongated few mm.	geochem	4315-4319	
31921	163.61-163.83	sil alt L.T. feldspar xstals; xstals are clear and round qtz xtals(7%), (3% white subround xstals, lap fragmetns are typically light to me dgrey with fewer darker grey laps. **Felsic L.T (f.g)**	geochem	4320-4323	
31922	179.79-180.02	chl alt xstal tuff; soft to cut. Plag (white,< 10%) and qtz (clear <10%) (5% carb rhombs). F.g matrix is dark grey somewhat green (chl alt), carb overprint is evident on outside.	geochem	4324-4328	
31923	197.62-197.84	sil alt L.T ser or FF?; appears to look like L.T because of dark grey chl? Alt in filling space or could just be felsic flow with chl alt veinlets with f.g py. Dark grey chl veinlets or blotches. 3% py dises in veinlets. Light grey in color.	geochem	4329-4332	

31924	226.34-226.71	mod sil alt A.T; f.g AT, with thin veinlets of py and ser (5%). Most veinlets are concordant, 1 rare one is discordant an x-cutting. Some are discontinous.	geochem	4333-4337	
31925	230.7-230.85	mafic dyke, f.g dark green grey.	geochem	4338-4340	
31926	246.94-247.09	L.T mod sil MC; light grey lap tuff with dark grey blotches of elongated lap-looking fragments or could be chl alt, pretty sure it's just alteration of different fragments. Pale white round xstals (<5%).	geochem	4341-4344	
31927	263.1-263.32	alt dyke? Or felsic dyke, f.g light grey, dark f.g speckles, clear/white qtz amygdules? Some void vesicles with py in it.	geochem* (T	4345-4348	
31928	284.06-284.3	hetero L.T ser>chl alt; pale grey, grey, thiner dark grey laps, some armored clasts, 10% round white plag (?) xstals. F.g lath-like po.	geochem	4349-4352	
31929	305.75-305.95	tuff?! Wk sil?; chl alt f.g tuff. Some visible qtz xstals.	geochem (TS	4353-4356	
31930	321.72-321.91	graded tuff; mod ser alt, rare MC (elongated), m-gr tuff with fine ash layer, white round <1mm-2mm plag (?) xstals.	geochem	4357-4359	
31931	336.1-336.3	mafic dyke; f.g with f.g carb laths in it.	geochem	4360-4363	
31932a	354.69-354.92	VMS chl alt with py; ser alt tuff with dentritic carb/qtz veining (15%) with chl+py stringer veinlets (15%), gn (4%) and sp (>10%) is assocaited with py veinlets with rare cp .	geochem	5458-5466	
31932b		ser alt tuff with dentritic carb/qtz veining (15%) with chl+py stringer veinlets (5%).	geochem	4364-4368	
31933	390.7-390.92	ser>sil alt and py (10%) stwk	geochem	5439-5446	
31934	407.5-407.70	ser and sil alt stwk with py stringers and pods of clustered py (m-g) in darker halo	geochem	5447-5452	
31935	448.7-448.95	ser alt stwk - more grey then 2 above, just ser alt, maybe wk chl as well with disem f-g py	geochem	5453-5455	
31936	469.5-469.7	ser alt stwk	geochem	5456-5457	

Section 4050

GA-10-274

Tag	Depth (m)	Rock Type (initial)	Purpose	Photo #	Thin Section Photo #
32054	6.18-6.37	flow.. This kinda looks like it says fragments of felsic flow. See other pictures	GC	5179-5182	

32055	26.64-26.84	sil alt tuff with plag xstals, same with this, but has clusters of f-m-gr py	GC	5183-5188
32056	44.64-44.84	tuff and xstals of felds mod sil and ser, with disem py (fg)	GC	5189-5192
32057	53.24-53.41	v. sil alt L.T; new unit change in alt; but it could also be a felsic flow.. Has wormy ghostly qtz veins	GC	5193-5195
32058	55.96-55.24	MD; beige; could be intermediate?? Has round clusters of f-m-gr py	GC	5196-5202
32059	66.46-66.71	sil alt L.T. white dry, could be flow with alt in cracks..	GC	5203-5205
32060	74.06-74.36	hetero L.T; clusters of py in elongated discont veins (5%)	GC	5206-5214
32061	87.84-88.06	hetero tuff wk chl and sil	GC	5215-5219
32062	95.7-95.91	MD; green wk chl	GC	5220-5221
32063	115.1-115.3	tuff with 10% qtz-feld xstals mod chl	GC	5222-5227
32064	120.16-120.33	hetero L.T mod ser/sil graded	GC/rep	5228-5230
32065	125.66-125.94	ash tuff cont' of L.T	GC/rep	5231-5235
32066	141.46-141.73	hetero L.T (compare); disem py f-g. matrix support, matrix is light grey and f.g, lap are grey and apantihic, py is mostly in matrix but is also in some clasts	GC	5236-5244
32067	154.9-155.1	tuff? Wk chl?; looks like xstal rich tuff, sandy like. Mostly qtz xstals. Wk alt	GC	5245-5249
32068	166.28-166.51	f.g. tuff mod sil	GC	5250-5254
32069	179.84-179.99	alt dyke? Or FD	GC	5255-5257
32070	186.15-186.35	arg beds and m-gr sub-euhedral py in mg. tuff	GC/rep/TS?	5258-5262
32071	197.35-197.63	felsic dyke?	GC	5263-5267
32072	198.75-199.03	hetero L.T ser alt mod/wk chl, 5% disem f-m gr py	GC	5268-5273
32073	222.68-222.89	**mafic sill**	GC	5274-5276
32074	250.1-250.32	tuff w/ wk sil/ser; in contact with mD; could make coool TS to see contact	GC	5277-5284
32075	261.05-261.32	mafic sill	GC	5285-5287
32076	270.9-271.1	chl alt (VMS) tuff;	GC	5288-5296
32077	272.23-27.5	ser alt tuff w/ chl stringers, f.g- py is assoicated with chl stringers (30%) (with rare gn, and possible 5-10% sp-unsure) but f.g disem py is also in ser alt (15-20%) tuffs, lower is GC sample	GC	5297-5304
32078	296.34-296.54	v. ser alt FW	GC	5305-5309
32079	307.2-307.4	v. ser alt FW; popcorn looking lap?? Py; some green micas in footwall sericite altered rocks	GC	5310-5317
32080	319.36-319.56	v. ser alt FW; had qtz vein, cut most of it out I think	GC	5318-5321

GA-14-277

Tag	Depth (m)	Rock Type (initial)	Purpose	Photo #	Thin Section Photo #
32155	6.7-6.92	x-stal bearing tuff mod sil	GC	4975-4982	
32156	29.5-29.73	xstal tuff or porphyritic flow? Fe-carb rhombs	GC/TS	4983-4990	
32157	45.8-46.0	felsic flow? Or sil alt tuff, contact? 15% sericite veinlets, v sil.	GC/TS	4991-4995	
32158	51.0-51.18	mafic dyke (could be AT??) light olive green run off	GC	4996-4999	
32159	56.16-56.44	sil alt L.T. or **felsic flow (pretty sure) v. sil, v. hard**	GC	5000-5005	
32160	67.57-57.97	**felsic flow**? Or sil alt L.T vil sil alt, very hard to cut, wormy qtz veins	GC (REP LI	5006-5010	
32161	70.02-70.2	mafic dyke	GC	5011-5015	
32162	81.5-81.7	porphyritic felsic flow?	GC/TS	5016-5021	
32163	93.96-94.2	chl alt xstal tuff	GC	5022-5028	
32164	114.41-114.63	xstal rich tuff	GC	5029-5037	
32165	136.14-136.32	felsic dyke? Or **A.T**	GC	5038-5042	
32166	139.04-13.22	arg	GC	5043-5047	
32167	139.29-139.5	graded At w/ wrg +MC+chert+ clusters of m-gr py (3%) in veinish	TS	5048-5053	
32168	153.27-153.5	mafic dyke	GC	5054-5058	
32169	159.36-159.56	mod ser alt tuff + m-c disem py (<5%) with wk chl	GC	5059-5062	
32170	165-165.22	mafic dyke beige	GC	5063-5066	
32171	190.52-190.74	mafic sill	GC	5067-5070	
32172	209.24-209.54	felsic tuff, white round xstals	GC	5071-5076	
32173	232.72-232.96	ser alt tuff w/ bands of py+chl stringers	GC	5082-5088	
32174	243.2-243.45	ser alt tuff w/ bands of py	GC	5077-5081	

GA-14-278

Tag	Depth (m)	Rock Type (initial)	Purpose	Photo #	Thin Section Photo #
32175	18.5-18.7	sil alt xstal bearing tuf/**porphyritic flow**; pale beige grey in color, mod sil alt, 15% plag xstals 2mm, coherent, felsic, f.g. discont bands of anhedral **f**-m py (2-3 cm in lenth, 1-2mm in width, 7%). Resembles a porphyritic flow rather then a tuff, however, could be "homo" LT? but most likely porphyritic flow	GC/rep(TS)	4462-4468	

32176	38.51-38.73	tuff w/ sil/beige; plagiclase xstals, light-med grey in color, 10% plag xstals.lap are med-coarse-gr pale grey and med grey. Few more white bands of more sil alt. strong sol, mod sil, wk ser.	GC/ts	4469-4472
32177	42.91-43.09	porphyritic felsic flow; light/med/pinky grey, 10% 1-3mm plag xstals, clusters of m-gr py. Could be lap tuff, laps looks made of qtz and felsic fragments. There are also smaller clear qtz xstals (few mm) and round. Mod sil alt, wk chl. However, does look like 75. **ASK**	GC/ts	4473-4478
32178	60.90-61.15	felsic flow; pale pink, coherent, f.g, few spaced out qtz xstals, 3% py, v. sil alt. massive, wormy qtz veins	rep litho	4479-4485
32179	70.51-70.81	mafic dyke/pillow basalt; possible multi gen MD, with selvages of v.f.g green/grey in wavy bands in f.g mafic dyke? Or could be chl alt tuff? Possible ts? F.g clusters of disem py. Mod chl alt	GC?	4486-4490
32180	84.0-84.24	xstal tuff w/ ser and chl wk; approx 45% xstals total. With 25% clear/ dark qtz, 15% white pale qtz and 5% broken up plag xstals. Rare wormy qtz veins, matrix is grey and f.g. mod sil, wk ser, wk chl.	GC	4491-4498
32181	94.81-95.02	tuff, visibile qtz xstals, mostly clear, some pale white, matrix is replaced by chl, dark green grey in color, f.g, 3% carb amygdules	ts	4499-4505
32182	111.39-111.63	chl alt tuff see qtz xstals; same as above.	GC	4506-4513
32183	119.34-119.63	awesome graded med-gr L.T-ash, could be considered "sandy" looking, but is a heterolithic felsic tuff.	rep litho/TS	4514-4521
32184	130.69-130.9	v. sil alt, could be L.T or felsic flow, or autoclastite	GC	4522-4525
32185	138.28-138.52	same unit, colors are pale grey and dark grey in "matrix", strong sil, wk chl?	GC	4526-4529
32186	153.63-153.84	wk alt A.T?; v.f.g tuff, pale grey, matrix looks replaced by ser? Can see fl qtz xstals but has patchy light grey matrix. Thin dark grey veinlets of chl? 3% fine discont veinlets of f.g py clusters.	GC	4530-4535
32187	163.51-163.71	same unit? Xstal tuff w/ chl alt, similar to above, but with bands of more black chl alteration with interlayered with bands of more ser alt tuff. Chl alt is difficult to see on cut side?	GC/ts?	4536-4541

32188	176.41-176.62	either A.T or dyke w/ fe-carb; still not sure, f.g pale beige grey in color, looks granular, black 0.5-1mm somewhat concordant veins. **Ask**	GC	4542-4547
32189	183.72-183.92	wk-mod ser alt tuff thin A.T/chert; med-gr tuff into chert layer, below chert layer there is a fine-gr darker layer only a few mm.. Looks like gn?? But probably not.. Above chert layer is fu/ml light grey tuff, with 1% euhdral f-m py. Wk-mod ser	GC	4548-4555
32190	190.48-190.64	ser/sil alt MD; light grey, coherent, m-c-gr. Very siliceous, looks like round xstals all together.. With few thin black cont and discont veinlets.	GC	4556-4560
32191	201.54-201.78	mod ser alt med hetero tuff; med grey in color with light grey elongated felsic lap fragments (5%), black thin and elongated (3%), clear and pale white qtz xstals. Matrix is grey and f-m gr. And disem f.g py (<5%).	GC	4561-4566
32192	215.31-215.48	mod chl ser alt hetero tuff; similar to the unit above but more chl alt. dark grey in color this one has 2-6mm mud clasts in 0.5-3mm round pale white qtz xstals. Matrix is fu, approx 25% xstals. Rare euhedral py xstals. Mod chl + wk ser.	GC+change	4567-4571
32193	234.41-234.58	xstal rich v chl alt? dark green grey ml/mu xstal tuff, strongly chl alt. clear dark and pale white qtz xstals.	GC	4572-4577
32194	263.-263.22	chl alt tuff or sill?; does look like it has very fine (fl) dark clear qtz xstals but it also has clusters of plagioclase xstals or they could be broken up. Overall, f.g (fl/fu) with patches of pale white (could be carbonate because very soft) **ask!**	GC	4578-4584
32195	269.82-270.0	ser alt tuff above sill; pale grey in color, fu/ml tuff with <10% creamy white round (1mm) plag xstals? Band of f.g py xstals, still has clear dark qtz xstals, (15%). Mod ser alt, wk chl.	GC	4585-4591
32196	280.08-280.29	ser alt tuff above sill w/ white xstals; med-c gr tuff, **v.f**-m-gr py disem clusters (3%) med grey > darker grey lap.	GC/TS	4592-4599

32197	300.01-300.30	mafic sill; or chl alt tuff. F.g dark green grey, granular -looking, black laths (could be MC? Or mafic minerals?, very soft), >5% plag and qtz xstals (few mm), could be sill.. F.g subhedral py xstals.	GC/rep litho	4600-4604	
32198	305.4-305.52	L.T w/ sulphide chl replacement in matrix	GC	4605-4608	
32199	306.7-306.95	chl + py + ser stringer in L.T/tuff; chl alt is more dominant in left hand side whereas ser alt is dominant on left. But get irregular chl/py stringers in ser alt zone. Approx 35-40% py. Get thin discont bands of chl in ser alt part as well. Patchy blobs of dolomite? some relict qtz?	GC	4609-4615	
32200	309.3-309.51	v. chl alt +sp+py; vein of gn surrounded by pale white (could be carb?, not overly soft..) and discont bands of sp.	GC/ replitho	4616-4624	
32201	320.36-320.53	strongly ser alt +carb and py, broken in a bunch of small pieces.	GC	4625-4626	
32202	328.28-328.51	v. chl alt + carb and py (15%). However, looks like there are still plagiclase xstals in matrix. I think that cut in half it's chalked full of qtz and plag xstals with the matrix completely altered to chl.	GC **(TS)**	4627-4638	
32203	332.65-332.83	ser alt tuff +py stringer + chl	GC	4639-4643	

Section 4100

GA-06-176

Tag	Depth (m)	Rock Type (initial)	Purpose	Photo #	Thin Section Photo #
32222	314.11-314.31	mafic sill	GC	6263-6268	
32221	329.99-330.12	MS w/ weird black mineral	rep litho	6269-6274	

GA-06-180

Tag	Depth (m)	Rock Type (initial)	Purpose	Photo #	Thin Section Photo #
32081	20.25-20.47	strong sil alt + ser tuff (white round xstals of qtz) 8% f-m gr anehdral py in thin discont veinlets - could be a flow? Or instrusive		4799-4803	
32082	40.79-41.08	strong sil alt + ser tuff , ser veinlets, rare chl-looking veinlets, white round qtz xstals, rare wormy qtz vein		4804-4809	
32083	57.1-57.37	strong sil alt + ser L.T-- this is probably a flow, pale white/grey/ink, 10% ser veinlets, white round and tabular qtz and plag xtals, looks coherent. 3% f.gr py veinlets associated with ser veining		4810-4816	

32084	69.56-69.37	chl + ser + strong sil L.T; lap fragments look like they're made of coherent rhyolite with plag xstals. Kind of look similar to above or other felsic flows in the area. Matrix is altered to chl.		4817-4821
32085	82.96-83.2	tuff w/ A.T beds, new alt - this has similar fragments as above (pink coherent with white plag xstals but has more of a f-m-gr matrix associated with it. Matrix looks like its wkly chl altered and is chalked full of f-m-gr anhedral py parallel to fol. double check for other sulphide minerals. tuff with lap sized fragments (above) py is in la fragments as well, must be late? even a mud clast. this would be heterolithic tuff. probably re-worked but could be primary?		4822-4826
32086	99.02-99.22	dyke (mafic?), chalked full of pale white rhombs of carb (60%), check photos for contacts, could be felsic.. Or be AT.. b/c wasn't green when cut.. But is v.f.g. and dark. 2% f.g. py disem clusters		4827-4831
32087	111.19-111.44	tuff wk chl; mod-strong sil alt in pale grey l.tuff? Pale grey is lap frags with dark grey/black thin bands in matrix space which is prob chl alt v.f.g py (7%) is in chl bands. Some plag ± qtz xstals 20%) in lap fragments. Could be potentially part of a flow. carb rhomb OP (20-30%)??		4832-4839
32088	123.77-124.04	sil alt L.T.- lap fragments are rhyolitic, look like flow fragments. Clear round qtz xstals in fragments but in "matrix" too, could be felsic flow with fracturing being altered causing the colors to appear to look lie diff lap fragments.		4840-4848
32089	146.69-146.94	chl plag- bearing tuff/porphyritic felsic volcanic , mod -strong sil alt, 3% cluster 1cm veinlets of f.g py		4849-4855
32090	163.72-163.95	wk chl, mod sil alt tuff, f.g tuff with few lap in it and plag and qtz xstals. Pinkish wormy blobs look similar to flows.. And contain same xstals as matrix. Carb OP		4856-4859
32091	187.4-187.59	wk chl alt tuff + fe-carb OP +clustered f.g py (5%) in distcon veinlets (2-5mm thick)		4860-4864

32092	195.54-195.81	wk chl mu/ml tuff with 10% lap size fragments of dark grey aphantic material and creamy white elongated blobs (less 1%) def a tuff. 5% disem clusters of f.g. py		4865-4871
32093	210.49-210.66	felsic dyke? 3% f.g disem py, qtz amy, qtz vein		4872-4878
32094	219.79-219.93	felsic dyke? Xstals - int? **prob massive xstal tuff, def a tuff, mu/ml, pale grey, qtz xstals.**		4880-4882
32095	236.22-236.45	tuff w/ AT or silt beds topped with arg and thin arg beds. Subhedral py xstals mostly f.g with rare m usually in finer beds or in arg (disem) with lesser in tuffaceous beds. Some of the args beds could be slightly deforme giving them a wavy/wormy apperance compared to the more compotent tuffs		4883-4890
32096	236.73-236.92	fl/vfu tuff?? Or just sed rock (greywacke?)With elgonated MC in it, capped by arg with discont fl tuff in between with chert layers?/ then more thinly bedded arg with v.f.l tuff seq. arg layers are hard,, tuff is only soft one eu-subhedral py (3%) mostly in arg units or chert		4891-4901
32097	242.67-242.89	sil/ser alt felsic dyke?; pale grey pink, looks coherent with small qtz xstals in it, mod sil, possible wk ser?		4902-4904
32098	261.1-261.32	wk-mod ser alt ± chl heterolithic tuff with lap fragments		4905-4910
32099	285.15-285.45	xstal rich M sill? Wk chl + amy		4911-4916
32100	300.4-300.6	mafic sill chl alt		4917-4921
32101	321.68-321.91	heterolithic tuff with white round xstlas, mod ser alt, 5% mc, wk py		4922-4926
32102	327.2-327.4	py stringer-f-c py 1-5cm py bands hosted in ser alt tuff. Can see relict qtz xstals in py stringers.		4937-4949
32103	338.39-38.58	ser alt tuff + chl py (f-m lesser c)(25%) stringers, py mostly contained in chl stringers but can be finely disem in ser alt tuffs, rare gn +cp (1%) asso w/ py		4927-4932
32104	339.67-339.87	ser alt tuff+ chl py stringers py (20%) is mostly f.g , there aren't as many veinlets in this one but mostly finely disem py in ser alt with few chl stringers.		4933-4936

32105	341.85-342.05	MS ; bands of sp (20%- red and gold) and py (30%) (dominant, f-c) with lesser (1-2%) cp and gn (8%). Gn is hosted within sp bands and cp looks later in interstitial space. Still reliect qtz veins and few xstals		4950-4961
32106	361.9-362.14	mafic sill strong chl alt		4962-4965
32107	391.9-392.18	ser alt tuff/ fault B		4966
32108	397.9-398.08	ser alt tuff/ fault B		4967-4970
32150	341.01-341.26	ser/chl py stwk; 5cm chl stwk vein with f-c py (15%) sp (5%), rest of ser alt with thin veins of py and disem f.g py (25%).		4971-4974

Section 4150
GA-14-279

Tag	Depth (m)	Rock Type (initial)	Purpose	Photo #
32109	17.35-17.65	coarse L.T ; med L.T with felsic lap fragments, average gr size is 0.5-2 cm with larger lap fragments up to 3-4 cm (light grey, med grey and clustered fragments of py). With darker grey matrix of fu/ml (85:15). Contact with light grey f.g mu with 2-5mm qtz xstals (oval; 15%). looks like sharp contact on cut side but not as obvious on rounded side, < few mm to few mm py xstals subhedral disem through matrix and surrounded by black.. could be replacing??). wk to mod ser/ wk chl.	G.C	4370-4374
32110	31.11-31.29	~~Mafic?;~~ xstal tuff- qtz-rich felsic xstal tuff. Qtz xstals are white and clear. Clear ones seem to be more fl/fu whereas white are fu/ml/mu with some being CL (<5%). Approx 60% xstals. Very xstal rich . <5% plag xstals. Qtz xstals are round to oval/subrounded. matrix is v.f.u. light grey in color. wk ser alt most likely.	G.C	4375-4380
32111	41.92-42.13	Mafic dyke; f.g. MD dark green grey in color. <2% clusters of anhedral py (0.5 mm- 2mm). Wk chl alt	G.C	4381-4384
32112	56.29-56.53	f.g qtz-bearing tuff. Mod ser alt wk sil. Wk chl. qtz xstals are v.f.u. with rare CU. light grey in color, pale beige ser veinlets are crenulated and are 45 from fol. Get some bands of slightly darker grey (2 cm in width).	G.C	4385-4390

32113	70.17-70.47	Could be autoclastic rhyloite? Pictures from section resemble that.. 1-2% plagioclase xstals subhedral and 2-5 mm, black v. thin veinlets (<1mm) could be outlining autoclastic clasts? Rare py (euhedral-subhedral), thin qtz vein (or carb). mod ser	G.C	4391-4398
32114	90.14-90.34	sil/ser tuff; heterolithhic felsic tuff/LT (med grain) clast range in size from mu-granule (1-1.5 cm). 7% plag xstals and 5% qtz xstals, clast supported. 5% 1mm subhedral py in lap fragments.	G.C	4399-4405
32115	100-100.23	chl tuff; chl altered with qtz> plag xstals (20%) and fine (0.5-1cm) lap felsic fragments. Matrix supported, matrix is altered to chl, could have some arg particles. When cut had "oily" run off like arg beds. Xstal fragments are 1-3 mm.	G.C	4406-4410
32116	103.82-103.98	felsic dyke? Could be felsic dyke, it's f.g pale beige grey, however there are small (mm-scale; vfl) qtz xstals (clear) in matrix. And <5% larger (mu/cu) pale white qtz elongated xstals. V. thin black lats/speckles. Mod ser alt.	G.C	4411-4416
32117	120.0-120.30	m. sill; is in mafic sill section however this looks like it could be an chl altered xstal-bearing tuffaceous rock. Both qtz and plag are present. ASK*	G.C (TS!!)	4417-4425
32118	141.24-141.50	ser>sil L.T.; f-m gr L.T with plagiclase xstals (15%) and qtz xstals (25%) most lap fragments are filled with xstals fragments. Chl is in filling f.g matrix, looks mostly clast supportd though. Lap fragments are felsic. Mod ser and chl alt.	G.C	4426-4433
32119	155.62-156.0	mafic sill; again part of mafic sill but very crystal-rich. Xstals are fu-cl with rare granule sized fragments. Qtz> plag again, 35% qtz, 10% plag, dark green grey in color. V. chl alt. looks tuffaceous. ASK. Also, broken up clast.	G.C	4434-4442
32120	176.48-176.73	mafic sill; same as above, less xstals and finer grained. And very fissile. Broken in a bunch of pieces when cut. V. chl alt.	G.C	4443-4446
32121	195.67-195.87	ser alt tuff; looks similar to 18, xstal-bearing tuff. Xstals are in lap fragments though, no in matrix. Like 18.. Very ser alt with chl in filling matrix. Very fissile.	G.C	4447-4450

32122	217.34-217.64	felsic dyke? Light grey, very fragmental/broken up. Hard to tell.. Strong sericite alteration	G.C	4451-4453
32123	220.5-220.3	black tuff; strongly chl alt? **arg beds**?? Fault zone, strongly gouged (lowered). Black and f.g. rare py cubes.	G.C	4454-4457
32124	223.223.25	tuff? Fault zone, felsic tuff? Strongly sericite alt, wk chl.	G.C	4458-4461